

The Nuclear Safety Impacts of Fuel Deposits in Nuclear Power Plants

NNL 16670

ISSUE 3

This document is prepared by National Nuclear Laboratory Limited ("NNL") for Frazer-Nash Consultancy, on behalf of ONR pursuant to a contract, dated 17 August 2023, reference ONRT864 ("the Contract"). The ownership of this document, and the material contained within it, shall be treated in accordance with the provisions of the Contract

The Nuclear Safety Impacts of Fuel Deposits in Nuclear Power Plants

NNL 16670

ISSUE 3

[REDACTED]

	Name	Signature	Date
Checked By	[REDACTED]	[REDACTED]	04/07/2024
Approved By	[REDACTED]	[REDACTED]	05/7/24
Work Order Number	09304.100		

Keywords

NUCLEAR FUEL; PWR CHEMISTRY; FUEL CRUD; MODELLING; MECHANISMS; CRUD INDUCED POWER SHIFT; CIPS; CRUD INDUCED LOCALISED CORROSION; CILC; AXIAL OFFSET ANOMALY; AOA; ACTIVITY TRANSPORT; NICKEL BASED ALLOYS; ZIRCONIUM ALLOYS; ACTIVATED CORROSION PRODUCTS; OPERATING EXPERIENCE; BORON HIDEOUT; CORROSION PRODUCT RELEASE

Executive Summary

This report presents a review of the topic of corrosion product deposits on nuclear fuel (widely referred to as "crud"), with the aim of facilitating future assessments by the Office for Nuclear Regulation (ONR), as new or modified reactor designs or fuel designs are proposed. The primary focus of this report is fuel deposits in pressurised water reactor (PWR) systems, although other systems are also considered in less depth. This report is structured as follows; Part A with sections presenting summary, knowledge gaps and conclusions, to identify the key findings and Part B containing the technical details which underpin the key findings.

The formation of thick PWR fuel crud depends on there being a sufficiently large corrosion release rate of nickel from the steam generator (SG) tubes into the primary coolant, and whether the thermal hydraulic and chemistry conditions in the core lead to this nickel depositing on the fuel rods. The nickel release rate depends on the composition and fabrication of the SG tubes, where the latter is linked to individual tubing vendors, and on the primary water chemistry. There are different mechanisms by which soluble and particulate forms of nickel deposit on fuel rods, but both are promoted by localised boiling in the upper spans of fuel assemblies. Thick PWR fuel crud is nickel rich.

Thick fuel crud raises the temperature at the fuel cladding surface, promoting accelerated cladding oxidation; a process known as crud induced localised corrosion (CILC). This can result in cladding failure, but only a very limited number of CILC fuel failures have been experienced by PWRs. Moreover, it has not been possible to identify any instances of crud related fuel failures contributing to reactor accidents.

Instead, a more common PWR observation has been that of crud induced power shift (CIPS); a larger than expected shift in the axial power distribution towards the bottom half of the reactor core, caused by accumulation of boron in thick fuel crud deposits formed preferentially in the top half of the core. CIPS can necessitate reactor de-rating to maintain safe shutdown margins, but it is now well recognised and managed effectively.

In addition, corrosion products that deposit on fuel rods become activated while in the core. A proportion of this activity is released back into the coolant and returned to out-of-core surfaces, where it causes radiation fields. The associated occupational radiation exposure (ORE) is a concern for all plants and provides motivation for minimising fuel crud well below levels that would be required solely to avoid CIPS or CILC.

Establishing core design principles that minimise localised boiling is likely to reduce the risk of forming thick fuel crud, and crud may be removed from reload assemblies using ultrasonic fuel cleaning (UFC). Chemistry options for mitigating fuel crud formation and its effects include specifying appropriate conditions for hot functional tests, optimising the primary water chemistry pH_T , and implementing zinc injection. Use of potassium hydroxide (KOH) and enriched boric acid (EBA) may assist in optimising the primary water chemistry.

Thick fuel crud is not removed to any considerable extent under PWR shutdown chemistry conditions, but shutdown operations can be modified to alleviate specific concerns, such as particulate releases of fuel crud activity. However, these operational changes may be at the expense of leaving more crud on reload fuel, unless the reload fuel is subsequently cleaned.

Modelling of the activity transport processes within the primary circuit has been developed over many years, and the degree of sophistication has continued to increase with time. Current efforts are focused on “multi-physics” approaches which include various modules to address different aspects of circuit performance, and the systems architecture for the software is currently a highly specialised field. The completeness of the multi-physics approaches is always a matter for discussion as different approaches have different strengths and weaknesses. Across the global effort, some specific effects appear to need further attention. Validation of the different modules is being pursued by comparison with results from test loops. It is important to recognise that various industry programmes exist concerned with fuel crud where information is not in the public domain.

The management of spent fuel with adherent crud is not widely regarded to be an issue. It is recognised and accepted that most fuel will have some crud attached to it, but provided the fuel has not failed, it is generally considered appropriate to store the fuel for the short, medium, and long term. There may be a procedural aspect in that fuel with substantial crud may be more difficult to dry, as the crud may provide microscopic locations for water hideout, but the overall inventory of water needs to be evaluated.

There are a significant number of knowledge gaps and knowledge retention issues identified in this document. Full remediation of these matters would be both costly and time consuming.

The implications of the potential use of other reactor designs where crud is a possibility have been considered. None of these (BWR, VVER, CANDU/PHWR, SCWR) give rise to significant concerns regarding fuel crud. It is well known that BWR fuel often exhibits substantial crud, but this is within the normal operating regime of such reactors and within normal management control to maintain reactor safety. Other water-cooled reactor designs have not recorded fuel crud as a significant issue.

Recommendations

It is intended that this review of fuel crud issues should be of value to ONR as a means of both updating the regulatory perspective on existing power reactors and in assessing new reactor designs if or when approval is requested. There is a wealth of technical detail in this document which will prove of much assistance in such matters.

This document also identifies a number of knowledge gaps or knowledge retention concerns associated with reactor chemistry and fuel crud. It is recommended that ONR gives consideration to these matters, some of which are deemed urgent. In particular, the loss of critical knowledge based on the age demography of subject matter experts is a key concern and a firm recommendation is that this should be addressed, ideally by a cross-industry arrangement similar to past critical knowledge retention issues with pressure vessel steels.

Verification Statement

This document has been verified and approved in accordance with NNL's procedures for the reporting of work.

History Sheet

Issue Number	Date	Comments
Draft 1	17 April 2024	Draft for internal peer review
Issue 1	3 May 2024	Issue for customer review
Issue 2	5 July 2024	Revision after customer feedback
Issue 3	17 April 2025	Revised Classification (Frazer-Nash Consultancy)

Table of Contents		Page
1.	Introduction and Background.....	16
1.1.	Aspects of the ONR Safety Assessment Principles and Technical Assessment Guides which have Relevance to Fuel Deposits	17
1.2.	The structure of this report	20
2.	Summary	25
2.1.	Suggested Focus Areas for Regulatory Enquiry	32
3.	Gaps in Understanding and Long-Term Knowledge Retention	35
3.1.	Knowledge Gaps in Reactor Chemistry	35
3.2.	Knowledge Gaps Associated with Modelling of Crud Formation	37
3.3.	Knowledge Gaps Associated with Non-PWR Types of Reactor Design	38
3.4.	Knowledge Retention	39
4.	Recommendations	41
5.	Historical Occurrences of PWR Fuel Crud.....	43
5.1.	Obrigheim	43
5.2.	Callaway	43
5.3.	Three Mile Island Unit 1	46
6.	Mechanism of Fuel Crud Formation in PWR Systems	48
6.1.	Corrosion Product Source Term	48
6.1.1.	Corrosion and Corrosion Product Release	49
6.1.2.	Tubing Manufacture	52
6.1.3.	Primary Water Chemistry	57
6.2.	Corrosion Product Deposition on Fuel Rods	58
6.2.1.	Solubility Changes and Precipitation.....	58
6.2.2.	Subcooled Nucleate Boiling.....	61
6.2.3.	Particulate Deposition.....	63
7.	Fuel Crud Properties and Chemistry	64
7.1.	Crud Scrapes	64
7.1.1.	Limitations	64
7.1.2.	CIPS Root Cause Investigations (US)	64

	Page
7.1.3. Ringhals Observations	68
7.1.4. Korean Experience.....	69
7.2. Laboratory Tests.....	69
7.3. Summary	71
8. Modelling Fuel Crud Formation.....	72
8.1. Introduction to Modelling of Fuel Crud	72
8.2. The Object of the Modelling	73
8.2.1. Primary Circuit Chemistry and EPRI Guidelines	75
8.2.2. Early PWR Crud Mechanisms and Models	80
8.3. Modelling Codes that have been Widely Used	82
8.3.1. The BOA Code.....	82
8.3.2. The APACT Code.....	85
8.3.3. The Wick Boiling Model	86
8.3.4. The VIPRE Code	89
8.3.5. The LANL ChemPac Model	90
8.3.6. The MOOSE / BISON Crud Chemistry Models.....	90
8.3.7. The MAMBA Model / Code	93
8.3.8. The PACTOLE and OSCAR Codes	94
8.3.9. The CASL / VERA Approach	96
8.3.10. The Electrostatic Deposition Effect	98
8.4. Summary and Discussion on Modelling Codes	101
8.4.1. The IAEA Model Cross-comparison.....	101
8.4.2. The Latest Models.....	104
8.4.3. The Present Situation	105
9. Impact of Fuel Crud on Radiation Levels.....	107
9.1. Sources of Radioactivity	107
9.2. Radiation Field Behaviour	109
9.3. Measurement Techniques	112
9.4. Plant Shutdowns.....	115
9.4.1. Pre-shutdown pH Control	116

Table of Contents		Page
9.4.2.	Post-shutdown pH Control.....	117
9.4.3.	RCP Operation and Peroxide Addition	117
9.4.4.	Coolant Purification	120
9.4.5.	Refuelling Cavity Decontamination.....	121
10.	Safe Plant Operations.....	123
10.1.	Potassium Hydroxide	124
10.1.1.	Fuel Compatibility	125
10.1.2.	Structural Materials.....	127
10.1.3.	Chemistry and Radiation	128
10.2.	Enriched Boric Acid.....	128
10.3.	Zinc Injection	131
10.3.1.	Strategies	131
10.3.2.	Thermodynamics	132
10.3.3.	General Corrosion	133
10.3.4.	Primary Water Chemistry	133
10.3.5.	Mechanism	135
10.3.6.	Radiation Fields.....	139
10.3.7.	Fuel Performance.....	141
10.3.8.	Other Considerations.....	143
10.4.	Hot Functional Testing	145
10.4.1.	Sizewell B HFT Chemistry	145
10.4.2.	EDF Experience with SGR.....	148
10.4.3.	HFT with Zinc Injection.....	149
10.4.4.	AP1000 HFT Chemistry	151
10.4.5.	EPR HFT Chemistry	152
10.5.	Ultrasonic Fuel Cleaning	154
10.5.1.	Laboratory Tests	155
10.5.2.	Field Demonstrations.....	155
10.5.3.	Production Cleaning	157
10.5.4.	Second Generation Equipment.....	158

	Page
10.5.5. Benefits, ALARA and LLW Impacts	160
10.6. Plant Monitoring to Identify Crud Related Problems.....	162
11. Impact of Fuel Crud under Accident Conditions	164
11.1. Consideration of Relevant Accident Conditions	164
11.2. The Adverse Consequences of Fuel Crud	164
11.3. Role of Fuel Crud as a Transient Initiator	164
11.4. Reactor Accidents where Fuel Crud Influences the Progression.....	166
11.5. Review of Fuel Failures.....	166
11.6. Major Reactor Accidents	170
11.6.1. Reactor Safety Post-Three Mile Island (1979)	170
11.6.2. The Paks Fuel Accident (2003).....	171
11.6.3. Reactor Safety Post-Fukushima (2011).....	172
11.7. Operational Experience Feedback.....	173
11.8. Summary of Accidents featuring Fuel Crud	173
12. Crud Implications for Spent Nuclear Fuel Storage.....	175
12.1. PWR Spent Fuel	175
12.2. UK Experience	177
12.3. Other fuel types - CANDU.....	178
12.4. Other fuel types - SCWR	179
12.5. Summary of Crud Implications for Spent Fuel Storage.....	179
13. Fuel Crud in non-PWR systems	181
13.1. Crud in Boiling Water Reactors	182
13.1.1. Introduction to BWR Reactor Cooling Systems.....	182
13.1.2. Fuel Deposits in BWRs	183
13.1.3. Summary considerations on BWR designs	190
13.2. Crud in VVERs	191
13.2.1. Introduction to VVER Reactor Cooling Systems	191
13.2.2. Fuel Deposits in VVER reactors.....	193
13.2.3. Summary of Considerations on VVER Designs.....	198
13.3. Crud in Pressurised Heavy Water Reactors	198

	Page
Table of Contents	
13.3.1. Operating PHWR Reactors	198
13.3.2. Crud and Spent CANDU Fuel	202
13.3.3. Summary of Considerations on PHWR Fuel Deposits	203
13.4. Crud in Supercritical Water Reactors	203
13.4.1. The Canadian Design of SCWR	203
13.4.2. Other designs of SCWR	205
13.4.3. Summary considerations on SCWR designs	206
14. References	208

	Page
List of Tables	
Table 1 Ni, Fe and Cr Indicative Content of Selected PWR Materials	50
Table 2 Approximate Corrosion and Corrosion Release Rates	51
Table 3: Participating countries, organisations, and models / roles in the IAEA 2012 cross-comparison of modelling codes.....	102
Table 4: Comparison of Ultrasonic Fuel Cleaning Technologies	159
Table 5: Summary of UFC LLW Generation at PWR Stations.....	162
Table 6: Causes of fuel rod failures (from [236])	167
Table 7: PWR fuel failures in incidents involving more than ten assemblies, 1989-1994 (from [236])	168
Table 8: PWR fuel failures in incidents involving more than ten assemblies, 1995-2005 [237].....	170
Table 9: BWR Fuel crud scraping analysis results (from [256])	184
Table 10: BWR Fuel failure analysis results (from [238]).....	190
Table 11: A comparison of key parameters for VVER-440, VVER-1000 and typical PWR (from [270] and [271]).....	192
Table 12: A comparison of SG materials in VVER-440, VVER-1000 and typical PWR (from [270])	193
Table 13: Composition of Inconel 800 series Alloys (from [284])	199

	Page
List of Figures	
Figure 1: An Example of CIPS for a Westinghouse PWR (From [17]).....	44
Figure 2: Factors Contributing to AOA or CIPS (From [17]).....	45
Figure 3: Flow of Corrosion Products through a PWR Primary Circuit (From [31])	48
Figure 4 Oxides Formed on Stainless Steel and Alloy 600/690 Surfaces (From [39])	51
Figure 5: Post Replacement Co-58 Shutdown Peaks following Peroxide Addition.....	53
Figure 6: Soluble and Particulate Co-58 and C-60 Concentrations for Sizewell B.....	54
Figure 7: Co-58 Peaks at Forced Oxygenation for EDF Plants with Alloy 600TT SG Tubes	56
Figure 8: Corrosion Rates of Alloy 600 and Stainless Steel Relative to pH _T = 6.9	58

List of Figures	Page
Figure 9: Variations in Nickel Solubility from Core Inlet to Outlet with pH at 300°C.....	60
Figure 10: Formation of a Bubble on a Heated Surface (From [68])	61
Figure 11: Illustration of Transition from Non-Boiling to Wick Boiling Conditions (From [68])	62
Figure 12: Backscattered SEM Image of a Callaway Cycle 9 Crud Cross Section (From [16])	65
Figure 13: Lister’s visualisation [89] of crud formation and erosion (after [90])	74
Figure 14: High magnification SEM of a crud flake, showing steam chimneys. (From [17]) .	77
Figure 15: Cross sectional view of a Seabrook Cycle 5 crud flake. (From [17]).....	78
Figure 16: Model and plant data for Zn at Vogtle Unit 1. (From [99])	84
Figure 17: Experimental data and APACT fit for the distribution of boric acid between the liquid and vapour phases. (From [77]).....	85
Figure 18: Schematic diagram of heat transport during wick boiling. q_e is the evaporative heat flux and q_c the conductive heat flux. (From [103]).....	87
Figure 19: Model and plant data for shutdown Ni releases at Vandellos. (From [99]).....	89
Figure 20: Loop nodalisation for ECP model. (From [107]).....	91
Figure 21: The 2-D model of steam chimneys, after Pan et al [111], as implemented by Jin and Short [108]	93
Figure 22: Flowchart of the MPO crud (MAMBA) model. (From [105]).....	94
Figure 23: A schematic of the PACTOLE code (From [112]).....	95
Figure 24: A schematic of the VERA performance simulation environment, (From [120])	97
Figure 25: A schematic of the CASL-CRUD model as a demonstrator. (From [119])	98
Figure 26: A schematic of the processes modelled by the DISER code (From [39])	99
Figure 27: PWR Corrosion Product Formation, Transport and Deposition Mechanisms (From [97])	108
Figure 28: Radiation Field Trends in PWRs (From [42])	110
Figure 29: Variation of Co-58/Co-60 Ratio based on Steam Generator Tube Measurements (From [97])	110
Figure 30: SRMP Survey Points for Typical Westinghouse 4-Loop PWR.....	114
Figure 31: Projected Clean-up Times based on Purification Flows and Resin Efficiencies.....	121
Figure 32: Comparison of the Li/H ₃ BO ₃ and K/H ₃ BO ₃ Strategies used in PWRs and VVERs.	125

List of Figures	Page
Figure 33: Effect of LiOH, KOH and a LiOH+KOH+H ₃ BO ₃ Mixture on Zircaloy-4 Corrosion (From [161])	126
Figure 34: Weight Gain of Zircaloy-4 versus Ionic Radius of Alkali Hydroxide Cation (From [162]).....	126
Figure 35: Effect of Void Fraction on Zircaloy-4 Oxide Thickness in LiOH and KOH (From [163]).....	127
Figure 36: Average Co-58 Activity in Cycles 1-5 after SGR	135
Figure 37: STEM-EDS Images of Alloy 600 Specimen Exposed to Zinc	137
Figure 38: SEM Observations of Alloy 690TT Sample Oxidised at 325°C.....	138
Figure 39: Dose Impact from Zinc Injection (From [182])	140
Figure 40: Schematic of Callaway (First Generation) UFC Equipment (From [221])	156
Figure 41: Images of Callaway Fuel Assembly G32 Before and After Cleaning (From [221])	157
Figure 42: Schematic of STP 1 and 2 (Second Generation) UFC Equipment (From [224]) .	159
Figure 43: Distribution of fuel failure causes between 1987 and 1994 from [236].....	168
Figure 44: Trends in fuel burnups between 1970 and 2005 [From [237]	169
Figure 45: Average discharge burnup data (2005) across all reactor fleets (From [252])	181
Figure 46: Fuel crud arisings and analysis at Tokai-2 BWR (From [258]).....	185
Figure 47: Differences between midspan (general) corrosion, shadow corrosion and enhanced spacer shadow corrosion (From [260])	186
Figure 48: Number of leaking BWR fuel bundles per 1000 discharged bundles and leaking rods per million rods. (From [237] and [238])	189
Figure 49: Layout of VVER-1000 reactor cooling loops (From [272])	192
Figure 50: Fuel integrity and SG dose rate correlation for two VVER-400 reactors (From [277]).....	194
Figure 51: The amount of deposit and acceleration of cladding corrosion along fuel rod N7 under spacer grids plates of fuel assembly after 4 years operation (From [281]).....	196
Figure 52: Number of leaking VVER fuel bundles per 1000 discharged bundles and leaking rods per million rods. (From [237] and [238])	197
Figure 53: Nodular corrosion (after crud removal) on CANDU fuel rod Zircaloy-4 cladding tested 90 days in TRIGA reactor using irradiation capsule. (From [283]).....	200
Figure 54: Number of leaking PHWR fuel bundles per 1000 discharged bundles. (From [237] and [238])	202

List of Figures

Page

Figure 55: (A) Canadian SCWR core schematic and flow streams and (B) fuel channel schematic and flow streams (From [287]).....	204
Figure 56: (A) Canadian SCWR fuel channel schematic and (B) fuel bundle schematic. (From [287]).....	205

PART A

SUMMARY AND KEY FINDINGS

1. Introduction and Background

This document is a review of the open literature concerning the state of the art describing PWR fuel deposits and the consequent safety implications, as regards fuel performance during reactor operations, under both normal operation and fault conditions. This review is provided at the request of the ONR in order to assist with the review of various reactor designs which may be advanced for approval or modifications to operations of existing plant.

This document is intended to provide detailed information which will assist in the technical assessments of new reactor designs or operations which, nonetheless, are based on the PWR concept and which base their operational and safety arguments on the extensive world-wide experience in operating PWRs. PWRs have been in operation world-wide since the 1950s and have evolved from early design patterns (Generation I) to the more recent patterns (Generation III+). Most recently a new category of nuclear reactors, known as Generation IV, have been brought forward with a wide range of operating principles, with at least some designs which derive from light water reactor (LWR) origins, although sometimes possessing characteristics of modularity, smaller unit size, or novel aspects of operational infrastructure.

The objective of this review is to furnish the ONR with independent advice, notwithstanding the claims of the reactor design Requesting Parties (or Site Licensee), to assist ONR in its role of judging the suitability of the proposed designs in regard to certain key safety considerations associated with fuel deposits.

It is understood that ONR will need to judge the capacity and capability of Requesting Parties concerning the various approaches and resources available to fully evaluate the nuclear safety impacts of PWR fuel deposits. The arrangements concerning approval and permissioning of nuclear power stations have been described in [1]. This document is intended to inform ONR concerning fuel deposits and to present relevant good practice together with consideration of risks and their reasonable mitigation.

This document is also intended to support ONR in any future requirement to review the Safety Assessment Principles (SAPs) and Technical Assessment Guides (TAGs) relevant to PWR reactor chemistry and fuel deposits, and any potential update or revision, if necessary. The information contained within this document will be of assistance in any future reconsideration of these guidance documents.

This document will also identify any evident gaps in the knowledge, across the industry, and indicate where further information would be desirable.

It should be noted that in many documents the term "crud" is generic for corrosion deposit in any part of the primary circuit, including deposits within steam generator (SG) tubes. For this study we only consider deposits on fuel surfaces. The terms "crud" and "fuel deposit" may then be used interchangeably.

1.1. Aspects of the ONR Safety Assessment Principles and Technical Assessment Guides which have Relevance to Fuel Deposits

The SAPs which govern the topic of nuclear fuel and any fuel deposits are presented in [2] which is an over-arching document dealing with all aspects of nuclear facilities. In [2] there is no explicit mention of fuel deposits, but on the matter of nuclear fuel more generally there are several statements which convey the general requirement that safety must be considered in

regard to the way fuel is used and stored. The following points consider a few of these specifics which may be relevant to fuel deposits.

- The requirement is laid out that, as regarding the reactor core, the SAPs relate to the need to control reactivity, heat generation and removal, and other design aspects, in order to assure that the reactor stays within specified limits to ensure safety during operation and design basis fault conditions. Since fuel deposits can affect both reactivity and fuel cladding temperature, these matters are of primary concern in application of the SAPs.
- Fuel deposits may be a factor influencing clad corrosion through to failure, and SAPs identify the need for core monitoring and the criteria and strategy for dealing with failed fuel.
- The SAPs draw attention to the need to prevent overheating of the fuel, to avoid detrimental consequences on reactor safety in the widest sense. Since fuel deposits may affect heat transfer from the fuel to the coolant, again the relevance of fuel deposits to compliance with SAPs is evident.
- The SAPs point out that reactor chemistry can have a significant effect on the performance of systems and structures. Since the corrosion of the coolant circuit, which is the source of the material incorporated as fuel deposits, is principally subject to the circuit chemistry, then chemistry must be a significant aspect of assessing the likelihood of fuel deposits.
- The SAPs confirm that the safe and correct management of fuel includes spent fuel as well as fuel within the operations of a nuclear reactor during its fuel cycle. Thus, any impact of fuel deposits on spent fuel needs to be considered.
- The need for inspection of fuel assemblies, including post-irradiation inspection, is confirmed on the SAPs and this will pick up on any incidences of fuel deposits.
- The SAPs make clear that a nuclear reactor should be subject to a probabilistic safety analysis and severe accident analysis. Whilst all the factors which might feed into such an analysis are not individually prescribed, the possible effects of fuel deposits in affecting fuel reactivity, temperature and corrosion / failure would provide reasonable basis for expecting fuel deposits to be factored in.
- In relation to graphite-moderated reactors, the interaction between the various reactor components, including fuel, the consequential mode of failure and spatial and temporal distribution all need to be estimated and thus predict the condition of components and structures. The development of analytical models is expected, and predictions made concerning the condition of reactor components and fuel assemblies etc. It would not be unreasonable to extend that expectation to water-moderated reactors and since fuel deposits may have some bearing on interactions it is reasonable to consider models of the effects of fuel deposits.

In addition to the SAPs are the TAGs. The principal TAGs are these:

- NS-TAST-GD-088 (Issue 3): Chemistry of Operating Civil Nuclear Reactors [3]
- NS-TAST-GD-089 (Issue 1.1): Chemistry Assessment [4]
- NS-TAST-GD-075 (Issue 3.1): Safety of Nuclear Fuel in Power Reactors [5]
- Of further relevance may also be NS-TAST-GD-081: Storage of Spent Nuclear Fuel [6].

In relation to the topic of fuel deposits, these TAGs include discussions of the following points.

TAG document NS-TAST-GD-088 [3] mentions "fuel" a number of times. Mostly this is in connection with the need to ensure the coolant chemistry preserves fuel integrity. That

document includes mention of chemistry as a factor in controlling crud induced power shift (CIPS) and circuit corrosion in general. There is a requirement to preserve the integrity of the fuel and limit the formation of deposits which could contribute to failures or limit the degradation rate to acceptable levels. It is also noted that the chemistry arrangements should be appropriately selected after giving due consideration to fuel cladding corrosion and deposition. In terms of the ongoing reactor chemistry there is a requirement that the system should be able to remove activated corrosion products (and fission products deriving from the fuel) from the reactor coolant. Reference [3] also mentions that the Safety Standard on the design of the reactor core [7], notes the general problem of fuel deposits and emphasises correct control of coolant chemistry. However, [7] has more recently been superseded by [8] which is similar to [7] in that fuel deposits are mentioned as a problem, and at this instance [8] the further complication of having boron as a constituent of the fuel deposit is noted. However, there is no detailed examination of why and how deposits arise or their mitigation.

There is also due note that the lithium concentration in the coolant must be controlled so as to limit the extent of corrosion of the fuel cladding. It is evident that control of coolant pH will also have an impact on the solubility of corrosion products, and therefore on fuel deposits. Normally this is not a problem, but any mechanism (such as CIPS) which increases the lithium concentration must be taken into consideration. Whilst the lithium concentration enhancement due to boron-10 neutron capture will be outweighed by concentration from thermal hydraulic effects (e.g., wick-boiling) for a conventional Li-B chemistry, this will have an influence for any non-Li chemistry such as a prospective potassium based chemistry.

It is also recognised that throughout each reactor fuel cycle, the boron concentration will need to be adjusted to achieve the intended reactivity profile, and this in turn requires adjustment of the bulk lithium concentration in order to retain the intended pH, under the “coordinated”, “modified” or “elevated” chemistry regimes intended for each plant. Alongside the effect of lithium are the effects of radiolysis in producing short lived oxidising species, whose presence is counteracted by the addition of dissolved hydrogen in the reactor coolant, but subject to the constraint that too much hydrogen could promote hydriding of the zirconium alloy fuel cladding, which is undesirable. Even this is subtly affected by Reaction (1)



Equation 1: Neutron capture by boron

whereby the resulting alpha particle (^4He) causes more local radiolysis of the water molecules in the coolant within the pores and steam chimneys and the production of additional oxidising species.

Reference [3] also notes the involvement of other trace components within the coolant (such as Si, Mg, Ca) to exacerbate deposits of corrosion product on the fuel surface. As a summary perspective, there is guidance that the quantity of corrosion products in the system should be kept low and that contamination of the primary circuit surfaces, including fuel, should be kept to a minimum particularly as regards deposition on heat-transfer surfaces, such as fuel assemblies.

In the context of spent fuel ponds or pools (SFPs) the guidance is that further corrosion of fuel should be prevented or minimised, and that in order to prevent formation of further tenacious deposits the concentrations of silica, magnesium and calcium should be paid close attention.

Similar concerns apply to BWR reactor chemistry although recognising that by definition boiling will occur, nevertheless the deposition of coolant impurities on the fuel surface should be

minimised by good control of the water purity. Unavoidably there are some corrosion deposits on the fuel and the implementation of a hydrogen water chemistry regime (to protect austenitic stainless steels in the core structure) may cause a crud burst with radioactivity release at shutdown, which must be carefully managed.

The impact of zinc addition (which is carried out for both PWRs and BWRs) is noted in [3] with the possible effect of densifying the corrosion product, which may also be more adherent (for example, zinc silicate – based deposits). Further, by reducing the quantity of out-of-core corrosion product and exchanging zinc atoms for cobalt atoms in the spinel structure found in oxides on nickel based alloys (commonly found in SGs), zinc injection results in less radioactive cobalt being retained in deposits, and deposit activity levels are reduced. It has been considered a possibility that denser and more adherent fuel deposits could have a role in fuel failures.

The chemistry assessment TAG [4] recognises that a number of factors influence the deposition of corrosion products onto surfaces and that the deposition process may be affected by the system chemistry and by temperature. Within [4] there is no specific mention of fuel deposits, however, there is the observation that the ability to cool irradiated nuclear fuel is paramount and that failure to do so may culminate in severe accidents. In practical terms, fuel surface deposits are not expected to completely prevent fuel cooling but may act as a thin layer of insulator and make heat ejection partly more restricted.

Reference [5] (the TAG relating to reactor fuel) makes several references to the topic of fuel deposits and this reinforces the perspective gained through the other TAGs that fuel deposits are problematic and should be avoided or minimised by good practice, including coolant chemistry control. The majority of the control measures are embodied in the chemistry, described in the other relevant TAGs, [3] and [4]. However specific mention of fuel deposits is in the following regards.

- The (fuel and core) design should consider the possibility of fuel failure by cladding corrosion and embrittlement, including the effect of surface deposits.
- The issues of corrosion, hydriding and surface deposits are grouped together as matters of concern. There is note of possible rapid fuel failure, but also an implicit or tacit linkage of under-deposit corrosion with hydriding and embrittlement, possibly as ancillary factors in the rapid failure mechanism.
- The permitted rate of sub cooled boiling is raised as a possible mitigation of the rate of deposit formation.
- Surveillance of the fuel, after each operating cycle, is required in order to assure that the condition of the fuel (including any deposits) is consistent with safety case assumptions.
- The possibility of deposits including boron is noted, with the guidance that the impact of such deposits on core neutronics must be assessed.

Reference [5] clearly reinforces the TAGs relating to coolant chemistry control and views the problem more from the perspective of the fuel itself.

Regarding spent nuclear fuel, [6] makes no specific reference to fuel having surface deposits; however, the generic guidance is that spent fuel must be managed appropriately and with due regard for safety. There are specific requirements in the following regards (inter alia):

- In any assessment, consideration must be given to providing confidence in the continuing cladding and structural integrity of the spent nuclear fuel.
- Consideration must also be given to the potential impact of radiation, heat generation, corrosion, or other chemical reactions on spent nuclear fuel and facility equipment.

Therefore, whilst fuel deposits are not specifically mentioned, their effects on cladding integrity and heat ejection are clearly deserving of consideration in and safety assessment.

In summary, the key SAP and the associated TAGs demonstrate a well-established awareness of the issues of fuel deposits, and the ramifications that should be expected from fuel having surface deposits. There is no detailed mechanistic description of deposit formation or mitigation techniques, but it is noteworthy that some mitigation technologies such as zinc injection are recognised, as are the high-level requirements for demonstrable reactor control when boron-containing deposits are causing CIPS. The SAP and TAG documentation is in generally good order but would benefit from a source document such as this to provide the underpinning detail on fuel deposits and their consequences.

1.2. The structure of this report

This detailed technical review and discussion arise from the various subject topics which were identified in the NNL proposal to ONR in response to the original specification. These topics were intended to give a wide-ranging coverage to the field of fuel deposits arising on PWR fuel. The individual sections and their immediate applications are as follows. The numbering of these sections has been modified from the original NNL proposal, in accordance with comments from the ONR on Issue 1 of this report.

PART A of this report.

1. Introduction and Background

This (present) section provides context and introduces the reader to the topic more generally in terms of ONR requirement and very high-level technical background.

2. Summary and Discussion

In the summary section we present a focus on aspects considered important to the regulator, particularly with regard to new build plant. This summary section discusses the following matters.

- The minimisation of fuel deposit and its consequences by aspects of plant design.
- The minimisation of fuel deposit by appropriate hot functional testing (HFT).
- The minimisation of fuel deposit and its consequences by appropriate fuel and core design,
- The minimisation of fuel deposits by optimised plant chemistry and operational procedures.
- Identification of fuel deposit related problems by best practice chemistry monitoring and power/flow monitoring.
- The safety implications of plants experiencing fuel crud problems.
- The safety issues associated with fuel having deposits which will need to be stored for short, medium and long term periods.

These important points are presented as a checklist of key questions which ONR inspectors may wish to ask duty holders when considering safety case submissions covering fuel deposit chemistry.

The discussions presented in this document relate these topics to the ONR SAPs and TAGs, which have been summarised above. It is the intention that this document will provide guidance for ONR to assess the following matters.

- Where to focus their regulatory attention.
- The relative importance of Operational Experience (OPEX) versus modelling.
- Their goal setting approach to regulation and making the "Chemistry Safety Case".
- How fuel crud chemistry assessment approaches may compare between the UK and other countries (possibly from both the operator's and regulator's points of view).
- The relative importance of any possible knowledge gaps.
- Identify the next steps required to address these potential knowledge gaps.

3. Gaps in Understanding and Long-Term Knowledge Retention

There are a number of aspects of fuel crud behaviour that are still not understood, and which merit discussion. This section reviews various organisations' approaches to the assessment of fuel crud particularly from a chemistry perspective. Around the world there are currently a number of research initiatives, both theoretical and experimental in order to more fully explore this matter.

This document summarises these present efforts and points out the best available tools, techniques, resources and accumulated experience available to model, analyse, evaluate and understand fuel crud deposits and to appreciate their nuclear safety impacts. The current state of knowledge in the UK and elsewhere is summarised, along with where that knowledge resides and the risks in respect of losing that knowledge.

A particular issue is that in the UK nuclear industry much of this understanding resides in an ageing work force. Since the UK is currently building reactors to operate for the next 60 years, a lack of supporting expertise is questionably an unsustainable position.

In the technical and modelling fields, any knowledge gaps identified are also identified and included in the general topic of “knowledge gaps”. In such cases any knowledge retention mechanism will be indicated.

4. Recommendations

This section presents the overall recommendations of this report in a concise summary.

PART B of this report.

5. Historical Occurrences of PWR Fuel Crud

This section discusses early experiences of fuel deposits in various plants. The section discusses the causes of early crud observations, and insights still useful today. The historical account moves on to describe CIPS – formerly known as axial offset anomaly (AOA) - and crud induced localised corrosion (CILC) events. The likely correlation of more recent events with the practice of operating the reactor cores at high power density will be explored, and is most relevant considering the current trend to increase the power obtained from the core.

6. Mechanism of Fuel Crud Formation in PWR Systems

An essential aspect of this document (and the topic at large) is to describe what is known about how PWR fuel deposit is formed. The overall formation route is discussed in detail and shown to be a consequence of out-of-core corrosion followed by corrosion product release and solubility gradients arising from in-core thermal hydraulics. The impact of reactor chemistry on the general corrosion behaviour of out-of-core materials is also important and merits a detailed consideration, along with some aspects of core thermal hydraulics. The various possible deposition mechanisms are discussed in the context of PWR fuel crud formation.

7. Fuel Crud Properties and Chemistry

The nature of PWR fuel deposit is considered, particularly its properties and composition. Also provided is a brief overview of how this information can be derived or measured; such properties (for example thermal conductivity) are important because they impact the heat transfer mechanism across fuel deposit and this in turn impacts local temperature and chemistry at the clad-deposit interface. The CIPS and CILC phenomena are described in terms of fuel deposit chemistry and temperature distribution.

8. Modelling Fuel Crud Formation

This section provides a review of the key parameters amenable to modelling and surveys the range of numerical simulation tools, with some reference to the way such tools have evolved with time. Future assessments of fuel deposit formation will likely depend increasingly on modelling for reactor designs which differ from historical standard designs (Gen I to Gen III+), therefore an understanding of such models, their basis and their deficiencies is provided. Such tools are also important in assessing the impact of changes in core design or coolant chemistry for existing plants.

9. Impact of Fuel Crud on Radiation Levels

As deposits derived from corrosion of out-of-core materials accumulate in the core they are subsequently activated by neutrons. This leads to an inventory of radionuclides that can be released to the coolant and subsequently re-deposit out-of-core. During outage inspection and maintenance, the out-of-core components may need to be accessed by workers who would then receive radiological dose. It is imperative that the radiation dose levels in these areas are kept as low as is reasonably practicable. During normal operation most of the inventory of corrosion product radioisotopes is located in the core. However,

at shut-down the various thermal and chemical perturbations to the fuel deposit environment may give rise to a "crud burst" in which significant amounts of crud are released from the fuel and find their way throughout the primary circuit. Some may become fixed in out of core locations, despite circuit flushing and chemical cleaning operations. Understanding the relationship between the amounts of fuel crud and out-of-core activity levels and how plant operators manage this, and links to shutdown practices, is therefore important and is discussed here.

10. Safe Plant Operations

It has already been noted that fuel crud may have some consequences on the safe operation of the plant. Additional effects of a secondary nature are also possible, and these include:

- Impact on shutdown procedure. During the shutdown process the plant operators have some latitude regarding any crud removal as a consequence of the various chemistry / regime steps required during the shutdown process. Operators may choose to shut down the reactor whilst retaining much of the crud on the fuel, or conversely whilst attempting to remove as much crud as possible. As a consequence, the radioactive corrosion product inventory (following shutdown) may be disposed in differing locations. In attempting to remove a significant portion of the crud at shutdown, one effect is that significant quantities of radioactive material may end up on the system clean-up filters/resins, alternatively a shutdown where the aim is to retain fuel deposits on the fuel during shutdown will therefore have fuel with crud in the refuelling pool (as fuel is always shuffled from one fuel cycle to the next). It has long been an international aim to minimise dose to operators during reactor outage and the location of radioactive crud needs to be assessed.
- In view of the normal operating practice of irradiating PWR fuel through typically three fuel cycles, the retention of fuel with surface deposits has the advantage of minimising secondary wastes; but re-use of fuel with adherent crud may lead to accumulation of thick crud which could have the consequence of local overheating and fuel failure. Fuel failure may lead to high inventories of mobile fission products such as radioactive iodine and tramp fuel, which can persist in the plant for decades.
- There are widespread differences in the way PWR plants are operated, in relation to chemistry and procedures. Some plants will include zinc addition in the chemistry regime, whilst some plants perform Ultrasonic Fuel Cleaning (UFC) during refuelling. Conversely other plants will do neither or only one of these things. The importance of these differences and the impact they have on fuel crud has to be appreciated, in the selection of plant management options. Furthermore, other options such as the extent and the conditions of HFT during the commissioning of new plants have a bearing on the extent of crud formation and these factors also should be understood.

11. Impact of Fuel Crud under Accident Conditions

The growth of thick crud on the fuel surface not only impedes heat transfer, but also affects coolant flow through the core; insufficient coolant flow may lead to an abnormal pressure differential across the core, and possibly affect the ability to remove heat. The impact of fuel crud on fuel behaviour under accident conditions has been reported a number of times, and such information is summarised.

12. Crud Implications for Spent Nuclear Fuel Storage

This Section describes the issues which may arise, in terms of hindering the drying of spent fuel (through water hide-out in thick crud) and also repeated heating and cooling

of the fuel cladding leading to realignment of hydride precipitates and the possibility of delayed hydride cracking.

13. Fuel Crud in Non-PWR Systems

The onset of fuel crud is observed in reactor systems such as BWR, CANDU, and (to a much lesser extent) in VVERs. This section provides an overview of fuel crud in these reactors as regards the history of such observations, crud formation mechanisms, the type and structure of non-PWR cruds, the assessment methods and the consequences of crud in these reactor types. An understanding of such fuel crud phenomena provides an added appreciation of observations which are relevant to PWRs, or not. It is recognised that BWR fuel typically has much more adherent crud than PWR fuel, since the basis of a BWR is that it permits boiling throughout the core. Consequently, BWRs see more fuel failures as a consequence of fuel crud. For example, there have probably been more fuel clad failures in BWRs relating to fuel crud than in PWRs. However, the mechanism of failure involves factors which are unlikely in PWRs, for example involving Zn-silicate formation and/or Cu chemistry. Since there now are some emerging designs which incorporate both PWR and BWR features it then follows that an understanding of fuel crud in all the current designs has relevance for assessing new Advanced Nuclear Technology (ANT) designs.

2. Summary

The main nuclear safety implications of PWR fuel crud are CIPS and CILC. Re-deposited activity is also inherent in the production of ex-core radiation fields, which are responsible for shutdown dose rates. CIPS refers to a larger than expected shift in the axial power distribution towards the bottom half of the reactor core, caused by accumulation of boron in fuel crud deposits formed preferentially in the top half of the core. CILC occurs when fuel crud raises the temperature of the fuel cladding surface, thereby promoting accelerated zirconium oxidation rates. In severe cases, CILC can cause fuel failures.

The fuel crud responsible for the first observation of CIPS (at Obrigheim PWR) was attributed to shortfalls in the primary water chemistry; namely, insufficient dissolved hydrogen to suppress the formation of oxidising species in the core, and the absence of lithium hydroxide (LiOH) for pH_T control. Addressing these issues was sufficient to preclude any further instances of CIPS for many years, until more examples followed in the late-1980s and 1990s. The re-emergence of CIPS coincided with the use of high-duty core designs, which were required to support longer fuel cycles and power uprates. Two features of high-duty cores are: (1) a propensity for sub-cooled nucleate boiling (SNB) in the upper spans of fuel assemblies, and (2) beginning-of-cycle (BOC) boron concentrations that are even higher than usual. For the CIPS cycles, the thickest crud coincided with regions of SNB. In the past 30 years, only three PWR fuel cycles have experienced CILC-related fuel failures, and each of these cycles was also affected by CIPS.

Iron and nickel are the main constituents of PWR fuel crud, and they originate from general corrosion of ex-core surfaces. Thin fuel crud is comprised of nickel ferrite (NiFe₂O₄) with a Ni/Fe ratio of 0.5 or less, but nickel-rich fuel crud may deposit if the nickel input to the coolant is sufficient. The excess nickel is deposited as nickel metal and nickel oxide (NiO) fuel crud, leading to higher Ni/Fe ratios of up to 5. For most PWRs, the main source of nickel is from general corrosion of the SG tubes. Certainly, this is the case if they are fabricated from the nickel-based alloys 600 or 690. The alternative is Alloy 800, which is iron based, and this partly explains why Siemens/KWU-designed plants do not experience CIPS.

Mill-annealed Alloy 600 (600MA) was the first nickel-based alloy to be used for PWR SG tubes, followed by thermally treated 600TT, and then, most recently, Alloy 690TT. The principal objective was to improve resistance to PWSCC (pressurised water stress corrosion cracking), but the compositional changes and thermal treatment also resulted in lower rates of general corrosion and corrosion product release, most notably for Alloy 690TT. Alloy 690 benefits from a higher chromium content and a lower nickel content than Alloy 600. The changes made were beneficial regarding fuel crud, but they are not the full story.

Operating experience gained by replacing older (Alloy 600) SGs with newer models fitted with Alloy 690TT tubes, plus evidence from laboratory tests, confirms the importance of the manufacturing process on nickel release rates. This is manifest as markedly different performance – a corrosion rate that falls rapidly after a few cycles versus a corrosion rate that is sustained at the higher level for several cycles – depending on the tubing manufacturer: Sandvik, Sumitomo or Valinox. Significantly, improvements in the performance of Valinox tubes are relatable to different periods in the evolution of the Valinox process. In- reactor performance was assessed by monitoring Co-58 surface activities and shutdown oxygenation peaks. This works because Co-58 is produced from nickel activation and has a short enough half-life to contribute only to the cycle in which it was produced. The advantageous behaviour observed for Sandvik and Valinox-manufactured Alloy 690TT tubing is seen both for replacement SGs and for new plants with original SGs, with only one potential exception

identified (Ringhals 4). It is likely that the evolving manufacturing processes resulted in surface-finish improvements that promoted the formation of a protective, chromium-rich passivation film. It has not been possible to confirm similar behaviour for Sumitomo-manufactured Alloy 690TT tubing, but it is known that Sumitomo has been developing a chromia pre-filming process.

Historically, chemistry attempts to minimise fuel crud formation have focused on maintaining a sufficiently alkaline primary coolant pH_T during power operation. Initially, it was considered optimum to maintain $\text{pH}_T \geq 6.9$ because of a corresponding change in the magnetite coefficient of solubility from negative (retrograde solubility) to positive (normal solubility), meaning that iron would become more soluble with increasing temperature on passing through the core, and hence, less likely to precipitate. This also coincided with a broad minimum in the magnetite solubility, thereby reducing dissolution from ex-core surfaces. However, the optimum range was subsequently revised upwards to $\text{pH}_T = 7.4$ based on the properties of nickel ferrite.

Current thinking is that the optimum pH_T should be based on nickel solubility because thick fuel crud in high-duty PWRs is nickel rich, and the solubility of Ni metal and NiO is lower than the iron solubility of nickel ferrite. It is not possible to operate PWRs with a pH_T for which nickel solubility behaves normally under oxidising conditions, but the nickel solubility at the core inlet decreases with increasing pH_T . Therefore, maintaining $\text{pH}_T = 7.4$ is predicted to minimise the nickel inventory available to deposit on fuel. However, this approach is limited in that it does not consider deposition from colloidal or particulate species, or the effects of localised boiling. Moreover, many plants are not able to achieve $\text{pH}_T = 7.4$ at beginning of cycle without operating above conservative lithium concentration limits. It is then a matter of weighing the potential fuel crud and radiation field benefits against the risks of fuel cladding corrosion and possible adverse effects on Alloy 600 PWSCC and on SCC of stainless steel. With fuel vendor support, some plants have justified operating with elevated lithium concentrations up to 6 ppm, thereby allowing them to maintain pH_T close to 7.4 throughout the whole fuel cycle. While there have been some reports of benefits arising from such operation, the evidence is not yet supportive of a systematic effect. This contrasts with the convincing case for maintaining $\text{pH}_T \geq 6.9$ from criticality, which EPRI raised to $\text{pH}_T \geq 7.0$ for full power conditions.

The properties of fuel crud have been studied using flakes scraped off fuel rods after reactor shutdown and simulated crud produced in laboratories. Flakes up to $\sim 100\text{-}125\ \mu\text{m}$ in thickness were obtained from Callaway fuel at the end of Cycle 9; a severe CIPS cycle. They were retrieved from the upper spans of fuel rods and exhibited a layered structure comprising needles or rods of bonaccordite (Ni_2FeBO_5) at the cladding-crud interface, zirconium oxide (ZrO_2) particles in the middle layer, clustered around wick-boiling chimneys, and a highly porous outer layer of NiO needles, capping the boiling chimneys. The condition of the crud would have been modified by the reactor shutdown chemistry, when species such as Ni metal and lithium borates become soluble. Nevertheless, it was apparent that the local chemistry conditions in the pores of thick fuel crud on rods undergoing SNB must be very different to those in the bulk coolant.

Computational models of the deposition process and crud chemistry were developed based on LiOH and boric acid becoming concentrated in the deposit pores under the action of boiling and causing boiling point elevation to a temperature hot enough for bonaccordite to form. The resulting pH-profile of the deposit promotes ZrO_2 dissolution at the cladding surface, which re-precipitates deeper in the deposit. There is debate about the form in which boron accumulates in thick fuel crud, either as lithium borate precipitates or by physisorption onto NiO whiskers, but laboratory experiments show that the amount of boron retained increases with the NiO

content of the crud. Furthermore, laboratory simulations have found that fuel crud increases with steaming rate, heat flux, and Ni/Fe ratio in the coolant, but falls with increasing pH_T .

Activated corrosion products dominate shutdown radiation fields, especially Co-58 and Co-60, which typically account for most of the dose received by workers. Nickel released from SG tubes is deposited on fuel cladding to form thick fuel crud and is also the source of Co-58 activity. This is different to Co-60, which is formed by activation of cobalt, and the main source of cobalt is usually from Stellite hard facings. Hence, some correlation of fuel crud with Co-58 activity is to be expected, but less so for Co-60. Another important consideration is that Co-60 has a much longer half-life than Co-58 and so any correlation between fuel crud and general dose rates becomes less likely as a plant ages.

A small proportion of the Reactor Coolant System (RCS) corrosion product inventory, including activated corrosion products, is released into the coolant during shutdown evolutions. At the start of a shutdown, the behaviour is explained by the increased solubility of oxide species during cooling under acid-reducing conditions, but this is followed by a prompt release of nickel and associated Co-58 when oxidising conditions are created. Nickel metal is soluble under acid-oxidising conditions. While the release represents only a small proportion (<10%) of the activity present on the fuel cladding and ex-core surfaces, and therefore should not be thought of as a decontamination process, the released activity must be cleaned up by the Chemical and Volume Control System (CVCS) purification system before the shutdown progresses, principally to avoid increased refuelling platform dose rates. The intent is to promote soluble releases that are readily removed by the ion-exchange demineralisers, whereas particulate releases tend to re-deposit, especially in low flow regions. Plants with thick fuel crud are more susceptible to unexpected releases of particulate activity, which contaminate out-of-core surfaces leading to higher dose rates.

Some plants have developed modified shutdown procedures, either to minimise the time taken to achieve activity clean-up criteria or to avoid particulate releases. The main modification is that all Reactor Coolant Pumps (RCPs) are stopped before adding hydrogen peroxide. This may leave more crud on the fuel rods, as opposed to it being released into the coolant and cleaned up, which is not a bad thing from a dose perspective because radioactive fuel assemblies are shielded, but the downside is additional crud carryover to the next cycle via reload fuel. The possibility then exists of relocating crudded fuel within the core and thereby causing core reactivity tilt, as well as CIPS. However, the proportion of fuel crud removed during shutdowns is invariably small because species such as NiO and bonaccordite are not readily soluble under shutdown chemistry conditions. Therefore, some plants choose to implement UFC, to remove crud from the reload fuel assemblies and, hence, minimise the risk of crud-related issues in the following cycle.

The likelihood of depositing thick crud on PWR fuel rods can be minimised at the plant design stage by selecting a SG tubing manufacturer whose processes have been shown to promote formation of a protective oxide layer during normal reactor operation, leading to lower corrosion rates and releases of nickel. Risks can be further reduced by designing cores in which SNB is minimised, especially in the early part of the fuel cycle when boron concentrations are highest. There is industry consensus that a primary coolant $\text{pH}_T \geq 6.9$ should be achieved at criticality for reactor start-ups, followed by $\text{pH}_T \geq 7.0$ for full power operation, and there is a theoretical possibility of increased benefits up to $\text{pH}_T = 7.4$.

If a core design is incompatible with a plant operating at its optimum pH_T due to constraints on maximum lithium concentration, then use of enriched boric acid (EBA) and potassium hydroxide (KOH) may be considered as alternatives to normal boric acid and LiOH, respectively.

EBA is already used in some western PWRs, and VVERs have considerable experience of using KOH. It may be the case that EBA is best considered at the plant design stage because of implications for tank volumes and the requirement for boron recovery, but a switch to KOH is likely to be an option for established plants, and a demonstration has been planned at Sequoyah PWR. It has been suggested that EBA and KOH might offer an additional benefit for CIPS mitigation, beyond that associated with pH_T , by reducing the accumulation of boron-containing species in fuel crud. However, any such benefit appears to remain speculative.

Other options are available to reduce the risk of forming thick fuel crud, and to mitigate its consequences. For new plants, there is an opportunity to influence the growth of protective oxide films during HFT. Industry consensus is that this should take the form of a passivation step under alkaline conditions, followed by a clean-up step under oxidising conditions, to remove corrosion products before they become activated. However, there are differing views regarding whether it is necessary to have dissolved hydrogen present for the passivation step, or just deaerated water. Operating experience from EPR and AP1000 plants may help resolve this question. It has been pointed out that some replacement SGs went on to perform well despite having received no such chemical conditioning. This presumably indicates simply that the improvements in tube manufacturing can outweigh those of chemical conditioning during HFT, in some cases.

There is a convincing case for zinc injection. Most but not all plants will experience dose rate reductions, with the magnitude of the reduction depending, among other things, on the relative contributions of Co-58, Co-60, and other radionuclides, to the shutdown radiation fields. If zinc injection is initiated while oxide films are forming, zinc becomes incorporated in the inner layer as it grows, making it more stable and protective. This has a dramatic effect on the corrosion rates of stainless steels and nickel-based alloys, resulting in significantly lower corrosion releases. Therefore, zinc injection should begin as early in a plant's lifetime as possible, and ideally during HFT for new plants. For established plants, there is industry consensus that zinc injection should be implemented for at least one cycle prior to Steam Generator Replacement (SGR).

Incorporation of zinc in oxide films initially results in elevated Co-58 and Co-60 concentrations in the reactor coolant, but they return to normal, or to even lower levels, within a few cycles. Concerns were raised that zinc injection may also lead to significantly elevated releases of nickel to begin with, adding to the nickel inventory available to deposit on fuel cladding, but analyses have found little indication of this. Instead, the longer-term beneficial effect of reduced corrosion rates appears to be dominant. Zinc is also incorporated in fuel crud, sometimes resulting in thinner and darker deposits, but extensive fuel examinations have observed no effect on the thickness of the ZrO_2 layer, and hence cladding corrosion. Concerns were also raised that zinc may precipitate as oxide or silicate species, especially in the pores of fuel crud, but a combination of loop tests, chemical modelling and operational experience shows that plants can operate safely with up to 5 ppb zinc. This is on the proviso that silica levels, and those of the make-up water impurities aluminium, calcium, and magnesium, are all within normal limits.

An ultrasonic cleaning technique has been developed that removes crud from reload fuel assemblies before they are put back in the reactor. The need for such equipment was identified after it was shown that CIPS behaviour at the outset of Callaway Cycle 10 was driven by residual fuel crud carried over on the once-burned fuel assemblies that were reloaded at the end of Cycle 9. Fuel crud formed for high-duty cores in plants with nickel-releasing SGs is resilient to shutdown chemistry conditions. However, tests show that UFC removes ~85% or more of deposit, which is then retained on installed filter elements. This mitigates the CIPS

risk both for the reload fuel and for feed fuel, because crud is known to redistribute from reload fuel to higher-power assemblies at the start of fuel cycles. UFC may be carried out in response to general concerns about elevated CIPS risk, but also by plants that have changed their shutdown chemistry conditions, and by plants that are replacing their SGs. In other words, when there is a perceived risk of an increased nickel inventory.

Modelling of the activity transport processes within the primary circuit has been developed over many years. A range of different models have been developed (some of which are no longer in use or supported) and the degree of sophistication has continued to increase with time. Current efforts are focused on "multi-physics" approaches which include various modules to address different aspects of circuit performance such as thermal hydraulics, heat balance, corrosion, erosion, coolant chemistry; each module produces information which becomes input data for another module, and the systems architecture for the software is currently a highly specialised field. The different modules may address effects at different scales, for example the macro scale aspects of fluid dynamics and the microscopic scale effects of steam chimneys on the fuel cladding surface. Currently the UK effort in this field (which is very limited) is supporting a multi-physics approach led by EPRI and including other major US organisations such as Westinghouse and various utilities. There is no uniquely UK-led multi-physics approach; competing consortia include Chinese and South Korean academia, who have published recently. The completeness of the multi-physics approaches is always a matter for discussion, different approaches have different strengths and weaknesses, perceived concerns at present include the role of colloids in activity transport and the radiation chemistry within the steam chimneys. Across the global effort, some specific effects appear to need further attention. Validation of the different modules is being pursued by comparison with results from test loops, particularly the WALT loop (Westinghouse, USA) and the DISNY loop (South Korea). The UK has a very limited number of reactor chemistry test loops, notably the Royce Institute loop at Manchester (which however lacks any input of radiation) and the DCF test loop (Cumbria) which operates with a very low fluid flow rate. Neither of these has yet been used in reactor coolant zinc chemistry simulation, because it is subsequently very difficult to clean up a loop once zinc-modified oxides have been formed within it. There are UK high temperature pressurised water loops which have been deployed for dedicated zinc injection corrosion exposures (University of Manchester and University of Bristol) but have not been developed for crud formation studies. There are loops outside the UK which have been used for tests on reactor coolant chemistry with zinc injection.

The implications of the possible use of other reactor designs where crud is a possibility have been described. None of these (BWR, VVER, CANDU or other PHWR, SCWR) give rise to particular concerns regarding fuel crud. It is well known that BWR fuel, particularly, normally exhibits substantial crud formation but this is within the normal operating regime of such reactors and within normal management control to maintain reactor safety. Other water-cooled reactor designs have not recorded fuel crud as a significant issue.

The impact of crud on reactor safety, particularly core reactivity control and fuel integrity, has been surveyed. The most common faults giving rise to fuel failures have been reviewed, the most common being fretting wear and manufacture faults. Historically some instances of fuel failure due to "corrosion" have been recorded, but these instances had a variety of different root causes and contributing factors. No instances of crud-related fuel failure leading to an accident have been identified, in particular with reference to the major historic LWR reactor accidents.

The management of spent fuel with adherent crud is not widely recognised as a specific issue. It is recognised and accepted that most fuel will have some crud attached to it, but provided

the fuel has not failed it is generally considered appropriate to store the fuel for short time scale (usually the station fuel pool) and medium timescale (some interim storage measure, often dry storage for PWR fuel) and ultimately for long term storage / disposal in a GDF. There may be a procedural aspect in that heavily crudded fuel may be more difficult to dry, as the crud may provide microscopic locations for water hide out, but the overall inventory of water needs to be evaluated.

The requirements of the ONR as regards the approval and licensing of a nuclear power reactor are set out in the relevant SAPs and TAGs (see Section 1). In particular TAG NS-TAST-GD-089 Issue 1.1 [4] sets out the requirement for a Chemistry Safety Case, which also presents the guidance that "Safety Cases should, by applying a systematic process, address all chemistry effects important to safety".

Therefore, it will be apparent that fuel crud is only one facet of the complex set of interactions which are (or could be) included in the term "all chemistry effects". Nonetheless, it is self-evident that limiting the corrosion of plant components in order to minimise crud deposition must be a desirable attribute, not least from the perspective of extending the service life of the various plant components.

The Chemistry Safety Case must also address procedural considerations such as "Defence in depth" and Operating Rules (reflecting Limits and Conditions), which provide a multi-layered structure to ensure that plant safety is not compromised for chemistry-related reasons.

A list of knowledge gaps (and knowledge retention matters) is presented below in Section 3. They fall essentially into three categories.

- Expertise in understanding and being able to assess the safety significance of crud as it affects both station performance and fuel integrity. This includes exposure to station data and OEF and the ability to evaluate such data.
- Development of information sources to better predict crud formation, and to quantify corrosion product source terms for ranges of operational variables; these would include materials, coolant chemistry, flow rate, temperature, heat exchange, radiation chemistry, etc. Such information sources are likely to consist of loop studies, additionally any in-reactor data should also be evaluated.
- Development of modelling approaches. The generally accepted consensus is that multi-physics models are the way forward, and the UK is making a small but important contribution to the EPRI-led consortium. The UK does not have a cohesive multi-physics crud modelling capability of its own.

These three categories all require some attention, there is particularly a knowledge gap where experts have a detailed overview of more than one of these categories. To make the point, whilst it would be helpful to have renewed modelling capability, it would be better if the modellers had appreciation of how the plant worked, and the limitations of loops in representing the plant. And similarly for the other categories and their crossover into each other; an all-round measure of capability by a number of subject matter experts would be a significant improvement on the present position.

There are a significant number of knowledge gaps and knowledge retention issues identified in this document. Full remediation of these matters would be both costly and time consuming. Yet time is probably of the essence, since UK expertise rests significantly with subject matter experts who are approaching retirement, or indeed have already retired but are "working on" in some part-time capacity. It is considered urgent that at least some knowledge capture approach should be adopted and implemented before this source of knowledge is lost completely. A first step would be to set up some cross-industry collaboration along the same

lines as been done for irradiated pressure vessel materials [9].

Further steps to address knowledge by way of loop studies or modelling studies are much more complex and are likely to involve international collaboration. The UK expertise is essentially locked into the EPRI programme for multi-physics modelling and the Westinghouse programme for experimental loop studies. Nevertheless, it would be helpful for the UK to develop at least an ongoing capability in the field, to remain current (if no more than as an “intelligent customer”) after the current subject matter experts have retired completely. Of necessity this must mean engaging with academia and providing training to a new generation of experts, as well as development of skills of (the relatively few) present early-career workers who are already embarked on the path towards subject matter expert capability in this area.

It would not be possible to outline costs for these suggested approaches, but the knowledge retention activities should be considerably less expensive and more immediate than any experimental programmes. Consideration should be given to constructing a high flow rate loop which can be irradiated and accommodate zinc chemistry. This combination is a key missing capability both in the UK and the EPRI group.

2.1. Suggested Focus Areas for Regulatory Enquiry

1	<p>Have the SG tubes been manufactured using materials and processes that have been shown to promote formation of a protective oxide layer with a low corrosion release during normal operation?</p> <p>The details of the manufacturing process are likely to be proprietary, but the requestor may be able to provide information on which to form a view.</p>
2	<p>Do the core design principles minimise, as far as is reasonably practicable, the occurrence of SNB, especially during the early part of the cycle when the boron concentration is at its highest?</p> <p>If this is not the case, the importance of other potential mitigations will increase.</p>
3	<p>Is a period of chemical conditioning planned during HFT, and does this include a passivation step under alkaline conditions and a clean-up step under oxidising conditions?</p> <p>There are differing views in the industry regarding whether it is also necessary to have dissolved hydrogen present during the passivation step, or if deaerated water will suffice.</p>
4	<p>Does the primary water chemistry pH_T regime adequately address the risk of fuel crud deposition by precipitation of soluble species?</p> <p>The minimum requirement (according to EPRI) is to achieve pH_T≥6.9 at criticality and then maintain pH_T≥7.0 during full-power operation, but there may be additional benefits up to pH_T=7.4. However, this approach does not take account of deposition from colloidal or particulate species, or SNB in the core.</p>
5	<p>Has proper consideration been given, where it is warranted, to using EBA and/or potassium hydroxide to assist with maintaining a sufficiently alkaline pH_T?</p> <p>Whether such an approach is needed from a fuel crud perspective will depend on the pH_T regime deemed to be optimal and the boron concentrations predicted for a representative fuel cycle.</p>
6	<p>Will zinc be injected into the primary coolant beginning with the period of chemical conditioning during HFT, and does the target concentration represent an appropriate balance between the benefits and risks?</p> <p>There is a compelling case to inject zinc during HFT onwards for new plants. For established plants, zinc should be injected as soon as possible and certainly for at least one cycle prior to SGR. EPRI considers that, in terms of fuel performance, plants can operate safely up to 5 ppb zinc. Using zinc to delay the initiation of PWSCC also favours early implementation.</p>

7	<p>Do the chemistry specifications include appropriate controls to prevent the precipitation of aluminium, calcium, and magnesium silicates in fuel crud?</p> <p>In combination, these species may precipitate as zeolites, especially if subject to a concentration factor in the pores of thick fuel crud. They are crud modifiers in that they densify fuel crud, impairing coolant access to the fuel cladding surface. This can result in accelerated corrosion.</p>
8	<p>What level of CIPS risk is predicted by models, and what assumptions are made regarding nickel release rates from the SGs?</p> <p>It is likely that reliance on computer modelling will continue for new plants and for established plants that have recently made a major modification, such as SGR, at least until passivation behaviour is confirmed. In which case, it will be necessary to understand what assumptions the models are making about nickel behaviour, both in terms of release from SG tubes and deposition in core.</p>
9	<p>Is operating experience available to corroborate or otherwise the assessed CIPS risk?</p> <p>Computer models will invariably have their limitations and so it is important to always perform a credibility check regarding their predictions. Furthermore, in straightforward cases, an assessment based on operating experience may suffice. If the core design and chemistry for a proposed fuel cycle is clearly bounded by previous cycles for which there were no indications of crud-related problems, and the trends in relevant chemistry and radiochemistry parameters are stable or improving and provide no cause for concern, then detailed CIPS modelling might reasonably be dispensed with.</p>
10	<p>Is a robust chemistry and radiochemistry monitoring programme established and are the observations being trended?</p> <p>Routine monitoring of coolant radionuclide concentrations and component dose rates may usefully be supplemented by plant gamma spectrometry surveys and monitoring of elemental corrosion product concentrations. The focus should be on long-term trending to detect changes in behaviour.</p>
11	<p>Has proper consideration been given to cleaning reload fuel assemblies using UFC if computer modelling, operating experience, or plant changes suggest a high CIPS risk?</p> <p>UFC removes ~85% or more of the deposit from reload fuel assemblies. It may be appropriate to employ UFC for reactors with already high levels of fuel crud, or if operational changes carry a risk of increased fuel crud.</p>

12	<p>Before consigning spent fuel to dry storage, has the possible water hideout and duration / number of vacuum / hot gas cycles been considered?</p> <p>The drying of heavily crudded spent fuel could require additional cycle steps or longer time at high temperature, both of which may contribute to zirconium hydride crystal reorientation, leading to delayed hydride cracking.</p>
----	--

3. Gaps in Understanding and Long-Term Knowledge Retention

This section identifies a number of knowledge gaps which have become apparent through the preparation of this review.

3.1. Knowledge Gaps in Reactor Chemistry

Considerable progress has been made over the past 30 years or so towards understanding fuel crud and its relationship to CIPS and CILC in PWR cores, including the role of primary water chemistry during HFT, power operation, and reactor shutdowns. Strategies to minimise fuel crud have been developed focussing on the corrosion release of nickel and iron from out-of-core surfaces, their transport in the reactor coolant as soluble species, and ultimately, their propensity to deposit on fuel rods. As a result, the impact of fuel crud on PWR operations appears much reduced compared to the 1990s and early-2000s. This is inferred from the relative sparsity of crud-related operational issues reported in the accessible literature and is a view supported by statements that there are few instances of CIPS affecting plants injecting zinc. Nonetheless, there remain knowledge gaps regarding the underlying mechanisms. These include understanding the role of particulate corrosion product transport and deposition in fuel crud formation. There is also uncertainty about the form in which boron accumulates in porous fuel crud, whether by physisorption or precipitation, and the precise nature of boron precipitates formed. Resolution of this issue is hindered by the fact that implicated lithium borate precipitates are unstable under shutdown chemistry conditions and so are not observed in crud samples obtained from irradiated fuel rods.

Chemistry strategies are only one part of the picture. These have coincided with evolutions in SG tube manufacturing leading to improved Alloy 690TT passivation behaviour, better understanding of core designs that reduce the risk of CIPS, and technology to remove deposits from reload fuel assemblies. While there has been considerable success in alleviating the problems of PWR fuel crud, the multitude of variables means that it is difficult to quantify the operational benefit attributable to any one factor. Some plants have justified operation with elevated pH_T up 7.4, well above the EPRI-recommended minimum values of 6.9 at criticality and 7.0 at full power. This is expected to be optimum for minimising ex-core corrosion release rates and deposition by precipitation of soluble nickel and iron in the core. However, such operation requires elevated lithium concentrations, especially for PWRs using normal rather than enriched boric acid for reactivity control, and concerns have been expressed about the potential implications of high lithium concentrations for fuel cladding corrosion, as well as the possibility of PWSCC of nickel-based alloys, and SCC of stainless steel. Some benefits have been observed and attributed to operating in this way, but it has also been pointed out that not all the candidate plants experience these benefits, and an assessment of radiation field data did not support any strong conclusions regarding the impact of high pH_T . Hence, there would be value in obtaining a better understanding of the benefits of elevated pH_T operation, as this might affect whether the associated risk of potential downsides is considered worthwhile.

Potassium hydroxide has long been identified as a potential alternative to lithium hydroxide for maintaining an alkaline pH_T in PWR primary coolant. It is already used for this purpose in VVERs. One of the advantages of KOH is that potassium is relatively benign for fuel cladding corrosion

at the required concentrations. It has been suggested that KOH could offer additional benefits for CIPS mitigation beyond facilitating operation at elevated pH_T , and this is due to the higher solubility of potassium borate salts compared to the corresponding lithium species. However, recent calculations by NNL suggest that this may not be the case after all, because enough lithium would form quickly by neutron irradiation of boron-10 for lithium borate still to precipitate in fuel crud. Given renewed interest in the use of KOH, mainly due to concerns about the long-term cost and availability of LiOH, there may be benefit in obtaining a more complete understanding of the behaviour of boron species in fuel crud for a mixed-alkali system. Moreover, boron-free chemistries have been proposed for some advanced PWRs and this will impact on crud behaviour, but there is little relevant information available in the open literature.

Maintaining optimum water chemistry conditions for HFT during commissioning of new reactors is expected to be beneficial towards establishing protective oxides on ex-core components. In turn, this contributes to minimising corrosion product releases, and there are plant data to support this view. It is agreed that the optimum chemistry should be comprised of a passivation step under alkaline conditions followed by a clean-up step under oxidising conditions, but there are differing views about whether dissolved hydrogen is also required, in addition to deaerated water, for the first step. The decision is usually taken to add dissolved hydrogen because it was employed successfully in commissioning Sizewell B and other PWRs. However, EDF decided against this approach for Flamanville 3 (FA3), despite dissolved hydrogen having been used for the other EPRs; Taishan 1 (TSN1) and Olkiluoto 3 (OL3). The benefits of using dissolved hydrogen were considered unclear for the specific case of Alloy 690TT tubing in combination with correctly deaerated water, and insufficient compared to the risks of forming explosive gas mixtures and nitrogen asphyxiation. It may be possible to address this knowledge gap regarding optimum HFT chemistry conditions by comparing operational data for the three EPR units. Chemistry data collected during HFT suggest that zinc addition at OL3 and FA3 had a much larger effect on stabilising the inner oxide and reducing the corrosion release than adding hydrogen at TSN1 and OL3, but it will be necessary to see if this is also borne out by experience during the first few cycles.

In around 2010, EDF devised a similar two-step conditioning process for replacement SGs. It was not possible to identify a significant positive impact when the process was tested at Bugey 3, but further R&D followed using the Boreal loop and this validated the beneficial effect of carrying out an initial conditioning process for replacement SGs. However, it is not known how the project progressed from there.

It is believed that the rate at which ex-core components release corrosion products including nickel and iron into the primary coolant depends, in part, on how close the respective coolant concentrations of those species are to saturation. In the event of localised boiling conditions in the core, which promote deposition on the fuel rods, the core will act as a sink for corrosion products, reducing their coolant concentrations, and promoting increased rates of ex-core release. The difference in concentration may be small but nonetheless significant due to the very high coolant mass flow rates. The implication is that fully passivated SG tubes would not be able to support the nickel release rates required to form the thick, porous fuel crud deposits associated with CIPS. While this appears to be the status of many PWRs, there remains the question of what would happen if the extent of SNB were to be increased above current levels.

3.2. Knowledge Gaps Associated with Modelling of Crud Formation

The modelling of crud deposition has progressed significantly over the past ten years or so. The availability of high power computing has been a contributory factor, along with the recognition that there are several physical processes in play, including thermal hydraulics, heat transfer, fluid dynamics, solution chemistry, corrosion and erosion. These multiple physical effects have been captured in a number of multi-physics models, which have become very complex and sophisticated. There is still room for improvement, however, since the multi-physics codes consider the “big picture”, the whole of the primary circuit, nodalised into many segments, but some appear not to properly capture the microscopic scale effects occurring within steam chimneys. Alternatively, there are some models at the atomistic level – as addressed by the LANL and CASL approaches – where the microscopic scale is simulated but the connection back to the “big picture” is more challenging (“big picture” multi-physics approaches appear to have poor representation of the extreme conditions at the base of a steam chimney such as supercritical temperatures and alpha radiolysis, but these have fundamental effects on the chemical makeup and morphology of the crud). No doubt this will be attended to as the models become increasingly more complex and the nodalisation goes down to ever finer scale resolution. At the present moment the models are constantly in development and there is a significant push towards this particularly in East Asia. In the past year alone, some 40 papers have been published on “Fuel crud in PWR Primary Coolant, deposition or erosion” and of these the vast majority of modelling papers come from China or South Korea.

It is reasonable to see how corrosion is modelled as a “general corrosion” phenomenon, a certain thickness of material lost from surfaces in a certain time, in accordance with general corrosion rates. Likewise, generalised deposition assuming that material deposits on all surfaces with appropriate thermal hydraulic conditions. However, it is much more difficult to model localised corrosion or localised deposition, and that represents the current frontier in the modelling world.

There are a number of specific mechanistic details which appear not to be recognised in the current set of chemistry models. These are now identified:

1. The absence of colloidal species from crud deposition models (in the main, the exception being DISER, for VVERs). This author can state, with the experience of managing an in-pile PWR corrosion test loop [10], that a cycle-end crud burst contains a lot of both particulate and colloidal material. To ignore this source of material transport and which could potentially supply the formation of crud seems inappropriate, unless there is good evidence that the colloids destabilise as soon as reducing conditions are reimposed.
2. An additional difficulty (identified in Section 8.4.3) is the radiation chemistry phenomenon of “track and spur” transmission of ionising radiation through a medium such as water, where transmission of particles such as neutrons and gamma rays proceed via a “track” and cause discrete Compton interactions leading to “spurs” (very small local regions where the products of radiolysis interact with each other and with water molecules, solutes). At the atomistic level – as addressed by the LANL and CASL approaches – (and at scales representing porous surfaces below around 10 nm, such as a ZrO₂ surface on fuel cladding) there is physically not the space for a spur to form, therefore the active radicals etc will react with surfaces and not with each other, therefore the familiar “G values” for radiolysis product yields will suffer interference at the precursor stage (in a time resolved sense) and will not be suitable for plugging into a model. A new approach to radiation chemistry, as a fundamental point, is required for modelling at the atomistic scale in proximity to surfaces. This also ignores the (well known) effects of heterogenous energy transfer, where radiation energy absorbed in

the solid phase is transmitted through mobile solid crystal lattice energy centres (“excitons”) to surface sites where adsorbed water molecules are split, apparently enhancing radiolysis and giving rise to observed “G values” in excess of theoretical maximum for pure water. This can be ignored within bulk coolant but will be significant within a steam chimney. No published computer model presently addresses heterogenous energy transfer.

3. There are various other deficiencies associated with available reference data for mechanistic benchmarking, notably temperature extrapolation and detailed kinetic data for complex reaction schemes. These are being addressed, to some measure by ongoing loop studies, however the present position is that not all the necessary information is in place.

3.3. Knowledge Gaps Associated with Non-PWR Types of Reactor Design

The current generation water reactor global fleets are supported by utility or national programmes to address technical issues, including fuel deposits where appropriate. From the UK perspective, accessing the outputs and learning from these programmes (which are not necessarily in the public domain) can be a key constraint, particularly where the domestic capability in the reactor chemistry discipline is limited.

Most of the prospective Generation IV designs, particularly supercritical water reactors, have no operational plant life experience although there have been some test loops. However, the principle of operation, that the heat from the fuel will take water from a sub-critical temperature to a supercritical temperature as the water flows along the length of a fuel pin, should mean that at some point – as the water changes from a liquid to steam and then a supercritical fluid – there will likely be a change in the solubility of corrosion products in the fluid, compared with water. There is very little data on this, which would be an essential part of an appreciation of the likelihood of corrosion product deposition on the fuel pin, possibly at some localised zone along the fuel pin as the fluid undergoes transition. The little data from the test loops suggests there is less deposition in the supercritical fluid zone than in the water zone or steam zone, but it is not clear if this represents an increase in water zone deposition compared with, for example, a VVER of similar boiling duty.

The cladding of supercritical water reactor fuel is a matter of concern. In the discussion concerning the Canadian design of SCWR (see Section 13) it has been noted that the proposed Canadian SCWR would use a zirconium alloy cladding whereas the IAEA advise that zirconium alloys would not be suitable. Beloyarsk test loops use stainless steel fuel cladding. However, there is a concern that austenitic stainless steels irradiated above the critical temperature for water ($T_{crit} = 374 \text{ }^{\circ}\text{C}$) will encounter radiation induced sensitisation – as is commonly encountered in AGR fuel in the UK – and therefore will require special measures to prevent widespread corrosion and failure of spent fuel if stored in a pond environment.

3.4. Knowledge Retention

In regard to reactor chemistry for PWR systems, the UK has a problem in that true subject matter experts are few, and most of those are approaching (or already past) retirement age. For the moment that capability remains, but it is not a tenable situation for more than a few years hence.

It has already been stated that in the field of reactor chemistry modelling, the UK expertise is already very stretched and is heavily reliant on a single subject matter expert who is already

retired, and now with limited availability. Additionally, there is a team of a few individuals in supporting roles, including some emerging subject matter experts but whose depth of experience is still developing.

It is therefore apparent that some form of knowledge retention scheme is needed, in association with some training or upskilling programme for current early career workers. These are now discussed.

A good working example of a knowledge retention scheme is that devised for the topic of degradation of metals such as pressure vessel steels, under prolonged irradiation. This is fully described in [9] where some 20 years ago the International Group on Radiation Degradation of Materials (IGRDM) launched a project to capture the information needed to preserve knowledge on that topic. The so-called "Ageing Community project" developed into a successful approach which has positive outcomes which endure today, although nearly all the experts involved 20 years ago are now completely retired.

In terms of upskilling early career workers, the NNL has some internal training provision for that process. However, a recurring problem is that in today's job market, staff are frequently leaving and being replaced, usually replaced at the most junior level, this continuing "churn" in the early-career staff means that the benefits of training and a few years' experience are often lost to the industry. It is for this reason that only a handful of young scientists are continuing on the path to becoming subject matter experts. Furthermore, the subject matter experts available to impart training are at (or have passed) retirement age and their expertise is no longer a given. Moreover, the incoming junior staff have frequently little or no experience of reactor operations (there are no academic institutions with training reactors left in the UK) and the upskilling has to start from "the back of the grid". Some new initiative in at least PhD level studies in reactor chemistry would be of assistance. NNL supports an internally funded core science "theme" in reactor chemistry and corrosion, however this initiative has very limited resources but nevertheless has made some inroads in this general area in the topics discussed above.

Currently PhD studies in nuclear technology are funded by bursary from either the NDA decommissioning portfolio, or from the EPSRC via the CINDe programme. Additionally, there is a Centre for Doctoral Training (CDT) in nuclear technology (the SATURN CDT) involving six universities, although the range of interests includes (for example) radioactive waste management, groundwater analysis, and radioactive materials storage. At present there is only one PhD project in progress relevant to the crud chemistry or general reactor chemistry of commercial PWRs, which concerns the relative corrosion performance of SG tube materials (Inconel Alloy 690 with different surface treatments). Previous CDTs – now completed - included TRANSCEND (focused on decommissioning), PACIFIC (focused on fuels). The current CDT in green industrial futures is a more broadly based approach where nuclear technology is not the primary focus. Other PWR technology projects may exist as one-off instances and are not easily identified. It is clear that this low rate of skills development will not be sufficient to address the known needs for reactor technology skills retention in the UK.

4. Recommendations

It is intended that this review of fuel crud issues should be of value to ONR as a means of both updating the regulatory perspective on existing power reactors and in assessing new reactor designs if or when approval is requested. There is a wealth of technical detail in this document which will prove of much assistance in such matters.

This document also identifies a number of knowledge gaps or knowledge retention concerns associated with reactor chemistry and fuel crud. It is recommended that ONR gives consideration to these matters, some of which are deemed urgent. In particular, the loss of critical knowledge based on the age demography of Subject Matter Experts is a key concern and a firm recommendation is that this should be addressed, ideally by a cross-industry arrangement similar to past critical knowledge retention issues with pressure vessel steels.

PART B

TECHNICAL REVIEW AND DISCUSSION

5. Historical Occurrences of PWR Fuel Crud

It is instructive to review some notable historical occurrences of PWR fuel deposits as a prelude to the main technical sections of this report. This establishes the main nuclear safety implications of fuel crud and hints at its properties and some of the factors associated with its formation.

The term “crud” is introduced as an alternative term for fuel deposits, although the original meaning of the term “crud” is debatable and is often presented as an abbreviation. Some maintain that it originated as “Chalk River unidentified deposit” in reference to early tests at Chalk River laboratories (Canada) where a related phenomenon was first observed; others insist it means “corrosion related unidentified deposit” since the deposits originate as corrosion product derived from other parts of the reactor coolant circuit. An alternative view is that it is simply the technical adoption of the vernacular English language term “crud” pertaining broadly to any undesired deposit.

5.1. Obrigheim

The 2-loop Kraftwerk Union (KWU) plant, Obrigheim (KWO), provided one of the first examples of thick PWR fuel crud [11]. This was a 2-loop plant that became operational in 1969. By today’s standards, its rating of 345 MWe/1050 MWth was modest. Substantial deposits were observed on the fuel rods after each of the first two operating cycles. The deposits had a maximum area density of 8 mg cm^{-2} , corresponding to a maximum thickness of $\sim 67 \text{ }\mu\text{m}$ if a crud density of 1.2 g cm^{-3} is assumed [12]. The fuel crud increased in thickness, porosity and NiO content between the bottom and top of the core. A shift in the reactivity maximum to the lower portion of the core was observed during the first cycle and was postulated to be due to hide-out of neutron-absorbing boron in the thicker fuel crud formed in the upper portion of the core.

The thick fuel crud was attributed to identified shortfalls in the primary water chemistry, including insufficient hydrogen overpressure to suppress the formation of oxidising species (resulting in dissolved oxygen concentrations of up to 300 ppb) and the absence of lithium hydroxide additions for pH control. It may also be noteworthy that the SGs were not subject to any hot preconditioning.

5.2. Callaway

While primary-water chemistry was much improved for subsequent PWRs, thick fuel crud leading to boron hideout was encountered again, many years later, for reactors operating with high-duty cores [13]. These core designs were a response to market demands for improved fuel economics, including longer cycles and power uprates, and the resulting operational changes led to increased rates of subcooled nucleate boiling (SNB) in the upper spans of fuel assemblies, and higher boron concentrations at the start of fuel cycles [14]. Subsequently, it became evident that the chemistry conditions that supported good fuel performance under the previous operating strategy were not adequate for the demands of core power up-rates and longer operating cycles [15].

The first example in the US was in 1989 for Callaway [16]; a 4-loop Westinghouse-designed plant rated at 3565 MWth. Upper-core flux depressions were detected during Cycles 4-11 following a 4.7% thermal power uprate in mid-Cycle 3. Such events were known initially as AOA before Westinghouse adopted the term CIPS to reflect improved understanding of the key role played by fuel crud in the phenomenon.

An axial offset (AO) is the difference in power between the top and bottom halves of a core ($P_t - P_b$) relative to the total core power ($P_t + P_b$), and is normally expressed as a percentage according to the following expression:

$$AO = \frac{(P_t - P_b)}{(P_t + P_b)} \times 100$$

It is normal for an AO to occur, and this is predicted by core models. However, boron hideout in fuel crud may cause the measured AO to deviate from, and become more negative than, the predicted AO. CIPS is the absolute difference (in percentage points) between the measured and predicted AOs. Given uncertainties, a deviation greater than 3% is usually regarded as being significant and is described as "core-wide" CIPS [17]. Figure 1 shows an example of core-wide CIPS for a Westinghouse plant.

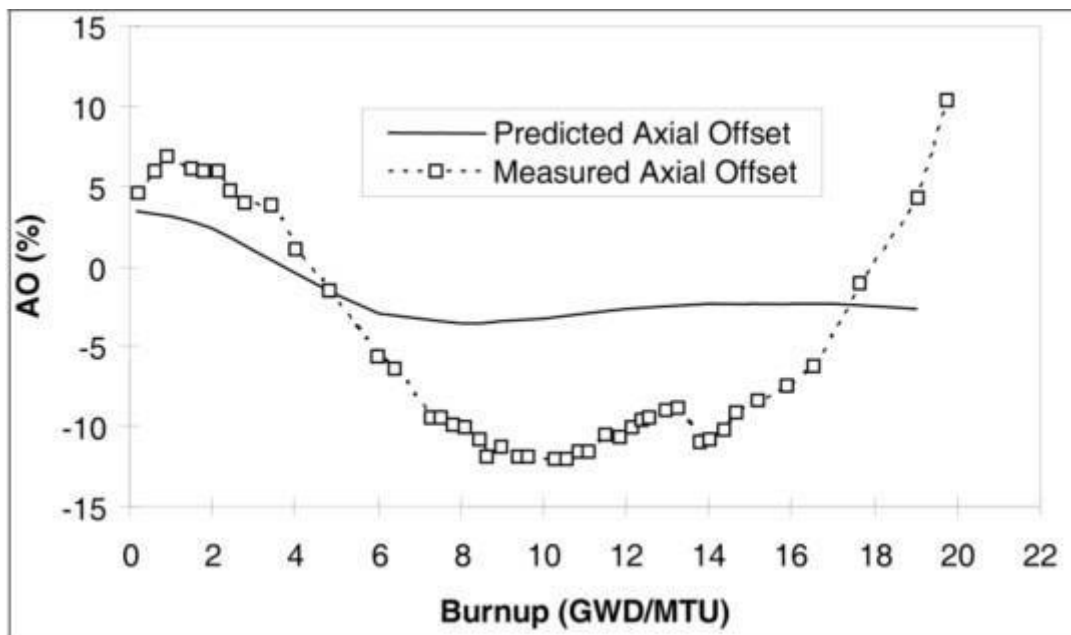


Figure 1: An Example of CIPS for a Westinghouse PWR (From [17])

The most severe CIPS to affect Callaway (-14%) was during Cycle 9. To maintain a safe shutdown margin, reactor de-rating to as low as 70% power was necessary during the final eight months of the cycle [18]. Flakes of fuel crud collected at the end of the cycle were up to 125 μm in thickness and displayed a novel structure comprising of three layers: a dense layer of the mineral bonaccordite (Ni_2FeBO_5) on the cladding side, a middle layer rich in ZrO_2 particles, and a highly porous layer of NiO needles at the coolant interface. Since then, CIPS has been reported for many cycles of PWR operation, including in France [19] and Korea [20], as well as for other US stations [21].

Early investigations [17] [18] determined three principal factors contributing to the occurrence of CIPS: coolant-borne corrosion products, SNB duty, and soluble boron in the coolant (see Figure 2).

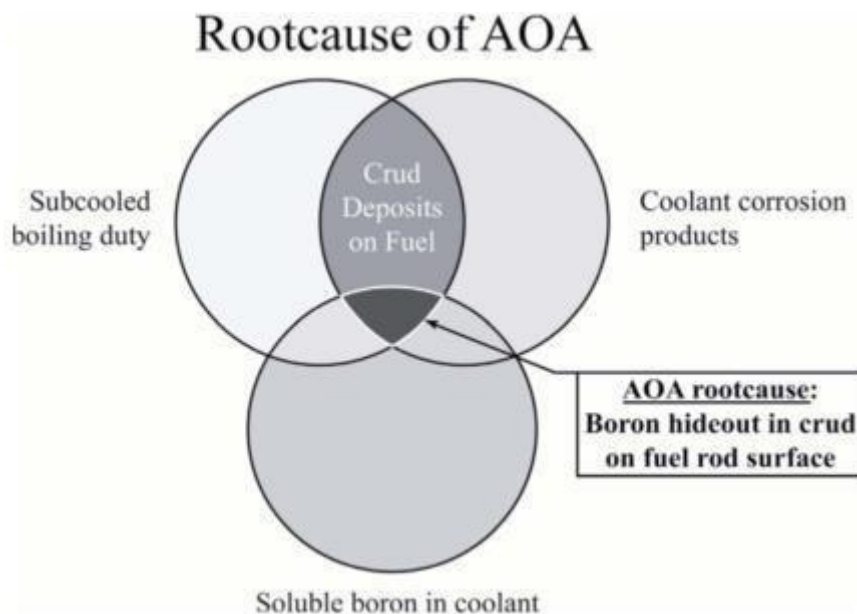


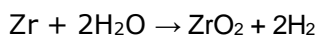
Figure 2: Factors Contributing to AOA or CIPS (From [17])

For high-duty cores, localised SNB promotes corrosion product deposition onto the upper half of fuel assemblies, forming porous crud that is rich in nickel (compared to non-AOA crud), and into which boron becomes entrained and concentrated. However, it is important to note that these conditions, while being necessary for CIPS, do not always result in CIPS. In other words, there must be additional factors at play. Notable examples [17] include VC Summer (a Westinghouse 3-loop plant), which did not exhibit thick crud (or CIPS) for Cycle 12 despite having very high SNB, and Vandellos 2, which is also a Westinghouse 3-loop plant, but has never experienced CIPS despite a high core duty (although it has produced thick fuel crud). These observations are in marked contrast with the experience of Westinghouse 4-loop plants, which accounted for six out of the first seven US PWRs to experience CIPS [22], and the instances of “localised” CIPS (i.e., CIPS for an individual fuel assembly rather than at the whole-core level) for 3-loop Framatome/AREVA (EDF) PWRs.

A comparison of US high-temperature PWRs with three European PWRs designed by Siemens/KWU noted that no fuel crud or CIPS had been observed over the lifetime of the latter, despite the European plants being of higher thermal duty than the CIPS-susceptible US plants [23]. The different behaviour was attributed to the Alloy 800 SG tubes used for the European plants, which have a lower nickel-content and corrosion rate than the Alloy 600 tubes used for the US plants included in the work. In the context of the present discussion, it is noted that Obrigheim and Callaway both had Alloy 600MA SG tubes when they experienced CIPS, as did VC Summer (no CIPS), although they were subsequently replaced with improved materials, whereas Vandellos 2 has its original Alloy 600TT tubes to this day [24].

5.3. Three Mile Island Unit 1

PWR fuel cladding is manufactured from different types of zirconium-based alloy and operating temperatures are high enough that thermally driven oxidation occurs in primary water during normal operation according to the reaction:



The ZrO_2 layer has low thermal conductivity, which results in higher temperatures at the cladding-oxide interface and, hence, a corrosion rate (and oxide thickness) that increases non-linearly with burnup. Zircaloy-4 was used for fuel cladding until the late-1980s, when vendors introduced variants, such as ZIRLO and M5, with improved corrosion performance. This facilitated operation to higher burnups and fuel cycles beyond the usual 12 months.

Not surprisingly, the presence of fuel crud may also promote increased cladding corrosion by raising the surface temperature. This is known as CILC. IAEA periodically reviews fuel failures worldwide and Table 3 of [25] provides statistics for the period 1987-2015. Corrosion failures of fuel are not typical for PWRs, and this is especially so for cases where fuel crud is implicated. It appears that only three PWR cycles have been affected by CILC-related fuel failures in the last 30 years [26]: Three Mile Island Unit 1 (TMI-1) Cycle 10 (~1995), Seabrook Cycle 5 (~1997) and Palo Verde-2 Cycle 9 (~2000). TMI-1 was a Babcock and Wilcox 2-loop plant (now decommissioning), Seabrook is a Westinghouse-designed 4-loop plant, and Palo Verde Unit-2 is a Combustion Engineering 2-loop plant. The fuel failures for one of these plants (unnamed) were for ZIRLO cladding, demonstrating that advanced cladding materials are not immune to CILC under adverse conditions [15].

EPRI performed a detailed evaluation regarding the root cause of the TMI-1 fuel failures [27], in which some of the fresh fuel loaded for Cycle 10 experienced localised cladding corrosion damage in the upper span, characterised by a distinct corrosion pattern. The abnormal conditions appeared predominantly at the interface between neighbouring fresh fuel assemblies and corner locations in fresh fuel assemblies. Instances of damage were isolated to surfaces facing outward and toward the fuel assembly gap. In total, 9 fresh fuel rods failed, 101 had eddy-current indications suggestive of cladding thinning, and 253 exhibited a localised corrosion pattern as determined by poolside non-destructive techniques. For context, the core would have contained ca. 39,825 fuel rods (177 fuel assemblies of 15x15 array), neglecting that some array positions would have been taken up by control rods and instrument tubes.

Hot cell examination of four rods, one of which had failed, observed that local regions of the exterior surfaces were subjected to temperatures well above normal operating temperatures and concluded that the only mechanism that could reasonably account for this was retention of vapour within a thick crud layer. Other supporting information included an unusually high Ni to Fe ratio in the fuel crud (with the presence of NiO indicated), and the fact that TMI-1 Cycle 10 was a CIPS cycle attributable to boron hideout in thick, porous fuel crud deposits.

It is unlikely to be coincidence that Seabrook and Palo Verde-2 also exhibited CIPS behaviour during the cycles affected by CILC-related fuel failures [28] [14]. All three units (TMI-1, Seabrook, and Palo Verde-2) were among the US plants operating with high-duty cores [18] and had SGs tubed with Alloy 600 at the time [24], although TMI-1 and Palo Verde-2 both subsequently replaced theirs.

6. Mechanism of Fuel Crud Formation in PWR Systems

Corrosion release from out-of-core surfaces provides the material source term for PWR fuel crud. The corrosion products are transported in the primary coolant to the core, where they form deposits and become activated. Some of the activated corrosion products are then returned to ex-core surfaces, where they generate radiation fields that give rise to occupational exposure during refuelling outages and other maintenance activities. Figure 3 is a schematic illustration of corrosion product transport for a PWR primary circuit.

It is a moot point whether corrosion products are transported mainly as soluble, particulate, or colloidal species and there may be differences between plants, but there are strong arguments for the role of soluble species in forming fuel crud [29]. These include the layered structure observed for Callaway crud, for which it is considered unlikely that the Ni_2FeBO_5 layer could be formed between the cladding and the ZrO_2 layer by particulate deposition, and the fact that predictions of crud thickness have achieved good agreement with observations for models based primarily on deposition of soluble material. Accordingly, chemistry efforts to minimise fuel crud formation have tended to focus on establishing primary water pH_T regimes that minimise dissolution in the SGs and discourage precipitation of iron and nickel – the principal constituents of fuel crud – as they pass through the core (see, for example, Section 2 of [30], which summarises how EPRI industry guidance developed during the 1980s and 1990s).

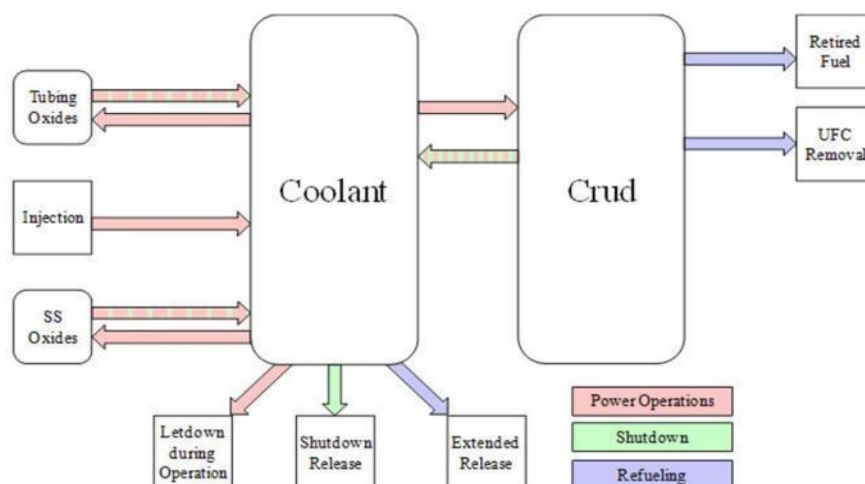


Figure 3: Flow of Corrosion Products through a PWR Primary Circuit (From [31])

6.1. Corrosion Product Source Term

Alloy surfaces in contact with the primary water of a PWR undergo a general, low-level form of corrosion that has no consequence for their structural integrity (i.e., in contrast to SCC), but which releases corrosion products into the coolant for transport around the circuit. These include the materials used for the SG tubes – either Alloy 600, 690 or 800, depending on the plant – and the stainless steels used for the loop pipework and to protectively clad the internal surfaces of some components in the RCS.

Except for PWRs designed by Siemens/KWU, the SGs in most first-generation PWRs in service in the 1960s and 1970s had mill-annealed Alloy 600 (Alloy 600MA) tubing. However, OPEX showed that the Alloy 600MA tubes were susceptible to significant degradation, including pitting, thinning, and stress-corrosion cracking, that could initiate from the primary and secondary sides. The resulting tube leaks and ruptures caused reliability issues and output reductions, which

resulted in additional inspections and, ultimately, a need to replace many of the original SGs.

The next generation of SGs used Alloy 600TT; Alloy 600 that had been subjected to a thermal treatment to relieve fabrication stresses and improve the microstructure of the tubes. This was partially successful in that degradation was delayed until after a much longer period of operation [28]. Some of the early replacement SGs in the 1980s used Alloy 600TT, as did some plants constructed around that time. Nuclear-grade Alloy 800 (Alloy 800NG), which is used mostly for Siemens/KWU-designed PWRs, is also expected to have corrosion resistance at least as good as Alloy 600TT [28], although the improvement over Alloy 600MA is due to compositional differences rather than heat-treatment.

Alloy 690 was developed to have improved corrosion resistance attributable to a higher chromium content than Alloy 600 (and Alloy 800). Laboratory results confirmed this to be the case [28] and thermally treated Alloy 690 (Alloy 690TT) has usually been the preferred choice (with a few exceptions) for replacement SGs and new-build PWRs from the late 1980s onwards. A useful summary of SGR for US PWRs up to 2004, including details of the tube material and manufacturer (i.e., Sandvik/Sweden, Sumitomo/Japan, or Valinox/France) is available in [32], which also notes that no corrosion or cracking of the Alloy 690TT tubes had been detected, although this was also partly attributable to design improvements for the replacement SGs. Useful information on SGR (and zinc injection) for the French fleet up to 2018 is found in [33] [34].

6.1.1. Corrosion and Corrosion Product Release

The nominal nickel, iron, and chromium content of PWR materials contributing to the general corrosion release is given in Table 1. In relative terms, the stainless steels (Types 304, 316 and 347) are iron-rich, whereas Alloys 600 and 690 are nickel-rich. Alloy 800 has intermediate values of nickel and iron content. This explains why PWRs with Alloy 600 or Alloy 690 SGs tend to have excess nickel in their fuel deposits and are described as nickel-rich plants, whereas PWRs with Alloy 800 SGs are iron-rich plants. In terms of chromium content, the stainless steels and Alloy 800 fall between the Alloys 600 (lower chromium) and 690 (higher chromium).

Table 1 Ni, Fe and Cr Indicative Content of Selected PWR Materials

Material	Nominal/%		
	Nickel	Iron	Chromium
Alloy 600	76	8	15
Alloy 690	60	9.5	30
Alloy 800	33	38	21
Stainless Steel Type 304	10	69	19
Stainless Steel Type 316	12	~66	17
Stainless Steel Type 347	11	~66	18

Notes: This Table is reproduced from [30].

Corrosion release from the internal (primary coolant facing) surface of SG tubes is the main source of nickel in fuel crud, whereas the stainless-steel loop pipework provides most of the iron [35]. These corrosion products (and others) become radioactive if they are held-up in the core. Nickel undergoes neutron activation to form Co-58 by the $^{58}\text{Ni}(n,p)^{58}\text{Co}$ reaction, and this is important for radiation fields because Co-58 is a gamma emitter ($T_{1/2} \sim 71$ days).

Co-60 – another gamma emitter ($T_{1/2} \sim 5.3$ years) – is also important for radiation fields but is produced by the $^{59}\text{Co}(n,\gamma)^{60}\text{Co}$ reaction, where the parent Co-59 does not contribute significantly to the formation of fuel crud. Moreover, the normal corrosion release is unlikely to be the main source of Co-60 for many plants, especially if low-cobalt alloys were specified. Instead, the dominant source term is typically from wear of Stellite-6 hard-facings present in the RCS [36]. For nickel-rich plants, Co-58 is responsible for most of the out-of-core surface activity during the first few operational cycles, including with replacement SGs, but Co-60 grows in and becomes progressively more important due to its longer half-life, and eventually dominates radiation fields as plants age.

General corrosion of SG tubes has been much studied and essentially leads to the formation of a duplex oxide [29], although the layers are sometimes considered to be subdivided [37]). There is an inner layer of iron-chromium-nickel normal spinels (chromites) based on FeCr_2O_4 at the alloy surface and an outer layer of iron-nickel inverse spinels (ferrites), including NiFe_2O_4 , at the interface with the primary coolant [38] [39]; see Figure 4. The inner layer, which is generally enriched in chromium, controls the outward diffusion of cations from the underlying base alloy and, hence, the material corrosion rate. In other words, it is a passivation film. The outer layer dissolves in the primary water and re-precipitates large crystals on the surface. It is not protective from a corrosion point of view, but it has a large surface area for adsorbing activated corrosion products from the coolant.

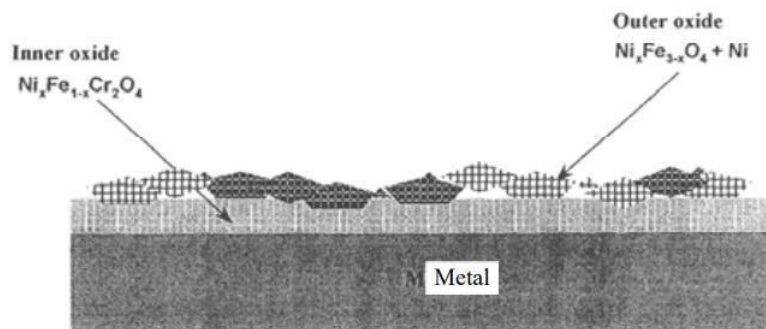


Figure 4 Oxides Formed on Stainless Steel and Alloy 600/690 Surfaces (From [39])

Table 2 presents approximate corrosion rates and corrosion release rates (after 3.5 months exposure) for the main structural PWR primary-circuit materials, both with and without zinc injection (zinc is injected into the primary water of many PWRs for dose rate control and this is discussed in Section 7.3). They are taken from [40], which, in turn, states that the values are based on information in [41]. The corrosion rate for Alloy 690TT is a factor of 2.0 less than that for Alloy 600MA in the absence of zinc injection, and a factor of 7.5 less with zinc injection. Likewise, the corrosion release rate for Alloy 690TT is a factor of 1.3 less than that for Alloy 600MA in the absence of zinc injection, and a factor of 3.0 less with zinc injection. More generally, it is evident that the corrosion release rate corresponds to ~30-50% of the corrosion rate and that zinc injection reduces the corrosion rate and corrosion release rate for all the materials shown. Other work [38] [42] concluded that the corrosion release rate of Alloy 690TT should be ~2.7 times less than for Alloy 600 MA based on the results of laboratory tests.

Table 2 Approximate Corrosion and Corrosion Release Rates

Material	Corrosion Rate		Corrosion Release Rate	
	With Zn	Without Zn	With Zn	Without Zn
Stainless Steel Type 304	1.1	3.5	0.1	1.3
Stainless Steel Type 316	1.3	3.5	0.1	1.4
Alloy 600MA	1.5	2.6	0.3	0.8
Alloy 600TT	0.5	2.1	0.2	0.9
Alloy 690TT	0.2	1.3	0.1	0.6

Notes: Rates are approximate and in units of $\text{mg dm}^{-2} \text{ month}^{-1}$. This Table is reproduced from [40].

Table 2 does not include any data for Alloy 800, but [38] states that, for identical surface finish, the extent of corrosion/corrosion release reduces in the following order:

$$\text{Alloy 600} > \text{Stainless Steel} > \text{Alloy 690} > \text{Alloy 800}$$

This is consistent with the observation that KWU/Siemens-designed plants with Alloy 800 tubing have never experienced anything more than negligible fuel crud deposits despite some very high core duties; a fact that is attributed mainly to the low corrosion product input into the primary coolant from the SGs [43].

It is important to recognise the distinction between corrosion rate and corrosion release rate [17]. Corrosion is a process in which the exposed surface forms an oxide. For systems that form a passivating or protective corrosion film, the corrosion rate slows down as the oxidation process continues and may reduce to a very low rate or become near-constant depending on the system and environment. In the current context, this would mean that the corrosion rate of SG tubes would be highest in Cycle 1 and then become progressively lower. Corrosion product release accompanies the corrosion process and occurs by diffusion and dissolution of metals through the protective oxide, after which they enter the primary coolant in either ionic or particulate form. As well as being dependant on the appropriate diffusion coefficient and the oxide thickness, the rate at which a metal enters the coolant will also depend on how close to saturation its coolant concentration is. The implication is that operating with a high-duty core, which promotes deposition on fuel rods and so reduces the coolant nickel concentration at the core outlet/SG inlet, may lead to increased rates of nickel release from the SG tubes unless the tube surfaces have become fully passivated and are no longer able to support such releases [44]. Fuel crud will form from corrosion product concentrations of just tens of ppb due to the very high mass flow rates.

6.1.2. Tubing Manufacture

The corrosion rates and corrosion release rates measured in laboratory for the different PWR SG alloys provide a useful indication of the expected behaviour in reactor, but they are by no means the whole story. Surface activities inside the primary system (hot legs, crossover legs and SG tubes) were studied, along with Co-58 peak activities released into the coolant during refuelling outages, for five plants with either Alloy 600TT, Alloy 690TT or Alloy 800 replacement SGs [45]. It was found that the levels of Co-58 activity reached after several cycles did not depend significantly on the alloy composition; for example, Alloy 600TT led, on occasion, to similar Co-58 coolant activities as observed for Alloy 690TT, while the surface activity inside Alloy 690TT tubes could be comparable to that inside Alloy 800 tubes. Moreover, significant differences (up to a factor of ~ 100) were observed between stations with nominally the same Alloy 690TT tubing composition. This behaviour was attributed to differences in surface finish associated with manufacturing.

EPRI analysed 22 US PWRs with Alloy 690TT replacement SGs by using the total (cumulative) shutdown releases of nickel and Co-58 as indicators of the corrosion release behaviour [31]. The objective was to identify parameters that could then be manipulated to reduce the corrosion release rate and, hence, the challenges to fuel performance via CIPS and CILC. The most striking result of this analysis was a clear division between plants that exhibited corrosion with a falling rate, following an exponential decay, and those that showed a constant corrosion rate sustained for many outages. Despite significant convolution between potentially significant parameters, the difference appeared to be most closely correlated with the tubing manufacturer; manufacturer 'A' having lower long-term releases than manufacturers 'B' or 'C'. The PWRs supplied by manufacturer 'A' included Callaway, South Texas Project Units 1 and 2, and V C Summer, such that manufacturer 'A' is readily identifiable (using [32]) as Sandvik. EPRI observed similar behaviour for Sandvik Alloy 690TT tubing based on Co-58 shutdown peaks for a mixture of Westinghouse 2, 3 and 4-loop units [42], as shown in Figure 5, where TV1 and TV3

can be identified as Sumitomo and Sandvik, respectively, using [32]. With one exception, these had fallen to low values within 6-8 EFPY of operation post-SGR, whereas Co-58 peaks for Westinghouse 4-loop units with replacement Sumitomo tubes were much higher and, if anything, increasing in magnitude.

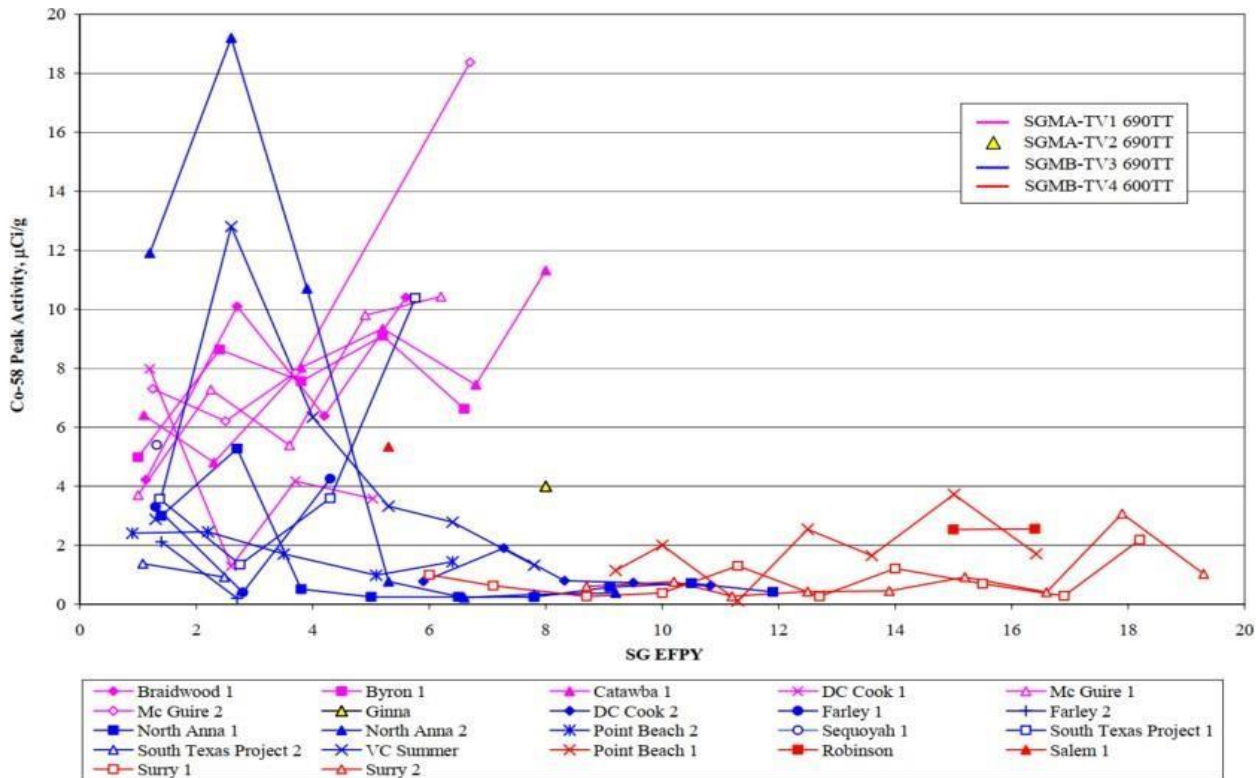


Figure 5: Post Replacement Co-58 Shutdown Peaks following Peroxide Addition

Notes: The data are for plants with Westinghouse nuclear steam supply systems (NSSS) and are sorted by tubing manufacturer. This plot is taken from [42].

Sandvik has studied the nickel release from four of its Alloy 690TT tubes when exposed to simulated PWR primary water conditions in a rig [46]. The status of the tubes ranged from 'new', through one previous rig cycle, to 'old' (>10 previous rig cycles). Not surprisingly, nickel release was highest for the new tube. This fell by 50% over 25 hours and was relatively low by the end of the test (~300 hours), but the tube had not fully passivated. However, the remaining three tubes all behaved similarly (lower releases) with passivation reached after ~50 hours. In other words, optimal behaviour was achieved after just one rig cycle. Overall, the tests provided evidence of very low nickel releases for Sandvik-manufactured Alloy 690TT SG tubes and their fast passivation.

Favourable performance of Sandvik-manufactured Alloy 690TT tubing is evident for Sizewell B based on the representative corrosion product data available since reactor commissioning in 1995 [47]. The SG surfaces were effectively passive after the first five fuel cycles, leading to a major reduction in soluble and insoluble corrosion product releases, both for shutdowns and start-ups. As of Refuelling Outage 15, Co-58 releases were several hundred times lower than in first four cycles (see Figure 6). That the reduction was greater for Co-58 than for other corrosion product species implies that it was mainly due to lower nickel release rate from the SGs. While black fuel crud was present after cycle 4, subsequent cores were essentially free of any visible deposits.

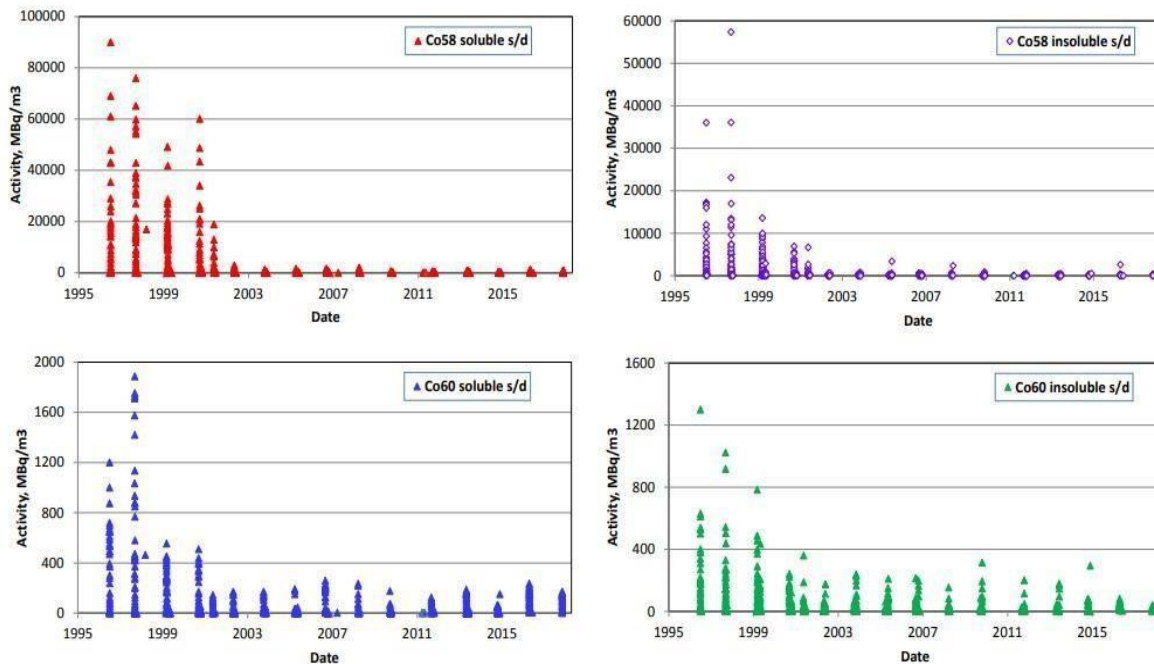


Figure 6: Soluble and Particulate Co-58 and C-60 Concentrations for Sizewell B

Notes: The activity concentrations are for 15 refuelling shutdowns (s/d) and two forced outages. These plots are taken from [47].

Sandvik also supplied the Alloy 690TT tubing for Ringhals 2 and 3 replacement SGs; the original ones were 600MA. In combination with the reintroduction of an elevated pH_T /lithium programme, this led to a significant reduction in general corrosion of SG surfaces, resulting in lower fuel crud build-up, plant dose rates and radioactive discharges over time [48]. The excellent results relative to Ringhals 4, which still had Alloy 600MA SGs at that time, were attributed, in part, to passivation of the Alloy 690TT surfaces. However, the delay in Unit 2 passivating (10 years) compared to Unit 3 (5 years), despite the Alloy 690TT tubing being nominally identical in both cases, suggested that the elevated pH_T /lithium programme was also a contributory factor (for both units, the improved behaviour was observed relatively soon after the pH-programme changes). In contrast to Ringhals 2 and 3, it is understood that the corrosion release for Ringhals 4 did not passivate when its SGs were subsequently replaced, also with (Sandvik) Alloy 609TT tubing, but this remains to be confirmed.

Turning attention to Valinox-manufactured tubes, OPEX for 900 MWe, 1300 MWe, and N4 series French PWRs equipped with Alloy 690TT SGs (either original or replacement models) has revealed different groupings for how the Co-58 coolant activity peak measured at forced oxygenation during refuelling varies with the number of operational cycles experienced by the SGs [49]. The groups correspond to the four main periods in the evolution of the manufacturing process for SG tubes used in EDF reactors (i.e., up to end 1988, 1989-1992, 1993-1995, and post 1995).

The general shape of the curves (Figure 7) indicates that the peak Co-58 activities are generally higher for the shutdown at the end of the second or third cycle than for the first cycle or subsequent cycles, but that the rate of decrease after the first two or three cycles can vary markedly. The decrease in the magnitude of Co-58 coolant activity peaks with number of cycles is more pronounced (i.e., the benefits of manufacturing changes are more visible) for the changes from the first to the second period of manufacturing, than for the subsequent

manufacturing changes. In other words, the behaviour observed for the second, third and fourth manufacturing periods was similarly favourable. One possible exception to this was for two units with replacement SGs in the fourth group (i.e., the post-1995 manufacturing period), which showed higher than expected peak Co-58 activities after one or two cycles of operation, and for which the long-term trend was yet to be observed. It was noted that for these two cases, the surface area of the tubes was greater for the replacement SGs, but that this would not totally explain the observations. Instead, the apparently anomalous results were attributed to RCS cleanliness issues after SGR. Abnormally elevated quantities of non-radioactive insoluble and soluble species were detected from the beginning of reactor start-up, which become activated during the following cycle and gave rise to high shutdown peaks.

Some years later, EDF reported that while these two 900 MWe plants (for which SGR was performed in 2003-2005) had experienced 'record' Co-58 peak activities for a few cycles, the elevated peaks then decreased, following the general behaviour observed for other Alloy 690TT SGs [50]. It was also confirmed that the 'material effect' of improved manufacturing processes on surface passivation also applies to newer plants with original Alloy 690TT tubes, with a 'first manufacturing process' leading to Co-58 peak activities that fell only slowly over 10 or more cycles (a continuous Ni release), and a 'second manufacturing process' for which the Co-58 peaks fell rapidly and had all but disappeared within 7 cycles. Changes to the Valinox manufacturing process over the years include improvement of the cold rolling, use of a hydrogen atmosphere for the final thermal treatment, and suppression of the final sand blasting [51].

Similar behaviour has been observed for Co-58 activity deposited on primary-system surfaces at EDF plants, with levels initially increasing after SGR before falling for subsequent cycles, sometimes to practically the lowest values in the history of the French fleet [52].

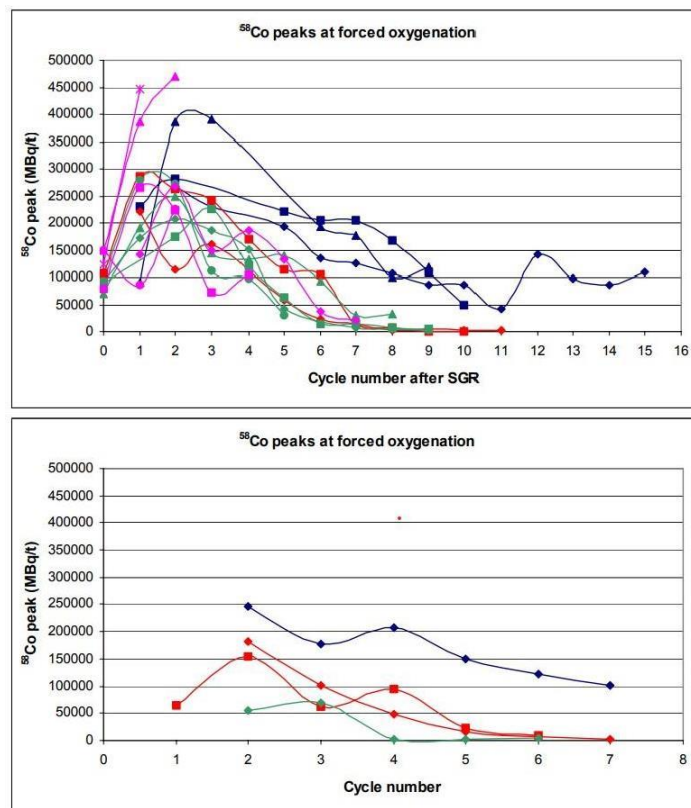


Figure 7: Co-58 Peaks at Forced Oxygenation for EDF Plants with Alloy 600TT SG Tubes

Notes: The upper plot is for 900 MWe and 1300 MWe series of reactors, and the lower plot is for N4 series of reactors. In both cases, blue is 1st manufacturing process, red is 2nd manufacturing process, green is 3rd manufacturing process and pink is 4th manufacturing process (N.B., there is no pink for the lower plot). These plots are taken from Ref [49]

French workers have investigated the corrosion release behaviour of Alloy 690TT tubing in the laboratory using the highly sensitive BOREAL loop [49]. Five different tubes, all having a chemical composition compliant with specification, were exposed to simulated primary water at 325°C. Despite the same experimental conditions being applied in each case, the different tubes exhibited differing behaviours towards corrosion release, in terms of both the size of the release and how quickly the release rate reduced with time. It was determined that most of the metal release occurs during the first 200 hours. The release rate then decreases and becomes constant, but this can take 300-600 hours to plateau. The first part of the behaviour corresponds to formation of oxide scale, which leads to corrosion release, while the second part corresponds to growth of the oxide scale, which reduces the release rate. Surface state greatly influences both processes, but this could not be explained in terms of simple surface parameters. In particular, the surface roughness of the within-specification tubes had no impact on the release. Moreover, all the tubes had similar cold-working but different release kinetics and so other parameters must have been influential. It was concluded that the microstructure and the chemical composition (with impurities) of the surface state, which is determined by the manufacturing process, can modify the formation and growth of the oxide film or scale, and hence, its properties.

Follow-up work [53] found that a small grain size at the surface seems to favour quick formation of protective oxides and low releases from SG tubes, and that a perturbed microstructure layer also has an effect. In another study, in which thermal treatments were applied to Alloy 690 samples to obtain homogenous grain sizes in the range of 25-100 µm before exposing them to simulated primary water conditions, it was determined that grain size does not affect the growth kinetics of the inner oxide layer, but smaller grains led to a higher proportion of chromium in the chromium-rich layer [54]. For samples with non-homogenous grain sizes, it has been observed that small subsurface grains are associated with higher corrosion releases [55].

Looking to the future, coatings are under development that could be applied to metallic components (including stainless steel and nickel-based alloys) during manufacture, with the aim of promoting passivation and, hence, reducing corrosion product release. These include EPRI's zinc-based passivation technology and Sumitomo's SM-ART process [56]. The former utilises zinc electroplating to form a stable ZnCr₂O₄ oxide, while the latter is based on selectively oxidising chromium during heat treatment to form a stable Cr₂O₃/MnCr₂O₄ film. Chromia films produced on Alloy 690 SG tubing by the SM-ART process have been characterised and tested in simulated primary water [57]. Pre-filming reduced nickel releases to about one third (for a test duration of 500-1000 hours) and the films remained stable during immersion lasting ~25,000 hours.

6.1.3. Primary Water Chemistry

General corrosion rates for Alloy 600 and stainless-steel, relative to $\text{pH}_T = 6.9$, are plotted in Figure 8. The primary coolant pH is expressed for a reference temperature, which is usually either the average core temperature (T_{ave}) or 300°C. Both materials behave almost identically in this respect and similar would be expected for Alloy 690. Moreover, corrosion release is likely to follow a similar trend. There is appreciable benefit of lithium addition to achieve primary water $\text{pH}_T \geq 6.9$, and this contrasts with the low pH_T that would have been experienced during historical operation of Obrigheim. Returning to modern-day chemistry regimes, operating at $\text{pH}_T = 7.2$

relative to 6.9 during the first cycle of operation would give rise to a source term reduction of ~5%, whereas the additional benefit of operating at $\text{pH}_T = 7.4$ is only 2%. Hence, the actual benefit of operating with elevated pH_T is to minimise solubility-driven transport to the bulk coolant and deposition on the core [38].

As noted previously, zinc injection reduces the corrosion release rate for stainless steel and Alloys 600, 690 and 800. This is an additional benefit of zinc injection as well as reducing radiocobalt re-deposition on out-of-core surfaces and mitigating primary water stress corrosion cracking (PWSCC) of nickel-based alloys.

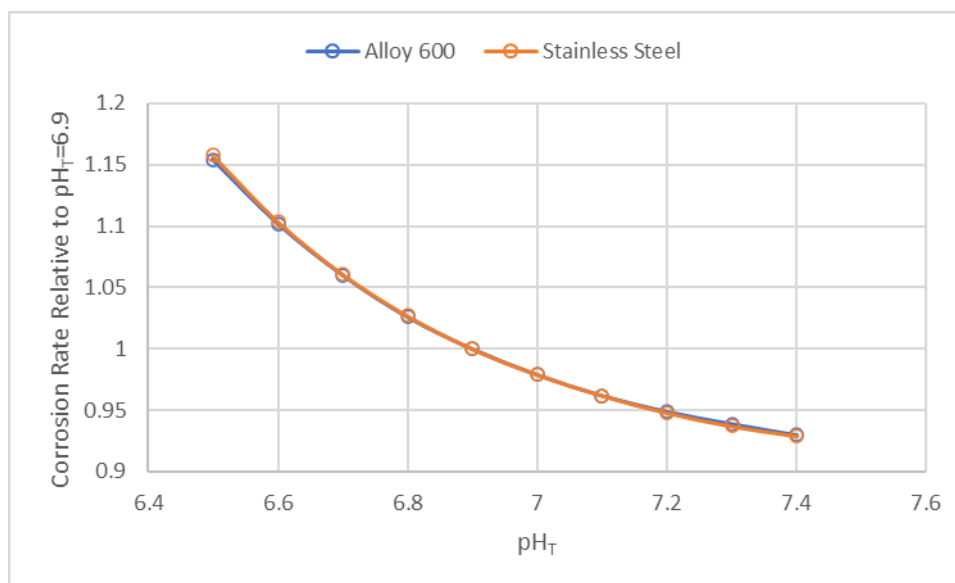


Figure 8: Corrosion Rates of Alloy 600 and Stainless Steel Relative to $\text{pH}_T = 6.9$

Notes: This plot is produced using data in [38].

6.2. Corrosion Product Deposition on Fuel Rods

Discussion of the PWR fuel crud mechanism up to this point has focussed on the corrosion product source term. However, it was noted in Section 5 that the occurrence of CIPS for US and other plants in the late-1980s and 1990s often coincided with high-duty operations following core uprates. Deregulation of the US power market around this time demanded better fuel economics, and the development of improved zirconium-based fuel cladding materials, such as ZIRLO and M5, facilitated higher fuel burnups and, hence, longer cycles. Modelling studies have shown that primary water chemistry and thermal hydraulics are coupled in terms of understanding and managing fuel crud risks, such as CIPS and CILC [14].

6.2.1. Solubility Changes and Precipitation

Corrosion product formation from soluble species is driven, in part, by thermodynamics (i.e., the solubility difference resulting from higher coolant temperature at the surface of the fuel cladding than in the bulk coolant). If the bulk coolant is near saturation for a species with retrograde solubility, its precipitation will be favoured at the hot surface of the fuel [14]. Liquid-phase mass transfer will also be important, with transport of species from the bulk coolant to the cladding surface being proportional to the concentration difference, but with build-up of crud limited by the kinetics of the mass flux.

The primary coolant experiences a temperature rise on passing through a PWR core; from an inlet temperature of ~ 270 - 290°C , to $\sim 325^{\circ}\text{C}$ at the core outlet. Iron is an important constituent of fuel crud and, historically, it was assumed that the in-core precipitation of iron was determined by the iron solubility from magnetite. Thermodynamic calculations showed that the temperature coefficient of solubility changed from retrograde solubility (i.e., decreasing solubility with increasing temperature) to normal solubility (i.e., increasing solubility with increasing temperature) at pH_T 6.9, which is an alkaline pH ($T=300^{\circ}\text{C}$ or T_{ave}), and so this was adopted as the target value for coordinating boron and lithium concentrations until around 1985 [58]. In addition, pH_T 6.9 coincided with a broad minimum in the magnetite solubility [59], thereby minimising the amount of soluble iron entering the core. However, it was subsequently determined that PWR fuel crud was composed mostly of nickel ferrite, and thermodynamic calculations showed that the iron solubility from nickel ferrite changed sign from retrograde to normal solubility at a pH_T of approximately 7.4 [58] [60]. Likewise, the minimum solubility of nickel ferrite also occurred at a higher pH_T than the minimum solubility of magnetite [59].

Bringing the story up to date, fuel crud in high-duty plants with nickel-releasing SGs is nickel rich, containing both nickel metal and NiO. Therefore, current thinking is to optimise pH based on nickel solubility because the solubility of nickel metal and NiO is significantly lower than the solubility of iron or nickel ferrite in most conditions [60]. Thermodynamic calculations show that as pH_T increases, the solubility of nickel decreases at core inlet temperatures (Figure 9), serving to limit the nickel concentration entering the core and reduce the nickel inventory available for forming crud. This approach holds even if localised oxidising conditions exist in the crud given, notwithstanding the fact that nickel has retrograde solubility over the operational range of pH_T with no dissolved hydrogen present (whereas its solubility behaves 'normally' under reducing conditions). With boiling at the cladding surface, the behaviour of dissolved gases is strongly influenced by water vapour generation, and this may cause their stripping out [61]. If boiling strips out hydrogen, then radiolysis of water will lead to local production of oxidants. Oxygen would also be stripped out, but hydrogen peroxide would remain in the liquid phase. Such a scenario might account for nickel oxide formation dominating over nickel in the fuel crud of high-duty PWRs affected by CIPS.

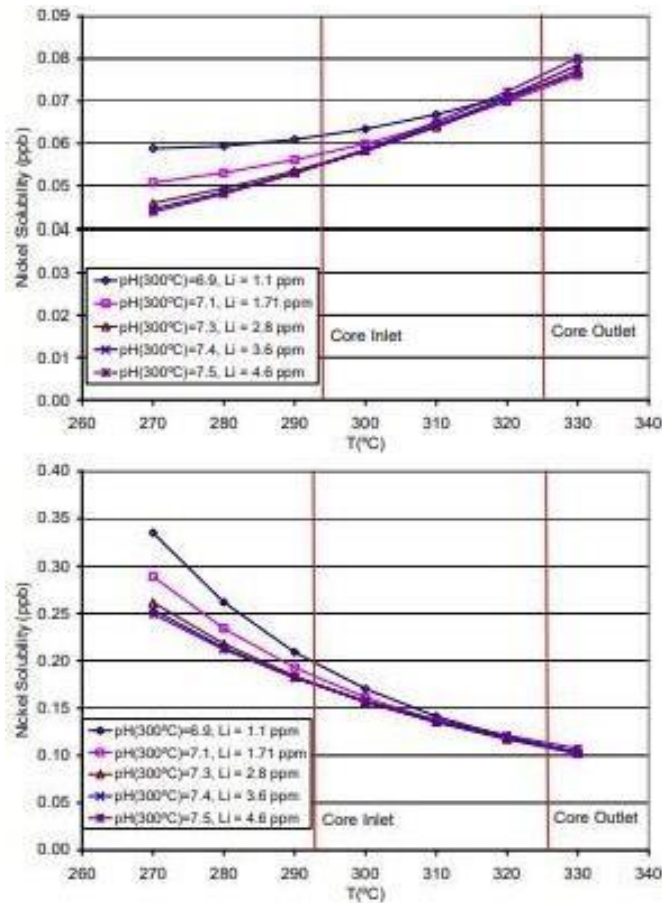


Figure 9: Variations in Nickel Solubility from Core Inlet to Outlet with pH at 300°C

Notes: The upper plot is for 600 ppm boron and $35 \text{ cm}^3 \text{ kg}^{-1}$ hydrogen (i.e., reducing conditions), and the lower plots is for 600 ppm boron and $0 \text{ cm}^3 \text{ kg}^{-1}$ hydrogen (i.e., oxidising conditions). These plots are taken from [60].

The benefits of operating at an elevated pH_T are enforced in the EPRI PWR primary-water chemistry guidelines, which require a minimum operating pH_T (at full power) of 7.0 [62]. The increase in the optimum target pH_T over the years has resulted in a dilemma for many plants, especially alongside the lengthening of fuel cycles to 18 months or more (with an accompanying increase in beginning-of-cycle boron concentrations). Some plants have increased maximum lithium concentrations up to 3.0-6.0 ppm to operate close to pH_T 7.4 [63] [64] [65] while other plants have decided that the potential benefits do not currently outweigh the risks of operating with lithium concentrations above ~ 3.5 ppm, and so are taking a more cautious approach [66]. The fuel vendors have expressed concerns about increased fuel cladding corrosion at high lithium concentrations (and operation outside of vendor-agreed limits is likely to invalidate the fuel warranty), and there remain some industry concerns regarding the potential impact of lithium on the PWSCC of Alloy 600 components and SCC of stainless-steel components in the RCS.

It has been suggested [67] that the nickel solubility (of nickel metal and nickel oxide) may be enhanced by complexation of nickel ions with boron species, thereby introducing a dependence on the boric acid concentration as well as pH_T , but this is based on an extrapolation of low-temperature experimental results that would need to be confirmed by high-temperature experiment.

6.2.2. Subcooled Nucleate Boiling

An important feature of high-duty cores is the increased propensity for subcooled nucleate boiling (SNB) to take place in the upper spans of high-rated fuel assemblies. Providing there is a sufficient inventory of corrosion products available in the coolant, SNB leads to increased deposition in the hottest regions by mechanisms including precipitation of soluble ions and electrokinetic deposition of particulate species.

The primary coolant at the inlet to a PWR core is in a subcooled state, but convective heat transfer from the fuel rods raises its temperature as it flows up the core. If a high heat flux is maintained, the liquid adjacent to the fuel cladding may be heated to slightly above its saturation temperature and become superheated, even though the bulk of the coolant in the core remains subcooled. Steam bubbles then start to form at surface imperfections known as nucleation sites [17]. Bubble growth initially occurs rapidly, with a microlayer of liquid stuck between the bubble and the cladding surface, and then more slowly as the microlayer evaporates leaving an area of dry surface at the base of the bubble [68] [69]. This process is illustrated schematically in Figure 10. Solute species in the fluid microlayer are deposited on the surface, giving rise to a boiling deposition velocity that is not present for single-phase heat transfer in non-boiling cores.

While liquid is being vaporised into the bubble at the cladding surface, steam is condensing back into liquid at other points on the bubble's surface. The rate of bubble growth depends on the relative rates of vaporisation and condensation. Equilibrium bubbles formed in this heat transfer regime eventually condense completely upon reaching a critical diameter, either locally by sticking out into the subcooled liquid, or in the main coolant flow after detaching from the surface.

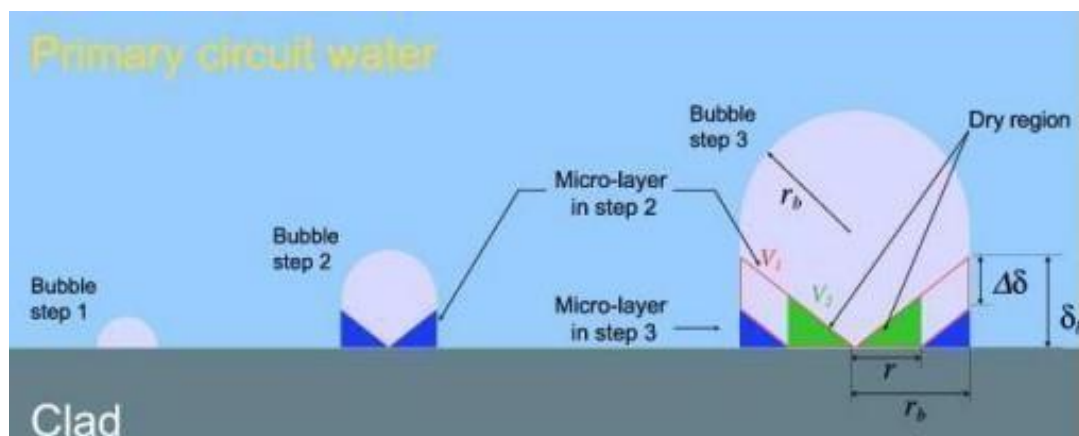


Figure 10: Formation of a Bubble on a Heated Surface (From [68])

SNB is most likely to occur when the extent of subcooling is lower (i.e., the core inlet temperature is higher), or when the heat flux is higher, or both [17]. The evaporation of liquid water into steam transfers large amounts of heat with very little difference in temperature, giving rise to a heat transfer coefficient that can be many times greater than for forced convection.

The mechanism of SNB is understood best in relation to clean surfaces. Boiling processes on surfaces affected by fuel crud are complex, but similar principles are likely to apply. It is postulated that convection causes an inflow of coolant through the pores in the crud, towards the fuel cladding surface, where evaporation takes place. As a result, dissolved species become more concentrated in the pores and may precipitate if they become saturated, thereby feeding deposit growth. Also, boiling creates steam that forms chimneys in the fuel crud through which

to escape, establishing a wick-boiling process for removing the heat flux, along with conduction through the deposit itself [70]. This process is illustrated schematically in Figure 11.

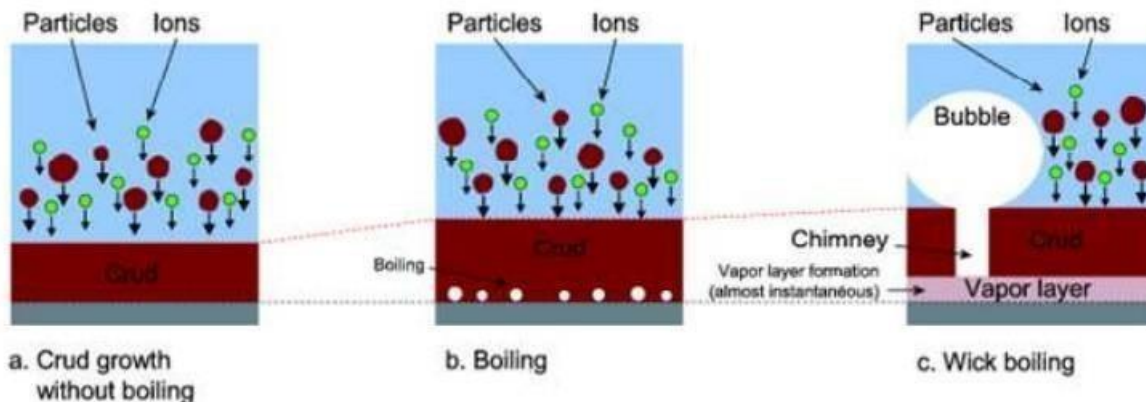


Figure 11: Illustration of Transition from Non-Boiling to Wick Boiling Conditions (From [68])

The thick crud that forms in the highest-power regions of high-duty cores provides a matrix for boron and lithium hideout. Concentrating lithium ions and boric acid in this region modifies the pH of the near-clad coolant, altering the solubility/precipitation characteristics of the water-borne species [14]. The transport arising from steaming also provides the chief driving force for particulate deposition [14].

In addition to feedback from operating experience, and the results of modelling studies, the role of SNB has also been investigated in the laboratory. A Korean group at KAERI used an acoustic emission technique to monitor SNB under conditions of high temperature and pressure [71]. ZIRLO fuel cladding was exposed to simulated PWR coolant in a recirculating rig, with water conditions in the test section maintained at 13.0 MPa and 328°C. A heating rod was inserted into the fuel cladding to keep its temperature above the saturation temperature and to attain SNB on the cladding surface. To study the relationship between SNB and fuel crud, a mixture of Fe and Ni ions was injected into the test section. Acoustic sounds of SNB emitted from the heated cladding surface during a series of tests were monitored, and the crud on the surface of the tubular segments was dissolved in aqua regia solution, and the concentrations of Fe and Ni analysed using ICP-AES. It was observed that SNB behaviour became active with increasing surface roughness, ZrO₂ thickness, and heat flux, but was not affected by dissolved hydrogen concentration over the range 0-70 cm³ kg⁻¹. As expected, the increased SNB behaviour resulted in an increase in the mass of crud deposited under all conditions.

Studies have also been carried out by a Japanese group at CRIEPI, using Zircaloy-4 fuel cladding samples exposed to simulated PWR coolant in a recirculating autoclave system [72]. The fuel cladding tube was again mounted with an electrical internal heater. The water conditions were 12.5 MPa/325°C and the steaming rate was calculated using a two-phase flow analysis, which revealed that up to 12 kg s⁻¹ m⁻² was reached in the middle of the test specimen – much higher than the 0.3 to 0.6 kg s⁻¹ m⁻² observed for Callaway, which suffered from severe CIPS. The Ni/Fe ratio in the tests was controlled to 0.2-0.4 (average 0.25) or 0.6-2.0 (average 1.3), and multiple techniques (SEM-EDX, ICP-AES and LRS) were used to analyse the thickness, chemical composition, and chemical formula of the resulting crud. It was found that the amount of deposited crud (NiFe₂O₄) increased with steaming rate, heat flux, and the Ni/Fe ratio in the test solution, but fell with increasing pH_T (i.e., less crud was deposited at pH_T ~7.7 than at pH_T ~7.2).

6.2.3. Particulate Deposition

The deposition of insoluble particles generally takes place by diffusional, inertial, and

thermophoretic mechanisms, although gravitational deposition may also take place if the deposition surface is not vertical. These mechanisms are described in [73].

Briefly, diffusional deposition affects particles under Brownian motion caused by the impact of water molecules and so is important when considering deposition from colloidal species <100 nm in size. Inertial effects become important for larger particles with diameters of 0.1-100 μm . When a flow stream containing a particle changes direction, the particle will continue to follow its original course due to inertia, and so inertia can contribute to deposition onto surfaces. In the presence of a temperature gradient (thermophoretic deposition), impingement of water molecules on a particle will be greater on the hot side of the particle than on its cold side due to greater water-molecule momentum in the higher temperature region. This promotes the movement of the particle down the temperature gradient from the hot to cold direction. Whilst this temperature effect may reduce deposition on hot surfaces, such as fuel pins, it can increase deposition on other areas of the primary circuit.

Particulate deposition is likely to be important regarding the release of deposits from reload fuel and their redistribution to feed fuel in the early part of a cycle. This mechanism is believed to be mostly via particulate transport and, in the case of heavily deposited reload fuel, may add to the generation of "new" material released from the SGs [14]. Modelling suggested that 10% reload deposit distribution may occur, contributing to CIPS, and this provided impetus for off-line UFC.

Electrostatic interactions between a surface and suspended species can either favour or disfavour deposition, and the behaviour is affected by temperature and pH, among other things [73]. An electrokinetic mechanism has been postulated for crud deposition in regions of flow acceleration, such as on the SG tubes at the sheet-to-tube transition [74] [75], but this is not closely relevant to fuel crud formation in the upper regions of the core.

7. Fuel Crud Properties and Chemistry

This section reviews the properties of PWR fuel crud deposits. The information is based on end-of-cycle deposit samples collected from fuel rods, and fuel crud produced in laboratory simulations. The observations indicate that the thermal-hydraulic conditions and chemistry environment within thick fuel crud deposits are significantly different to those in the bulk. Chemistry models have helped to understand this behaviour, which, in severe cases, may lead to CIPS or CILC.

7.1. Crud Scrapes

Samples of deposit can be scraped off fuel rods in the fuel pool after they have been offloaded from the core. The samples can then be analysed by various techniques. An automated scraping system was developed for use initially at Callaway and is described in [18] [21]. Hard blades were used to remove deposit, which was drawn into a stainless-steel tank using a funnel. The fluid in the tank was then pressure filtered using a 0.45 µm Millipore membrane.

7.1.1. Limitations

While analyses of crud scrape samples have provided extremely useful information, it is important to recognise that the samples would not have been fully representative of the fuel crud that existed at power. This is because the shutdown chemistry and SFP conditions would affect the thermodynamic stability of some of the chemical species present. A good example being nickel metal, which is rarely detected in ex-reactor fuel crud samples because it is soluble under acid-oxidising conditions. Hydrogen peroxide addition therefore leads to dissolution of Ni, along with Co-58 derived from nickel sites in the crud. Similarly, nickel ferrites and LiBO_2 (see later) both have retrograde solubility and so become more soluble during cooldown. When a PWR shuts down, several kilograms of nickel and several hundred grams of iron can dissolve into the primary water [21], and an increasing Co-58/Co-60 ratio and Co-58 specific activity (i.e., Co-58/Ni) indicate an in-core source of release [52].

7.1.2. CIPS Root Cause Investigations (US)

Prior to operation with high-duty cores, PWR fuel crud was reported to consist of nickel ferrite, $\text{Ni}_x\text{Fe}_{3-x}\text{O}_4$, with a typical x-value of between 0.25 and unity [18] [69], or, in other words, with a Ni/Fe ratio of 0.5 or lower. In the limit of $x=1$, this corresponds to the mineral trevorite, which has an inverse spinel structure where the divalent ion (Ni^{2+}) occupies the octahedral sites, and the trivalent ion (Fe^{3+}) occupies both the tetrahedral and octahedral sites. Hence, a Ni/Fe ratio of 0.5 has long been considered an indication of predominantly nickel ferrite in PWR fuel crud [28].

Video examinations of Callaway Cycles 5 and 6 fuel showed crud deposited in the top of the core with coverage following the pattern of boiling, both within and between fuel assemblies [16]. Crud samples scraped off Callaway fuel at the end of Cycles 6 and 7, and Millstone-3 fuel at the end of Cycle 4 – all CIPS cycles – were sent for analysis as part of an initial root-cause investigation. The deposits were found to consist of mainly Fe and Ni oxides with Ni/Fe in the range of 0.5 to 1.5. This suggested that the crud contained other forms of nickel in addition to “blocky” nickel ferrites, most likely NiO or Ni metal.

Following the severe CIPS experienced by Callaway in Cycle 9, end-of-cycle crud samples scraped from span 6A of two high-CIPS feed assemblies were sent to AECL for characterisation

using advanced techniques [16] [18] [21]. These were taken from near the top of the core, where deposits were observed to be especially thick in the regions of intense SNB. As already mentioned briefly in Section 5.2, ~100- μm thick flakes retrieved from the samples were found to contain sizeable fractions of bonaccordite (Ni_2FeBO_5) and ZrO_2 (~50 wt% and ~30 wt%, respectively) along with small amounts of NiFe_2O_4 and NiO (in the region of 10-15 wt%). These species were arranged in a layered structure, as shown in Figure 12, and described as follows:

- Needles or rods of Ni_2FeBO_5 at what would have been the clad-crud interface.
- ZrO_2 particles in the middle layer of the flake, mostly clustered around wick-boiling chimneys, and some 30-50 μm away from the clad-crud interface (where the bulk of the ZrO_2 would normally be found)
- Needles of NiO at the crud-coolant interface, forming a highly porous structure capping the boiling chimneys.

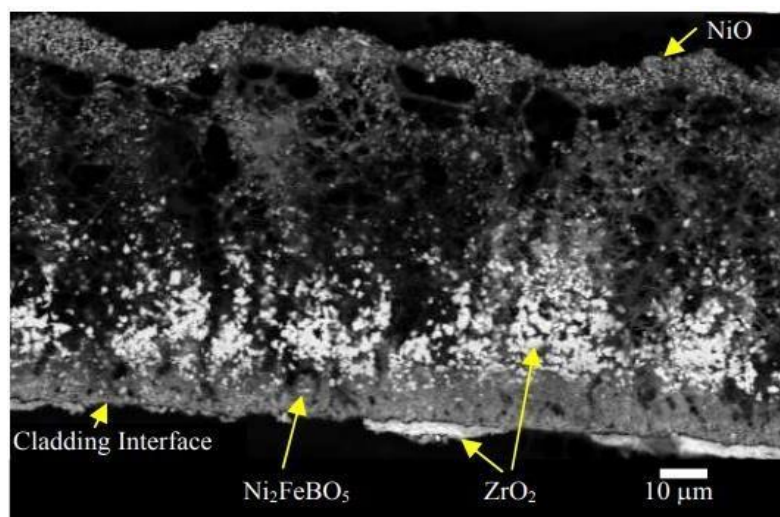


Figure 12: Backscattered SEM Image of a Callaway Cycle 9 Crud Cross Section (From [16])

The Ni/Fe ratio in the Callaway Cycle 9 crud samples was very high (~5) and it was noted that recent Westinghouse analyses of primary coolant grab samples for 11 PWRs showed Callaway to have very high nickel concentrations, ranging from 11 ppb to 53 ppb, whereas plants without CIPS typically had nickel concentrations in the range of 1-5 ppb. Iron concentration for Callaway's coolant was also high (12-17 ppb), although no correlation between iron concentration and CIPS was evident from the data.

Bonaccordite had not positively been identified in PWR fuel crud before, although it was acknowledged that its presence had probably been detected qualitatively in earlier fuel-deposit examinations. The B-10 abundance in the Ni_2FeBO_5 needles was significantly depleted compared to its natural abundance and the B-10 abundance in the Callaway coolant at the end of the cycle, meaning that a corresponding amount of Li-7 must have been formed and released into the crud matrix, along with α -radiation by the $^{10}\text{B}(n,\alpha)^7\text{Li}$ reaction. However, the evident lack of isotopic exchange with the coolant suggested that while the boron captured in Ni_2FeBO_5 deposits could initially have contributed directly to CIPS, its impact in later stages of the cycle was likely to be lessened, as the B-10 became depleted.

CIPS tended to affect Callaway and other US PWRs during the latter half or two-thirds of the fuel cycle, and so this pointed to additional boron hideout contributions from LiBO_2 (lithium metaborate) precipitation or boric acid physisorption. The hypothesis is difficult to prove because LiBO_2 is soluble in SFP conditions and so its presence would not be anticipated in crud samples. Instead, support for LiBO_2 precipitation was provided (despite unfavourable thermodynamics)

by the release and subsequent re-adsorption of lithium during a short down-power to 30% in Cycle 9. Similar behaviour was then observed during Cycle 10.

The root cause investigation was extended to nine additional cores, including from other units, and these were selected to span a range of core performance from severe CIPS to no CIPS [17] [21]. Notable observations included the implied presence of Ni_2FeBO_5 in crud scrape samples from fuel offloaded at the end of Seabrook Cycle 5, and its confirmed presence for Callaway Cycle 10 fuel. There was also a ZrO_2 layer, like that observed for the Callaway Cycle 9, in flakes from both samples. The immediate appearance of CIPS in Callaway Cycle 10 suggested that the 16 once-burnt fuel assemblies reloaded from Cycle 9 must have retained their crud [16]. To mitigate the risk of CIPS becoming worse, the core duty was reduced midcycle by lowering T_{ave} . This prompted a release of Co-58 particulate activity into the coolant. The subsequent crud scrapes suggested that some of the bonaccordite and NiO had dissolved (the crud was thinner than for Cycle 9), and that nickel ferrite formation was favoured in the new environment (nickel ferrite had grown under the original deposit).

More generally, the findings of the extended investigation [17] [21] were as follows:

1. CIPS correlates with deposit thickness and the presence of layering within fuel crud.
2. The amount of crud is roughly proportional to the degree of SNB, which only occurs in the upper spans of fuel assemblies.
3. Nickel and iron are the main components of crud.
4. The Ni/Fe ratio tends to increase with assembly height for high-SNB cores, either because rising pH in the deposit due to concentrating lithium increases iron solubility relative to nickel, or due to the presence of a nickel deposit that is less soluble under shutdown conditions (e.g., Ni_2FeBO_5 or NiO).
5. Ni metal is typically absent in (thicker) deposits on rods undergoing significant SNB but has been measured in thinner deposits from low power rods (high-temperature coolant sampling of crud particles).
6. NiO is more prevalent in deposits undergoing SNB but is also found in deposits from low-duty cores.
7. Thick crud from rods undergoing significant SNB can have fully substituted nickel ferrite (contains only Fe^{3+}), whereas thinner crud contains partially substituted nickel ferrite (contains Fe^{2+} and Fe^{3+}).

The observations indicated that the local chemistry environment within the thick deposits on fuel rods undergoing significant SNB must be very different to that in the bulk coolant. Some possibilities [17] [18] included:

- Undissociated boric acid and dissociated LiOH concentrating in the pores due to SNB and causing the coolant boiling temperature to rise sufficiently to form Ni_2FeBO_5 , which was synthesisable (in the laboratory) at temperatures of 350-550°C (i.e., mostly in the supercritical water regime).
- An elevated pH at the fuel cladding promoting ZrO_2 dissolution, which then re-precipitates deeper in the deposit. Along with the elevated temperatures caused by thick deposits, this chemistry would be expected to promote increased fuel-cladding corrosion (i.e., CILC).
- Formation of radiolytically-produced oxidising species (aided by the local alpha dose from neutron activation of B-10, and not suppressed due to hydrogen being stripped from coolant in the deposit) raising the electrochemical potential and changing the deposit composition.

A crud deposition model (CDM) and a crud chemistry model (CCM) were used to investigate

CIPS problems in PWRs [70] [76] [77]. CDM included material transport from the bulk coolant to the fuel surface, while CCM focussed on the chemistry taking place within crud once it is formed, coupling this with the local thermal hydraulic conditions. The models were based on fundamental chemistry and physical principles. Modelling fuel crud formation is the subject of Section 8. For now, it is sufficient to note that CDM and CRM were found to be consistent with the plant data and supported the interpretation summarised in the bullet points, above. In addition, they predicted that:

- Soluble material (alone) can account for fuel crud deposits 10-100 μm in thickness formed over a 12-month cycle under boiling conditions, although the presence of particulates will further exacerbate matters.
- A temperature of $\sim 385^\circ\text{C}$ is achieved at the cladding-crud interface for a 60 μm thick deposit. Increasing solute concentrations in the deposit pores lead to boiling point elevation, which, in turn, lowers the enthalpy of vaporisation (of water).
- There are two possible forms of NiO: one from direct precipitation of NiO from bulk solution, and the other from conversion of nickel ferrite to NiO.
- LiBO_2 becomes less soluble as temperature increases and precipitates out in fuel crud once it reaches a thickness of $\sim 30 \mu\text{m}$, depending on the heat flux. This is comparable to when CIPS is observed to occur. Once formed, LiBO_2 becomes the main source of boron in the deposit and acts to buffer the pH in the vicinity of the fuel cladding.
- Adsorbed boron accounts for $<1\%$ of the boron in fuel crud.

However, there was debate regarding the main form of boron responsible for boron hideout in fuel crud – a key aspect of CIPS. For example, Beverskog [78] argued against the assumed role of a precipitated borates (such as LiBO_2) on the grounds that normal changes in the bulk concentrations of lithium and boron during a fuel cycle would cause an outflow of these species from the porous deposit, making such precipitates dissolve. Instead, he favoured boron physisorption onto NiO whiskers, which have very high surface area. While there remains some uncertainty, it will be seen in Section 7.2 that the presence of lithium tetraborate ($\text{Li}_2\text{B}_4\text{O}_7$) precipitates has been confirmed in fuel crud grown under PWR conditions simulated in laboratory.

7.1.3. Ringhals Observations

More recently, Studsvik and Ringhals have embarked on a significant effort to determine the phases of fuel crud present in the Ringhals PWRs.

Crud was scraped and collected from two Ringhals 4 fuel assemblies: a once-burned rod and a third-burned rod [79]. For the once-burned rod, crud was scraped from rod levels of 1615, 2830 and 3190 mm, whereas for the third-burned rod, only the levels of 1615 and 2940 mm were scraped. This was pre-SGR, when the unit was operating with Alloy 600MA SG tubes and a medium-low duty core. The general pattern of results for both rods was that phase fractions of the spinel species Fe_3O_4 and $(\text{Ni,Cr,Fe})_3\text{O}_4$ increased at lower levels, and phase fractions of NiO and a new solid phase with the tentative composition Ni_2FeO_3 (or possibly bonaccordite – see below) increased at higher levels, where water temperature and reactor power are higher. It was noted that increasing temperature from 300°C to 330°C would shift the thermodynamics from favouring nickel ferrite formation towards NiO, and that NiO would be more stable than nickel metal with an elevated electrochemical potential at the fuel cladding surface, as might arise from radiolysis in the deposit. In addition, more NiO was found in the crud from the once-burned rod than that from the third-burned rod (when comparing similar heights), while the latter contained a much higher fraction of $(\text{Ni,Cr,Fe})_3\text{O}_4$. Once-burned fuel operates at a higher power than third-burned fuel, leading to more favourable conditions for forming NiO.

Crud scrapes were later collected from two Ringhals 2 fuel assemblies: a once-burned rod representing the highest duty for the cycle and a high burnup rod that was of low power and which did not experience boiling in its most-recent cycle [80]. The assemblies were in-core post-SGR (i.e., with Alloy 690TT SG tubes) and experienced medium-high core duty. For the once-burned rod, crud was scraped from various rod levels ranging from 2590 to 3540 mm, while only the level of 2950 mm was scraped for the high burnup rod. The crud from the once-burned rod contained mainly NiO, Ni₂FeO₃ (or possibly bonaccordite – see below) and (Ni,Cr,Fe)₃O₄ at 2590-3255 mm, but only (Ni,Cr,Fe)₃O₄ at 3540 mm. The temperature had flattened-out at the very top of the rod, where there was less boiling than at the lower levels sampled. The crud from the highest sample of the high-duty rod resembled the crud scraped from the high burnup rod at 2950 mm in that it too contained virtually only (Ni,Cr,Fe)₃O₄; the common factor being insufficient local boiling. In other words, NiO-rich crud was produced preferentially for locations of SNB on the high-duty rod.

The composition of the crud phase that had tentatively been identified as Ni₂FeO₃, but which has the same Ni/Fe ratio as bonaccordite (Ni₂FeBO₅), and a similar crystal morphology, was subsequently re-evaluated using a sample scraped (at 2403 mm) from a once-burned Ringhals 4 fuel assembly, pre-SGR [81]. Application of electron energy loss spectroscopy (EELS), which was not used on previous occasions, confirmed the boron content to be in good agreement with that of bonaccordite, as was the diffraction pattern and Ni/Fe ratio. Interestingly, some thread-like crud crystals present on an Alloy 600MA specimen that was exposed to simulated PWR primary water in a PWSCC rig also appeared to be the same material, although the diffraction pattern lacked the required precision for unambiguous identification. The crystals grew in runs with 5 cm³ kg⁻¹ dissolved hydrogen, but not for higher dissolved hydrogen concentrations. This raises questions about whether bonaccordite forms more regularly in operating cores, including those without CIPS, or if it might even be a common phase in PWR primary circuits, but is only present in sufficient quantities to be problematic in cores with thick crud.

7.1.4. Korean Experience

It is known that Korean PWRs experienced CIPS during several cycles between the late-1990s and mid-2000s [20], including one cycle each at the Kori (K-a) and Younggwang (Y-a) sites, and three cycles each for two reactors at the Ulchin site (U-a and U-b). Most Korean units had high duty cores (High Duty Core Index (HDCI)>150) at the time. Anecdotally, the risk of CIPS was observed to increase with fuel burn-up and cycle length.

End-of-cycle crud samples were obtained for various CIPS and non-CIPS cores, either by scraping, taping, or smearing the cladding surface, or from filters in a UFC system. Crud flakes were up to 10-15 µm thick in the upper part of fuel rods, and the Ni/Fe ratio was higher in crud from CIPS cycles (1.2-1.4) than for non-CIPS cycles (0.9-1.2). A crystal of pure boron was detected in the crud from one U-b cycle, and it was postulated that this might be related to the observation of CIPS.

In other work [82], differences in morphology were reported for crud collected from three units; Y-a, Y-b and U-b. Crud from U-b had many needle-shaped crystals mixed with relatively large grains, whereas the crud from Y-a was comprised mainly of pyramid-shaped crystals. The crud from Y-b also had needles, but in less abundance. The needles were Ni-rich, suggesting that they could be NiO whiskers. It was questioned whether morphological differences such as these might help in understanding differences in the CIPS behaviour of Korean PWRs.

7.2. Laboratory Tests

In addition to providing laboratory evidence supporting the role of SNB in forming thick fuel crud (see Section 3.2.2), workers at KAERI and CRIEPI have used their experimental facilities to provide further insights into fuel crud properties, particularly in relation to NiO formation. An advantage of laboratory simulations is that the crud can be collected and analysed without firstly having to expose it to PWR shutdown chemistry, which modifies its properties. Moreover, the KAERI rig was equipped with a rapid cooling system to minimise the dissolution of retrograde solubility species that might otherwise occur during slow cooldown.

KAERI investigated the effect of different coolant ratios of Ni:Fe on fuel crud for simulated PWR primary water (3.5 ppm Li, 1500 ppm B and $5 \text{ cm}^3\text{kg}^{-1} \text{ H}_2$) undergoing SNB at the surface of a Zirlo cladding sample [83]. The three test cases were 20 ppm Ni and 20 ppm Fe, 39 ppm Ni and 1 ppm Fe, and 1 ppm Ni and 39 ppm Fe. In two cases, interpretation of the results was straightforward; nickel ferrites with a polyhedral structure were formed in the 20 ppm Ni and 20 ppm Fe test (Ni/Fe=1), whereas NiO deposits were formed in the 39 ppm Ni and 1 ppm Fe test (Ni/Fe=39). Polyhedral iron oxides were formed in the remaining case – 1 ppm Ni and 39 ppm Fe (Ni/Fe<0.03) – but these were accompanied by sparse needle-like nickel oxides. After reviewing the experimental traces recorded for the Ni and Fe concentrations, the result was explained by the polyhedral structures forming in the early stages when significant amounts of iron were present, and the sparse needle-like deposits forming in the later stages when the iron concentrations were depleted. It was suggested that a needle-like deposit morphology is required to form porous deposits, which create a stagnant coolant zone supporting boron enrichment.

Similarly, CRIEPI investigated the effect of Ni concentration, Ni/Fe ratio and dissolved hydrogen concentration on fuel crud for simulated PWR coolant boiling at the surface of a Zircaloy-4 cladding sample [84] [85]. NiFe_2O_4 formed in all the tests, but this was accompanied by NiO for those runs when the circulating nickel concentration and the Ni/Fe ratio were both at the high end of their tested ranges (i.e., when $\text{Ni} > 33 \text{ ppb}$ and $\text{Ni/Fe} > 0.5$). Also, the detected NiO peak was larger for runs with lower dissolved hydrogen, consistent with thermodynamic calculations for the Ni/NiO phase transition showing NiO to be more stable than Ni metal in the range of $< 10 \text{ cm}^3 \text{ kg}^{-1}$ dissolved hydrogen (at 325°C). Grains and needle-like NiO were formed, and boron was detected in the crud layer, but not bonaccordite. The boron content in the crud increased with boron and nickel concentration in solution.

A co-sponsored experimental programme [86] [87] was set up at Studsvik to identify the boron-containing species that are deposited in thick crud, causing CIPS. Fuel cladding samples were coated with crud (a tenacious inner layer containing nickel and iron oxides, and a loose outer layer mainly consisting of iron oxides) in a pre-treatment before exposing them to simulated PWR primary coolant conditions in an autoclave. During the autoclave exposure, loop water was preheated to achieve the required test temperature, and further heated by an element mounted in the cladding sample to achieve SNB. A rapid drainage technique was employed to preserve the chemical and physical characteristics of the crud after each test, and this involved forcing the solution out of the autoclave while using nitrogen gas to maintain high pressure. The heated section of each cladding sample was divided axially into three sections (lower, middle, and upper) and crud powders were collected for analysis from each section by scraping with a knife. It was possible to scrape the inner and outer layers separately when sampling the lower zone, and this is where the crud was thickest.

Boiling was found to promote the formation of lithium and boron-containing oxide precipitates; only a small amount of boron was detected on the cladding surface for non-boiling conditions.

Boron deposited in the inner crud layer, which was also rich in nickel oxide, and its concentration increased with increasing nickel concentration in the crud. The main metallic constituents of the crud, after exposure to simulated PWR primary coolant, were Fe, Ni, B and Li, but the atomic ratios (Li/B) did not match those for any single known lithium borate. Instead, XRD suggested the possible presence of LiBO_2 , $\text{Li}_2\text{B}_4\text{O}_7$, $\text{Li}_3\text{B}_7\text{O}_{12}$ and $\text{Li}_4\text{B}_{10}\text{O}_7$ (important diffraction peaks were either overlapping or too few for conclusive identification), and Scanning Transmission Electron Microscopy (STEM) was able to confirm the presence of crystalline $\text{Li}_2\text{B}_4\text{O}_7$.

A small amount of boron was detected in the crud for a special case of the pre-coating consisting only of iron oxides, but this was considerably less than for other tests with nickel oxide also present. It was suggested that the iron-oxide crud was more porous than the crud containing nickel oxide. For lithium and boron to precipitate in porous crud their local concentrations must be high. In the more-porous crud layer, hideout could be difficult due to lower concentration factors.

7.3. Summary

The main points from this discussion of fuel crud properties may be summarised as follows:

- Low-duty, non-boiling PWRs tend to have thin fuel crud comprised of non-stoichiometric nickel ferrites, $\text{Ni}_x\text{Fe}_{3-x}\text{O}_4$, where x is between 0.25 and 1.0, and hence, $\text{Ni}/\text{Fe} \leq 0.5$.
- On the other hand, for reactors with high-duty cores and non-passivated Alloy 600 or Alloy 690 SG tubes, thick crud enriched in nickel may form on the hottest fuel rods. Ni/Fe values up to ~ 5 have been observed for deposit samples.
- Crud samples may be obtained after fuel has been offloaded from the core. They are unlikely to be fully representative of the deposit that was present at power, not least because nickel metal is unstable under acid-oxidising coolant conditions, which are established when a reactor shuts down for refuelling.
- Nickel may also be present in fuel crud as nickel metal, nickel oxide (NiO) and bonaccordite (Ni_2FeBO_5). Fuel crud is known to form layered deposit structures up to ~ 100 - $125 \mu\text{m}$ in thickness, with boiling chimneys evident. The presence of NiO needles or whiskers increases the deposit porosity, and bonaccordite is a source of boron hideout contributing to observations of CIPS. Thick fuel crud has also been observed to contain a ZrO_2 layer, 30 - $50 \mu\text{m}$ away from the fuel cladding-crud interface.
- NiO is abundant in thick fuel crud and its formation increases with the extent of SNB, which occurs in the upper spans. NiO formation is also favoured by a high nickel concentration in the coolant, a high Ni:Fe coolant concentration ratio, and a low dissolved hydrogen concentration. Ni metal is absent from samples of thick fuel crud but is likely to be present in the lower spans and for low-duty cores.
- Computational models of the deposition process and crud chemistry were developed to aid interpretation of the fuel crud observations. They show that LiOH and boric acid concentration in the deposit pores due to SNB will cause sufficient boiling point elevation to form bonaccordite, and that the pH-profile through thick fuel crud will promote ZrO_2 dissolution at the fuel cladding (a potential CILC risk), which re-precipitates deeper in the deposit.
- Isotopic analysis of bonaccordite in deposit samples indicates that other forms of boron also have a role in CIPS. There is debate as to whether these are lithium borate precipitates, or boron that is physisorbed onto the surface of NiO whiskers, or both. Lithium borates would not be stable under reactor shutdown conditions but have been observed in laboratory simulations. The amount of boron deposited in simulated crud was found to increase with the NiO content of the crud.

8. Modelling Fuel Crud Formation

8.1. Introduction to Modelling of Fuel Crud

Over the past thirty years or so there have been multiple initiatives to attempt to model the chemistry within the PWR bulk coolant and the crud deposited on PWR zirconium alloy-clad fuel. The physical evidence of fuel crud and its formation conditions, chemistry and structure have evolved over recent decades and as more information has become available, so the modelling approaches have become more sophisticated.

The physical evidence of fuel deposits on, for example, BWR fuel has been clear since the outset of BWR technology. There, the consequences of fuel deposits (in the main) have been a reduction of heat transfer from the fuel to the coolant, although the consequent arising of hot spots and possible fuel failure sites is a concern. However, for PWR fuel the build-up of deposits has a more profound effect, besides heat transfer, in that the deposits may contain boron (as boric acid is deliberately added to the coolant for reactivity control). Additional boron trapped on the fuel surface may then affect the reactivity of the reactor in a manner that is not controllable by operators, and this has rightly been the source of more focused concerns. Over the past thirty years or so, evidence has been built up which includes measurements of reactor power (often as neutron flux) and inspection of fuel after irradiation, and also removal of crud flakes (via scraping techniques) so that the crud structure and chemistry may be investigated. Each new development of the information available adds to the scope of fine detail to be modelled.

The ONR requirement on this topic is to review what computer modelling tools are available to simulate fuel crud formation, and to discuss their basis and their deficiencies. ONR recognise that such tools are important in assessing the behaviour of fuel crud in new reactors and for assessing any impact of changes in core design or coolant chemistry for existing plants. The relevant TAGs are [5] NS-TAST-GD-075 (Issue 3.1) "Safety of Nuclear Fuel in Power Reactors" and [3] NS-TAST-GD-088 (Issue 3) "Chemistry of Operating Civil Nuclear Reactors". Within these documents, [5] refers to modelling only in the context of nucleonics and fuel design, and not in the context of fuel crud (save to say that in paragraph 145 of [5] there is a recommendation that the potential impact of any boron-containing crud on fuel nucleonics should be addressed). In [3] the term "model" only arises once, in the context of Appendix 8 therein (BWR chemistry, radiolysis and electrochemistry). Whereas the terms "crud" and "deposit" – which are often used interchangeably – do occur several times in [3] but without the context of a calculational model. It is clear that modelling of crud formation / fuel deposit formation is a new topic which ONR may wish to consider for inclusion in any future revision to these TAGs.

There have been a considerable number of published papers on the topic of modelling of crud formation, the literature has grown over the years and the level of sophistication and general understanding of the phenomenon have developed with time. This present review has been conducted with "a fresh pair of eyes" and has not borrowed from any particular summary or review, except to summarise their findings as any other reference might be addressed.

There is a matter of nomenclature to clarify at the outset. In the phenomenon of crud deposition and redistribution there are several processes in play. Each process may have been studied and reported on, and often the selected mechanism is then referred to as a model. The literature frequently interweaves and interchanges the terms "model" and "mechanism" (e.g. a model for particle deposition, or a model for radiolysis inside a crud pore). In this review, the term model

has only one specific meaning, which is a numerical simulation for calculating the chemistry, deposition, erosion, precipitation, dissolution, flow dynamics and radiolysis in the context of a fuel assembly surface (or any combination of these separate effects). Whilst a mechanism should be describable in terms of mathematical equations, which in turn can be converted into algorithms or expressions in a computer program, the general concept of a mechanism covering one of the processes is here not described as model.

In keeping with the agreed specification this review will not address detailed aspects of the model algorithms, but will describe the overall scope of each model, and its strengths and deficiencies. This will enable ONR to appreciate each model in the light of the appropriate SAPs and TAGs.

This review follows a broadly chronological sequence and addresses modelling efforts over approximately the last thirty-years. Some greater level of detail will be given to models from around 2005 (\pm 5 years) since these reflect the time zone when greatest progress was made, and more recent models tend to be developments of the fundamental approaches developed just over ten years ago.

In this introductory subsection, attention should be drawn to the textbook on the subject, by Castelli [88]. Dating from 2009, this source outlines the general approaches which might be adopted. However, the book has some disadvantages, such as the principal emphasis is the spread of activated cobalt as a source term for workers (ORE), not crud on fuel surfaces; also, the emphasis on zinc as a cobalt mitigation approach, and further the simplification that on fuel, crud is simply one layer of a spinel type oxide, which had already (by 2009) been demonstrated to possibly consist of up to three layers. The field was rapidly evolving in 2009 and this source [88] was very soon overtaken by new information. Therefore, whilst acknowledging that there is a text book on the subject, the reader is advised that there is much more detail, and more recent, which should be included in a review such as this.

8.2. The Object of the Modelling

Before embarking on a discussion of the various models, it may be helpful to simply recap what it is that these models are attempting to emulate.

The deposition of additional material on fuel assembly surfaces exposed to the primary circuit water in a PWR is generally described as crud formation. Generally, the deposited material may be oxides derived from corrosion of other parts of the primary circuit (and particularly SGs, which have a large exposed surface area) although the pipework surfaces connecting the core, SG, pumps, and pressuriser may contribute some smaller component of the corrosion product which ends up as fuel crud. The fuel itself presents a large surface area of a zirconium-based alloy, which conventionally has a strongly adherent oxide film, but which may corrode in part and re-re-precipitate if local conditions are appropriate.

The deposition mechanism may consist of particle deposition out of a turbulent flow, and precipitation of ionic species which have locally exceeded their solubility limit. Conversely, crud may be removed by processes including spallation and erosion of oxide particles, as well as dissolution of deposits back to their constituent ionic components, if the solubility limit is locally not saturated (for example, due to a change in temperature). Further, crud deposits may be modified, after deposition, by changes to their mineral phase, composition, stoichiometry, bulk density, porosity, due to any one (or a combination) of effects such as reactor control manoeuvres, redox chemistry, radiation chemistry and thermal hydraulics. Due to local redox and radiation chemistry effects, some metal oxide species may be chemically modified into solid

metal precipitates, which may also comprise part of the crud. This combination of effects has been visually summarised by Lister in Figure 13.

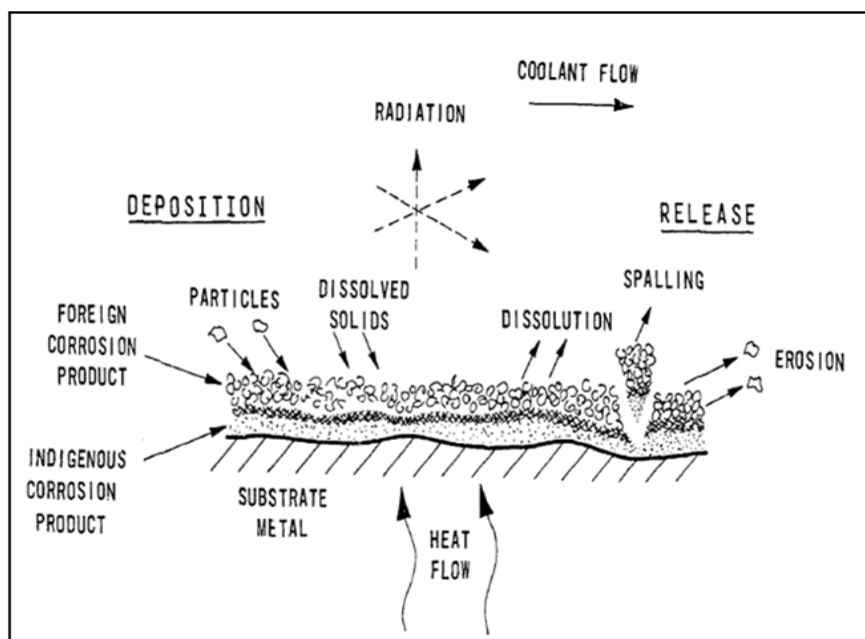


Figure 13: Lister's visualisation [89] of crud formation and erosion (after [90]).

Further complications arise due to the necessity of operating PWR reactors with boric acid dissolved in the coolant as a reactivity control, and correspondingly lithium hydroxide being added to control the system pH within a tolerance band being appropriate for the corroding SG and pipework surfaces (in general, the higher the pH the less corrosion) and the integrity of the zirconium alloy fuel cladding, (not too high a pH, else the cladding alloy suffers). Further, some plants may add zinc acetate to restrict out-of-core surface corrosion, with consequent cobalt activation and deposition out-of-core.

Most models are developed with a specific purpose (or mechanism) in mind. In the decade from around the mid-1990s to mid-2000s, the major emerging problem was AOA, where crud including some boron-containing oxide phases was deposited and this in turn affected fuel reactivity in the regions where such deposits were formed (usually the upper spans of the fuel assemblies where coolant and clad temperatures are at their greatest). This transferred power along the axis of the fuel, to the lower spans of the assembly, hence the term AOA. More recently this term has been superseded by the term CIPS which is a more straightforward way of describing the same effect.

In light of these many processes, all occurring simultaneously, models have a multiplicity of processes to simulate. Not all these processes are well supported by data, in terms of for example, rate constants at the relevant conditions. There are frequently several unknowns in the mechanisms represented in any model, including the in-situ crud morphology, localised redox chemistry at the micro-scale, radiation chemistry in the context of micro or nano scale surface interactions, and thermal-hydraulic conditions. It is therefore unsurprising that modelling of crud formation has taxed the abilities of the reactor chemistry community for some decades, and that a considerable (and growing) body of information has arisen to address the many and varied aspects of crud formation and CIPS. There is now a very considerable body of information available; however the reader should also be aware that certain fundamental data (e.g. the solubility of some mineral phases at elevated temperature) has evolved over recent times, and early papers on such matters may have been superseded. Attention needs to be paid to the details of what fundamental data each model relies upon.

8.2.1. Primary Circuit Chemistry and EPRI Guidelines

Many of the manufacturers of PWR reactors and fuel, worldwide, have developed chemistry regimes in which the competing demands of boron addition and lithium hydroxide pH control are balanced within a control band to provide optimum pH values throughout the fuel cycle. It is then a given, that models of crud formation should recognise that broadly, the overall reactor chemistry should be within the envelope set by the relevant primary coolant chemistry constraints. There are several of these coordinated chemistry regimes, with variations developed by Westinghouse, VGB, CEA, and Mitsubishi. The envelope has some latitude because the fuel may include different zirconium alloys as cladding, and different SG tubing alloys, depending on manufacturer; nevertheless the broad intention is to add sufficient boron, as boric acid, to allow for reactivity control through the reactor fuel cycle, and also to add sufficient lithium hydroxide to balance the pH into a slightly alkaline regime and inhibit SG tube corrosion, but not too alkaline in order not to attack or corrode the zirconium alloy fuel cladding.

The US-based approach to coordinated chemistry has been formalised by the Electric Power Research Institute (EPRI) into various versions of guidelines for PWRs. These guidelines are regularly updated, but the most up to date versions are not publicly available and are restricted to EPRI members. Therefore, reviews based on publicly available data are unavoidably dealing with superseded documentation. Nevertheless, the EPRI guidelines (most recent public versions) are of great assistance in framing the context for any model describing crud formation in a PWR primary circuit.

In 2004 EPRI published a revised set of guidelines [17] concerning AOA / CIPS. The main outputs of the guidelines provide background information to support the management of plant by diagnosing and monitoring the progression of a CIPS cycle, and also a guided decision-tree risk assessment tool, to assist in the design of in-pile and out-of-pile plant components, and any changes to chemistry. As part of the integrated approach, other codes are mentioned, such as VIPRE (for calculating core steaming rates) and BOA (for integrating steaming rates with chemistry and analysis of proposed core and chemistry changes). An example of a change that might be brought about is core up-rating with subsequent increased rates of sub-cooled nucleate boiling, or any revision to pH control.

That report [17] presents the CIPS phenomenon from the industrial end-user (power station) perspective. There is helpful background on the history of AOA observations, first at Obrigheim, then Calvert Cliffs (both in 1979) then a number of stations including Callaway, Wolf Creek, Catawba, Seabrook and Comanche Peak (in the 1980s). There appeared to be a linkage of going to longer fuel cycles, with increased fuel thermal duty, higher peaking factors and plant uprates. In response, fuels that had undergone AOA were subject to close inspection and fuel crud scrapes, which are reported in [77] and discussed below.

An important point is made, in that axial power deviations may occur for reasons other than CIPS; chief among these reasons is that real-life reactor operations often differ from the idealised mode. Ideally, reactors run with the control rods fully withdrawn, however in reality at both start-up and shut-down there may be control rods partly in place (and always at the upper side of the core) for several days. These affect the burnup of fuel (and depletion of the fissile content) in ways that predispose the plant to an axial imbalance at the next fuel cycle, because of multiple cycle fuel assembly dwell. The difference between measured and predicted Axial Offset is known as Axial Offset Deviation (or AOD). (See Section 5.2 for calculation detail). AOD is more likely to be manifest in fuel assemblies incorporating burnable poisons.

Putting the AOA phenomenon in perspective, Bosma et al [17] note that the typical 4-loop PWR fuel inventory has a total fuel surface area of around 5600 m², and that sub cooled nucleate

boiling, of some form occurs at around 5% of the fuel surface (280 to 370 m²). In order to measure an AOA power shift of around 3%, it requires that over a period of 4 to 8 months there must be crud deposition of around 3.6 kg over this surface and that this crud must incorporate around 0.3 kg of boron.

Another factor identified by EPRI is that when multiple cycle fuel dwell is implemented, then crud built up in the first cycle may be thinned (eroded or dissolved) if subsequent use is in a lower power zone of the core. This creates a source of crud material, in the core, to deposit on newer fuel in high power core locations. This emphasises the importance of recognising deposition of crud fragments or particulate displaced from other fuel assemblies when constructing models of crud formation.

The solubility of various metal ions will vary as a function of the local temperature, pH, and dissolved H₂ concentration. However, the theoretical solubility of each metal ion (e.g. Fe, Ni) is not easily measurable, and often has to be calculated on the basis of some measurements and a theoretical solubility model. However, the various solubility models may differ when it comes to precise calculations, according to [17] sometimes by a factor of 5 in the solubility of a specific species. This makes the task of the plant chemist rather difficult, especially considering that the coolant sampling arrangements for PWRs were generally not designed for accurate measurement of corrosion products.

In a report of coolant sampling at Diablo Canyon-1 [17] it was noted that elemental carbon was present in the coolant particulate. It has been inferred, though not with certainty, that the carbon originates from reduction of acetate ions associated with zinc injection. It is possible that carbon uptake in crud is a feature to be increasingly expected with the wider application of zinc injection. Consequently, models should include this possibility. However, as a general observation, zinc injection tends to reduce the thickness of crud deposits and gives a more uniform dense crud coverage. Consequently, boron deposition (and CIPS) was expected (in 2004) to be less likely in plants with zinc injection.

Crud scrape and characterisation investigations have been carried out in the early 2000's, at a number of plants. Figure 14 shows a Scanning Electron Microscope (SEM) image of an intact crud flake from Span 6B of Vogtle-2 Cycle 8. This clearly shows the steam chimneys, with a diameter of less than 10 microns. Since steam chimney boiling is a key feature of a number of models, this image of the reality is particularly relevant.

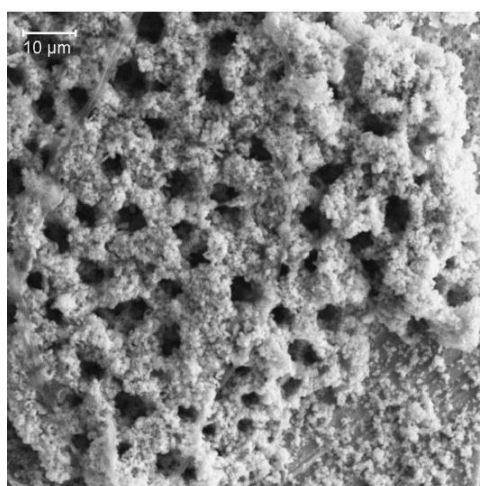


Figure 14: High magnification SEM of a crud flake, showing steam chimneys. (From [17])

One other important concept that needs to be accurately reproduced in models is the nickel / iron ratio. This ratio tends to increase with height up the fuel assembly, for cores with high SNB. (This also includes the isotope pairs $^{58}\text{Co}/^{59}\text{Fe}$ and $^{58}\text{Co}/^{54}\text{Mn}$, formed by activation of nickel and iron). Two possible explanations are credible. First, that as crud thickens it has the effect of concentrating lithium and boron, modifying the local pH, consequently precipitation of iron is inhibited at higher pH, whereas the solubility of nickel is relatively insensitive to pH. Second, that under shutdown conditions a less soluble nickel corrosion product may form, so that when fuel is examined (after shutdown) a higher nickel / iron ratio is found. There are several other effects which may have a bearing on crud chemistry, details should be consulted in section 2.3.4.2 of reference [17].

Nevertheless, the details of lithium and boron hide-out and concentration within crud pores remain a matter of active interest, with corroborating evidence (Callaway, Cycle 9) of power fluctuations linked to lithium concentration (in the bulk, presumed to be after release back from a hide-out process).

A detailed description of crud morphologies, from a number of power stations, is presented in [21]. This is the most complete survey of PWR crud morphologies to date.

Another feature of interest is that in some crud samples it has been found that the crud is layered, with one layer of primarily ZrO_2 (but containing some boron) sandwiched in between layers of Cr / Ni ferrite (see Figure 15). This is abnormal, as ZrO_2 is generally regarded as a very insoluble corrosion product and which forms via a progressive mechanism of amorphous then tetragonal then monoclinic crystals, all highly constrained / stressed by their mineral phase bulk densities being significantly different to the parent metal from which they are derived. Nonetheless, the zirconium oxide once formed on the parent metal surface is usually regarded as highly insoluble and not prone to redistribution.

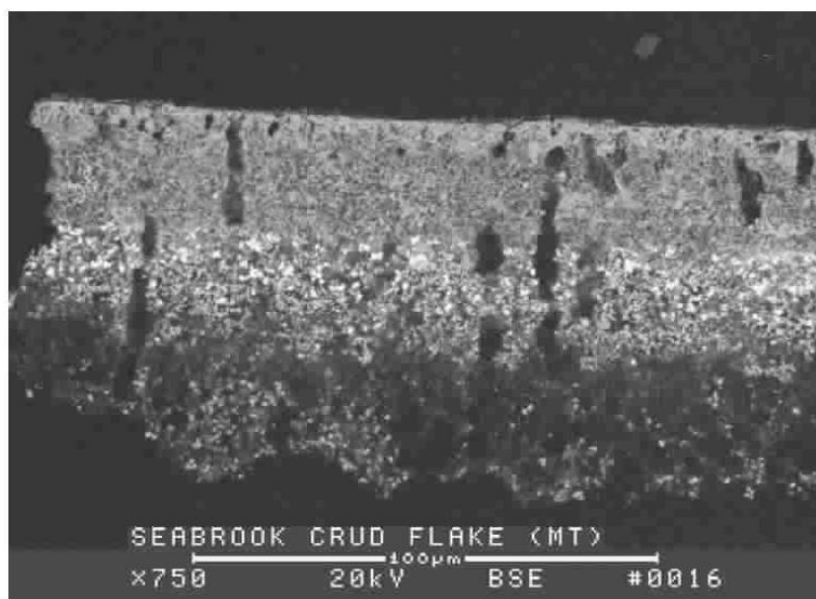


Figure 15: Cross sectional view of a Seabrook Cycle 5 crud flake. (From [17])

The one factor yet to consider is that zirconium alloys are more easily attacked at high pH (fuel vendors will normally have some conditions for their fuel warranty which include a safe pH regime). If lithium concentration has become elevated (and thus pH raised) micro scale attack on the zirconium alloy (with its adherent oxide) becomes possible and this may explain why

bands of ZrO_2 re-deposit within the crud. The re-deposition process is thought to involve Li ions associating with the negatively-charged ZrO_2 particles (OH^- ions may occupy edge sites on the crystal lattice) via an electrokinetic effect influencing the Electrical Double Layer (EDL – more of this later). This Li / ZrO_2 electrostatic attraction may provide a sufficiently electroneutral assembly for boron (as $B(OH)_3$) to become incorporated in the re-depositing crud band.

Reference [17] includes a section on measurements which indicate incipient CIPS, form both in core and ex-core measurement systems. Whilst these measurements are useful information, there has been (as yet) no attempt to construct a model which would replicate these early diagnostics and confirm a mechanistic reason why these specific measurements might be observed and linked to CIPS, although there are models to generate predicted power distribution within the core, based primarily on neutronics and shielding.

The effect of CIPS on fuel reactivity is primarily considered in terms of neutron flux suppression along the axial coordinate, as the name suggests. However, the reader (and modeller) should be aware that there are also second-order effects in a radial direction through the reactor core. A set of core flux maps taken at mid-cycle show that in proximity to a fuel assembly with known CIPS, the neighbour fuel assembly(s) also showed neutron flux suppression. This effect may take the form of both quadrant-based variations and in-out radial variations. If a fuel assembly in an inner high power, core centre location experiences CIPS, then the core as a whole responds by putting more power through the outer (peripheral) fuel assemblies, to maintain the overall reactor power. This represents the in-out power shift. Furthermore, plants with a history of radial power tilts (for other reasons) have found evidence of the onset of CIPS in the quadrant with the highest power before observing CIPS in the symmetrical opposite low power quadrant. These second-order effects have not, as far as can be established, been mechanistically modelled.

Since the mechanism for CIPS under stable plant conditions has been shown to be complex, and with many aspects of plant chemistry and physical processes interacting, it is no surprise to learn that under start-up and shutdown conditions, or other reactor power manoeuvres, CIPS modelling has made hardly any progress.

Reference [17] includes a useful section describing the various observations of CIPS made during power changes associated with reactor operations. One principal effect will dominate, that under reactor power changes, and consequent temperature changes, in general there will usually be a release of crud from all surfaces (ex-core and in-core) as the various metals and their overlaying oxides have different coefficients of expansion, and as temperature changes these different materials will expand or contract differently, and detach when the stress exceeds the local yield limit, depending on oxide (crud) morphology, composition, grain size, etc. It has been implicit throughout, that at the end of each fuel cycle there will normally be a crud burst, and that some of the trapped boron in the crud will probably be lost from the fuel surface (there have been some instances when crud loss from fuel has been minimal, corresponding loss of oxide from SG tubing not commented on). Smaller, but still very measurable, crud bursts will occur at events like control rod movements which may take place monthly (typically). In transient analysis terms, a common approach is to conservatively assume that under loss of coolant conditions, a rapid temperature excursion will mean a significant crud burst and release of all trapped boron back to the primary coolant, with associated increase in reactivity of the fuel which had experienced AOA.

One area where modelling is routinely used in conjunction with AOA effects is the Adjusted Core Model. This is a tool for estimating safety considerations arising from AOA in the fuel array. This requires the creation of a neutron absorber that can be positioned in such a way as to mimic the effect of neutron depletion due to boron containing crud deposits. The absorber must be movable to different axial positions and modifiable in terms of neutron capture properties. The model is

benchmarked against plant measurements and then affords a prediction tool for the consequences of AOA, should it occur on that plant. However, predictions for power manoeuvre events have met with limited success, therefore use of the model has more generally been for assessments of the impact of AOA on safety analysis parameters.

The assessment of AOA risk employs a range of calculational tools, which vary according to their level of complexity and are considered in “tiers” according to their sophistication.

- Level 1 methods. These are intended to be simple and fast. They must relate to measurements from actual plants (no relevant test loop data existed, in 2004). The methods include Core Radial Power Peaking calculations, and Single Dimensional Thermal Hydraulics calculations.
- Level 2 methods are more complex and require a three-dimensional analysis of the steaming rate (S_R). Model codes such as VIPRE are appropriate for this assessment.
- Level 3 methods are the most complex and are intended to provide an assessment of core performance for future / projected core designs. The BOA code (see section 8.3.1) is an example, although this requires a VIPRE (see section 8.3.4) analysis of S_R as a prerequisite.

The BOA and VIPRE models are described separately in sections 8.3.1 and 8.3.2 although reference [17] gives a thorough background to these models as they stood in 2004. In particular, in that reference there are four substantial Appendices covering case studies on the application of BOA to specific power stations.

8.2.2. Early PWR Crud Mechanisms and Models

The issue of corrosion product deposition and activity transport in a PWR was recognised as far back as 1979 (or earlier, since [91] gathers information from earlier times). At that point in time, there was already a recognition that radiation exposure to workers at outage times was largely controlled by re-deposited activity, mainly in the out-of-core sections of the primary circuit.

Berry [91] assembles a considerable amount of detailed information, however, there is no comprehensive model to utilise the data in a computer modelling sense; nevertheless Berry [91] does assemble the various theoretical understandings of corrosion rate and mechanisms, transport mechanisms, deposition rate and mechanisms, and solubility. Consequently, [91] is a good primer and starting point for anyone new to the area. Another early summary worth consulting for the general principles of PWR chemistry is Cohen’s textbook [92] which has gone through several Editions and remains a perennial starting point for those wishing to understand reactor coolant chemistry.

However, it was not very long before models of crud deposition and associated corrosion and transport were developed. In 1987 Morillon [93] reported an academic (MIT) study on modelling the overall process, using the CRUDSIM model but also referencing the CORA-2 model (developed by Westinghouse) and the PACTOLE model (developed in France by the CEA). The CRUDSIM model is based primarily on the limiting solubility of a cocktail of metal species in solution at high temperature and subject (or not) to a flux of gamma radiation. This is underpinned by experiments with all these components using a pair of stainless steel “slurry tanks” to replicate the core (deposition) region and the heat exchanger (corrosion product dissolution and erosion leading to small particulates). The CRUDSIM model is however based on 1980s data for solubility products and does not include several features relating to transport, which are bundled up in a factor (beta) which is experimentally determined, but which in detail represents several processes.

A similar academic study (and again from MIT) was presented by Chan [94] as a PhD thesis, in 1989. Again, this uses CRUDSIM as the main model, and including data obtained from the PWR Chemistry Control Loop (PCCL) attached to the MIT test reactor. Chan also references the CORA-2 code, and PACTOLE, noting some specific concerns with the former. The CORA-2 code, whilst good at thermal hydraulics, does not pay attention to the effects of temperature change on corrosion product solubility, which is nowadays considered one of the most significant effects. The PACTOLE code, by contrast is recognised by Chan as predicting PWR operational results rather well. As an appendix, Chan provides the entire listing (Fortran) of the CRUDSIM Code. Under the conditions covered, CRUDSIM provides a reasonable model for the precipitation deposition and erosion of PWR primary circuit crud. However, some of the solubility data etc will by now be obsolete.

In 2006 Beverskog advanced a theoretical approach to boron-rich crud deposition [78], in which he pointed out that the precipitation of (monocrystalline) needles of NiO (bunsenite) – as observed in PWRs – was more reasonable than precipitation of cubic spinel crystals of NiFe₂O₄ (trevorite) – as observed in BWRs – due to the significantly higher temperature of PWR high-duty cladding (around or >350 °C) compared with BWR fuel cladding (286 °C). Also, the more physically violent environment of SNB mitigates against complex crystal shapes such as cubic spinels, with their porous structure, and favours simple crystal habits such as monocrystalline (one-dimensional growth into needles).

A review of model codes was provided by Rafique et al in 2010 [95]. This review encompasses material in the public domain at the time of writing and notes that the first model was developed in relation to CANDU reactors (of marginal relevance to this review of PWR models, but relevant to Section **Error! Reference source not found.** of this report). Subsequently a number of other well-known models were developed, most of which are commented on elsewhere in this Section. These include the ACE-II code (a Japanese code), CRUDTRAN (a development of the CRUDSIM model from MIT), PACTOLE (from CEA, France), CORA-II (from Westinghouse), CPAIR and COTRAN. For VVER systems ¹ the models MIGA-RT and DISER are recorded. The description given for each of these codes is very brief, and does not permit a comparison of key features, they each have a slightly different approach and therefore their own strengths and weaknesses.

A long-standing example of modelling is the French code PACTOLE which has been developed by CEA / EDF / FRAMATOME. [96]. The code has been in development since 1979 and for many years was the default tool for studying PWR coolant chemistry in French reactors. PACTOLE and its successor model, OSCAR, are discussed in Section 8.3.8.

In 1992 there had been sufficient progress on all aspects of this topic for the IAEA to publish a four-volume set of documents [97] as follows.

Volume 1: Chemistry of Primary Coolant in Water Cooled Reactors

Volume 2: Corrosion in the Primary Coolant Systems of Water-Cooled Reactors

Volume 3: Activity Transport Mechanisms in Water-Cooled Reactors (of prime relevance here)

Volume 4: Decontamination of Water-Cooled Reactors.

These take the format of a collection of papers by invited experts in each of the four topics. In the volume concerning Activity transport mechanisms, and the first such review, Thornton commented that “*Many attempts have been made to construct models with a predictive ability. They all remain semi-empirical due to a lack of fundamental understanding of the processes involved. It follows from this that their predictive abilities are at present questionable*”.

¹ Note that the reactor type VVER (in the original Russian being Voda-Vodyanou Energesticheski Reaktor) meaning Water-(cooled) - Water (moderated) Energetic Reactor is sometimes also known as WWER.

In his paper, Thornton uses the outputs of CRUDSIM and PACTOLE models for comparison with plant, but (as his comments reflect) the confidence in the outputs was lacking.

Similarly, Alder et al (in the same volume [97]) reported on various models developed for BWR corrosion product transport, and in particular fuel failure and tramp uranium issues. Here something of greater interest is reported, that two papers emanating from the General Electric Company take complimentary (but different) views on fuel crud formation and out of pile deposition. Marble [98] then argues that the deposition of cobalt-rich species out of core is what drives the exposure dose rate to plant workers. The different mechanisms needed to support these viewpoints are sometimes referred to as "models", but they do not reflect fully functional calculational tools. Of course, these papers relate primarily to BWR chemistry, not PWR.

The IAEA report [97] includes a paper concerning electromigration of corrosion products, by Sedov et al. They propose that under shut down conditions the addition of hydrogen peroxide (or radiolytic H₂O₂, since they study a RBMK (Reaktor Bolshoy Moshchnosti Kanalnyi)) changes the overall electrical charge on spinel particles from negative to positive, and this affects the transport and deposition properties of such particles. The importance of electrochemical and electrical charge effects develops significance in much later models of deposition.

8.3. Modelling Codes that have been Widely Used

In this section we consider in turn some of the more widely used modelling codes, describing their essential features, together with strengths and deficiencies.

8.3.1. The BOA Code

The BOA (Boron Offset Anomaly) code has been developed by EPRI in collaboration with partners including NNL, in the UK. The BOA code has been described by Henshaw et al [99]. The BOA code consists of three coupled models described as follows.

- A bulk transport model which describes the movement of all species around the PWR primary circuit. This covers corrosion product formation (based on the molar fluxes of nickel and iron passing through the inner oxide layer on stainless steel as the typical out of pile surface) plus transport, release and deposition (in terms of both soluble and particulate species), and finally precipitation where the flux of material precipitating (or dissolving) is calculated from known parameters.
- A porous crud model which calculates material behaviour within steam channels on the Zircaloy fuel pin surface. This aspect of BOA draws heavily on the wick boiling model developed by NNL and discussed in detail in Section 8.3.3 below.
- A zinc model which calculates the extent of zinc uptake by the following pathways. Absorption on non-fuel surfaces, uptake in (out of core) outer oxide plus core crud, uptake in (out of core) inner oxide – via solid state diffusion from the outer oxide, and finally uptake by precipitation of zinc minerals within core crud.

The BOA model includes an extensive reaction set for chemical reactions, which is divided into

fuel surface reactions and out-of-core surface reactions. Fuel surface reactions include those involving lithium, boric acid, zinc and silicon. The reactions at out-of-core surfaces involving bulk coolant include the reactions of iron and nickel, and their hydroxides and oxide precipitates.

Added to all of this are reactions describing boron – lithium – hydrogen chemistry throughout the system. Where necessary equilibrium constants are calculated using a non-ideal thermodynamics approach, based on the Meissner method.

The model describing the primary water circuit is broken down into approximately 18,000 nodes (in a four-loop PWR) of which 50 to 100 are out-of-core. The reactions for lithium – boron – hydrogen are decoupled from the reactions for nickel and iron chemistry, in the bulk coolant. The model works by solving steady state equations, based on mole fractions (rather than absolute concentrations). This approach gives much greater stability and reliability. The model only solves the equations for fuel surface deposits in the nodes where fuel surfaces are present. The model recalculates the rate of SNB since the flux for a clean core (no crud) differs from the flux in a core with crud; thus the local thermal hydraulics are constantly being adjusted. The saturation temperature is recognised to be a function of the concentrations of boron, lithium and zinc, and this in turn affects the flux of SNB. Ultimately the crud deposition rate is recognised to be a function of all the chemistry, and within the relevant nodes, all the equations are coupled.

Comparisons of model prediction and plant observations are provided, principally in relation to Vandellos power station. Modelled and measured values for soluble and particulate nickel at Vandellos in Cycle 15 are presented and show generally good agreement. In regard to fuel crud composition, the in-core masses of nickel ferrite, nickel oxide and nickel metal are calculated, for two fuel cycles (15 and 16). A plot of both calculated and measured nickel to iron ratio is presented for Vandellos cycles 15 through 18 (copied here as Figure 16, showing very good agreement for the first three cycles, but some subsequent divergence. The overall trend though, of gradually increasing nickel in the core, is correct. Likewise, the model for nickel release at shutdown / end of cycle shows reasonable agreement with Vandellos plant data at Cycles 17 through 19, despite some inconsistencies at Cycles 15 and 16 (which may be due to some mid-cycle shutdowns, perturbing the normal plant conditions). The model makes the assumption that at shutdown only metallic nickel is released and that oxides of nickel and iron are not released.

Zinc bulk coolant concentration has been modelled and compared with plant operations, at Vogtle Unit 1. Across a three-cycle period, with one short period of zinc injection, the model reasonably well predicts the bulk zinc concentration. The coolant chemistry model is based on the specified zinc feed rate, and the model indicates that most of the zinc is captured in out of core surfaces, by diffusion into the inner oxide. The relevant diffusion rate decreases with successive zinc injection campaigns, and also the diffusion rate constant varies with the alloy type in the SGs, which comprise the vast majority of the out of core surface area.

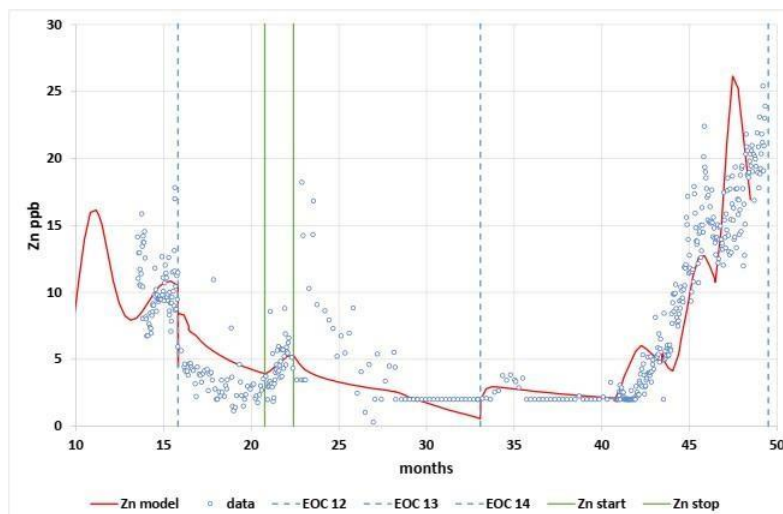


Figure 16: Model and plant data for Zn at Vogtle Unit 1. (From [99])

The reason for the significant increase in zinc beyond 42 months in the above Figure is not apparent, although it must have been due to some effect that was modelled correctly (possibly some unscheduled shutdowns, in mid cycle). At shutdown there must be some release of zinc back to the coolant as out-of-core outer oxide either spalls off or dissolves, and its constituents re-equilibrate with the bulk coolant. Byers et al [100] also present a comparison of plant and calculated values for zinc uptake, over a number of fuel cycles, at Watts Bar power station. The calculated and measured values agree well, indicating a decreasing trend as the system as a whole approaches zinc saturation.

The BOA code has been used to model an "ideal" PWR plant starting from a new and clean condition, calculating the mass of core crud as a function of time. Two crud formation routes are considered, firstly simple precipitation of solution species and secondly precipitation plus particulate deposition. Since the plant is initially clean and has no oxide anywhere, to act as a source for particulates, it is hardly surprising that for the first 100 days all crud deposits are from precipitation of solution species. However, as time progresses, and out to 500+ days cycle time, the mass of crud due to particulate deposition increases (as does crud from precipitation) towards an end situation where the mass of crud from each source is comparable.

In conclusion, Henshaw et al [99] state that the BOA model is based on basic chemistry with reasonable values for uncertain parameters. The BOA code predicts many plant chemistry variables and has been benchmarked against various sets of plant data. It is recognised that the model is not perfect, and benchmarking continues using loop data for zinc behaviour in crud. The stated aim is to make BOA a useful tool in understanding and predicting PWR primary circuit chemistry, along with understanding the CIPS phenomenon.

8.3.2. The APACT Code

The APACT (associated-perturbed-anisotropic-chain theory) code is indirectly required to model crud chemistry in the BOA code. The model is described by Dickinson et al in [77]. APACT, amongst other things, covers the chemistry and distribution of boric acid, and it accounts for hydrogen bonding, dispersion, and polar interactions according to an equation of state. The APACT approach has been used previously for modelling the physical chemistry of water, and since aqueous boric acid has these same types of interactions, APACT is well suited to describe the boric acid aspects of PWR coolant chemistry.

Noting that at elevated temperature, and in contact with a gas phase (steam) boric acid may partition into the gas phase so there are both aqueous and gaseous aspects to the concentration, Activity, fugacity, concentration and molar density of both the boric acid molecule ($B(OH)_3$) and its polymerised forms, principally the dimer and trimer formulations. APACT then predicts all the necessary physical parameters and species distributions for these forms of boric acid, in both phases and as a function of pressure, temperature, initial boric acid concentration, pH, etc.

The APACT model has been calibrated against a literature methodology (IAWPS95) for calculating the vapour pressure of pure water from zero Centigrade up to the critical point (374 °C). The agreement was essentially identical. Similarly, the distribution coefficient for boric acid partitioning between aqueous and gas phases across a wide temperature range has been modelled and compared against experimental data, with the results seen in Figure 17.

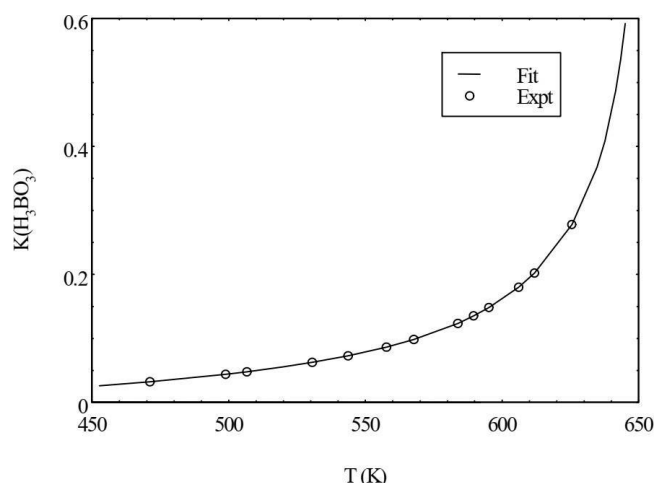


Figure 17: Experimental data and APACT fit for the distribution of boric acid between the liquid and vapour phases. (From [77])

Similar good agreement was obtained in plots of $B(OH)_3$ mole fraction versus pressure, over the temperature range 80, 90 and 100 °C, using thermodynamic parameters evaluated from optimised APACT calculations. From this basis, other (otherwise unknown) thermodynamic parameters for boric acid chemistry have been evaluated.

From this foundation, APACT has been used to evaluate boric acid chemistry parameters required for the modelling of crud chemistry.

One particular claim made of the APACT code is that it provides very accurate information concerning the boric acid chemistry inside the crud pores. However, this is a 2005 claim, based

on the understanding at that point in time that crud porewater temperature is never more than one degree in variance from bulk water temperature. The basis of that claim was later overturned by the wick-boiling model (see Section 8.3.3) which indicated significant departures (to above critical point) for the water in the bottom of a steam chimney in thick crud.

Since 2005 our understanding of the aqueous chemistry of boric acid has been advanced through the recognition that at Beginning-of-Cycle (BOC) PWR concentrations ($> \sim 2000$ ppm B) and at high temperatures, boric acid may form dimer and trimer molecules [101] [102]. However, it must also be recognised that these calculations and experiments are in the absence of a radiation field which, through the agency of radiolytic products, may have a further influence on the chemical speciation of boric acid.

8.3.3. The Wick Boiling Model

One approach to the chemistry within a crud pore is the wick boiling mechanism, developed by Henshaw and co-workers [77]. The wick boiling mechanism is comprised within a code known as the Crud Chemistry Model (CCM). This is a one-dimensional model that describes the process of a steam bubble forming in a pore within the crud layer, and the chemical and physical processes which occur at the various phase interfaces. There is the water / steam interface at the bottom of the pore, and again a water / steam interface at the mouth of the pore where the bubble meets bulk coolant. At the various interfaces there are processes including (a) chemistry resulting from the radiolysis of water, taking into account the alpha dose from the $^{10}\text{B}(n,\alpha)^7\text{Li}$ reaction (b) magnetite dissolution and hydrolysis reactions of iron (c) nickel – iron ferrite dissolution and nickel hydrolysis reactions (d) nickel metal and nickel oxide formation (e) boric acid chemistry and the precipitation of lithium borate; (f) non-ideal solution thermodynamics and (g) the effect of solute concentration on the saturation temperature and vapourisation enthalpy of water. Figure 18 illustrates the principal features of the model.

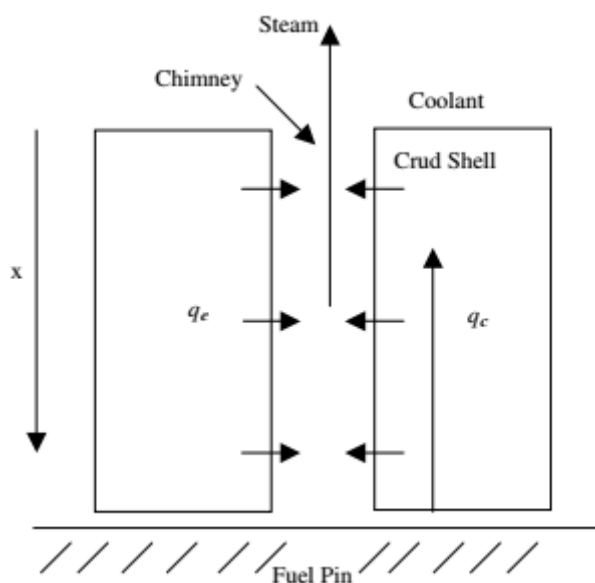


Figure 18: Schematic diagram of heat transport during wick boiling. q_e is the evaporative heat flux and q_c the conductive heat flux. (From [103])

The model addresses physical effects including thermal hydraulics, liquid flow and transport, solution and precipitation chemistry, the radiation chemistry (recognising the effects of gamma and neutron radiations, in addition to the in-situ alpha radiation from the $^{10}\text{B}(n,\alpha)^7\text{Li}$ reaction). The model as a whole is coded and solved using the FACSIMILE chemical modelling platform,

which is based on a predictor-corrector form of integration. Using a set of input conditions which are considered typical of PWR operating conditions and chemistry, the CCM has been used to address various crud features observed in crud scrapes and other measurements from operating plant, including the layering of different metal oxides within a single crud flake retrieved from a scrape sample (see Figure 15).

One significant finding, through use of this model, is that $\text{LiBO}_{2(s)}$ is precipitated at a particular depth (between 35 and 40 μm) down the steam chimney, which is in good agreement with plant scrape measurements for the crud depth at which CIPS occurs. This is now understood to be a reflection of the temperature gradient through the crud, and the required temperature for this precipitation reaction is reached at this particular depth down the steam chimney. The model also points to extreme conditions at the bottom of the steam chimney, if the chimney depth exceeds approximately 60 μm , whereby the temperature approaches 400 °C, well above the critical point for pure water. Also, though not explicitly commented in this paper, close to the initiation temperature for the runaway Zircaloy-steam reaction: there is a comment that the impact of such temperatures on cladding corrosion rates has not yet been reconciled. There is discussion of the implications of such temperatures on heat exchange rates, notably that the enthalpy of vaporisation decreases as a function of temperature and is zero at the critical point (364 °C). Thereby, at these high temperatures, one of the heat loss mechanisms ceases to function, leading to even higher temperatures at the bottom of the steam chimney, and thus the extreme conditions that may be needed for formation of the mineral bonaccordite (Ni_2FeBO_5) which has been observed in some crud scrapes (very thick crud flakes of over 80 μm thickness). Output from the model indicates that T_{crit} is achieved at a chimney depth of around 35 μm (and at the plant chemistry conditions specified).

The inclusion of nickel and iron in crud mineral phases has not been fully described or reconciled against observation, the paper recognises several factors that may underlie this difficulty. These principally relate to the variation of chemistry conditions through the course of a fuel cycle, in terms of boron concentration, pH, redox conditions, the varying form of the mineral deposits, and the rate of inter-conversion between various mineral forms. There is data reflecting the variation of deposit temperature as a function of crud thickness, for a range of coolant boron concentrations, for example for a crud depth of 60 μm the deposit temperature varies between 380 °C and 400 °C across a corresponding boron concentration range of 1800 to 300 ppm. Similarly the concentration of hydrogen peroxide (a key radiolysis product) at the bottom of the crud varies increasingly at greater crud depth, and becomes significant at crud depth greater than 50 μm : for example, at 60 μm depth the concentration of hydrogen peroxide (a strongly oxidising radiolysis product) is 0.1 molar when the coolant chemistry is set at 300 parts per million (ppm) boron, the concentration of hydrogen peroxide maximises as 0.35 molar at 600 ppm boron, then decreases to a consistent 0.02 molar at boron concentrations greater than 1200 ppm. The hydrogen peroxide concentration is linked to the dissolved hydrogen concentration (the two will react in a radiolytic system) and the hydrogen solubility is inversely proportional to temperature. There are thus competing effects, the effect of decreasing boron concentration is to minimise precipitation of boron-containing species that then give rise to alpha radiolysis and thus produce H_2O_2 , but at the same time for a given crud thickness, a lower boron concentration increases the temperature, decreases the dissolved hydrogen concentration, and enhances the H_2O_2 concentration. There is a complex interplay of many factors, which will influence the crud composition and interfacial processes. Henshaw et al [103] conclude with a remark that further work is planned to attempt to resolve the crud composition and in particular the amounts of Ni and Fe present.

There is an update to the BOA code from 2018 [99]. Here the BOA authors describe additional features to incorporate processes such as zinc uptake, in products such as zinc oxide and zinc

silicate. This is a new insight to the importance of silica in the coolant water, as well as having a number of zinc oxy-/hydroxy-boron compounds in the reaction scheme. The BOA V4 model seeks to simplify matters by only modelling crud in regions of the core where there actually is crud. Other simplifications are made, such as calculating using mole fractions not concentrations, which is much more mathematically stable. Additionally, the rate of SNB (originally calculated by VIPRE, see Section 8.3.4) is now recalculated because the thermal heat flux through an adherent crud is quite different to the heat flux from a clean surface (which is what VIPRE uses). The bulk transport model for movement of Li, B and H₂ around the circuit is now decoupled from Fe-Ni chemistry, which is most relevant to crud only in the core region.

The output of this upgraded BOA code is a good simulation of plant, in many respects, but not perfect. See Figure 16 for one such comparison, but also see Figure 19 illustrating some difficulties modelling plant nickel in shutdown releases, for the first couple of fuel cycles, but then a much-improved simulation in subsequent cycles after the plant had equilibrated.

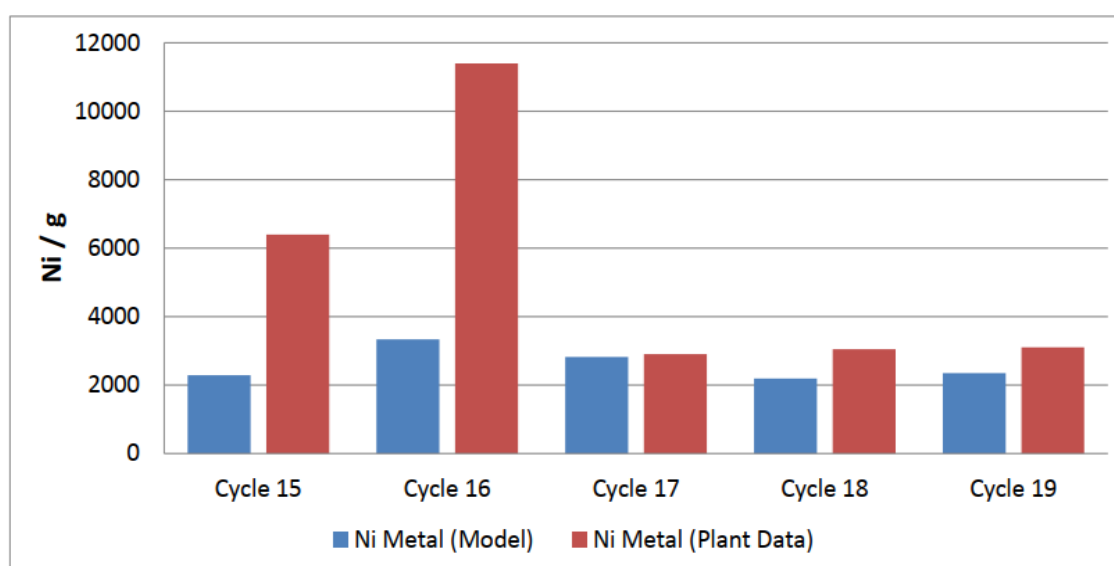


Figure 19: Model and plant data for shutdown Ni releases at Vandellos. (From [99])

BOA clearly represents a continuing and generally acceptable model for crud chemistry and deposition, with recognition that it contains many assumptions, which are being tested out in, for example further loop experiments.

8.3.4. The VIPRE Code

The VIPRE code is not a crud deposition model, but it is widely referred to in the context of crud formation and therefore merits some mention. This code calculates aspects of steam boiling parameters in a two-phase flow context, and thus feeds data into a number of other codes or models. A key factor in core performance is the void fraction, or the proportion of the core that is occupied by steam (rather than condensed water). Since steam has very different neutron moderation properties to water, the void fraction has a direct bearing on core neutronics. There are a number of codes which address this matter, such as RELAP, RETRAN-3D and CORETRAN-01 (often coupled with VIPRE-2) [104].

Since the formation of crud is attended by the deposition of dissolved material out of water as it turns into steam, the void fraction in a PWR is a guide to how much dissolved material is being deposited on the fuel surface. There are various codes which may address this; each covers some specific aspect of core thermal hydraulics, and codes are often used in combination. The

VIPRE code has evolved from the relatively simple VIPRE-1, to the more sophisticated VIPRE-2 and to the Westinghouse-specific VIPRE-W.

There is no obvious ranking of which of these void fraction / steam quality models is better, they are all used in the literature, however since VIPRE has been adopted by Westinghouse it is clearly one of the leading options for use with a crud deposition model.

8.3.5. The LANL ChemPac Model

The ChemPac model is referred to in [105]. In light of its very straightforward tenor, [105] provides an excellent primer for the non-expert to gain a first survey of the world of crud modelling, as reported by the Los Alamos National Laboratory (LANL). That paper provides a less theoretical introduction to the topic of crud modelling, and a survey of progress to date (2011). The objective of that paper is to review the history of the BOA model and the efforts to avoid CIPS and Crud-Induced Localised Corrosion (CILC). The stated intention is that these older models lead to the latest micro-scale model (MAMBA – see Section 8.3.7) for use in the Consortium for Advanced Light Water Reactor Simulation (CASL) program – see Section 8.3.9.

The progress to date is then applied forward, with a view to multiscale modelling anticipated through using LANL's ChemPac code (via its 2D grid structure and computational capability for coupling mass / heat transport with chemical kinetics). The intention being to use such code coupling at the macroscopic scale, then micro scale, and finally the finest scale anticipated is the atomistic. Descriptions are given for model development at each of these scales.

However, a word of caution should be exercised regarding the atomistic scale (and there are already included in that paper various caveats concerning the difficulties of calculations at this scale). An additional difficulty which those authors do not identify is the radiation chemistry phenomenon of "track and spur" transmission of ionising radiation through a medium such as water, where transmission of particles such as neutrons and gamma rays proceed via a "track" and cause discrete Compton interactions leading to "spurs" (very small local regions where the products of radiolysis interact with each other and with water molecules, solutes). At the atomistic level, (and at scales representing porous surfaces below around 10 nm) there is physically not the space for a spur to form, therefore the active radicals and their precursors will react with surfaces and not with each other, therefore the familiar "G values" for radiolysis product yields will not be suitable for plugging in to a model. A new approach to radiation chemistry, as a fundamental point, is required for modelling at the atomistic scale in proximity to finely porous surfaces.

8.3.6. The MOOSE / BISON Crud Chemistry Models

A good introduction to the MOOSE approach (Multiphysics Object Oriented Simulation Environment) is provided in [106]. Over the years since [93] [94] (1987 and 1990) the CRUD SIM model developed at MIT (see Section 8.3.2) has advanced into the MOOSE application platform, although the programming described in [106] is actually coded in C++ and MOOSE is a system architecture, not a coding language. The MOOSE framework uses an object-oriented approach to develop extensible sub-systems to represent physics, set up meshes, applying boundary conditions and material properties, and execute solves. The work described in [106] borrows from an activity transport model developed by Macdonald et al [107] in 2006. MIT also published a further (2018) paper based on the MOOSE architecture, but addressing the MAMBA crud deposition model [108] (see Section 8.3.7).

The work by Macdonald et al [107] set out with an electrochemical emphasis, to calculate the

ECP at specific locations within the reactor primary coolant circuit, using the Mixed Potential Model (MPM). As discussed in the introduction to this section, here the term “model” really means a mechanism or concept, rather than a fully-fledged computer model. One clear difficulty is that not all the required data is adequately known and an amount of assumption and educated estimation is necessary. Macdonald et al sought to overcome this problem by deploying the Point-Defect Model (PDM) however they found that this did not give satisfactory outcomes, largely because the PDM applies to a situation of passivity, where corrosion is not actively progressing.

Returning to CRUD SIM, Macdonald et al observe that this is a whole-loop crud build-up model (i.e. that “crud” refers to all corrosion products, wherever located in the primary circuit).

The primary circuit is nodalised by Macdonald et al [107] as follows in Figure 20. It is this same nodalisation which is adapted by Elliott [106] in the MIT MOOSE model.

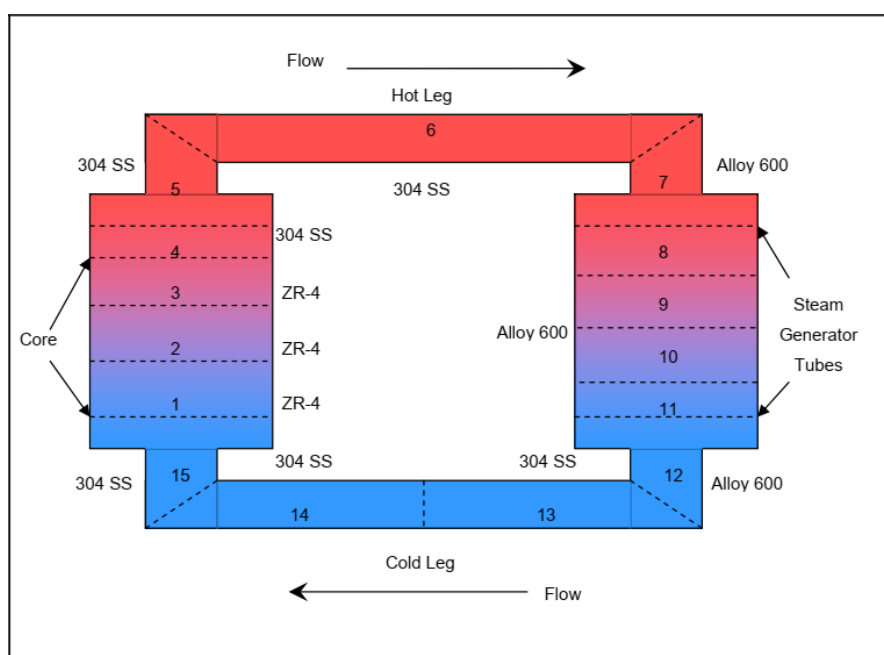


Figure 20: Loop nodalisation for ECP model. (From [107])

In applying this nodal model, Elliott used corrosion source terms derived from [88] which are probably an over-simplification, since Castelli [88] was primarily interested in out of core corrosion product deposition.

Elliott [106] points out that the MOOSE framework is a multi-physics solver which uses fully coupled and implicit approaches together with a finite element library (libMesh) to generate automatic parallelisation and mesh adaptivity. The MOOSE framework is designed to solve tightly coupled sets of partial differential equations (PDEs) on arbitrary geometries using implicit numerical and finite element methods, but is considered to be physics-agnostic; that is, the framework is not specifically adapted for any particular field or application. A variety of physics problems may be addressed through MOOSE-based applications including nuclear reactor fuel performance modelling (BISON). The distance and time scales of these applications can be varied to suit the problem being addressed.

The results of Elliott’s MOOSE model [106] indicate most activity deposition in the SG and the SG end of the hot leg, with another peak in deposition in the cold leg. Results are mainly

compared with those of Macdonald et al [107]. Clearly there is scope to improve on this initial study; particular areas for improvement include the fixed pH and ECP around the circuit, the loop temperature profile and the neutron flux profile in the core.

Using the MOOSE architecture, a further modelling development has been the BISON model, which specifically considers fuel in the reactor. This is reported by Williamson et al [109] who describe BISON as a nuclear fuel performance application built using the Multiphysics Object-Oriented Simulation environment (MOOSE) finite element library. Here the emphasis is on modelling fuel performance due to the multiple physical effects such as thermal stress, hoop stress and pellet-clad interaction. In a further development of BISON Gaston et al [110] describe a module which includes crud growth. However, it assumes that crud growth rate is uniform with time, and there is no indication that the model includes the fine detail of crud structure (the implication is that crud is treated as a homogenous material and that it has a role in impeding heat flow). There is no reason to suppose that a yet more complex model could not be devised, and since [110] was published in in 2015 there may well have been some development, however nothing further was identified in this current work.

A MOOSE model simulating fuel, particularly, has been reported by Jin and Short (Figure 21) [108]. On the basis of this model, and recognising the difficulties of mechanisms such as wick boiling to accurately simulate the observed heat transfer, they propose a new mechanism of "double dryout" specifically applied to thick crud deposits on fuel. Their view is that crud deposits will continue to form until the rate of deposition and crud growth are balanced by the rate of crud loss, through shear stresses from coolant and erosion, at which point equilibrium is achieved.

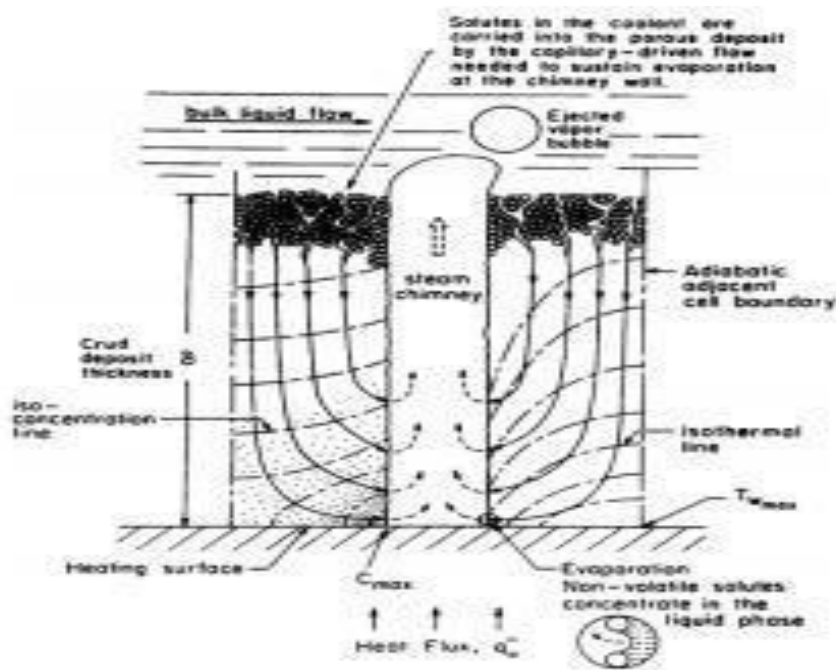


Figure 21: The 2-D model of steam chimneys, after Pan et al [111], as implemented by Jin and Short [108]

8.3.7. The MAMBA Model / Code

The MAMBA BDM (MPO Advanced Materials and Boron Analyzer: Boron Deposition Model) is an atomistically informed micro/meso scale program that tracks the evolution of the boron chemistry inside a single boiling chimney in the crud, coupled with precipitation as lithium tetraborate [105]. As described by Deshon et al [105], the approach has been to start with three

distinct dimensional scales, namely macroscopic, microscopic and atomistic.

The processes involved in this model are shown in Figure 22 indicating the relationship between the different phases, interfaces, and sub-models. The C_i values represent the concentrations of the i^{th} elemental species in each phase where $i = \text{Ni, Fe, B, Li, Zn, Zr, Cr, Co}$.

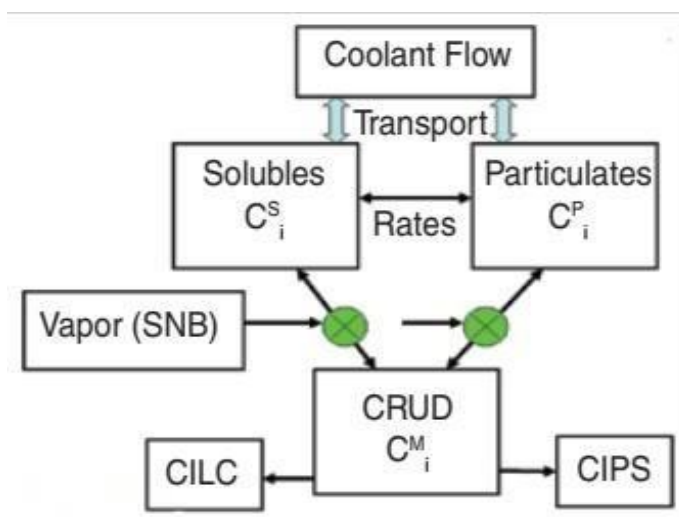


Figure 22: Flowchart of the MPO crud (MAMBA) model. (From [105])

Species concentrations for each phase (particulates, solubles, vapour and crud solids) are defined at each node. The time resolved evolution of these concentrations are then modelled using coupled transport and chemical kinetics calculations. Although aspirational, the atomistic scale of study is too small to be explicitly resolved within the MAMBA framework and such developments will be done separately using techniques such as density functional theory and molecular dynamics. The micro scale model operates at the node level and calculates parameters within the node volume, including time-dependent "sources" and "sinks" for the macro-scale model.

The intention is to incorporate MAMBA (and BOA and VIPRE) into the CASL framework approach (discussed below).

In summary, [105] is an excellent primer and overview of the EPRI consortium modelling progress up to 2011, identifying future aspirations, but also recognising the several caveats which will add complexity and difficulty to further development.

8.3.8. The PACTOLE and OSCAR Codes

The PACTOLE code has been available for many years and was reported in the first conference on water chemistry of nuclear power systems in 1978. It has subsequently become widely used for prediction of out of core radiation dose rates, which was its primary function. It includes aspects of all the primary processes, as shown in Figure 23 [112].

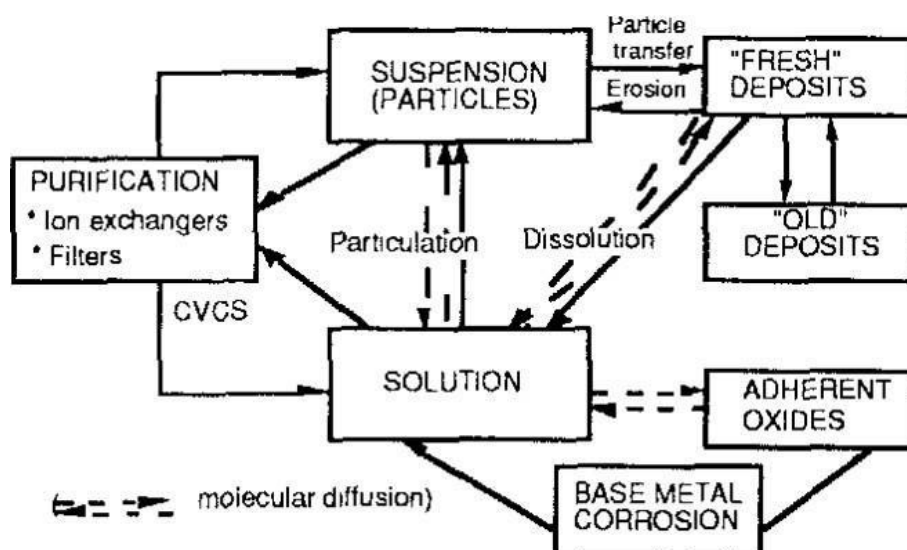


Figure 23: A schematic of the PACTOLE code (From [112])

According to Di Pace and Sandri [112], the PACTOLE model includes the following processes.

- Element concentration gradient between wall and bulk coolant
- Solubility
- Oxidation, Ion release, Oxide formation
- Dissolution
- Precipitation
- Particle growth
- Convection
- Mass transfer (Brownian diffusion, inertial projection, turbulence, gravitation)
- Thermophoresis (heat transfer across surfaces)
- Erosion, sticking probability and lift forces
- Molecular diffusion.

PACTOLE has much in common with other mechanistic models, in that it calculates metal corrosion, dissolution and precipitation, according to available solubility data. The classic reference texts on high temperature metal ion solubility were to be found in the writings of Mesmer, Sweeton and Baes (see for example [113] and [114]). However, the dissolution of magnetite (for example) in a nuclear reactor coolant system has more recently been shown to be partly controlled by dissolution kinetics, in addition to thermodynamic equilibrium solubility [115]. In PACTOLE the deposition of solid metal oxide particles is recognised to be dependent on flow conditions and Reynolds number (turbulence). The PACTOLE model focuses on out of core deposition and radiation exposure to workers. At the 1994 version of the model [96], and including proposed revisions to the model, there were no specific aspects of the model considering crud deposition on fuel assembly surfaces. PACTOLE has evolved, and a more recent version PACTITER is available, but not used for PWR coolant chemistry. Instead, the OSCAR code appears to have taken first place within French reactor chemistry community.

As regards fuel surface deposits, there is no apparent distinction made between out of core deposits and fuel surface deposits, they both consist of "new deposits" and "old deposits", with the supposition that "old deposits" are more fixed and difficult to remove by dissolution or erosion (but with little detail on the structure of the deposits). This really underlines the basis of PACTOLE as primarily for the prediction of out of core active deposits, where a duplex oxide is more commonly observed on stainless steel and nickel based alloy surfaces.

The OSCAR code is the current code available for modelling primary water chemistry in PWRs in France. According to [116] OSCAR has resulted from the merging of two former codes PACTOLE for Activated Corrosion Products (ACPs) and PROFIP for fission products and actinides. It is then the intention for the OSCAR code, by design, to predict the activation product transfer in a PWR reactor coolant environment. It also has application in the modelling of activity transfer within fast reactors and fusion reactors, which is the main subject of [116] with some derivative models such as OSCAR-Na and OSCAR-Fusion. The equilibrium concentrations of ionic products are obtained from an extension of the PHREEQ-C model, as adapted by CEA, this derivative being named PHREEQ-CEA.

One particular concern is the reliance on PHREEQ-CEA, noting that PHREEQ originated with the US Geological service as a tool for equilibrium thermodynamic species calculations at ambient temperature, and has been used for example in the geochemistry of a geological disposal facility. PHREEQ-C [117] is a version of PHREEQ programmed in the C++ language. The way that PHREEQ-C includes higher temperatures is primarily as a change to equilibrium constants, more than rate constants. There is a facility for adding some aspects of reaction kinetics, but only in a generic way. However, PHREEQ was primarily intended to be used over credible geological aqueous temperature ranges. (The highest temperature mentioned in [117] is 75 °C, in relation to the solubility of gypsum). The actual temperature dependency data are obscured in embedded data bases and are not easily visible or changeable. However, the extension of solubility data to PWR coolant temperatures is a considerable additional stretch. Dacquait et al [116] see this high temperature solubility capability as a strength for the OSCAR code, the details of exactly how this extrapolation to PWR temperatures has been made need to be clarified to give confidence. There appears to be very limited public information on PHREEQ-CEA. It is questionable whether equilibrium thermodynamics (which PHREEQ is based on) should be applied to a highly kinetic-controlled system, such as PWR primary chemistry. In other words, we know what the ideal reaction products should be, but the system may spend a long time getting there. (As noted above in relation to dissolution kinetics of magnetite [115]). The only public domain reference to PHREEQ-CEA is Wang et al [118] who point the reader to a "personal communication" from CEA. Whilst it is presumable that PHREEQ-CEA has received rigorous scrutiny within CEA, the lack of visibility of PHREEQ-CEA and any public domain verification is a residual concern.

The other clear distinction between PACTOLE and OSCAR is the inclusion of PROFIP capability for fission products and actinides. Unless fuel fails there should not be any significant transuranic or fission product chemistry in the coolant, excepting for tramp uranium originating on intact fuel surfaces ex-factory, and that should be very low indeed. But under reactor operations fuel cladding does fail, and that opens the possibility for these additions to the circuit chemistry. This review has not found this capability in any other reactor chemistry modelling code.

8.3.9. The CASL / VERA Approach

The Consortium for Advanced Simulation of Light water reactors (CASL) has endeavoured to simulate the crud formation process in a more complete sense, by coupling together several codes and having them inter-relate to one another [119]. The overall approach of CASL is to simulate every aspect of LWR fuel performance, with an overall modelling approach known as VERA (Virtual Environment for Reactor Applications), where six different challenges relevant to aspects of fuel performance are inter-linked. A schematic of these inter-linking challenges (from [120]) is shown in Figure 24. Note that VERA picks up the MAMBA model (discussed above) as one of its key components. Within the CASL consortium there is a Materials and Performance Optimization group (MPO) which performs model development in order to improve predictions of crud formation.

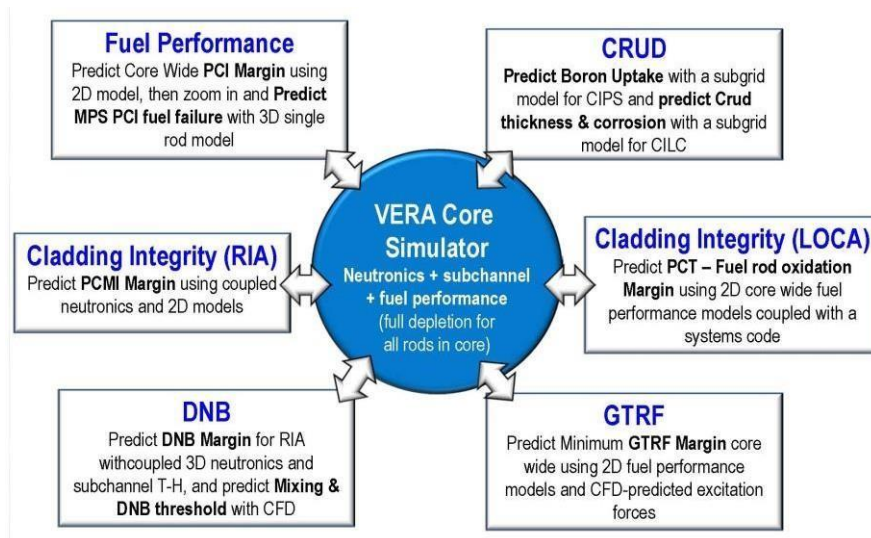


Figure 24: A schematic of the VERA performance simulation environment, (From [120])

The overall approach is to use a number of different models to address different parts of the problem, but in a way that feeds information from one model to another in an integrated and systematic manner.

Clearly, crud is only one of the challenges that VERA seeks to address, and specifically the intention is not only to model crud formation, but also CILC.

The exact method for calculating crud deposition and thickness has evolved with time. An early demonstration of the fuel crud code interactions from CASL is shown in Figure 25 [120]. This later paper on the same topic shows an updated approach to crud modelling, in which the various modules inter-relate and feed information to and from each other.

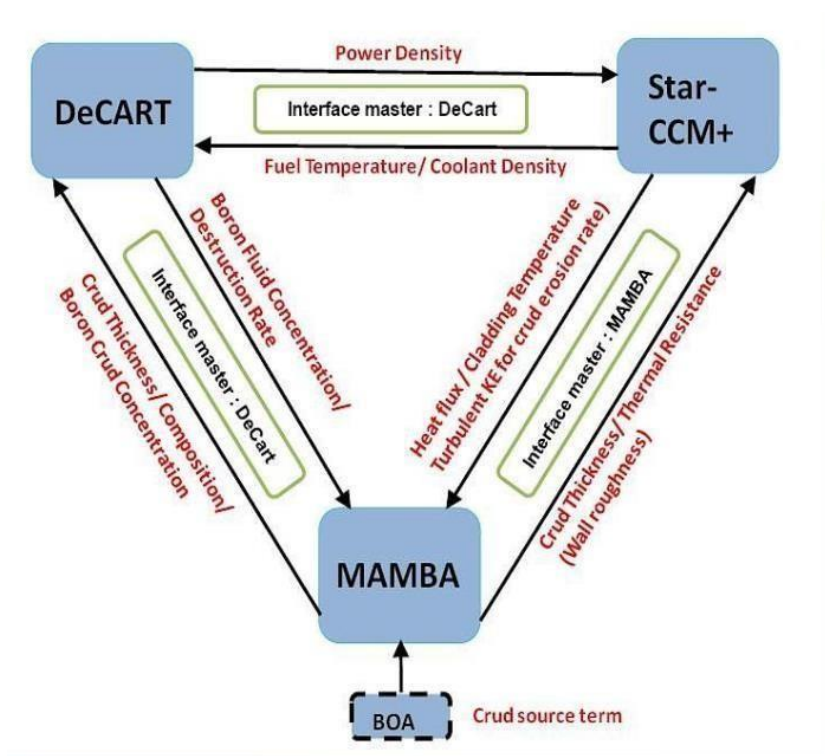


Figure 25: A schematic of the CASL-CRUD model as a demonstrator. (From [119])

The approach picks up various model approaches for processing specific data (such as crud deposition) and integrating them in an overall model of the PWR core.

8.3.10. The Electrostatic Deposition Effect

The effect of electrostatics on crud deposition is generally acknowledged, but modelling has been mainly confined to out-of-core scenarios.

The exception to this statement concerns models which include colloidal species as crud precursors, and the core chemistry model DISER does include this route within the overall material transport flux. DISER was more widely referred to and was included in a 2012 review of models by IAEA [121] and a paper describing the details [39].

However, DISER is primarily directed to VVER circuit simulations, and its colloid transport / electrostatic charge loss / deposition mechanism is not replicated elsewhere, as far as can be determined. There was a short-lived attempt at this by AEA Technology plc (2001) in a hybrid model of DISER applied to Mitsubishi PWR conditions, in a model named ACTRAN, however only one item was ever published [10] (mainly concerning loop tests on zinc injection and comparison with model results).

The various processes modelled in DISER are portrayed in Figure 26.

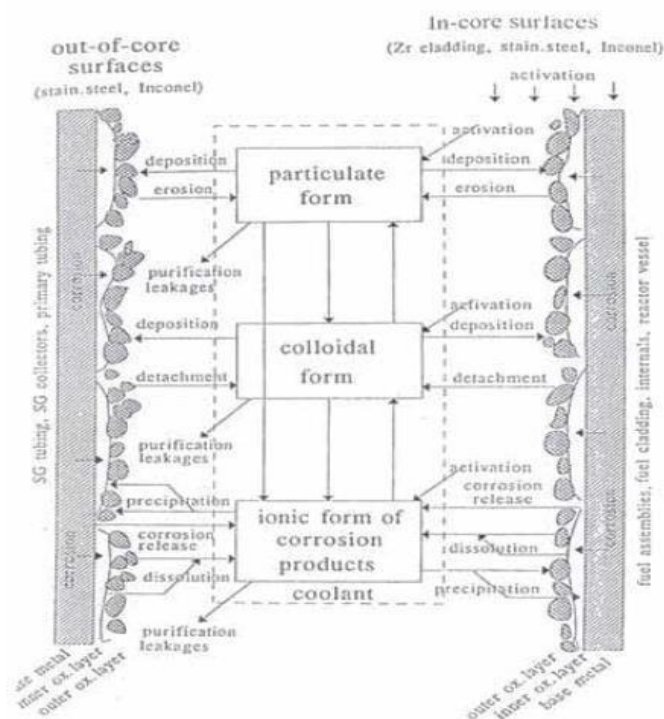


Figure 26: A schematic of the processes modelled by the DISER code (From [39])

The topic of electrostatic effects influencing crud deposition out of core deserves an extended discussion. It is often assumed that these effects do not apply in-core, but there is no convincing reason why that should be the case unless radiolytic perturbations are demonstrably stronger in terms of electron availability. There are a number of locations within the RPV where there is a change in flow path cross section / linear flow velocity, such as the transition from RPV bottom plenum to the flow path through the fuel rod bundles.

Concerning electrostatic effects, the literature on PWR crud deposition, as a whole, has been reviewed relatively recently (2019) as part of a doctoral thesis [122]. The aim of that thesis is stated to be "to facilitate the development of an all-inclusive deposition model, which will reproduce the morphology of deposits found in actual plants and assist in elucidating the electrokinetic mechanism". This was a highly aspirational target, and the programme of work was conducted using the finite element approach wherein multiple other models may feature. The principal approach was that of considering the relationship between fluid dynamics and the streaming current, which arises as an electrokinetic effect (particularly when pipework changes diameter) and then affects the EDL, in turn influencing the deposition of crud. This is in essence a study of "why does crud form in the locations it does, and what are the controlling factors?". Regarding location, it is noted that in the primary circuit as a whole, crud (and Wu uses this term to include out of core corrosion product deposits) forms at pipe locations with restrictions, which is identified as the type of location where electrokinetic influences may be greatest.

Wu's literature review section [122] is comprehensive, but only in regard to out of core surfaces, their crud deposits, and the details of iron, nickel and chromium hydroxy-oxides which make up

the various layers of corrosion product. In terms of orifice geometry, the SG tube sheet is a primary area of concern. Wu also presents a thorough review of the electrokinetic processes and the various concepts which define the electrical double layer.

Regarding fuel crud models, Wu notes some of the models discussed above.

He notes that these models describe the physics and chemistry taking place within the crud, not the original formation of the crud.

Since the main aim of this thesis is to investigate electrokinetic effects on crud deposition, Wu mainly describes hybrid models where one or other of the above chemistry models is coupled with an appropriate finite element model for electrokinetic effects. Specifically, he describes the following chemistry models.

- The wick boiling model (see Section 8.3.3).
- The Moose Crud Chemistry Model (MCCM) (see Section 8.3.6).
- There have been several particulate deposition models developed over the past few decades, which are briefly reviewed and summarised.
- Computational Fluid Dynamics (CFD) models which describe crud formation are described, noting that crud formation is actually a multi-physics problem. Here Wu begins to describe in more detail the flow conditions within a PWR fuel assembly, particularly noting the coolant swirl introduced by mixing vanes at the structural grids.
- Wu describes a number of models of the EDL, which reflects a charged surface (the cladding, minus some negatively charged species) and the layer of negatively charged species in solution attracted to the surface.
- Models of microfluidics are described; this concerns the manipulation of small volumes of fluid using channels with diameter of tens to hundreds of micrometres. This approach is of relevance to the electrokinetic aspects of crud deposition.
- Models of crystallisation fouling are discussed: these relate to the precipitation of material from solution in such a way as to block or foul flow paths. The effect follows the condition of supersaturation, followed by nucleation, followed by crystal growth.

In order to describe and model crud formation, Wu develops three models, of increasing complexity. First, a turbulence model, set up in COMSOL, to describe the turbulent flow within a PWR primary circuit. From this, he develops a fluid dynamics model in order to investigate the effect of shear rate on electrochemical streaming current. Second, a conductivity model to investigate how the current distribution is affected by the electric field. Thirdly, a Combined Electrochemistry, Conductivity and Fluid Dynamics (ECFD) model is developed.

The Fluid Dynamics model include descriptions of changes in diameter to flow paths, including varieties of joint profile, e.g. radial, chamfered, orthogonal. These physical arrangements are depicted by meshing configurations to convey the model in a computational finite element system. At each step various tests and sensitivity studies are made and reported. With each geometry possibility, further studies were made of deposition rate as a function of time, indicating zones of preferred principal deposition and ripples of increased deposition at distances away from the principal deposit. A flow facing step is introduced as a concept where flow is perturbed by a step-change in pile diameter or some feature such as a tube sheet or valve.

The Conductivity Model is actually a series of four incremental models constructed to investigate different attributes of the EDL and its effect on the deposition process. A range of flow path geometries are considered, and again meshing is used to create a representation of the various solid geometries. Specific aspects which are studied include the velocity field, the current path, the overpotential and normal current density, potential distribution in the solution, and (for the

fourth model only) deposition growth.

The results of the model indicate that the concentrations of solution species can vary significantly (orders of magnitude) between the metal surface and the EDL (around $1\text{E}-7$ m from the surface). There is consequently a dependency of the deposit thickness versus time, depending on the surface charge density. In summary, Wu remarks that in the one-dimensional model the EDL affects the solution species concentrations by a few orders of magnitude, changing the pH and the soluble iron concentration. In turn these may have an effect on magnetite solubility and deposition rate. The two-dimensional model was constructed with a hypothetical 90° cornered sudden reduction in tube diameter, this produces an array of fluid velocities around the tube constriction and in turn these affect the surface potential. In consequence, overpotential and net surface current values can be calculated, with the locations of anodes and cathodes. Deposition at the flow facing surface is both calculated and expected from plant observations. There is also some prediction of other deposit locations (embodied as ripples in the oxide) further along the restricted pipe length.

In summary, Wu's work is a thorough investigation of surface electrochemistry effects on crud (specifically magnetite) deposition, as a function of solution chemistry and consequent impact on the electrical Double Layer. It does not consider boric acid chemistry, but does lay down models for various aspects of electrochemistry and deposition chemistry that could be extended, if so desired.

8.4. Summary and Discussion on Modelling Codes

8.4.1. The IAEA Model Cross-comparison

Having discussed and reviewed the various models and the mechanisms behind them, the reader will wish to know "which model works best" and "which ones are actually available and supported today?" This very question was the subject of a round-robin blind simulation test carried out in 2012 under the auspices of the IAEA [39].

This stemmed from a symposium (1994) in Canada to bring some cohesion to the large number of models (even then) and to promote discussion amongst modellers, particularly for mechanisms applicable to CANDU reactors. The ensuing IAEA Coordinated Research Program (CRP) on Activity Transport Modelling ran for over a decade and included a blind benchmarking exercise. Unfortunately, the UK was not a party to that CRP. The participating countries and their level of involvement is shown in the following Table 3.

It is immediately apparent that the modern-day front-runners such as BOA, do not appear in this listing. Neither do the leading organisations such as Westinghouse or EPRI. This makes the exercise more of a historic record, than a guide to current performance.

Reference [39] also provides a summary history of the attempts to model reactor activity transport, as well as a summary of the main processes. However, this background material is without reference to any boron chemistry or the effects of zinc addition, and focuses on out of core activity deposition.

Table 3: Participating countries, organisations, and models / roles in the IAEA 2012 cross-comparison of modelling codes

Country	Organization	Model	Application	Role
Argentina	CNEA	-	-	Consultancy
Bulgaria	INRNE	MIGA-RT	VVER	Expert & Consultancy
Canada	AECL & UNB	CANDU AT	CANDU	Consultancy
Czech Republic	NRI	DISER	VVER	Expert & Consultancy
Finland	IVO	-	-	Consultancy *
France	CEA	PACTOLE 2.2	PWR	Expert & Consultancy *
Germany	SNP	-	-	Consultancy *
Hungary	VEIKI	RADTRAN	VVER	Expert & Consultancy
India	BARC	-	-	Consultancy
Japan	MHI	ACE	PWR	Expert & Consultancy
Norway	Halden	-	-	Consultancy
Rep of Korea	KAERI	CRUDTRAN	PWR	Expert & Consultancy
Russia	VNIPIET	-	-	Consultancy
Slovakia	Slovenske Elektrarne	-	-	Consultancy *
USA	Penn State University	-	-	Consultancy

Notes: The original designations of "Expert" and "Consultant" and other specialist roles were complex in nature. Here they simply mean that an "Expert" has a working model and a "Consultant" provides high level intellectual input. Those organisations marked * provided the benchmarking data.

In [39] each of the models is described in turn, given the date of the exercise was in the interval 2000 – 2002. Most models do not explicitly consider deposition in core, or even if they do, it is as a simplistic mixed metal oxide of a spinel (or inverse) formulation.

The PWR models ACE, PACTOLE and CRUDTRAN have been described above, in detail. These do bear reference to the coolant chemistry in terms of boron content and pH (Li⁺ ion control).

However, the stated aim of PACTOLE (at this point in time, and for the purpose of this comparison) is to determine the activity in the fluid and the deposited activity of out of flux surfaces. There is no detailed model of fuel crud, as such.

Within [39] are further discussions of an un-named Russian model and a summary of the German approach to modelling, with the implicit existence of a German model, but not one that was subject to this round robin comparison. However, the German model does focus more on the core than the SGs, whereby the core is split into three nodes, and the model works by calculating thermodynamic equilibrium solubility in core node 1 (cold end) then passing on the resulting aqueous chemistry to node 2, and so on. It also considers the involvement of zinc, and has been calibrated against measurements from Siemens plants. Comparisons indicate that for the core regions, the model consistently under-predicts crud distribution in-core.

There is also discussion of an American approach featuring the combined use of deterministic models and an artificial neural network (ANN). This uses a radiolysis / mixed potential mechanism to calculate ECP at four circuit locations, from which the local magnetite solubility is calculated. The model was initially calibrated against data from a VVER, then the ANN was trained to predict magnetite solubility for a different type of reactor (namely PWR). It should be noted that the solubility of magnetite in the primary coolant could be calculated without the ANN, but using the ANN greatly accelerated the calculation speed when large numbers of locations were considered.

For the benchmarking exercise data from two reactors (Cruas-1, France, and Neckarwestheim-2, Germany) were the PWR contributions. The cross comparison indicated that:

- ACE consistently under-predicted the activity of deposited Co-58 and Co-60 for several cycles of CRUAS-1 (although the trend was roughly correct). Whereas for GKN-2 the ACE model over predicted Co-58 but under predicted Co-60.
- CRUDTRAN consistently over-predicted the Co-60 activity in the CRUAS-1 SG and under predicted the Co-58 activity. Therefore, arbitrary adjustment factors were introduced to compensate, but this lack of fundamental agreement implies the model is either inadequate or fed with inaccurate physical data (e.g. solubilities). There was no comparison with GKN-2 due to a delay in plant data availability.
- PACTOLE showed consistently good performance for Co-58 and Co-60 activity deposited at CRUAS-1 and GKN-2. It fared less well when applied to simulations of VVERs, particularly Loviisa-1.

The outcome of the round robin comparison was the conclusion that PACTOLE should work well for French PWRs such as CRUAS, and that the Japanese code ACE should work less well for CRUAS-1 because it uses rate constants in its models based on Japanese PWR operating data. One of the conclusions of [39] (which had evidently been nearly a decade in the writing) was that further development seemed unlikely due to funding constraints. Also, that individual code authors would be unlikely to abandon their code for more purely mechanistic models because of the large investment costs which had already been made for each code.

Nevertheless, for present purposes, and out of this very limited selection of models, the PACTOLE model (and by extension, its modern successor OSCAR) should at least be a good option for modelling out of core activity deposition which infers reasonable in-core activation calculations.

-

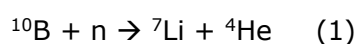
8.4.2. The Latest Models

The past few years (since 2018) have seen various further efforts in a number of specific regards.

- In 2018 a Korean team presented [123] a review of crud growth models compatible with multiphase thermal hydraulic codes. This really focused on only two codes, BOA and MAMBA. Comparatively little is said about BOA, significantly more concerning MAMBA. It emerges that one of the key parameters (determining the rate of loss of crud by erosion) is the Turbulent Kinetic Energy (TKE) which needs to be calculated, and there are various ways of doing so. They conclude with a view that the whole-core model which is addressed using integrated thermal hydraulics is actually inappropriate for calculating crud growth, which would be better approached using a subchannel model of fewer fuel pins.
- A Korean team have developed a multi-physics model known as BOTANI [124] (2021). This model incorporates key mechanisms such as Wick boiling, capillary flow, heat transfer, fluid transport and chemistry, The outputs are calculated temperature and SNB heat flux within the crud layer, the pressure and capillary flow velocity within the crud layer, and the concentrations of boric acid, hydroxide ion, borate anion, lithium ion, hydrogen ion and lithium diborate. The simulation object was an instance of CIPS at the Seabrook Unit-1 plant in 1995, which had separately been modelled using MAMBA. The results from BOTANI indicate the deposition of boron species above a certain temperature value, in the upper spans of the fuel rods, with the amount of boron deposited increasing with crud thickness.
- In 2021 the University of Tennessee published a PhD thesis by J Rizk concerning “thermochemical and continuum modelling to understand the chemical composition of PWR fuel crud” [125]. The main thrust of the thesis is the construction of mechanisms and a model to predict the formation of bonaccordite (Ni_2FeBO_5) a mineral that has been observed in crud and whose formation requires relatively extreme conditions, possibly including supercritical temperatures. This work was funded under the CASL program.
- In a 2022 conference held in China, a Chinese team reported [126] a multi-physics coupling model for thermal hydraulics and solute transport in crud deposits. Again, wick boiling is included, with capillary flow of fluid through the porous crud to the steam chimney base. Solutes are subject to transport and reaction, but again there is no apparent attention to radiolysis or radiation chemistry, although both neutron and gamma dose rates are amongst the feed data. The study confirms the quantity of deposited lithium tetraborate increases with crud thickness. Interestingly, a sensitivity study on the effect of steam chimney radius indicates that the quantity of deposited boron should decrease as the steam chimney diameter increases. There is also a similar dependency on steam chimney density (chimneys per unit area).
- At that same 2022 conference another Chinese research group reported [127] development of a new crud deposition model CAMPSIS. The authors claim the model can perform a quantitative calculation of crud. The software was validated with measured data from the power plant, and the results are claimed to fit the measured data well.
- A second Korean team have published a paper on the deposition and erosion of crud on fuel surfaces [128] (2023). The key feature here is that erosion of crud is poorly accounted for in other models such as BOA. Again, the object of study is the Seabrook-1 plant, and again pointing to the previous MAMBA calculations, the authors comment that models usually depend to some extent on empirical constants or experimentally determined data, leading to uncertainty in results. The absence of a well-defined theory for crud deposition is an additional problem, in their view. In this approach, the rate of

deposition is determined via the subcooled nucleate boiling and deposition area, whereas the rate of crud erosion was determined via the turbulent kinetic energy of the reactor coolant. Consequently, the tendencies of crud deposition to accelerate, decelerate and reach saturation were studied through a range of simulation calculations. Again, this appears to be a multi-physics approach but based mainly on material properties and imposed chemistry: no mention of radiolysis or radiation chemistry. The model calculates numerous results which are presented and discussed; they all point to thicker deposits and AOA occurring at Seabrook. The missing component is any direct comparison of the calculation results with data from Seabrook fuel, such as crud scrapes.

- In 2023 Zaczorowski and Roland [129] presented a summary of the radiation chemistry at a fuel pin surface and the corrosion of zirconium alloys, pointing out that the “critical hydrogen concentration” – the concentration of dissolved hydrogen necessary to inhibit radiolysis and avoid significant production of oxidising species – was affected by boiling, which would effectively strip out dissolved hydrogen into the steam bubbles, leaving the local chemistry unprotected against formation of oxidants. This, together with alpha radiolysis due to the reaction



Which also produces additional oxidising radiolysis products, could lead to unexpected high concentrations of oxidant. They modelled this using a radiolysis modelling code named ARCOL (Advanced Radiolysis COde for Lwr) – a Framatome development although based on the widely accepted Elliot and Bartels radiolysis reaction scheme. It was found that peaks in the dissolved concentrations of hydrogen peroxide and oxygen occurred around 3.5 m in vertical elevation along fuel assemblies. The variation of the applied dissolved hydrogen concentration identified that the critical hydrogen concentration quadrupled from around 0.5 ppm to 2.0 ppm, in order to inhibit oxidant production for all regimes of hydrogen stripping.

8.4.3. The Present Situation

As an overall summary, the situation is one where a number of major international organisations have, over a number of years, assembled a range of models that address PWR fuel crud deposition. Some models developed over 20 years ago now appear to have become disused, possibly because their expert creators have retired or moved on. In the main, the most recent models employ some form of multi-physics approach whereby the physical properties of the system and its materials are coupled with the chemistry to define conditions under which multiple physical-chemical processes influencing the fuel surfaces can be modelled, and indicating whether deposition (or erosion) may occur – often both at the same time. There appears to have been something of a hiatus over the past few years, particularly in the UK, possibly because the models are now becoming so sophisticated that programming is in itself a specialist skillset requiring a multi-discipline team. This is particularly true when advanced programming techniques such as neural networks and machine learning are deployed.

The most recent advances have come from research teams from China and South Korea. Their models are in many ways very similar to the published models from the more established organisations. There appears to be very little to set them apart, although direct comparisons with plant data are few, and comparisons with test loop data are by nature imperfect. This does not develop confidence in a widely applicable capability, from any research team. The leading modelling scheme available to the UK would be the CASL consortium, into which the NNL modelling capability has contributed via BOA and APACT. Alternatively, the OSCAR / PACTOLE model scheme could be accessible via EDF Energy.

The CASL / VERA model continues to be developed and this is likely to be the best UK-based source of information for the ONR, over the longer term. However, a RP could draw on modelling support from any organisation, internationally. But the industry has not yet arrived at the ultimate goal of a fully capable model that can be deployed to successfully simulate any reactor station or with confidence predict any proposed new design. Trends and likelihoods are “attainable outputs” but quantitative replication of reactor data has not yet been realised.

There remains something of a gap in each model scheme, whether it be the apparent neglect of radiation chemistry (in a physics-dominated approach) or the apparent neglect of colloidal species as a contributor to mass transport of activated or corrosion product materials, or the naïve application of radiation chemistry into nanoporous environments where “track and spur” Compton interactions are prohibited. This is further complicated by the lack of reliable data on matters such as solubilities of certain mineral phases at all the temperatures and chemistries of interest; often these parameters are needed and are calculated, but without a wide pool of data for verification. There are aspects that still require improvement.

Whilst the models continue to improve, the skilled practitioners able to evaluate model outputs and assess real plant data appear to be a diminishing resource (due to reactor closures and demographic reasons). Also, the number of skilled programmers with plant awareness, able to implement multi-physics models into this field of endeavour appear to be unrealistically few for the rate of progress to accelerate measurably. Accepting that modelling has a major role in the assessment and management of fuel deposits, and that substantial further development remains, then considerably greater resources will need to be brought to bear.

9. Impact of Fuel Crud on Radiation Levels

9.1. Sources of Radioactivity

The production of radioactivity is an unavoidable consequence of operating a nuclear power station. This follows because the fission process, which releases energy, also produces radioactive fission products, including radioisotopes of krypton, xenon, caesium, and iodine, whose nuclei are unstable and dissipate excess energy by spontaneously emitting radiation. The fuel cladding provides a containment barrier to minimise release of these species into the primary circuit, and reactors are designed to shield workers from the radioactivity within the fuel rods, including during refuelling operations. Therefore, with intact fuel cladding, fission products are not normally a major contributor to occupational radiation exposure (ORE). However, fuel cladding defects may result in fission products and 'tramp' fuel being released into the circuit, and this can then become a radiological protection (RP) issue [130].

Coolant activation products are another source of radioactivity for PWRs, and these include radionuclides formed by neutron interactions with the primary water itself, the dosing chemicals, and adventitious impurities. In general, they are not a concern for worker dose, but some radionuclides are of considerable importance for active effluent control [130]. Notable examples include N-16, C-14, and H-3 (tritium).

For a PWR with intact fuel cladding, and which also has low levels of 'tramp' fuel material, it is activated corrosion products that make the biggest contribution to ORE due to their incorporation into out-of-core oxides, and the associated radiation fields generated by their γ -decay [130]. This occurs by two mechanisms, depending on whether the corrosion products originate from out-of-core surfaces or in-core materials, including the fuel assemblies. For the former, the main steps are as follows:

1. Corrosion product release from out-of-core surfaces.
2. Transport to the core and deposition on fuel cladding surfaces.
3. Activation of the metallic corrosion product.
4. Release of the activated corrosion product from the fuel cladding surface and transport from the core.
5. Deposition or uptake of the corrosion product on out-of-core surfaces.

In the case of corrosion products from in-core materials, the mechanism simplifies to:

1. Activation of fuel assembly or in-core structural material.
2. Release of highly activated corrosion product and transport from the core.
3. Deposition or uptake of the corrosion product on out-of-core surfaces.

For in-core materials, neutron activation in-situ can lead to the release of radioactive corrosion products directly, whereas release from out-of-core surfaces must result in transport and deposition in-core before activation and re-release to the coolant can occur [97]. It follows that in-core materials are likely to release mostly radioactive corrosion products, whereas out-of-core sources will also provide a source of inactive elemental species. Corrosion products may be transported in the coolant as soluble, colloidal, or particulate species. The various processes involved in the formation, transport, and deposition of corrosion products are summarised in Figure 27.

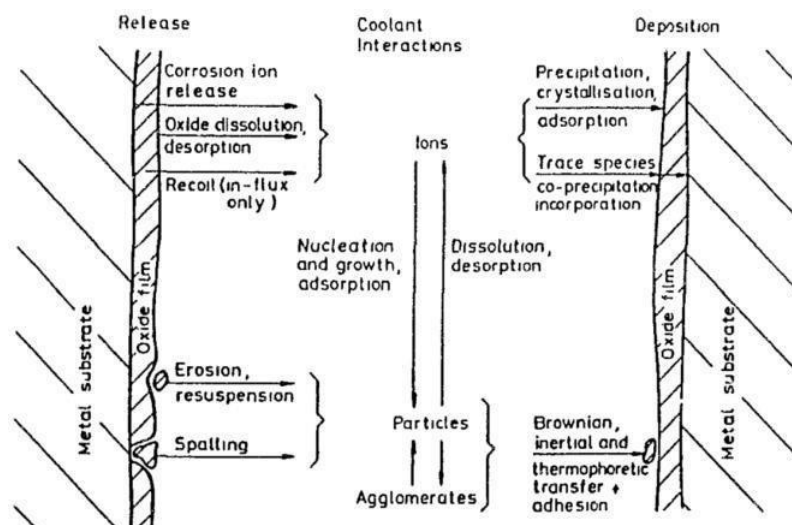


Figure 27: PWR Corrosion Product Formation, Transport and Deposition Mechanisms (From [97])

The activated corrosion products dominating PWR out-of-core radiation fields are generally Co-58 and Co-60, with lesser contributions from Fe-59, Mn-54, Cr-51, and others [97]. In some cases, antimony or silver radionuclides may also pose problems for outage operations, but this is related to specific plant issues. For example, there is OPEX of elevated Ag-110m activity in PWRs affected by Ag-In-Cd control rod wear, or silver releases from the reactor head (Helicoflex) seal, and antimony leakage from secondary neutron sources, and antimony impregnated graphite pump seals and bearings, are known sources of Sb-122 and Sb-124 [130].

Of the two radionuclides that are usually dominant, Co-58 is formed from the neutron-proton activation of Ni-58 (the most abundant stable isotope of nickel), and Co-60 is formed from the neutron-gamma activation of Co-59 (the only stable isotope of cobalt):



Co-58 decays with a half-life of ~ 70.8 days, emitting γ -rays with an energy of 0.81 MeV, while Co-60 has a much longer half-life of ~ 5.27 years and emits two high-energy γ -rays of 1.17 MeV and 1.33 MeV upon decay.

The main source of nickel in PWRs is corrosion release from the SG tubes (see Section 6), although the nickel content of tubes depends on the alloy and decreases in the order Alloy 600 > Alloy 690 > Alloy 800. Lower corrosion and release rates have been observed in laboratory tests for Alloy 690TT compared to Alloys 600MA and 600TT, and there is plant OPEX of the nickel release falling to very low levels after just a few cycles of operation history for some PWRs with Alloy 690TT (replacement) SG tubes, depending on their manufacturing history.

General corrosion of SG tubes and the stainless-steel loop pipework also releases cobalt into the reactor coolant, but this is mitigated by specifying low-cobalt alloys at the design stage. Wear of high-cobalt materials, such as Stellites, used in hard facings is often a more important source. Siemens/KWU PWRs sought to minimise the inventory of high-cobalt hard facings in successive generations of plants by introducing cobalt-free alternatives where practicable [131]. Initially, Stellites were present in the control rod drive mechanisms (CRDMs), in-vessel pins and bolts, the main coolant pumps, and valves. However, by the final generation of (KONVOI) plants, the Stellite surface area had been reduced markedly for all components except the CRDMs, from

greater than $>11 \text{ m}^2$ (total area) to $\sim 2 \text{ m}^2$. Compared to the early plants, cycle-average coolant concentrations of Co-60 were 4-5 times lower for the KONVOI plants, and similar trends were also observed for deposited Co-60 activity and shutdown radiation fields. This was sufficient for Co-58 to replace Co-60 as the dominant contributor to radiation fields. Overall, the data showed that eliminating the in-vessel Stellites had the biggest effect on reducing shutdown radiation fields, whereas the Stellite inventory in the CRDMs was probably not the main source of the remaining Co-60.

9.2. Radiation Field Behaviour

Radiation fields tend to build-up over a few years before an equilibrium level is reached following the initial start-up, as shown in Figure 28. The initial rise is associated mainly with nickel released from the SG tubes before protective oxides have formed, which is activated to form Co-58. However, the half-life of Co-58 is short enough that it contributes to shutdown radiation fields for only one cycle, and subject to favourable SG performance and chemistry, it is produced in decreasing quantities as the corrosion rate falls. This is very different to the behaviour of Co-60, whose contribution to shutdown radiation fields increases as high-cobalt hard facings start to wear, and then continues to accumulate or 'grow-in' from cycle-to-cycle due to its much longer half-life. Figure 29 shows that Co-58 is dominant in the first year or two of operation, accounting for most of the surface activity, whereas Co-60 then becomes the more important radionuclide for radiation fields. The effects of the different γ -ray energies (Co-60 $>$ Co-58) is also illustrated. Take exposure rates in the SG channel head, for example, a Co-58 surface activity three times that of Co-60 is required to make an equivalent contribution. The corresponding ratio (Co-58/Co-60) increases to about 10 outside the SG because the Co-58 and Co-60 γ -rays are attenuated differently by the thick shell wall.

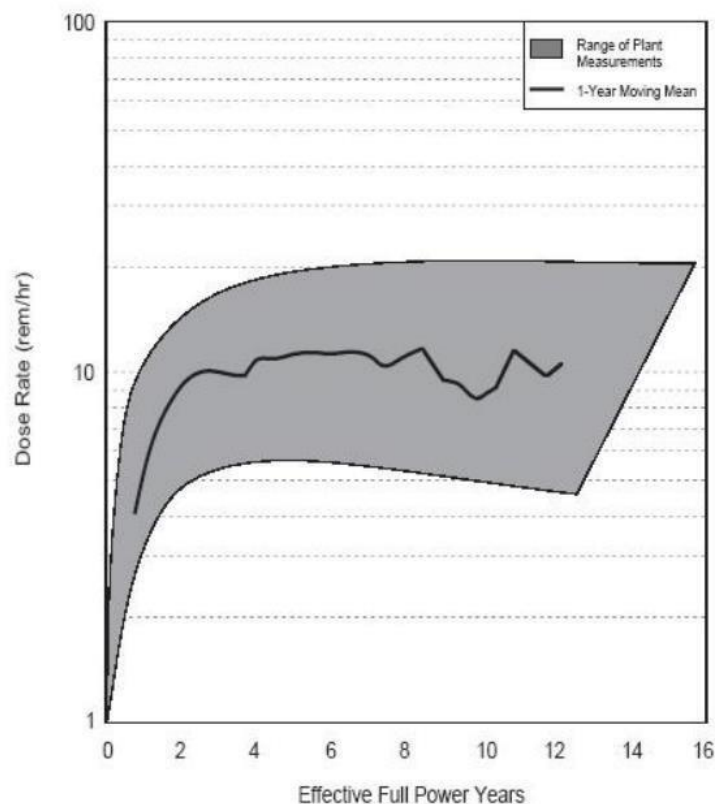


Figure 28: Radiation Field Trends in PWRs (From [42])

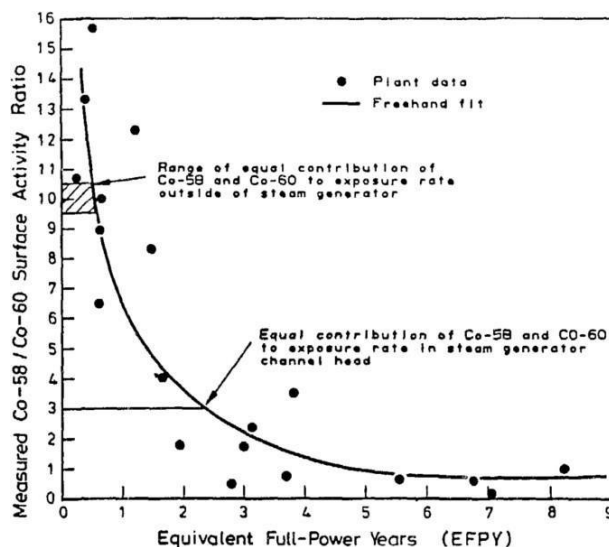


Figure 29: Variation of Co-58/Co-60 Ratio based on Steam Generator Tube Measurements (From [97])

It is understood that Figures 13 and 14 were included in some of the earlier revisions of the EPRI PWR Primary Water Chemistry Guidelines and so they are probably based on data for US plants with Alloy 600 SG tubes. Similar behaviour is likely to apply for other plants although the details may differ depending, for example, on:

- Surface area and location of Stellite sources.
- Choice of alloy used for SG tubes, and its passivation behaviour (including HFT).
- SGR, which resets the SG surface activity and may result in different corrosion behaviour.
- Implementation of zinc injection to reduce the corrosion release rate and the deposition or uptake of cobalt radionuclides on out-of-core surfaces.
- Use of surface treatments, such as electropolishing of SG channel heads, to reduce the deposition or uptake of activated corrosion products.

Given the complexities outlined above, it is perhaps unsurprising that simple correlations of shutdown dose rates to cycle average coolant concentrations of Co-58 and Co-60 are rarely, if ever, observed [132]. Historically, there have also been difficulties obtaining representative coolant samples from which to determine soluble and particulate activity concentrations.

EPRI therefore attempted to model radiocobalt incorporation into out-of-core films using data obtained mostly from Ringhals 2, 3 and 4, since these units have historically benefitted from effective coolant sampling and regular (gamma scan) campaigns of surface activity concentrations for the stainless-steel loop pipework [132]. In total, 26 cycles of Ringhals data were used. In terms of plant design and operation, there were similarities between Ringhals 2 and 3 that were also a source of contrast to Ringhals 4. Another attraction of the data was that it preceded the implementation of zinc injection, thereby simplifying interpretation.

The empirical models were of the following general form:

$$\frac{dC_f}{dt} = k(C_c)^n - \lambda C_f$$

where C_f is the film concentration, C_c is the (soluble) coolant concentration, λ is the decay constant, t is time, k is the incorporation rate constant, and n is an exponent. Numerical integration allowed incorporation rate constants for Co-58 and Co-60 to be calculated for

individual cycles in units of (atoms cm⁻² s⁻¹)/(atoms g⁻¹). For Co-58, the only surface activities needed were for EOC because BOC surface activity decays to negligible levels, whereas for Co-60, determination of incorporation rate constants was based on the difference between BOC and EOC surface activities, and subject to much greater error.

Initially, it was assumed that net incorporation rate depends linearly on the coolant activity concentrations (i.e., $n=1$). However, the rate constants obtained for Co-58 were similar for Ringhals 2 and 4, and markedly different to those for Ringhals 3, which increased significantly with time. The rate constants for Co-60 were more encouraging in that they were relatively constant with time, similar for Ringhals 2 and 3, and different (lower) for Ringhals 4, but it was further concern that the Co-60 incorporation rate constants were significantly lower than those for Co-58. The chemical behaviour of both cobalt radionuclides should be identical and their incorporation rate constants equal.

Looking more closely at the Ringhals 3 results, a clear relationship between rate constant and coolant concentration was noted for Co-58, suggesting that n might not be unity. The exercise was therefore repeated, but with $n=0$ as a limiting case. The coolant concentration term in the model is then a constant incorporation rate, A , viz:

$$\frac{dC_f}{dt} = A - \lambda C_f$$

While an apparent lack of dependence on coolant concentration was considered unlikely, it could occur if the incorporation rate (in atoms cm⁻² s⁻¹) was primarily dependent on the diffusion rate of Co-58 and Co-60 into the oxide film, and the oxide film vacancies at the interface became saturated at a very low coolant concentration. Results were encouraging for Co-58 in that the incorporation rates were similar for Ringhals 2 and 3, decreasing with time for both (which could be viewed as passivation of the Alloy 690 SG tubes), whereas incorporation rates tended to increase for Ringhals 4 (with Alloy 600 tubes). However, the Co-58 incorporation rate now varied almost linearly with coolant concentration for Ringhals 3, suggesting that an intermediate value $0 < n < 1$ might lead to further improvements. Variability in the Co-60 incorporation rate was also a concern. It was concluded that an improved model might seek to also include the impact of particulate Co-58 and Co-60 on incorporation rates.

9.3. Measurement Techniques

Station health physics personnel have always collected radiation field data, but this was often concerned primarily with exposure rates for locations requiring worker access. In many cases, such information was not suitable for quantitative trending or benchmarking due to irregular measurement frequencies, inconsistencies in measurement location, and/or background interference from nearby components or radiation hot spots [133]. General area measurements may provide a good indication of potential personnel exposure, whereas time-dependant dose rates on piping (from which workers could be shielded) are more closely linked with operations and chemistry modifications made to mitigate radiation fields [130]. This led EPRI to establish the Standard Radiation Monitoring Program (SRMP) for Westinghouse PWRs in the late 1970s [133]. The SRMP provided a meaningful, consistent, and systematic approach to monitoring radiation field build-up on out-of-core surfaces, based on performing dose measurements at permanently marked (tagged) locations during plant shutdowns.

The specified radiation monitoring points were chosen to be representative of the behaviour of the activated corrosion product γ -radiation source on out-of-core surfaces and were common from plant-to-plant. In addition, they were easily accessible and limited in number to maintain

low personnel doses while performing surveys. Dose rates measured inside the SG channel heads (if accessible prior to primary-side inspection or SG maintenance) were considered the best available source of information because they are not attenuated by shielding, and because the common geometry facilitates comparison between plants. The outside of reactor coolant piping (hot, cold and crossover legs) was also a desirable location for assessing radiation field build-up owing to its geometry and lack of features that could constitute localised crud traps. It was recommended that surveys should be conducted with a portable instrument, equipped with an extending or telescopic probe, that had been calibrated by exposure to known γ -radiation fields.

Consistent efforts were made to collect SRMP data during the period 1985-1996, but the programme was discontinued in 1996 due to lack of funding. Data collection was then limited mainly to those plants implementing changes such as elevated primary coolant pH, zinc injection or SGR. However, the SRMP was reinstated in the mid-2000s in response to industry changes that affected the radiological behaviour of plants (e.g., core uprating). This supported an initiative to promote radiation dose reduction by emphasising RP fundamentals and reducing the radioactive source term [134]. Separate procedures were provided for Westinghouse, Combustion Engineering and Babcock and Wilcox plants, and the survey locations were recast in terms of being required, recommended or optional. Dose rate monitoring at recommended points was requested, but could be skipped in cases of personal safety, poor accessibility, or significant ALARA impact. The optional survey locations, for which information was requested 'only if available' included monitoring points in the CVCS and the Residual Heat Removal System (RHRS), as well as at the surface of the refuelling water. The required and recommended SRMP survey points for Westinghouse PWRs are shown in Figure 30.

The reinstated SRMP also contained the explicit recommendation to include gamma spectroscopy, either in the form of 'smears', gamma scan campaigns or coupon analysis. While total gamma radiation fields offer valuable insights, they do not provide information about radionuclide distribution, which is often required to understand the basis of observed trends. However, gamma scan campaigns normally require specialist equipment, whereas total gamma measurements can be collected by station personnel. High-purity collimated germanium detectors offer the highest commercially available resolution and can separate and identify the contributions of specific gamma-emitting radionuclides, but their use as a mobile tool is hindered by practical considerations including requirements for liquid-nitrogen cooling and heavy shielding, and measurement times are counted in hours [130]. Computer software is employed to calculate surface activities from the spectra considering the effects of different types and thicknesses of thermal insulation, the wall thickness, and whether the pipe or component is full or drained [135]. Surface activity concentrations can be measured if the primary circuit is full or drained because the volume activity contribution can be removed, and are generally reported in terms of Bq/m² of the corresponding radionuclide, e.g., Co-58, Co-60, etc.

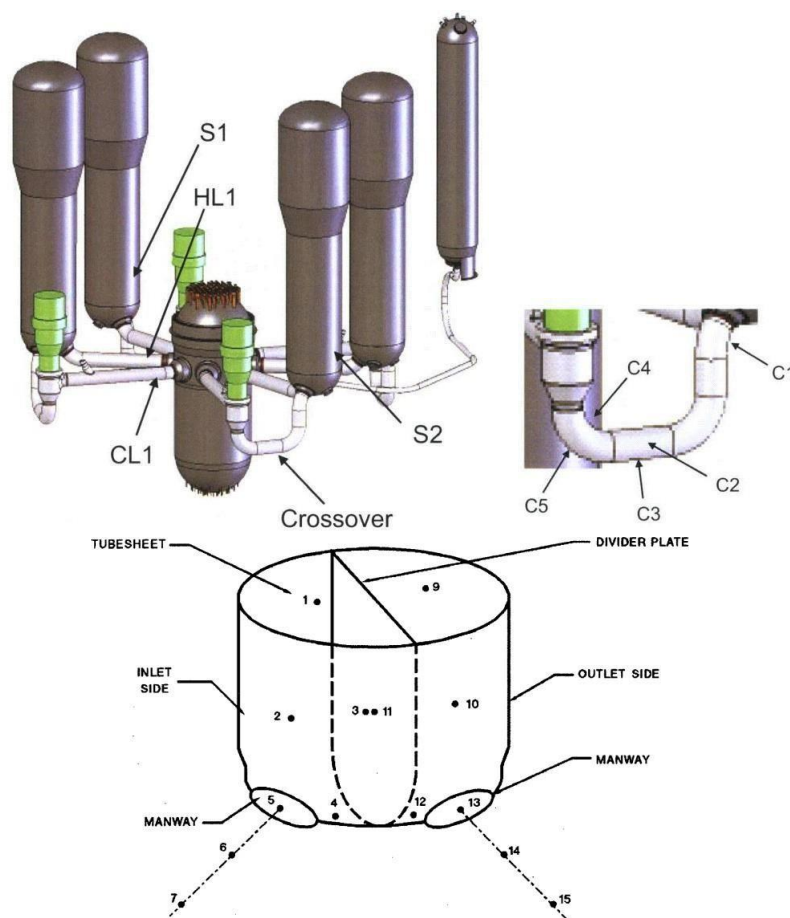


Figure 30: SRMP Survey Points for Typical Westinghouse 4-Loop PWR

Notes: The upper illustrations, which include an expanded version of the crossover leg, are for the reactor coolant piping survey points, where C2, HL1 and CL1 are 'Required Points' and C1, C3, C4 and C5 are 'Recommended Points'. S1 and S2 are 'Required Points' if taken previously, or else are 'Recommend Points'. The lower illustration is for the SG channel head, where points 1-4 and 9-12 are 'Required' and points 5-7 and 13-15 are 'Recommended' if there is access. These illustrations are taken from [134].

Conventional gamma scan campaigns produce high-quality data, but deployment of the technique depends on the availability of specialist equipment and suitably trained personnel, which is a substantial constraint. Therefore, EDF has developed a supplementary tool which uses a CZT (Cd-Zn-Te) semi-conductor probe [81]. The CZT device has lower resolution than a high-purity germanium detector (as used in EDF's EMECC device) but can quantify satisfactorily the main radionuclide contributions to dose equivalent rates. While the EMECC is more accurate, the CZT device is lighter and more manageable. The CZT device does not produce deposited surface activities (although technical upgrades were planned), but the radionuclide contributions to dose equivalent rates agree with EMECC to within about 10%. The largest differences were for the hot and cold legs, and these were explained by the absence of a collimator for the CZT detector, resulting in background interference. It was noted that there may be a requirement to take measurements at different times during a shutdown and with different water levels. This may be a limitation for CZT analysis because it is not possible to subtract the volume activity contribution, whereas it is possible when using EMECC. All EDF PWRs were equipped with a CZT gamma spectrometer to analyse, during shutdowns, the radionuclide activity present on out-of-core surfaces for specified locations in the reactor building (RCS, SIS and RHRS), the auxiliary

building (CVCS), and the fuel building (SFPCTS). Following on from the EDF experience, KHNP has investigated using the CZT detection technique, albeit qualitatively in the first instance [136].

9.4. Plant Shutdowns

During a refuelling outage or other cold shutdown in which the RCS is opened to air, the system conditions go from being hot, alkaline, and reducing to cold, acidic, and oxidising. Hydrogen peroxide is dosed to the reactor coolant to accelerate the release of activated corrosion products, which would otherwise occur when the primary circuit is vented to atmosphere [137]. Obtaining a controlled release at a time when it can be easily cleaned-up by the coolant purification system avoids delaying refuelling and impacting the outage schedule. Clean-up is necessary to avoid increased refuelling platform dose rates and may also benefit refuelling water clarity [138]. In addition, dose rates from activity in the coolant would add to those from activity deposited on out-of-core surfaces, leading to increased area dose rates if not cleaned-up to a very low level prior to maintenance. Therefore, radiochemical criteria are set that must be achieved before proceeding beyond various stages in the shutdown, such as stopping the last RCP, lifting the vessel head, and flooding-up the refuelling cavity.

Shutdown chemistry programmes should not be confused with surface decontaminations. The radioactivity released during shutdown is less than 10% of the RCS inventory [139] and most of the out-of-core Co-58 and Co-60 surface activity is incorporated in chromium-enriched oxide films that are protective and very stable in both operating and shutdown chemistry environments. Instead, most of the activity released into the coolant during a shutdown is from fuel crud deposits in the core. Even then, only a small proportion of the total fuel crud mass is likely affected (illustrative calculations in [42] for trends in activity release with EFPY assumed 20% of the corrosion product burden on fuel is released during shutdown). The intent is to promote soluble releases, which are cleaned-up by the CVCS ion-exchange demineralisers, while minimising particulate releases, which can re-deposit around the circuit, especially in low-flow regions.

There are two main chemistry phases to a shutdown: an acid-reducing phase followed by an acid-oxidising phase. Acidic conditions are generated by adding boric acid to achieve the required shutdown boron concentration, and the change from acid-reducing to acid-oxidising conditions is achieved by hydrogen peroxide addition. Hydrogen must be removed from the system before going oxidising to avoid the formation of H₂/O₂ explosive gas mixtures. This is achieved by a combination of mechanical and chemical methods, including nitrogen overpressure, venting, and burping. Removal can be slow and so EPRI states that the hydrogen concentration may be reduced to 15 cm³ kg⁻¹ up to 24 hours prior to a planned shutdown [130].

Shutdown chemistry guidance was developed to manage releases from fuel crud comprised mainly of nickel ferrite. However, it was seen in Section 6 that high-duty cores associated with power up-rates and extended fuel cycles (i.e., core designs with high levels of SNB) tend to produce a thicker, more porous fuel crud containing tenacious species such as NiO and, under extreme conditions, bonaccordite. SGR may also impact on the fuel crud inventory [140], at least to begin with, because replacement tubes initially corrode at a faster rate than the ones replaced. However, the longer-term behaviour of Alloy 690TT replacement tubes vary, with passivation and very low material release rates tending to occur relatively quickly for tubes from some manufacturers.

In terms of refuelling outages, one of the problems encountered for high-duty plants is that of unexpected particulate releases accompanying the increased soluble releases, leading to

contamination of out-of-core surfaces and increased dose rates [141]. EPRI offered some suggestions for better shutdown management of particulate crud releases based on a review of shutdown practices for the period 1998-2001 [140]. This was followed, in 2006, by a thorough benchmarking review [141] of its guiding principles for shutdown chemistry control against the following modified goal: "Prepare the plant for a refuelling (or mid-cycle) outage in as short a time as possible, without negatively impacting on shutdown dose rates or particulate contamination levels and associated contamination events". Shutdown chemistry considerations relevant to fuel crud and/or radiation field management are summarised in the following subsections, which draw heavily on [140] [141], but also include other sources of information. The focus here is on end-of-cycle refuelling outages (i.e., cold shutdowns with oxygenation), but guidance is also available for mid-cycle shutdowns [142] [143].

9.4.1. Pre-shutdown pH Control

Particulate crud release is often observed at the end of an operating cycle, although this does not necessarily predict an anomalous shutdown particulate release. Initially, EPRI suggested that consideration be given to reducing pH_T to 6.9 towards the end of a cycle for two reasons: (a) because it may stabilise fuel crud, and (b) to aid in establishing acid-reducing conditions for the outage [140]. However, [141] subsequently made no mention of stabilising fuel crud in this way, focussing instead on minimising pH_T to increase the solubility of nickel and iron. In 1994, Palo Verde Unit 2 experienced an increase in core pressure drop and a reduction in core flow during a 36-hour period preceding power reduction for a mid-cycle shutdown. Lithium removal was started 3 days prior to the shutdown and pH_T was ~ 6.3 when the pressure drop increase began. The problem was attributed to deposit build-up and/or re-distribution within the core. Therefore, EPRI considers that the minimum pH_T without significant risk of crud redistribution is 6.5, and states that reductions below pH_T 6.9 should be minimised [141]. Lithium reduction in this way was not expected to have any significant effect on particulate releases or shutdown dose rates.

At least three EDF reactors (Belleville Unit 2 in 1988, and Chinon Units B1 and B4, both in 2009) have also experienced instances of abnormal RCS pressure loss during prolonged periods (20-40 days) of hot shutdown conditions, either prior to a shutdown or start-up [144]. In all cases, pH_T was below the recommended value of 6.9 (and sometimes < 6.5) and hydrogen was not added systematically, although a sufficient concentration was present for Chinon B1. For Chinon B1, raising the pH_T to within specification was successful in re-establishing normal behaviour, whereas for Chinon B4, it was necessary to implement acid-reducing chemistry at 180°C [145]. Previous experience at Belleville 2 showed that forced oxygenation would not resolve the issue, and neither did an initial Chinon B4 chemical treatment of lithium addition to raise the pH_T . EDF suspects that anomalous behaviour of these plants was due to the formation of iron and nickel-containing deposits, such as nickel ferrite, at the entrance of flow restrictions, where electrokinetic factors may cause particulates to deposit. Accordingly, EDF guidance is now to adjust the shutdown pH to the target value ($\text{pH}_T > 6.9$) and add a minimum concentration of hydrogen as soon as possible during a prolonged (> 24 hours duration) hot shutdown.

9.4.2. Post-shutdown pH Control

EPRI recommends prompt and rapid boration to maximise the time spent with acid-reducing conditions [141]. Likewise, the lithium concentration in the coolant shutdown should be decreased as quickly as plant conditions permit after shutdown. Both actions decrease the coolant pH_T . Originally, it was thought that this would promote reductive decomposition of nickel ferrite to nickel metal and magnetite, and reduction of NiO to nickel metal, which would be advantageous because nickel metal is then readily dissolved and cleaned-up under acid-oxidising conditions. However, tests have since shown that neither reduction reaction takes place to any

significant extent in the primary coolant of a shutdown PWR due to slow kinetics [146]. Historically, EPRI recommended an acid-reducing phase hold of at least 16 hours (at 120-150°C) to promote nickel ferrite decomposition, but this was discontinued based on the improved understanding. Maintaining acid-reducing conditions may still be beneficial for some shutdowns though, particularly for managing iodine radionuclides following cycles affected by fuel failures.

While the original optimisation of the acid-reducing phase may not have been correct, the solubilities of nickel-ferrite, nickel oxide and nickel metal (in-core and out-of-core) all increase with decreasing pH_T under shutdown chemistry conditions [140], and so the EPRI shutdown principles are consistent with promoting dissolution. Nickel-containing species activated in-core contain Co-58, and nickel ferrites may also contain a small cobalt/Co-60 impurity. Hence, solubilisation of crud during cooldown under acid-reducing conditions is accompanied by radiocobalt release, where the latter is mainly from the core.

Care should be taken to avoid any significant increases in lithium concentration (e.g., due to lithium present in the RHRS) because the resulting pH_T increase, and nickel and iron solubility decrease, may lead to precipitation and an increase in particulate concentrations. Similarly, the release of soluble iron (from nickel ferrite) during cooldown, if combined with small amounts of dissolved oxygen, will result in ferric hydroxide precipitation. Ferric hydroxide co-precipitates cobalt-58 and other radionuclides and may result in localised hot spots throughout the plant [147]. Preventative measures include dosing the RHR trains with hydrazine several weeks before shutdown (the oxygen scavenging reaction is slow in the absence of γ -radiation) or flushing them to waste, as well as ensuring there is sufficient dissolved hydrogen in the coolant at shutdown to maintain a reducing environment until ready for forced oxygenation. The latter may include making allowance for the effects of boration with partially aerated coolant, which reduces the hydrogen concentration.

9.4.3. RCP Operation and Peroxide Addition

RCP strategy varies considerably between PWRs, mainly in terms of how many pumps are operating when hydrogen peroxide is added (and EDF, for example, permits injection of hydrogen peroxide at $T \leq 80^\circ\text{C}$, [143]. EPRI recommends maximising the time with at least one pump operating [140] [141]. By maximising mass flow and mixing through the core (and the loops), and providing the driving head for CVCS operation, this enhances corrosion product dissolution and clean-up, although stagnant or reverse-flow conditions may occur along with particulate deposition in loops with idled pumps. Cycling of pumps is discouraged due to risk of re-suspending previously deposited material. However, extending pump operation (without cycling) following an abnormal particulate release is recommended to minimise out-of-core deposition, by keeping particulate suspended for clean-up by the CVCS.

Wall shear is the major factor impacting on particulate release and deposition. It follows that minimisation of core shear values could be achieved by shutting down all RCPs before adding hydrogen peroxide, and then relying on the RHRS to provide adequate mixing [141]. In theory, this approach could be particularly beneficial for PWRs with substantial amounts of nickel-rich fuel crud since nickel dissolution under acid-oxidising conditions is expected to destabilise the crud, leading to the risk of particulate releases. It has been used by a small number of plants even though it presents a challenge for ensuring explosive gas mixtures are avoided. On one occasion, a significant release of Co-58 occurred during the subsequent start-up. Another downside is that removal of fuel crud will be slower for RHRS flowrates than with an RCP running (each RHR pump operates with a flow rate corresponding to 2-5% of an operating RCP flow) and leaving behind a higher residual fuel crud loading may be a concern for plants at risk of CIPS. The decision-making process for stopping all RCPs before adding hydrogen peroxide is likely to

require detailed plant-specific evaluation.

Prompt releases of soluble nickel and Co-58 are usually observed adding hydrogen peroxide to establish acid-oxidising conditions. This indicates the presence of a significant nickel metal inventory since no effect on nickel ferrite or nickel oxide would be expected. An increasing Co-58/Ni specific activity shows that the release is mainly from the core. It is then necessary to clean up the coolant activity to meet specified limits before activities such as flooding-up the refuelling cavity can take place. This is achieved by maximising coolant flow to the purification system and assuring that the filter and ion-exchange demineraliser removal efficiencies are high. Reducing the clean-up volume (e.g., by closing loop-stop isolation valves, if fitted, or by draining to mid-loop under nitrogen overpressure) can also be beneficial in terms of achieving coolant activity criteria more quickly. EPRI investigated this approach in a study that classified the (individual cycle) shutdown operations of selected Westinghouse 4-loop plants according to the following three categories [148]:

Strategy 1: Operate at least one RCP during forced oxidation and clean-up.

Strategy 2: Secure RCPs before forced oxidation and clean-up the whole system volume.

Strategy 3: Secure RCPs and reduce system volume before forced oxidation and clean-up.

The two datasets evaluated, one for plants with original SGs with Alloy 600TT tubing and another for replacement Alloy 690TT SGs, were not large and most of the experience was for Strategy 1. In addition, there was some risk of confounding variables. The resulting observations were not capable of supporting strong recommendations, but some were worthy of note, in particular:

- The choice of RCP strategy had little or no effect on out-of-core radiation fields in high-flow areas of the plant.
- Securing RCPs prior to forced oxygenation may provide direct schedule savings by reducing RCP run time, and, in the case of Strategy 3 (reduced system volume), may potentially lead to further savings by decreasing the total clean-up time.
- There was indirect evidence that securing the RCPs prior to forced oxygenation could lead to increased deposit loading on fuel in future cycles, potentially increasing the risk of CIPS or CILC if no secondary fuel cleaning method is applied.

Hence, it was concluded that securing the RCPs before forced oxidation may not be advantageous if RCP maintenance is not on the critical path or if outage schedule is not a main driver for shutdown decisions. Instead, leaving RCPs in-service during forced oxygenation and allowing them to continue to run may be the most appropriate strategy to remove as much fuel crud from the core as possible, and to prevent particulate from settling out in the loops during clean-up. Moreover, any plants considering implementing Strategy 2 or 3 to realise outage schedule savings, should recognise the potential for increased crud carryover between cycles (relative to forced operation with RCPs running).

In 2015, Vandellos 2 – a high-duty Westinghouse 3-loop PWR with Alloy 600TT SG tubes and high crud levels – implemented a substantial change in shutdown strategy for refuelling outage 20 (R20). This was in response to an increase in collective dose recorded in the refuelling cavity for R19. The increase was partly due to the work schedule but was also caused by discharging into the cavity high-activity coolant that had been trapped in the SGs when the last RCP was shutdown. Normal practise up to and including R19 was to add hydrogen peroxide with one RCP in service, but there was concern that the time taken to clean up the coolant activity to meet the head-lift criteria would soon have unacceptable impact on outage critical path. Therefore, it was decided to reduce radiocobalt transport from the core to the SG U-tubes by oxygenating the

primary coolant with the RCPs stopped for R20 [149]. With no RCP running during forced oxygenation, and relying instead on the two RHRS trains, flow through each tube bundle is very low, and the activity in the coolant trapped in the SGs is commensurate with the lower levels in the RCS during acid-reducing conditions. Another advantage is that the clean-up volume is reduced with the SGs effectively isolated.

The changes made to the Vandellos 2 method of oxygenation were judged to be a success in reducing the overall collective dose for R20. Much less activity was trapped in the SG tube bundles, and the refuelling cavity activity for R20 (after breaking the SG siphons and flooding-up) was about one third of that for R19. The total amount of Co-58 and Co-60 removed from the RCS after oxygenation was ~30% lower for R20 than for R19, although this was attributed to unspecified events that occurred during cycle 20. Similarly, it appears that the release of radiocobalt into the RCS under acid-oxidising conditions was much slower for R20 than for R19, and this raises the possibility that more of the crud was left on the fuel. However, this is not a major concern for Vandellos 2 because the reload fuel has been cleaned ultrasonically since 2006, when zinc injection was also introduced.

EDF has reviewed the impact of its criteria for taking the last RCP offline ($[Co-58] < 50GBq/te$ and $[total-\gamma] < 100GBq/te$) on surface contamination and dose for refuelling outages [150]. Outage schedules typically allocate 15-20 hours after oxygenation for the coolant activity limits to be met. Through a combination of computer modelling and measurement campaigns, it was concluded that while coolant activity concentrations make a strong contribution to dose rates immediately after oxygenation, this effect is temporary because the coolant activity is cleaned-up. Different criteria were tested for stopping the last RCP and it was shown that regions suspected of having low flow in the absence of pump operation (e.g., the crossover leg and SG U-tubes etc.) were purified in the same way as other regions. Initial dose rates before oxygenation were restored. Maintaining RCP operation to lower coolant activities did not impact deposited activity levels to any significant extent. Similarly, there was no relationship between general area dose rates and the criteria for stopping RCPs. This showed that adopting more onerous criteria (i.e., achieving a higher degree of clean-up before stopping the last RCP) would not be expected to result in dose reduction benefits.

9.4.4. Coolant Purification

EPRI recommends that the purification flow rate is maximised, and that filter and demineraliser removal efficiencies are high during the clean-up phase of shutdowns [141]. In addition, clean-up should continue until activity levels are reduced to the limits specified in plant procedures.

Coolant purification is one of the key functions of the CVCS and is achieved by using a combination of filtration and ion-exchange units, where the ion-exchange demineralisers also provide some particulate filtration. The design intent of having a filter downstream of the demineralisers is to remove resin fines, but there has been an industry trend towards using much finer (submicron) filters that may also remove larger corrosion product particles [130].

During normal operation, corrosion products deposit on fuel surfaces faster than they can be removed by the coolant purification system. Hence, the coolant purification system has limited impact on the corrosion product inventory. However, the situation is reversed during refuelling outages (and other cold shutdowns with oxygenation), and the schedule demands that clean-up of the corrosion product release is optimised and achieved in minimal time.

In general, it may be considered that there is a fixed coolant volume to be cleaned up following a rapid release of activity, although securing the last RCP before peroxide addition is known to result in a continued release of activity after the initial peak [148]. The key factors in achieving

this are the purification flow (i.e., the letdown flow) and resin efficiency. The theoretical impact of flow optimisation (45-130 gpm) and resin optimisation (70-100% efficiency) on cleaning-up a constant volume of Co-58 activity is illustrated in Figure 31. Maximising the purification flow has a significant beneficial effect on clean-up as does improving the resin efficiency from 70 to 95%, whereas the effect of further improvements in resin efficiency (from 95 to 100%) is relatively small. In addition, the theoretical purification half-life is inversely proportional to the clean-up volume. EDF considers 65°C to be the optimum temperature for Co-58 clean-up, and this is also appropriate for antimony radionuclides, but the temperature is held at 75°C if clean-up of Ag-110m is the priority [143].

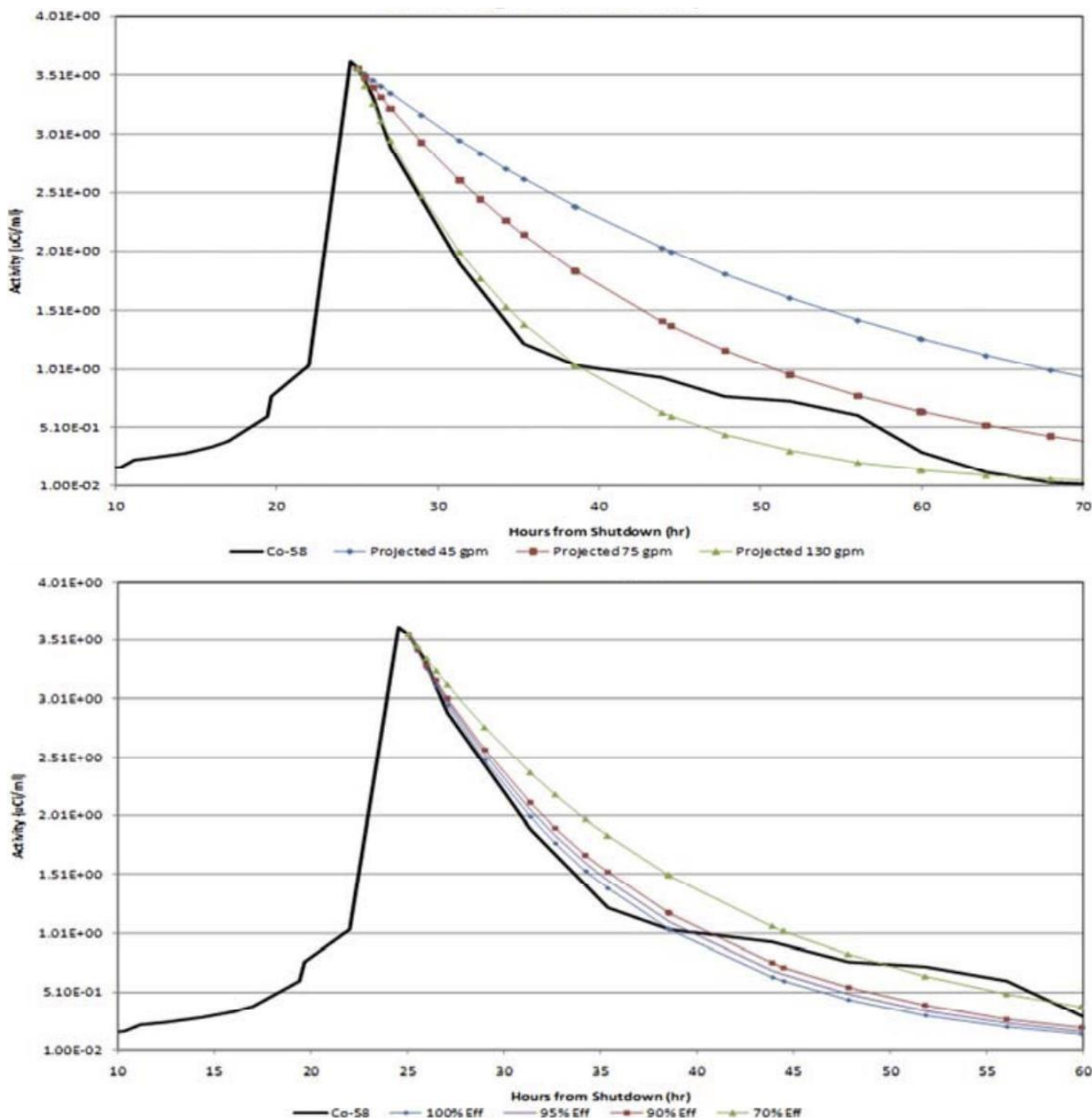


Figure 31: Projected Clean-up Times based on Purification Flows and Resin Efficiencies

Notes: Theoretical clean-up curves based on different purification flows (upper plot) and resin efficiencies (lower plot). These plots are taken from [130].

9.4.5. Refuelling Cavity Decontamination

A post-refuelling decontamination of the reactor cavity is undertaken to help reduce personnel exposure and/or contamination during vessel disassembly and reassembly activities. It is observed that reducing activity concentrations in the cavity water reduces the level of decontamination effort that is required after drain-down (e.g., water jetting and manual scrubbing), and this is important because decontamination efforts after drain-down may increase outage durations [151]. Several options are available for reducing the activity of the cavity water, but a detailed characterisation of cavity activity prior to decontamination is required to assess their effectiveness. To that end, EPRI developed a sampling and analysis protocol [152] based on sampling the refuelling cavity water at various depths, both after flood-up (before the core offload) and after the core reload is complete (before drain-down). The samples are then filtered using gradually smaller ratings of 5 μm , 0.45 μm and 0.1 μm , with a cation membrane on the outlet from the 0.1 μm filter. In testing the procedure for a PWR refuelling outage, various smear samples of refuelling cavity activity were also collected for comparison.

Initial consideration of the liquid-sample results found that activity was distributed uniformly around the cavity in terms of both location and depth. Co-58 and Cr-51 were the dominant nuclides, although their activities before and after refuelling were noticeably different. Overall, most of the activity passed through the three filters and was either captured on the cation membrane or passed through in the final effluent. For the smear samples, the activity on the cavity floor was much greater than that on the cavity walls, suggesting that activity accumulates on the floor because of particulate settling. Nb-95/Nb-95m and Zr-95 were much more abundant for the smear samples than they were for the liquid samples, and when they were present for the liquid samples, they were removed by the 5- μm filter, suggesting that they were present as particulate.

Potential mechanisms by which activity may attach to the cavity surfaces through chemical interactions (adsorption, ion exchange and covalent bonding) are discussed in [153] along with a summary of industry practices for cleaning-up refuelling cavity water. In terms of chemistry practices affecting cavity decontamination, it was recommended that the following main options should be considered:

- Optimise the primary chemistry during the operating cycle to minimise corrosion of wetted surfaces, release of corrosion products from out-of-core surfaces, and deposition of corrosion products in the core.
- Reduce the activity of the refuelling cavity water, either by extending primary coolant clean-up times to achieve lower coolant activity concentrations before head-lift and flood-up, or by purification of the refuelling cavity water before drain-down.
- Based on OPEX, addition of hydrogen peroxide to the refuelling cavity water (to a concentration of ~ 6 ppm) can reduce personnel exposure during subsequent decontamination activities.

10. Safe Plant Operations

This section is concerned with safe plant operations that may be employed to militate against the formation of operationally significant fuel crud in PWRs. The consequent benefits include reduced risk of nuclear-safety impacts such as CIPS, CILC and increased shutdown radiation fields.

It is worth recapping that general corrosion of out-of-core components provides the source of iron and nickel that is transported in the primary coolant to the fuel cladding, where it may deposit under steaming conditions of SNB. In terms of nuclear safety, the formation of thick, porous fuel crud is the main concern. This type of crud is nickel rich and so is usually observed only for units with Alloy 600 or Alloy 690 SG tubes.

The design and manufacture of SG tubing provides an early opportunity to mitigate the risk of substantial fuel crud forming during future operation and this was discussed in Section 6.1.2. Some manufacturers have made process improvements that result in Alloy 690TT tubes exhibiting passive behaviour (i.e., very low corrosion releases) within a small number of fuel cycles.

Core design is also a key factor because there is increased propensity for SNB to occur in the upper spans of fuel assemblies for high-duty cores, and this promotes deposition of circulating corrosion products onto the hottest regions of the fuel rods; see Section 6.2.2. Designing lower duty cores is potentially the simplest way to avoid severe fuel crud deposition, but may not be compatible with commercial objectives, such as power uprates, extended fuel cycles and fuel-cycle efficiency.

The importance of operating with an optimised primary water pH_T was discussed in Section 6.1.3. Maintaining an optimum pH_T not only minimises the general corrosion release within the primary circuit, but also minimises corrosion product transport to, and deposition on, fuel cladding surfaces in the core. Depending on the assumed conditions, the latter is achieved either by promoting normal as opposed to retrograde iron and nickel solubility behaviour with increasing temperature through the core, or by minimising the soluble nickel concentration entering the core. Understanding of the optimum pH_T has evolved over time, increasing from a minimum of 6.9 to a target of 7.2-7.4. In addition, the BOC pH_T should be as high as achievable without transgressing any fuel-vendor imposed limits on maximum lithium concentration (typically ~ 3.5 ppm lithium). With fuel vendor concurrence, some PWRs (e.g., Comanche Peak) have justified operating with up to 6.0 ppm lithium at BOC to enable operation at a constant pH_T of 7.4 for an entire 18-month fuel cycle.

Other safe plant operations are available and discussed below. These include the use of potassium hydroxide and/or enriched boric acid to allow primary water chemistry pH_T regime optimisation in favour of fuel crud and radiation field control whilst avoiding high lithium concentrations. More commonly, zinc injection is used to minimise incorporation of Co-58 and Co-60 – the radionuclides that usually dominate shutdown radiation fields – into the oxides present on the SG tubes and loop piping surfaces. In addition, HFT during reactor commissioning provides an opportunity to promote the formation of stable and protective oxide films on RCS surfaces and to clean-up releasable corrosion products prior to operation with fuel in the core. Finally, the technique of UFC has been developed and deployed to remove tenacious crud from reload fuel assemblies prior to them being reinserted into the reactor. This reduces the corrosion product inventory available in the core at the start of the next fuel cycle.

The section ends with a discussion of monitoring activities available to detect crud-related

problems.

10.1. Potassium Hydroxide

KOH has long been considered for use as an alkalizing agent in 'western' (non-VVER) PWRs, as an alternative to isotopically enriched $^7\text{LiOH}$ ($\text{Li-7} > 99.9\%$):

- Siemens/KWU initiated a study of alternative PWR water chemistry regimes in the early-1990s [154] because longer fuel cycles and higher-duty cores would result in higher beginning-of-cycle (BOC) boron concentrations. Increased concentrations of $^7\text{LiOH}$ would then be required to maintain the target pH_T , where a sufficiently alkaline pH_T (≥ 7.0) is important for minimising fuel crud formation and out-of-core radiation fields. However, high concentrations of LiOH are known to accelerate corrosion of Zircaloy fuel cladding. Hence, there was a conflict of objectives and an initial screening process identified KOH to be a feasible alternative to $^7\text{LiOH}$.
- In the late-1990s, EPRI identified use of KOH (in place of $^7\text{LiOH}$) to be a potential mitigation strategy for CIPS [155]. There was high confidence that the observed flux depressions were caused by precipitation of lithium borates, such as LiBO_2 , within porous fuel crud due to concentration of Li and B under conditions of sub-cooled nucleate boiling (SNB). Of the common alkali borates, LiBO_2 has the lowest solubility and the (retrograde) solubility decreases with increasing temperature. On the other hand, potassium forms three borate species (KBO_2 , $\text{K}_2\text{B}_4\text{O}_7$ and KB_5O_8) and the solubility of these K-borates is at least two orders of magnitude greater than that of LiBO_2 at 350°C . Furthermore, data indicate that the solubility of the K-borates behaves normally (i.e., it increases with increasing temperature). Therefore, it was suggested that changing from $^7\text{LiOH}$ to KOH would curtail the precipitation of normally soluble borates in porous fuel crud, and hence, the risk of CIPs would be greatly reduced. That said, recent crud chemistry modelling challenges this viewpoint, as discussed below in Section 10.1.1.
- Interest in qualifying KOH for use in PWRs was renewed in the mid-2010s because of $^7\text{LiOH}$ cost and supply issues. The problems were mainly driven by increased demand for lithium carbonate from the energy storage and automotive industries. This led EPRI to set out a plan to qualify KOH for use for PWRs across the industry [156], and Framatome re-established investigations with respect to using KOH for Siemens/KWU PWRs [157].

KOH is a strong base with similar dissociation constants to LiOH and so the same molar concentrations of KOH or $^7\text{LiOH}$ are needed for pH adjustment (although 2 ppm Li-7 is equivalent to ~ 11 ppm K due to the higher molar mass of potassium, [154]). One reason for initially choosing $^7\text{LiOH}$ to be the alkalizing agent for PWRs was that Li-7 is produced by neutron irradiation of B-10 according to $^{10}\text{B}(n, \alpha)^7\text{Li}$. In contrast, dosing KOH would result in a more complicated dual-component alkali control system requiring additional effort to control the potassium and lithium concentrations concurrently. There is considerable OPEX of using KOH as an alkalizing agent for the primary coolant of VVERs in eastern Europe and elsewhere, and Figure 32 shows that the pH-regimes of VVERs and PWRs are broadly similar.

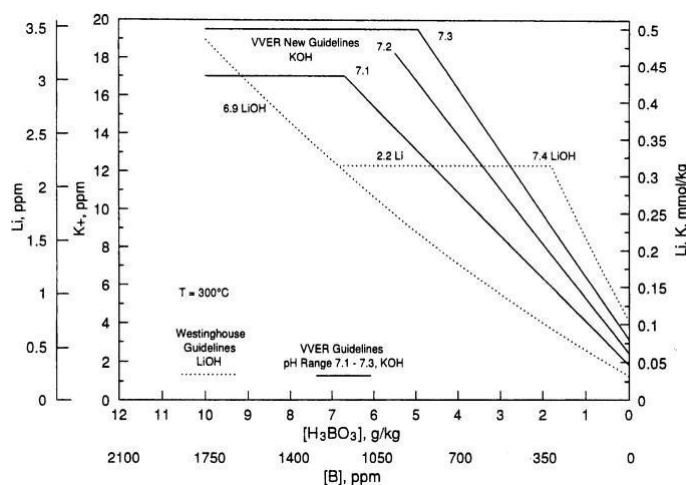


Figure 32: Comparison of the Li/H₃BO₃ and K/H₃BO₃ Strategies used in PWRs and VVERs

Notes: PWRs dose ⁷LiOH to maintain an alkaline pH_T in the presence of boric acid, whereas VVERs dose KOH. In molar concentration terms, the regimes are very similar. The mass concentrations of lithium and potassium differ due to their different molar masses. This plot is taken from [155].

Operating experience with KOH from the VVER units is overwhelmingly positive, although it should be interpreted cautiously because of materials and operational differences between VVERs and PWRs. These include the use of (titanium stabilised) stainless steel for the SG tubes in VVERs, whereas PWR SGs are tubed with the nickel-based alloys 600, 690 or 800. Also, VVERs tend to operate with lower-duty cores and produce less fuel crud than some PWRs [158]. A Westinghouse-designed PWR unit (Trino) in Italy, which is now shutdown, also used KOH but it too had stainless steel SG tubes [155]. As a result, the KOH qualification plan for PWRs [156] identified potential compatibility issues with the fuel and structural materials that needed to be addressed, as well as some chemistry and radiation effects. While materials testing work [159] is still completing, EPRI is collaborating with TVA for a (planned) monitored trial campaign using KOH at Sequoyah PWR, which will last for three cycles [160].

10.1.1. Fuel Compatibility

Several investigations have shown that while Zircaloy undergoes accelerated corrosion in concentrated solutions of LiOH at ~350°C, the corrosion rates are greatly reduced in KOH. For example, Siemens/KWU observed much lower Zircaloy-4 corrosion rates in ~0.01-0.1M aqueous KOH and LiOH+KOH+H₃BO₃ solutions than for equivalent molar concentrations of LiOH [161]; see Figure 33. Similarly, extended tests by KAERI and Siemens [162], in which Zircaloy-4 samples were exposed to 4.3 and 32.5 mmol aqueous solutions of Group 1 metal hydroxides, showed that the weight gain decreased with increasing cation radius (i.e., weight gain decreased in the order Li⁺>Na⁺>K⁺>Rb⁺>Cs⁺); see Figure 34. Unlike for LiOH, KOH did not lead to accelerated Zircaloy-4 corrosion at the higher of the two concentrations. The hydrogen pick-up fraction (i.e., the fraction of the hydrogen produced by corrosion that was retained in the oxide) also decreased in the order LiOH>NaOH>KOH.

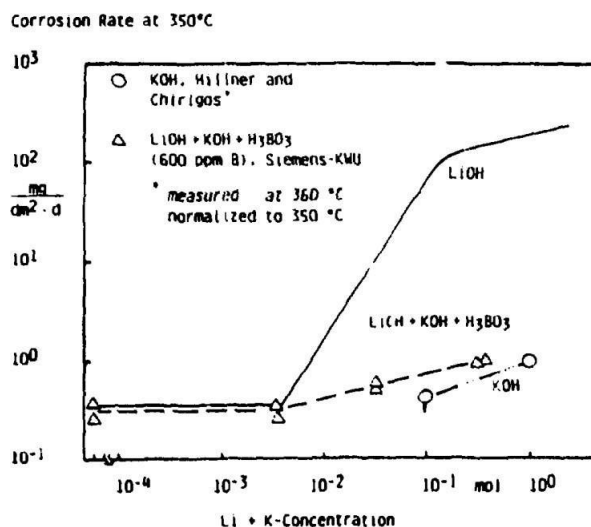


Figure 33: Effect of LiOH, KOH and a LiOH+KOH+H₃BO₃ Mixture on Zircaloy-4 Corrosion (From [161])

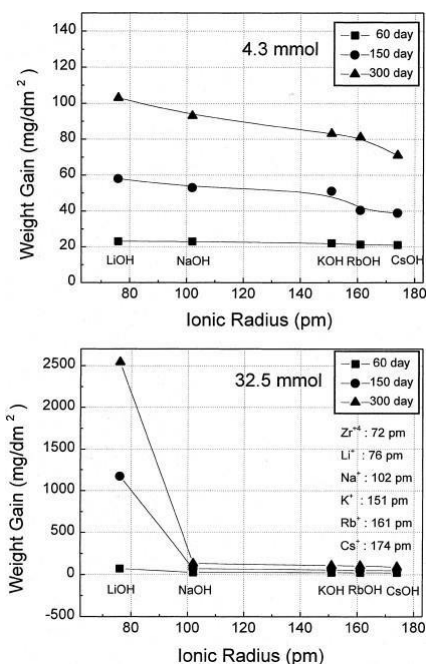


Figure 34: Weight Gain of Zircaloy-4 versus Ionic Radius of Alkali Hydroxide Cation (From [162])

Based on these experimental results, it is unsurprising that oxide growth for ZIRLO fuel in VVER conditions is comfortably in the lower half of the experience base in PWR conditions at normal end-of-life burn-up, and similarly reassuring comparisons are also available for M5-type cladding variants [158].

Experimental data are also available jointly from CEA and Framatome [163] for the effects of LiOH and KOH on Zircaloy-4 corrosion with two-phase heat transfer (i.e., partial boiling exposure at the surface of the fuel rod). They show a significant advantage for KOH compared to LiOH in that the corrosion increase observed in the boiling region with LiOH present was not observed for KOH at the same $\text{pH}_{300^\circ\text{C}}=7.7$; see Figure 35.

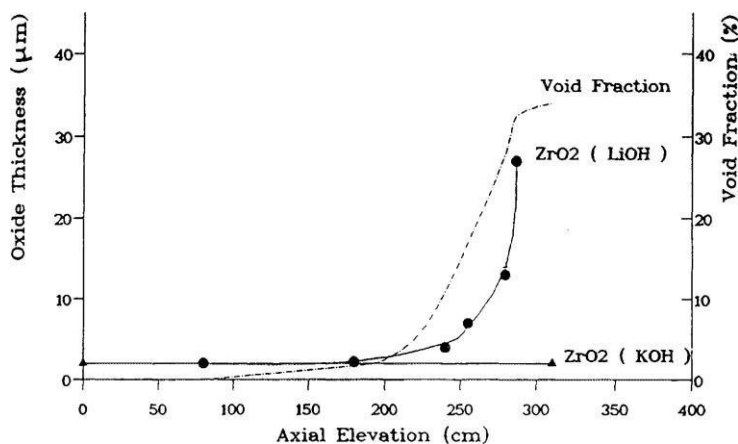


Figure 35: Effect of Void Fraction on Zircaloy-4 Oxide Thickness in LiOH and KOH (From [163])

NNL has modelled the fuel crud chemistry for a PWR coolant dosed with KOH [164]. Calculations suggest that enough lithium would be present within ~30 minutes of start-up (produced by neutron irradiation of B-10) that Li-borate salts would precipitate preferentially in fuel crud compared to the equivalent potassium salts because of the higher solubilities of the K-borates. It is also reported that the elevated temperatures and pH-values that could occur at the base of the crud if only potassium and boron were present (by concentration of soluble KOH) would be avoided. This is good news for KOH qualification, but it follows that using KOH in place of $^7\text{LiOH}$ in and of itself (i.e., for the same pH_T) will not necessarily result in avoidance of CIPS, if it were predisposed by other factors.

While the available fuel data are very encouraging, Westinghouse nonetheless requires a plant trial with fuel inspections to fully qualify KOH for use with its PWR fuel [158]. This would be to assess the impact of potentially different crud compositions (e.g., which might arise due to the different SG materials used by VVERs and PWRs), and to gain irradiation experience that is lacking from the experimental studies. Westinghouse is performing simulated (WALT) loop tests beforehand to predetermine any potential fuel risks associated with using KOH in high heat flux and thick crud environments. Results to date are reported to be satisfactory [159], although work is ongoing.

10.1.2. Structural Materials

The implications of KOH on the structural integrity of reactor materials have been assessed, including the effects of KOH on cracking of Type 304 stainless steel and Alloys 600, 182, 750, 718 and 82H; see [156], [165] and [166].

10.1.3. Chemistry and Radiation

It was recognised that CVCS operability issues might arise arising from using the ion-exchange resins to control the potassium and lithium concentrations in a PWR dual alkali control system. The situation is complicated by the fact that the ratio of lithium to potassium will change during a cycle due to changing rates of production and removal. A mass-balance model has been developed [167], which shows that the effects of KOH additions on lithium exchange are predictable and manageable for a 'western' PWR using the most common configuration of continuous mixed-bed operation and intermittent cation-bed operation. It was found that the simplest and most effective method for controlling the pH_T would be online conversion on an initially hydrogen-form mixed bed cation resin to a potassium-form resin via KOH additions

during the first few days of power operation (or during power ascension), which is like the strategy adopted for VVERs.

When it comes to controlling the chemistry, it is also important to know the precise contributions of lithium and potassium to the pH_T . Temperature-dependent equilibrium coefficients and volatilities were developed, as appropriate, for potassium species (including hydroxide and borates) and added into the MULTEQ database to predict relevant high temperature chemistries [159]. Assessment of mixed (Li+K) alkali systems indicated that they have comparable pH_T values to lithium on an equivalent molal (mmol/kg) basis [168]. Therefore, adopting an 'equivalent lithium' approach for control bands, as compared to lithium-only solutions, results in a largely insignificant change in the calculated pH_T .

Another (economic) advantage of KOH over $^7\text{LiOH}$ is that it is unnecessary to use potassium that has been isotopically enriched, whereas Li-6 would lead to significant tritium production. Potassium has three stable (or long lived) isotopes (K-39, K-40, and K-41) of which K-39 has the highest natural abundance (93.26%). When assessing radionuclide activation pathways, it is prudent to also consider the possibility of a sodium impurity in KOH. New nuclides formed by combinations of activation and decay are likely to include isotopes of Ar, K, Ca, Cl, S and P from potassium, as well as isotopes of Na, Ne, Mg and F from sodium. These include the high-energy gamma emitter K-42 ($T_{1/2}=12.3$ hours), which is a major contributor to VVER coolant activity during operation [156]. Hence, there is potential for K-42 to impact PWR radiation fields at power, but less so during shutdowns due to its relatively short half-life. Only six of the radionuclides formed by activation from K or Na have half-lives greater than 24 hours, and the maximum coolant activity concentration of these longer-lived radionuclides is predicted to be <3.7 Bq/g; an increase due to potassium addition of $<0.1\%$ of the total coolant activity [168]. These findings are being fed into a safety review to determine safe implementation of the KOH monitored campaign at Sequoyah.

10.2. Enriched Boric Acid

Boric acid is used for reactivity management in all civil PWRs, including as a chemical shim to control excess reactivity in the fuel assemblies during a fuel cycle [169]. The required amount of boric acid is greatest at BOC and then falls with burn-up. In addition, longer fuel cycles with high-duty cores require more boric acid to maintain reactivity control, although burnable poisons may also be employed to help with this.

The added boric acid reduces the pH of the coolant, which can adversely affect the integrity of the primary circuit. Hence, it is necessary to raise the pH by adding an alkali such as $^7\text{LiOH}$, which is the usual choice for western PWRs. However, at higher concentrations lithium may also affect some of the primary circuit materials adversely, including:

- Accelerated corrosion of Zircaloy fuel cladding.
- Possible effect on IASCC of Type 304 stainless steel.
- Possible effect on initiation of PWSCC in Alloy 600 components.

This limits the amount of LiOH that can be added to the coolant. Studies have shown that optimum PWR chemistry is to operate at constant pH throughout fuel cycle, preferably as high as $\text{pH}_T=7.4$, but certainly at $\text{pH}_T=7.2$ [170]. However, it is often the case that achieving high pH in the early fuel cycle would require additions of LiOH beyond conventional limits on lithium concentration. Hence, more customary practice is to begin the fuel cycle at a lower pH dictated by the lithium limit, then holding the pH_T constant (at 7.2 or 7.4) for as much of the fuel cycle as possible once the high BOC boric acid concentration has been reduced. In other words, some

PWRs are required to operate at RCS pH_T conditions that are not optimal due to limits on RCS lithium concentration.

The isotope of boron that is the effective thermal neutron absorber is B-10, but this only accounts for ~19.8% of natural boron – the rest being B-11. B-11 is of no use for reactivity control, but still acts to reduce the coolant pH_T [169]. Hence, there is scope [171] for operating with enriched boric acid (EBA) – boric acid enriched with B-10 – to increase the boron reactivity worth, and to reduce the total amount of boric acid required at all stages of the cycle. With sufficient isotopic enrichment, it becomes possible to operate the entire PWR fuel cycle with constant pH at the favoured value of 7.2-7.4 [170].

EBA can be used for two different reasons [169]:

1. To permit higher pH operation throughout a fuel cycle, either for radiation field control or to mitigate against the formation of fuel crud deposits that are implicated in the development of CIPS, or
2. To increase shutdown margins when part U/Pu mixed-oxide (MOX) cores or more highly enriched U-235 fuel is loaded.

Loading MOX fuel was the reason for Siemens/KWU-designed PWRs converting to EBA at an enrichment of ~30% B-10 [169]. The main cost saving arose from the improved fuel economy, whereas reduced radiation exposure was a minor factor. The fact that no significant changes in radiation fields were observed was not unexpected because these EBA plants operated at only slightly higher pH_T levels than they did previously. None of the units suffered from CIPS and this is usually attributed to low nickel releases from the Alloy 800 SG tubes. The transition from natural boric acid (NBA) to EBA necessitated several changes in plant systems and operating procedures. For example, efficient recovery of relatively expensive EBA using a boron recycle evaporator was considered essential, as was minimisation of EBA losses on anion resins by operating the mixed-bed units to exhaustion.

As of 2017, MOX was widely used in Europe and in Japan [172]. About 40 reactors in Europe (Belgium, Switzerland, Germany, and France) were licensed to use MOX, with over 30 doing so. In Japan, about ten reactors were licensed to use it. These reactors generally use MOX fuel as about one-third of their core, but some will accept up to 50% MOX assemblies (it is estimated that EBA must be used for PWRs when the core loading exceeds ~50% MOX fuel, [170]). France aims to have all its 900 MWe series of reactors running with at least one-third MOX fuel, and Japan also plans to use more MOX fuel. This includes construction of a 1383 MWe ABWR (at the Ohma site), which is nearing completion and capable of operating with a 100% MOX-fuel core. Other advanced light water reactor designs, such as the EPR or AP1000, are also able to accept complete fuel loadings of MOX, if required. China and Russia are new countries to embark upon MOX use, albeit with a focus on fast reactors.

Not surprisingly, consideration was given to using MOX fuel in US reactors, and a small number of test assemblies (up to 4) were loaded to Catawba 1 PWR in 2005 [170], but US NRC has since terminated its construction authorisation on a MOX fabrication facility at the Savannah River Site. Instead, US interest in EBA has been mostly from the perspective of facilitating higher pH operation to achieve radiation dose savings [169]. Cost-benefit evaluations such as those in [170] [173] were performed. In 1998, initial plant conversion costs were estimated to be \$2M for a partial conversion required to use EBA with 45% B-10 enrichment and \$4M for a full conversion to use EBA with 80% B-10 enrichment [173]. The payback period was assessed to be 3.5 to 6 years, but this was a conservative estimate because no credit was taken for the potential avoidance of CIPS. It was noted that EBA plants would likely require a silica-removal system (as well as a boron recycling system), especially those units with Boraflex spent fuel

racks.

It should be noted that there is now sufficient laboratory data and operating experience to underwrite PWR operation with a lithium limit of at least 3.5 ppm, and some PWRs have operated with up to 6.0 ppm lithium. Accordingly, EPR has been designed to use EBA enriched with B-10 to 37% (i.e., a lower figure than considered previously by EPRI) and this is sufficient to maintain a constant $\text{pH}_{300^\circ\text{C}}=7.2$ over the fuel cycle without exceeding 4.0 ppm lithium [174]. For operational convenience, EBA and Very Enriched Boric Acid (VEBA) will be supplied to EPR at 39.5% and $\geq 90\%$ B-10 enrichment, respectively. VEBA will be used to compensate for B-10 depletion.

The general thinking [169] is that the higher pH_T values achieved with EBA will reduce corrosion product release from primary system component surfaces and subsequent crud build-up on the reactor core. In addition, operation at high pH_T levels should reduce the potential for CIPS, which has been a continuing challenge for PWRs seeking to operate at higher power levels, but the potential effects of EBA on CIPS may be more complicated. EBA could potentially reduce CIPS, as high pH_T reduces crud formation. However, the CIPS benefits could be offset if crud still forms after the pH_T increase, or if there is crud already on fuel from a previous cycle, and the EBA enhances the precipitation of B-10 neutron adsorber in the crud layer [173]. It was recommended that further studies should be undertaken before definite conclusions concerning the impact of EBA on CIPS could be drawn.

This uncertainty was echoed by IAEA in [175], which points out that if crud formation is not dependant on total boron concentration, then the higher concentration of B-10 will balance the lower total boron concentration and not affect the risk of CIPS. In a presentation to IAEA FUWAC-2 [176], Chen and Bengtsson noted that Studsvik had participated in CIPS root-cause examination activities supported by EPRI and ENUSA, including testing boron deposition under EBA chemistry. An abstract of a 2007 paper summarising the Phase 3 experimental findings concluded that “the results of the EBA test calls for taking more cautious measure and further validation before EBA can be implemented in the PWRs with AOA [CIPS] risk”, but the full paper is not openly available. However, a subsequent Chen presentation to FUWAC-3 [177] concluded simply that while a change in pH can affect boron deposition in PWR cores in the longer term by reducing corrosion release rates and the amount of fuel crud formed, EBA would probably not be a better chemistry to adopt. Instead, he considered that the nickel fraction in the fuel crud was the deciding factor in the total amount of boron deposited.

10.3. Zinc Injection

As pointed out by Nordmann [66], the beneficial effect of zinc on shutdown dose rates was observed originally for BWRs with Cu/Zn alloy condensers. The first injection of zinc into BWR primary coolant took place at Hope Creek in 1987 [40]. Having established the benefit of zinc injection for BWRs, the PWR fleet followed in the 1990s, beginning with Farley 2 in 1994. Other PWR early-adopters of zinc injection included the US plants Farley 1, Diablo Canyon 1 and 2, and Palisades, and the German units Obrigheim, and Biblis A and B [178]. Understanding and experience up to the mid-2000s is summarised conveniently by EPRI in [179] [180]. As of today, zinc injection is a well-established PWR technology with around 93 units injecting zinc, which corresponds to $\sim 36\%$ of all PWRs worldwide [181]. The country with the largest number of PWRs injecting zinc is very likely the US, but there are also numerous examples in France, Spain, Sweden, Japan, and Korea.

PWRs inject zinc for one or more of the following reasons:

- Reduce shutdown radiation fields.
- Mitigate PWSCC of nickel-based alloys.
- Reduce CIPS/CILC fuel risks.

A detailed consideration of the PWSCC risk to primary-system components is beyond the scope of this report. Suffice to say that zinc has an important role in delaying PWSCC initiation, although any effects on crack-growth rates are less clear [182]. Instead, Sections 7.3.1 to 7.3.8 will focus predominantly on zinc injection in the context of radiation field reduction and managing fuel risks. Relating to this, the use of zinc injection specifically during the passivation stage of HFT is considered in Section 10.4.3.

10.3.1. Strategies

Zinc is injected to PWRs as zinc acetate because this form of zinc has solubility advantages over zinc borate and cost advantages over zinc formate, which is expensive when produced at the required high purity [183]. In the simplest case, the solubility of zinc in primary water is determined by ZnO solubility, and this corresponds to 104-220 ppb total dissolved zinc at representative PWR temperatures (150-350°C) and pH_T [178]. Power variations affect zinc solubility in a significant way, and this is explained by temperature changes and the retrograde solubility of zinc. For example, power reductions of 60% at Bugey 2 resulted in zinc concentration increasing by a factor of two [184]. Load following makes zinc control difficult.

In the early days, plants typically targeted zinc concentrations of 5-10 ppb for radiation field control, but 15-40 ppb if PWSCC mitigation was also an objective [180]. Natural zinc contains 48.6% Zn-64, which transmutes to Zn-65 under neutron irradiation. Zn-65 has a half-life of 244 days and decays by emitting γ -rays. Therefore, plants that injected zinc at the lower concentration for radiation field control used zinc depleted in Zn-64, whereas, owing to the increased cost of depleted zinc, plants that targeted higher zinc concentrations (for PWSCC mitigation) typically used natural zinc. However, strategies have since evolved to the point where most plants now inject zinc to 15 ppb or less [185].

When zinc injection is initiated, there is normally an incubation period before it is detected in the primary coolant. This may be up to ~50 days for the first zinc cycle [186], but the incubation period decreases to 5-10 days after a few cycles of injection [34]. This is good evidence for the incorporation of zinc in primary circuit materials. Some experience suggests that the time to detection may initially be longer for older units, presumably indicating that it takes longer for zinc to become incorporated in thicker corrosion films [187].

Zinc is incorporated in the out-of-core surface films, deposited on the fuel cladding, and removed by the CVCS demineralisers. It follows that the zinc retained in the circuit is given by zinc injected minus zinc removed, but this does not differentiate between zinc retained ex-core and on the fuel assemblies. The amount of injected zinc required to maintain the target zinc concentration tends to decrease with successive cycles of zinc injection [34].

10.3.2. Thermodynamics

Zinc interacts with the oxide films formed on RCS components; the SG tubes and loop piping having the largest surface areas. It may also interact with crud deposited on the fuel cladding. Lister explained the tendency of zinc to interact with ex-core corrosion films based on thermodynamic site preference energies of metal ions in spinel lattices [188]. The key feature being that Zn²⁺ ions have a very strong preference for tetrahedral sites over octahedral sites in the oxide crystal structures, and so they are much more stable in these sites than ions of other

metal species (e.g., Cr, Ni, Fe and Co).

As discussed in Section 6.1.1, the duplex oxides formed on ex-core surfaces have an inner layer comprised of nickel and iron chromites (NiCr_2O_4 and FeCr_2O_4) into which cobalt ions (including radiocobalt) are also incorporated. Given these inner oxides are normal spinels, the divalent cations (Ni^{2+} , Fe^{2+} and Co^{2+}) are in the tetrahedral sites, whereas the trivalent cations (Cr^{3+}) are in the octahedral sites. Hence, injected zinc will become incorporated into the inner corrosion films on nickel alloys and stainless steels, preferentially occupying the tetrahedral sites normally taken up by other divalent cations. This is especially so for cobalt because Zn^{2+} and Co^{2+} have almost identical ionic radii. On the other hand, the nickel ferrites (NiFe_2O_4) found in the outer oxides as well as in fuel crud have an inverse spinel structure, where the divalent cations are in the octahedral sites for which zinc does not have an affinity.

Henshaw points out [189] that the above treatment does not account for the hydration energies of the various ions involved, and in PWRs the exchange of Ni^{2+} and Fe^{2+} in chromites and ferrites by Zn^{2+} must be discussed based on aqueous ion reactions, taking account of the ionic speciation in solution. Such an assessment was performed to calculate the zinc concentrations required to achieve the complete replacement of the Ni^{2+} and Fe^{2+} ions for various oxides present in the different regions of the PWR primary circuit. The results were broadly consistent with those of Lister. For duplex oxides, zinc uptake in the inner layer (NiCr_2O_4 and FeCr_2O_4) will be largely complete at <1 ppb zinc, while uptake in the outer layer (NiFe_2O_4) will require much larger concentrations of zinc in the coolant (~130-330 ppb) and is much less likely, although partial substitution will occur. Based on plant data for Diablo Canyon and Vandelllos, it was suggested that outer-layer substitution by zinc was of order 15-20%. In addition, the assessment calculated that zinc completely replaces Fe^{2+} in the inverse spinel Fe_2O_3 at zinc concentrations in the range of ~7-15 ppb.

According to Tigeras [187], some authors suggest an energetic approach is not enough to completely explain the zinc interaction mechanism because an additional energy would have to be considered for atom reorganisation in the crystal lattice. In which case, zinc incorporation and the displacement of other ions would only take place on grains boundaries, where energy is lower.

10.3.3. General Corrosion

Incorporation of zinc into the crystal lattice of spinel-type oxides makes them more stable and more protective, thereby reducing the primary water corrosion rates of the SG tubes and the loop piping. This is evident from Table 2 in Section 6.1.1, where materials effects were initially the focus, but the impact of zinc is also included. Corrosion rates show an average improvement factor of 3.7 due to the presence of zinc for the various stainless steels and nickel alloys tested; the largest improvement factor being 6.5 for Alloy 690TT. The effect of zinc on corrosion release rates was markedly higher for the stainless steels compared to the nickel alloys (average improvement factors of 13.5 and 4.4, respectively), but the largest improvement among the nickel alloys was again for Alloy 690TT (factor of six improvement). These data are from loop tests and correspond to 3.5 months of zinc uptake in freshly forming surface oxides [182].

In the long-term, zinc injection would be expected to reduce the corrosion input to the primary water, with potential benefits both for fuel crud accumulation (thick fuel crud is nickel rich and contains iron) and shutdown radiation fields (Co-58 is a key contributor, and its formation is dominated by in-core activation of nickel released from the SGs). Zinc also reduces the corrosion rate of iron-rich Alloy 800 SG tubes [183], which is pertinent to Siemens/KWU designed plants and Westinghouse plants with Alloy 800 replacement SGs, such as Doel 3 and Asco 1 and 2.

However, long-term effects are not the only consideration. As will be seen below, when zinc is first introduced into the primary coolant, and it becomes incorporated in oxide films in preference to other divalent cations, this can result in increased coolant concentrations of those species. An effect on cobalt, nickel and iron concentrations might be expected, influenced by the choice of SG tubing alloy.

10.3.4. Primary Water Chemistry

For the first few cycles, zinc injection typically results in increased radiocobalt concentrations during normal operation [178]. Circulating activities increase soon after zinc injection starts and may then level off for the remainder of the cycle. The relative increase becomes smaller during subsequent cycles, and after a few cycles, equilibrium levels may be lower than those from before zinc injection. Initial increases in radiocobalt concentrations are observed irrespective of SG tubing alloy [187], but the effect is not systematic [34], and a statistically significant increase in radiocobalt concentrations is not seen (in the first zinc cycle) for all PWRs [190]. When zinc injection does promote an initial increase in radiocobalt concentrations during normal operation, it is attributable mainly to the soluble phase (e.g., Vandellos II, Asco II, and Watts Bar) due to zinc inhibiting or replacing Co in the oxide layer [187].

To begin with, EPRI observed that zinc injection increased the amount of radiocobalt activity released and removed during shutdown [178], although this trend became less clear as more units injected zinc. In some cases, Co-58 removed on shutdown following the first zinc cycle increased, whereas in other cases, the amounts decreased or remained unchanged [40]. EDF experience is that Co-58, Co-60, and Cr-51 peak concentrations following oxygenation at shutdown increase for the first and sometimes second zinc cycles, and more so than the concentrations during normal operation [34]. Moreover, an increase in the Co-58 peak after the first zinc cycles is observed for plants with Alloy 600, 690 and 800 SG tubes alike [187], noting that factors other than zinc may also contribute (e.g., longer fuel cycles). In terms of activity removed during shutdowns, EDF calculated, for several plants, the average value of the Co-58 release for the two shutdowns prior to starting zinc and compared this with the activity released during subsequent shutdowns for which there was zinc injection in the preceding cycle [186]. Ratios (post-zinc/pre-zinc) were in the range of ~ 1.3 -2.0 for the first zinc cycles and then tended to decrease for subsequent cycles.

For early zinc cycles, it was observed that increases in Co-58 activity during normal operation were greater than those in Co-60 activity, at least for nickel-rich plants. At the time, this was interpreted as an indication that zinc may cause greater releases of nickel than cobalt from ex-core oxides [178] [180], with the nickel depositing in the core where it is activated. However, a statistical analysis of plant data by EPRI, while reluctant to completely rule out the possibility that coolant nickel concentrations increase during the first cycle of zinc injection, found no evidence that they do [190]. Likewise, there was no statistically significant increase in the mass of nickel removed during shutdown following initial injection of zinc. This was despite an earlier EPRI review observing that shutdown nickel releases are increased for the first two cycles with zinc injection, according to [187]. Nonetheless, EDF notes that while an increase of a few ppb Ni may be encountered during the first few days of the first zinc cycle (a minor issue that is resolved by temporarily halting zinc injection), nickel concentrations are then low and stable (~ 1 ppb) during normal operation, irrespective of whether zinc is injected [34]. This all indicates that the early interpretation, while conservative in terms of potential risks, is likely to have been incorrect. Interestingly, [190] implies that the EPRI BOA code assumes close to a 1:1 molar substitution between zinc initially retained in the circuit and nickel deposited in the core, which would seem to be overly pessimistic in terms of evaluating fuel risks.

In line with the above, an EDF review of US, French and German experience [187] found that units with Alloy 800 observed no effect of zinc injection on their coolant nickel inventory, as was also the case for units with 600/690 alloys. However, the observed behaviour differed and diverged regarding iron. For the Alloy 600/690 units, iron concentrations stayed the same or decreased following zinc injection, whereas they increased for the alloy 800 units (from 1-2 to 2-8 ppb). Statistical analysis by EPRI also found evidence for a short-term increase in iron concentrations for some alloy 800 plants upon initial zinc injection [190].

Given the very favourable test-loop results for general corrosion and corrosion release rates, zinc injection was identified as an effective mitigation to be implemented in advance of SGRs [184]. Prior to this, it was observed that releases of cobalt and nickel were higher for several cycles after SGR than before because the replacement tubes were not preconditioned, and so the surfaces had higher corrosion release rates in the first cycles of operation. Early examples of units injecting zinc both before and after SGR apparently confirmed the passivation effect of zinc. For Farley 1 and 2, the nickel and Co-58 increases after SGR were lower than the increases experienced in units without zinc injection.

The Farley 2 experience led EDF to inject zinc for Bugey 4. For zinc plants, EDF now reports [34] a rapid reduction in the magnitude of shutdown Co-58 peaks to <50 GBq/t in the cycles soon after SGR (i.e., to lower than the criterion to stop last RCP); see Figure 36. The corresponding decrease in Co-58 for non-zinc SGR plants is slower and less systematic, with levels continuing to exceed 50 GBq/t (prior to clean-up) for several cycles after SGR. In other words, zinc leads to a gain in plant availability due to reduced purification time, encouraging EDF to continue injecting zinc and expand the practice to future reactors.

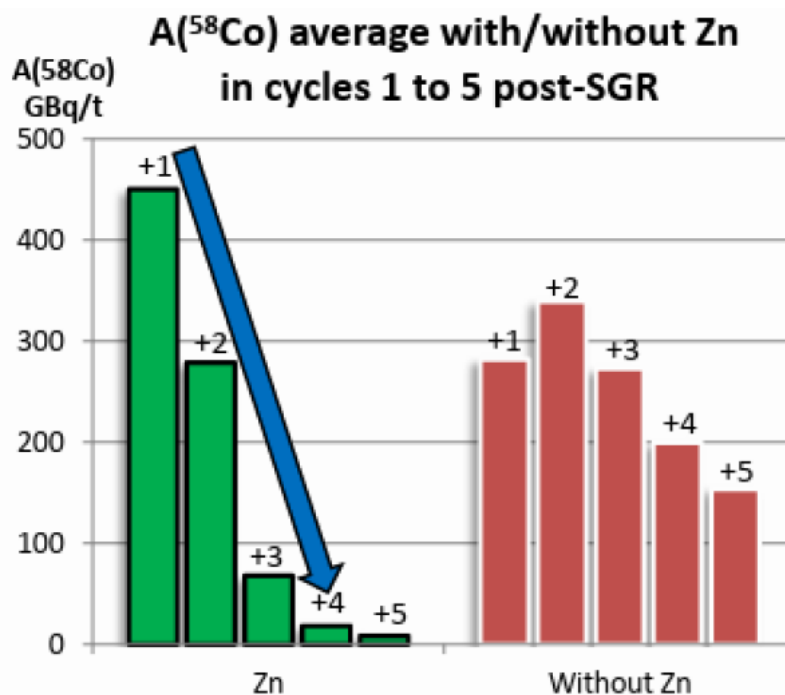


Figure 36: Average Co-58 Activity in Cycles 1-5 after SGR

Notes: Peak Co-58 activity following oxygenation is plotted for EDF PWRs that have undergone SGR. Data are averaged by cycle (1-5) for the first five shutdowns after replacement and are presented separately for units with/without zinc injection. This plot is taken from [34].

10.3.5. Mechanism

In 2014, EPRI carried out a comprehensive review of internationally available laboratory data and operating experience [191] to better understand the effect of zinc on corrosion product release, beyond the thermodynamics outlined in Section 10.3.2. The review considered each of the relevant surface materials (stainless steel and alloys 600, 690 and 800) separately, and drew a distinction between the zinc effect on freshly growing oxide films and pre-oxidised surfaces.

Common aspects of the zinc mechanism were described as follows:

- Mechanisms of zinc and cobalt incorporation in oxide films appear similar and involve reversible and rapid adsorption to available oxide binding sites, followed by gradual incorporation into the oxide film from the bound state through a diffusion-controlled process.
- Binding sites for zinc and cobalt appear to be similar resulting in a concentration driven competition for steady-state occupation. The coolant concentration of zinc is greater than that of cobalt and so zinc readily displaces cobalt present at surface binding sites, preventing further binding and incorporation.
- The implications are that (i) bound (but not incorporated) cobalt may be released rapidly from surfaces upon zinc injection, (ii) zinc incorporation occurs over multiple timescales, and (iii) zinc prevents binding and further incorporation of cobalt into oxide films.
- This initial process does not result in rapid exchange of zinc with divalent cations (Co or Ni) already incorporated in the metal oxide. Instead, Zinc incorporation occurs primarily at the oxide surface to begin with, and a decreasing penetration profile is indicative of a diffusion-limited process. Prolonged exposure results in increased zinc penetration. This is also the case when zinc is present during oxide growth.

The following conclusions were drawn specifically for zinc with freshly growing oxide films (i.e., for zinc injection in the case of new plants or replacement SGs):

- Average rates of corrosion release are all reduced by zinc exposure when oxide films are grown in the presence of zinc, and this is accompanied by changes in oxide morphology and reductions in thickness of the resulting film and corrosion rate of the base metal.
- Observed reductions in corrosion rate and corrosion release are attributable to initial growth of oxide to its mature state. Zinc incorporation in growing oxide may result in formation of a zinc spinel phase that stabilises the oxide and reduces its growth rate. A zinc chromite phase may be favoured, with zinc preferentially incorporated in Cr-rich oxides. This may prevent transport of corrosion products and oxidising species across the film.

However, the conclusions for zinc with mature oxide films (i.e., for zinc injection in the case of older plants) were as follows:

- The inhibitory effect of zinc on corrosion release from mature oxide films is not rigorously quantified (data are sparse). Moreover, the effects of zinc on mature films are not the same as for freshly growing films, other than with regards to cobalt-uptake. The mechanism by which corrosion product release is inhibited is not established, but zinc may inhibit transport of corrosion products and oxidising species across the film.
- Initial radiocobalt release may be more closely related to competition between zinc and cobalt for available binding sites rather than due to changes in underlying corrosion and release rates from the bulk oxide film.

To summarise, the effect of zinc on freshly grown oxides is dramatic and clearly different from the effects observed on mature oxides. Reductions in corrosion release rates measured experimentally pertain to freshly grown oxides in the presence of zinc. Quantitative measurements on long term corrosion, and on corrosion release rates from mature oxides exposed to zinc are extremely rare. It is not possible to isolate the long-term effects from plant data because they are frequently obfuscated by other more dominant factors.

EPRI has since investigated the role of zinc in relation to mature oxides using SG tube specimens obtained from several plants. A study using two Alloy 600 specimens from a Westinghouse 4-loop plant is described in [192]. One specimen was removed at EOC 11 after 3.6 EPFY of exposure to hot-leg conditions, while the other was removed at EOC 14. The plant started zinc injection towards EOC 12, and it is stated that the second sample experienced 2-3 cycles of zinc, with a mature oxide film present. On average, the oxide thickness of the zinc specimen was thinner than for the non-zinc specimen, suggesting that exposure to 2-3 cycles of zinc reduced the thickness of the mature oxide by ~26%. STEM-EDS revealed that zinc bypassed the bulk of the oxide and instead diffused rapidly through surface defects deep into the intergranular region and metal-oxide interface (Figure 41). In other words, the uptake of zinc was very localised, in marked contrast to how zinc diffuses gradually into the bulk of the oxide formed on type-304 stainless steels [35]. If the inference made from comparing the Alloy 600 specimens is correct, that zinc causes thinning of mature oxide, then the removed oxide may potentially provide additional source term for crud in the core, but this material will be taken-up partly by coolant purification, and the effects of an increased source term have not been observed in practice.

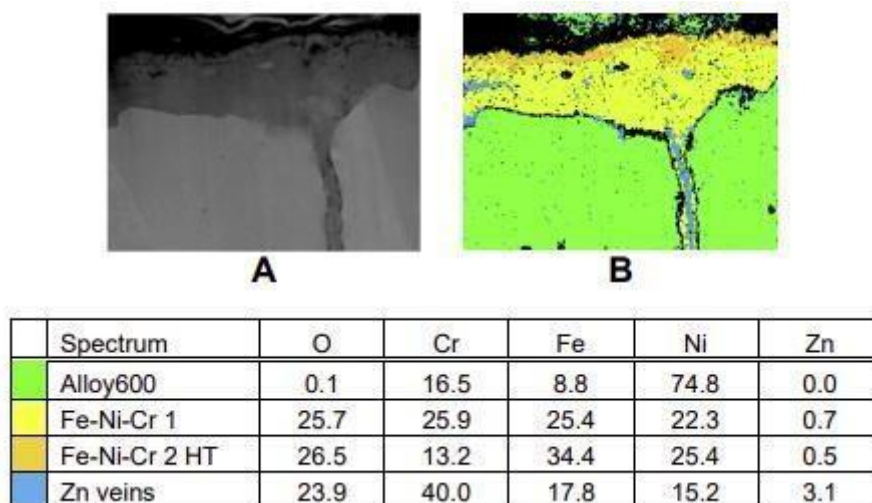


Figure 37: STEM-EDS Images of Alloy 600 Specimen Exposed to Zinc

Notes: The STEM image (A) and EDS phase map (B) are accompanied by a table giving the semi-quantitative composition of phases in weight%. This figure is taken from [192].

In addition, EDF has recently investigated the microstructural effects of zinc on Alloy 600TT and 690TT oxidation using their experimental ZINC-loop [181]. Samples of SG tubing were exposed to primary water chemistry conditions representative of BOC or mid-cycle, either at 285°C for 3000 hours or at 325°C for 1500 hours. The objective was to form a morphologically stable oxide in each case. Three different zinc scenarios were investigated, two of which were as follows:

1. Oxidation of as-received samples without zinc (i.e., reference cases for comparison).
2. Oxidation of as-received samples with 10 ppb zinc (i.e., effect of zinc with freshly forming oxide).

The third zinc scenario was oxidation of as-received samples without zinc followed by a second period of oxidation with 10 ppb zinc. These tests were twice the duration of the others and were designed to represent the effect of zinc with pre-oxidised surfaces. Upon completion of the tests, the various samples were analysed by SEM and ToF-SIMS.

A large matrix of results was obtained, but there was little effect of chemistry conditions (BOC versus mid-cycle) and both alloys (600 and 690) behaved similarly. Also, excluding zinc, the oxide layers formed had comparable compositions; an inner layer mostly enriched in Cr with lower Ni and Fe concentrations, and an outer layer comprised of hydroxides of Ni, Fe and Cr. On the other hand, the effect of temperature was significant. For the reference case, large crystals were formed on the surface at the higher temperature but not at the lower temperature, and the oxide was thicker at the higher temperature (~ 270 nm versus ~ 37 nm). A double layer was formed at the lower temperature, but it had probably not reached maximum thickness at 3000 hours.

Zinc injection from the start of oxidation, with freshly forming oxides, clearly affected the oxide morphology and thickness; see Figure 38. The large crystallites formed at 325°C without zinc were not present with zinc, and the oxides were thinner, especially at the higher temperature (~ 40 - 62 nm). However, this was not the case for zinc injection with the oxides pre-formed. There was little difference in the morphology compared to the reference case and the oxides were thicker than for the reference case, although arguably less so than might have been the case for two consecutive periods of oxidation without zinc (not tested). This was suggestive of a more complicated structural modification of pre-existing oxides (replacement of cobalt ions), and therefore slower. The value of a future test with an extended period of zinc exposure was identified, to see if the crystallites would eventually disappear.

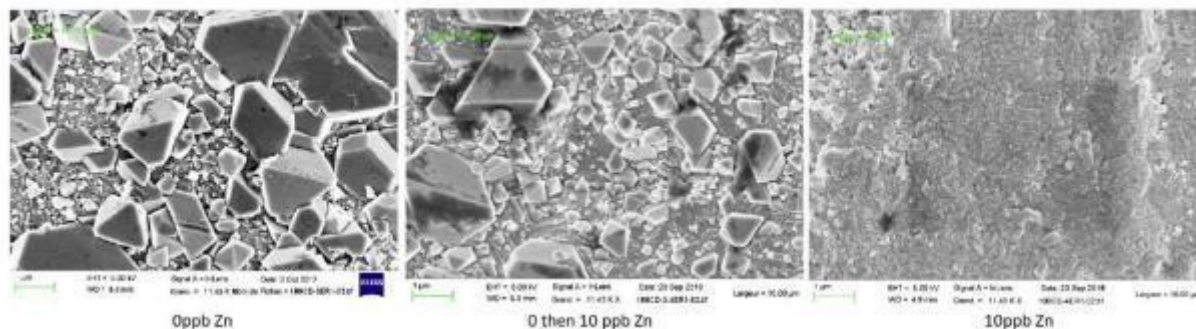


Figure 38: SEM Observations of Alloy 690TT Sample Oxidised at 325°C

Notes: The lefthand image is the reference case (0 ppb Zn), the righthand image shows the impact of 10 ppb Zn on freshly forming oxide, and the centre image represents the case for zinc addition with a pre-formed oxide. This figure is taken from [181].

To summarise the EDF findings, the effect of zinc on oxide thickness appears to depend on whether the oxides are freshly forming or are relatively mature. Regardless, the presence of zinc was detected in the oxides for the higher temperature runs with zinc exposure. Hence, zinc participates in the formation of oxides and penetrates previously formed oxides. Injected from the initial stages of oxidation, zinc enables the formation of a thinner layer, which is apparently more compact and does not have crystallites on the surface.

10.3.6. Radiation Fields

The PWR early adopters of zinc injection soon provided compelling evidence of lower shutdown dose rates and deposited radiocobalt activities (see, for example, [178] [186]). Operating experience from Diablo Canyon 1 and Farley 2, both injecting natural zinc to a concentration of 20-35 ppb, showed ~28% reduction in dose rates after one cycle of zinc, and ~50% reduction after 2-3 cycles. This was despite zinc being injected for less than half of any given cycle for Farley 2. Tellingly, there was also no dose rate improvement for Farley 2 Cycle 11, for which no zinc was injected (zinc was injected for Cycles 10 and 12). Plants with lower zinc concentrations (5-10 ppb) also benefited from reduced dose rates by 10-15% per year, e.g., Palisades, Biblis, and Obrigheim. This confirmed that lower levels of zinc were adequate to realise dose savings. International experience showed that ~25% reduction in deposited activity was possible with zinc.

Gamma spectrometry for Diablo Canyon 1 showed radiocobalt decreases greater than expected from decay only, indicating that zinc was exchanging with cobalt radionuclides. It should be noted that the dose savings for Diablo Canyon 1 were judged to be attributable to zinc injection and UFC in roughly equal measure, and that the replacement SGs at Farley 2 also benefited from electropolished channel heads. However, the Farley 2 channel head dose rates (6.2 mSv/h) compared favourably with those of other SGs with polished heads, but without zinc injection (typically ~20 mSv/h). Comparing average dose rates before and after oxygenation, it was observed that average dose rates were often lower by a greater fraction after oxygenation for those shutdowns following zinc cycles, suggesting that zinc led to corrosion product activity being more easily removable by hydrogen peroxide.

To recap, it was recognised [187] that zinc could reduce shutdown dose rate in three ways:

1. Inhibit cobalt incorporation into the oxide layer of ex-core surfaces.
2. Substitute cobalt ions already incorporated.
3. Diminish corrosion release from primary circuit materials.

For (1), dose rates would fall according to natural decay – by 10-15% per year for Co-60 – whereas reductions would be more significant if radiocobalt was also displaced by zinc.

It became apparent that a dose reduction of 60% was achieved for Biblis A and B after ~10 years of zinc, but this was not uniform for different areas of circuit, and that US Alloy 600/690 plants with 5-10 ppb depleted zinc reported average dose reduction of 40% after about 170 ppb months (or 2-3 cycles) of zinc. The cumulative effect of zinc was identified by a correlation between zinc exposure (in 'ppb months') and dose rate reduction, although it was recognised that zinc concentration and time of exposure would not be the only dominant factors. Dose reductions would presumably also be affected by surface contamination events, and operating conditions (power variations), etc. Siemens/KWU plants that had experienced frequent power reductions had not yet reported dose reductions after four cycles of zinc injection (2-5 ppb zinc), compared with 16% and 26% reduction after two and three cycles of zinc for another unit with stable operating history.

EPRI produced a plot (Figure 39) illustrating how the impact of zinc injection on shutdown dose rate evolves with cumulative zinc exposure [182]. Although individual plants and cycles are not identified, data are plotted and fitted separately for Alloy 600/690 plants injecting natural zinc, Alloy 600/690 plants injecting depleted zinc, and alloy 800 plants injecting depleted zinc. On average, plants achieve a 40% dose rate reduction before reaching 400 ppb-months of zinc exposure, but this is not the case for all plants.

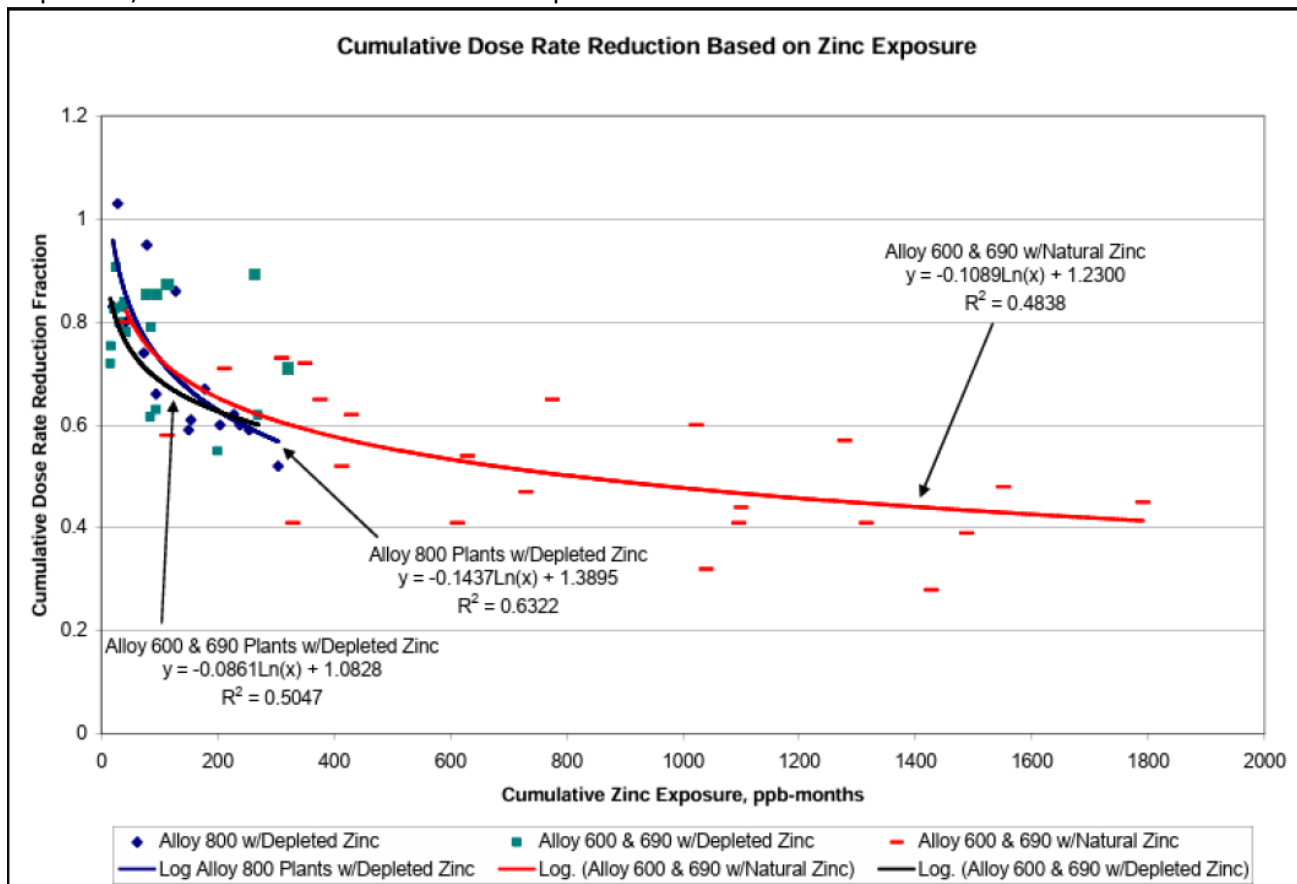


Figure 39: Dose Impact from Zinc Injection (From [182])

It is notable that EDF has not experienced a significant effect on the dosimetry of its many PWRs injecting zinc, which amounted to 34 campaigns between 2004 and 2017 at the time of [34]. This follows, in part, from the absence of an effect on deposited Co-60 activity, but EDF also comments that a dose effect is difficult to observe because of other influential factors, such as the behaviour of non-cobalt radionuclides (perhaps referring to silver or antimony radionuclides), and radiation hot spots, etc. This is at odds with Japanese experience, for example, where continually reducing dose rates were reported for 11 PWRs injecting zinc to a concentration of ~5 ppb [193].

EDF, on the other hand, does report a reduction in Co-58 surface activity in the SGs of those units injecting zinc, especially in the case of replacement SGs. A decrease in Co-58 surface activity is also observed for the crossover legs of units with replacement SGs. More generally, it is considered that the presence of zinc during passivation is important towards obtaining its optimal oxide-layer incorporation. EDF developed a very comprehensive follow-up programme

to monitor the impact of zinc injection on radiation fields, fuel performance and waste arisings for its PWRs, as described in [194].

EPRI's view is that most plants injecting zinc observe a decrease in shutdown dose rates, but a small fraction do not experience a clear benefit. Understanding this divergence in response is hindered by the fact that there are a range of factors that influence the evolution of radiation fields. Therefore, multivariate statistical analyses were performed for a population of Westinghouse-designed PWRs [195] [196]. These analyses used data for ~400 operating cycles (including 75 cycles with zinc) held in EPRI databases and compared radiation field responses at plants injecting and not injecting zinc, in concert with other factors. This was considered a more realistic approach than the single parameter hypothesis testing that was typically employed previously. Separate analyses were performed using hot and cold leg mean radiation fields as dependent variables.

The range of explanatory variables was arguably somewhat limited, and probably intended to demonstrate the usefulness or otherwise of the approach, ahead of possible follow-on work. They were comprised of plant design parameters, operational zinc parameters, and a chemistry parameter (pH_T during last days of cycle). A decision tree model was then used to uncover which factors may interact favourably on dose rates. The results confirmed the importance of zinc. On average, dose rates for zinc plants are about 50% lower than for non-zinc plants. Materials factors were also identified to be important for the hot-leg analysis, with the average predicted dose for Alloy 690TT about half of that for 600MA/600TT plants, which may reflect the lower corrosion release rates of nickel for Alloy 690TT SG tubes. Number of SGs was also significant for the cold-leg analysis, but box plots suggested this finding was largely due to a small number of high outliers for 3-loop plants, and so it should be treated with caution.

10.3.7. Fuel Performance

Laboratory testing suggested that a significant reduction in fuel crud deposit would be expected in the longer term for PWRs injecting zinc, mainly due to reduced rates of nickel release into the primary coolant from general corrosion of nickel-rich SG tubes as the ex-core oxides became stabilised and more protective. However, there was uncertainty about what the initial effects might be. As already discussed, there were concerns that the incorporation of zinc in ex-core oxides would lead to increased nickel releases, at least for the first cycles of zinc injection, before the longer-term benefit was realised. This nickel would then be available for deposition on the fuel cladding, especially in regions of the core undergoing boiling, with the risk of promoting CIPS. It was also recognised that localised boiling could promote precipitation of zinc-containing species in pre-existing fuel crud, potentially leading to CILC. Therefore, low-to-medium duty plants were selected for the first demonstrations of zinc injection.

Fuel inspections for the demonstration plants (as summarised in [178] [179] [180]) showed no effect of zinc, beneficial or otherwise, on the thickness of the zirconium oxide layer. Fuel crud tended to be thinner and more-evenly distributed along the full height of fuel assemblies, rather than concentrated in the upper spans, and contained <5 wt% zinc. Some deposits were observed to be unusually dark, but this feature of so-called 'zinc crud' was confined to those plants injecting zinc at higher concentrations for PWSCC mitigation and was not apparent for plants targeting a zinc concentration of 5-10 ppb. Crud scrapes of Palisades fuel found no evidence of zinc or silicates, despite silica concentrations of ~ 1 ppm.

Some years later, an EDF unit (Blayais 4) reported that a cloud of loose particulate was observed to emanate from a fuel assembly in the SFP during an extended outage [197]. It was assumed that contraction during cooling led to spalling of crud, and that this was likely related to zinc injection and modification of the fuel deposits. However, upon reaching out to international colleagues, it was ascertained that such observations were considered normal for zinc plants in the US and had been sentenced as unalarming by the fuel vendors and EPRI. EDF investigations determined that the phenomenon, which also affected another EDF plant, were associated with the first cycles of zinc injection and extension of the operating cycle (i.e., stretch-out), as well as prolonged time in the SFP [34]. In terms of mitigation, a mobile filtration unit may be employed at the bottom of the fuel pool to accelerate removal of deposits, supplementing the SFP purification system.

Following these promising results, zinc demonstrations were carried out for plants with progressively higher-duty cores, including Callaway, Vandellos 2, and Vogtle 1 [100]. Initially, zinc was restricted to the latter half of fuel cycles for high-duty plants, to militate against the risk of CIPS occurring at the beginning of cycle when boron concentrations and boiling are highest, but fuel vendors later relaxed this requirement following observations confirming the benign nature of zinc injection with respect to fuel performance [183]. For example, Callaway crud was scraped at the end of Cycles 13 and 14 after exposure to zinc concentrations up to 20 ppb, and crud up to 35 μm in thickness was observed [100]. No zinc oxide precipitate was detected, but zinc was incorporated into a variety of (spinel and inverse spinel) crud phases. Similar results were obtained after zinc injection up to 10 ppb at Vandellos 2. The crud was up to 39 μm thick, but no zinc-rich phases were detected, just zinc incorporation in spinel oxides. It is understood that only two units (Fort Calhoun and Vogtle) were affected by CIPS during zinc cycles, and both had reported CIPS in the previous cycles without zinc [187].

Much attention has been given to understanding the conditions for which zinc-containing species, such as ZnO, may precipitate in PWR cores. It is known that SNB provides a mechanism by which circulating corrosion products concentrate and deposit at the cladding surface, and once porous deposits are present, boiling will favour the localised concentration of any solute species present in the coolant. Hence, precipitation and deposition of zinc-containing species may occur in fuel crud even under conditions for which they are soluble in the bulk coolant [183] [100]. Such concerns are likely to become more significant for high-duty cores (and higher zinc concentrations).

Precipitation of zinc silicate is another potential concern. Silica is soluble under PWR conditions, but it forms silicates with Al, Ca, and Mg (the elements commonly responsible for water hardness), as well as with zinc [198]. It is well known that zeolite species (Al, Ca, and Mg silicates) precipitate preferentially on fuel rods and may cause densification of porous deposits leading to accelerated cladding corrosion, and potentially CILC. Silica is retained poorly by ion-exchange resins and so its accumulation in PWR coolant can be a problem, especially for plants with Boraflex spent fuel racks (a source of silica), and for plants that recycle boric acid. The silica concentration tends to behave like that of boron. It is highest at beginning of cycle before co-diluting with the boron concentration. Initially, the silica upper limit for zinc injection was fixed at <1 ppm by the fuel vendors [183], and inability to comply with this conservative requirement at BOC sometimes meant that zinc injection had to be delayed for several months, as was the case for Bugey 2 and Bugey 4 [186]. Similarly, primary water concentrations of Al, Ca and Mg are also limited by plant specifications, with or without zinc injection (e.g., to <50 ppb by EDF, [183]).

EPRI examined the solubility of zinc silicates in the late-1990s by extrapolating lower-

temperature solubility data to PWR operating temperatures. For an assessed zinc concentration of 80 ppb, [180] recounts that zinc silicate precipitation was not estimated to occur at 300°C unless the silica concentration reached 8 ppm. However, this assessment did not take account of the concentration mechanism available at the fuel cladding surface.

WALT tests funded by EPRI simulated zinc precipitation under the thermal hydraulic conditions of a high-duty PWR [100]. Nickel ferrite was deposited on a heater rod before zinc was added to simulated primary coolant at concentrations ranging from 0 to 60 ppb. During the 60-ppb run, a significant temperature increase was observed. Investigation revealed that the base of boiling chimneys formed in the deposit had been filled with a white material subsequently identified as ZnO. Given the solubility limit of ZnO was estimated to be ~200 ppm, this suggested a zinc concentration factor of ~3.3 due to boiling in the deposit layer, which was not considered unreasonable for a crud thickness of ~50 µm. However, laboratory testing and plant experience suggests that ZnO precipitation does not take place when crud is thinner, or zinc concentrations are lower.

Similar tests were then performed with varying quantities of impurities present, including silica. There appeared to be no interaction between zinc and silica, and zinc silicate was not detected in deposits [199]. This was true even in an experiment where the zinc concentration was 40 ppb and the silica concentration was 10 ppm; a result seemingly corroborated by the operational experience of some units injecting zinc with silica levels above 2 ppm.

Initial attempts [189] to model zinc behaviour in PWR cores, based on a wick-boiling model updated to include thermodynamic data for ZnO and Zn₂SiO₄, suggested that zinc precipitation was likely, even with relatively low zinc and silica concentrations, and for modest crud thicknesses, but this was inconsistent with plant observations. It was later realised that high concentrations of zinc and borate ions may lead to zinc-borate complex formation, as well as the possibility of complexation between borate and silicate. Little direct information existed for the thermodynamics of these complex species, but when uncertain estimates were added to the model, the predictions were in much better agreement with operational experience [200]. Zn₂SiO₄ was no longer predicted to precipitate before ZnO, except at higher silica concentrations of 1 ppm (raised to 5 ppm in later work, [199]), and the crud thicknesses required for precipitation to occur for the various modelled permutations of zinc and silica concentrations increased.

Plant observations, modelling results, and fuel deposit loop testing results appear sufficient to justify fuel vendor consideration of relaxation of the current primary coolant silica limits prior to zinc injection. The current consensus according to EPRI [199] is that plants can operate safely up to 5 ppb zinc, although the highest duty plants may require additional analysis and evaluation before, and potentially after, implementing zinc injection. This may include fuel examinations.

10.3.8. Other Considerations

An EPRI review of zinc injection experience for 19 plants confirmed that while zinc results in an initial increase in reactor coolant corrosion product concentrations, this was found not to significantly affect the performance of the CVCS demineralisers or filters [180]. One possible exception was that filter usage approximately doubled during the first cycle of zinc injection at Diablo Canyon 1, but this returned to normal after that cycle. Hence, it was concluded that zinc injection did not result in a significant increase in radwaste. EDF also observed that the amount of spent resins and filters was largely unchanged by zinc injection, based on three zinc cycles for Bugey 2 [183].

In terms of long-lived radionuclide surveillance, EDF was initially concerned that zinc injection

might influence Ni-63 and Fe-55 activities [186]. These are β -emitters and so do not contribute to radiation doses, but with half-lives of 100.1 and 2.73 years, respectively, they must be considered in reporting the activities of liquid wastes. However, NPP feedback (from the Bugey reactors) provided reassurance that effluent activity did not increase following zinc injection, and that the ratios used to report long-lived beta/gamma and pure β -emitters remained valid for units injecting zinc [183].

EDF had a similar concern regarding the potential impact of zinc injection on the isotopic distribution of solid radwaste arisings, for which a characteristic waste spectrum was routinely employed [186]. Gamma spectrometry of CVCS filters conditioned in concrete containers initially found that relative activities of Co-60 increased for the first zinc cycle, but that spectra obtained for second and third zinc-cycle filters were close to the reference spectrum [183]. However, with more data, it was concluded that a different isotopic distribution was observed for spent CVCS filters during the first three cycles of zinc injection, and the decision was taken to develop a specific waste spectrum, adapted to the first cycles of zinc [34]. In the interim, it was necessary to perform measurements on each waste package to ensure the accuracy of the radiological characterisation.

Questions were raised at a zinc workshop about whether the acetate form of injected zinc causes any problems [188]. In response, it was noted that the acetate breaks down and that the carbon precipitates out and is removed by filters or is incorporated in crud. Moreover, no deleterious effects of the acetate or resulting carbon were known. Theoretical calculations show negligible potential C-14 production from acetate addition; $<1-3 \times 10^{-4}$ % of C-14 produced from other sources [183].

The calculated C-14 production rate for a PWR rated at 2,775 MWth is approximately ~ 350 GBq $\text{GWe}^{-1} \text{y}^{-1}$, and it is evident that activation of O-17 is the main source term, accounting for $>99\%$ of the production; the next most important source being activation of N-14 [201]. A detailed investigation [201] using pre-zinc data for Ringhals 4 found that organic forms accounted for almost all (99.7%) of the C-14 in the coolant at the start of the fuel cycle, although inorganic forms increased to 27% towards the very end. Of the organic phase, $\sim 60\%$ was reduced gaseous compounds (probably CH_4), and $\sim 40\%$ was non-volatile organic compounds (NVOs), believed to be formate and acetate. The NVOs were not affected by purging or acid-stripping but were converted to CO_2 upon oxidation.

Of the C-14 produced in the Ringhals 4 coolant, $\sim 9\%$ ended up in the spent resins (N.B., organic compounds contributed only $\sim 30\%$ of the total C-14 activity in the spent resin samples) and $<0.5\%$ was released with liquid discharges. Gaseous releases should, therefore, have accounted for the remaining $\sim 90\%$, but stack measurements of C-14 activity accounted for only $\sim 78\%$. Hence, the fate of $\sim 12\%$ of the C-14 produced in the coolant was potentially unaccounted for.

While this was within the calculated uncertainties, the possibility of undiscovered sinks of C-14 was not completely ruled out. Interestingly, flakes of Diablo Canyon 1 fuel crud (from a zinc cycle) were found to be rich in carbon [188].

In summary, zinc injection will not affect the production rate of C-14 in PWR coolant, but it could affect how its fate is split between solid, liquid, and gaseous waste streams. Whether or not a PWR operates with a continual purge on its VCT might also influence the fate of acetate breakdown products, and hence C-14.

10.4. Hot Functional Testing

HFT is carried out during reactor commissioning and provides an opportunity to influence the development of oxide films on wetted metal surfaces in the primary circuit; the loop piping and SG tubes being of most interest because of their high surface areas. The chemistry objectives can be summarised as follows [202]:

- Formation of a stable and protective passive film, which minimises the corrosion release rate of metals during subsequent plant operation, and the incorporation of activated corrosion products once fuel is load in the core.
- Removal of releasable corrosion products prior to operation with fuel in the core to prevent their subsequent activation.

It is expected that oxide films will have at least partially developed their characteristic duplex structure by the end of a typical HFT process because laboratory testing indicates this happens over an initial period of 100-200 hours. In other words, HFT is sufficiently long for the chemistry objectives to be feasible. Some tests showed continued changes in the chemical properties of oxide layers for specimens with up to ~10 years of exposure to primary chemistry conditions, although the changes were most rapid during the first few thousand hours. As a general principle, EPRI notes that the oxide formed during HFT will be inherently unstable at operating conditions unless HFT was performed under similar conditions. Therefore, any HFT chemistry other than the planned operational chemistry should be subject to qualification testing.

Originally, conventional HFT was comprised simply of warming the PWR primary circuit to 260-300°C under alkaline conditions (1-2 ppm lithium) for a period of days or weeks. Boric acid might also be added to test the operability of various systems, but boron concentrations would be variable and lower than those experienced at beginning of cycle. However, this changed in the mid-1990s with the commissioning and HFT of Sizewell B.

10.4.1. Sizewell B HFT Chemistry

The recommended HFT chemistry for Sizewell B differed to what had gone before in three main respects [203]:

1. HFT operation with dissolved hydrogen present.
2. HFT operation with boric acid (and lithium) at BOC concentrations.
3. Implementation of 'refuelling outage' chemistry controls, including hydrogen peroxide addition, at the end of HFT.

Oxide morphology is affected by redox changes. Moreover, other workers had shown that dissolved hydrogen led to chromium enrichment of oxide films grown on nickel-based alloys in LiOH solutions, and this was expected to reduce oxide solubilities and corrosion release rates. Therefore, it was decided to operate with 25-50 cm³ kg⁻¹ dissolved hydrogen for HFT, starting with a 10-day 'passivation' stage with Li-7 present at 1-2 ppm (target range) and T>280°C. This was followed by a 'boric acid' stage lasting ≥4 days in which the circuit was borated to ~1200 ppm boron (target value), with hydrogen and lithium also present. Adding boric acid was known to cause a considerable increase in corrosion product concentrations and so it was considered better for this to take place at a time when deposition on fuel assemblies could not occur. Likewise, it was thought that adding hydrogen peroxide to achieve a forced oxidation at the end of HFT might be beneficial in removing outer-layer oxides (nickel ferrites), which might otherwise be released later and become activated on the fuel.

In practice, it was necessary to perform Sizewell B HFT in two steps to allow repair of a small leak from a SG drain line. The first step (HFT1) included the passivation stage in its entirety and part of the boric acid stage. The boric acid stage was then completed in the second step (HFT2) after a total of ~11 days during which typical beginning-of-cycle lithium, boron and hydrogen concentrations were maintained. Lithium was ~1.5 ppm during the 'passivation' stage (pH_{300°C}=7.65-7.75), rising to 1.8-2.0 ppm during the 'boric acid' stage, when boron was ~1130 ppm (pH_{300°C}=6.85-6.90). Hydrogen was maintained in the range of 30-45 cm³ kg⁻¹. It was not possible to add hydrogen peroxide during the interruption to HFT for the drain-line repair, and so the plant was cooled under acid-reducing conditions. However, a full 'shutdown' (with boratation, removal of lithium and hydrogen, and a forced oxidation) was carried out at the end of the second step.

Soluble transition metal concentrations were mostly very low during the passivation stage and decreased steadily indicating that a protective oxide layer was being formed. By the end of the passivation stage, Fe and Ni concentrations were very low at just ~2-3 ppt suggesting that corrosion release rates were also low. There was no detectable effect of adding hydrogen, but this was possibly due to much higher dissolved hydrogen concentrations being produced by initial corrosion reactions. Adding boric acid, on the other hand, had a major and very rapid effect on the soluble concentrations of all the transition metals. The concentrations of Fe, Ni and Co increased by up to 25,000 times to peak over 10 hours before falling during the remainder of HFT and then also during Cycle 1, suggestive of continuing slow passivation.

The fact that corrosion rates appeared to be significantly higher in boric acid/LiOH than during the passivation stage suggested that passivation in LiOH alone would have little impact on later behaviour of the primary circuit. Both HFT 'shutdowns' caused further increases in transition metal concentrations, but this was mainly when the boric acid concentration increased, and lithium was removed from the coolant. The hydrogen peroxide addition at the end of HFT2 did not cause the expected large increase in Ni, perhaps because fuel clad surfaces, which are usually the main source of nickel release under acid-oxidising conditions, were absent during HFT. It was concluded that adding boric acid during HFT is important and the length of the boric acid stage should be maximised. It was more difficult to identify clear evidence for the benefit of dissolved hydrogen, but it was considered probably beneficial. Meanwhile, it was thought that incorporation of a full shutdown chemistry may have been beneficial. EPRI has since remarked [202] that forced oxidation following HFT (through the addition of hydrogen peroxide) would be expected to accelerate the removal of corrosion products formed during HFT, although the extent to which such a procedure would be effective at removing any outer-layer oxide is uncertain.

Plant radiation fields at the end of Sizewell B Cycle 1 were lower than for other Westinghouse-designed PWRs commissioned with Inconel fuel grids [203]. Moreover, long-term monitoring of circulating corrosion product concentrations, shutdown releases, surface activities and radiation fields all showed that corrosion release rates from the Alloy 690 SGs quickly became passivated, within a few cycles. At the time, such behaviour was very unusual for PWRs with Alloy 600 or Alloy 690 SG tubes and so it was concluded that the improved HFT chemistry employed by Sizewell B was likely to have been a key factor [204]. However, other PWRs with replacement Alloy 690 SG tubes have since displayed similar behaviour to Sizewell B, even though no HFT passivation procedure was applied. This led to a view [52] that surface finish, achieved by means of an improved manufacturing process (see Section 6), was the key factor, and probably for Sizewell B, too [44]. Nonetheless, optimised HFT chemistry conditions should still be beneficial, and so this continues to receive much attention. The HFT chemistry conditions at Sizewell B may also have contributed to the good SG passivation behaviour, as well as other plant-specific factors including the extensive flushing carried out to remove any cobalt-bearing lapping debris, and the relatively high coordination $\text{pH}_{300^\circ\text{C}}$ of 7.4 adopted for Cycles 1-3.

Laboratory work has been undertaken that supports different aspects of the improved HFT chemistry employed by Sizewell B. Electrochemical research on the effect of water chemistry in simulated HFT conditions for Alloy 690 at 292°C , with solutions containing 0.5 to 2.0 ppm Li, and with or without 245-1200 ppm B, concluded that a HFT water chemistry with low-to-intermediate lithium concentrations (0.5-1.0 ppm) and boric acid addition produces oxide films that exhibit improved electrochemical stability and thus enhanced resistance against corrosion [205]. However, the pH was not held constant during the work, and so an alternative interpretation is that a $\text{pH}_{300^\circ\text{C}}$ in the range of 6.9 to 7.5 may be beneficial compared to higher pH values [202].

Japanese workers used a once-through autoclave to study the effects of four different HFT chemistries on the oxidation and corrosion behaviour of Alloy 600TT and Alloy 690TT [206]. The HFT chemistries were as follows:

- Deaerated water ($\text{O}_2 < 10$ ppb).
- Added LiOH (0.5 ppm Li, $\text{O}_2 < 10$ ppb)
- Added H_2 ($30 \text{ cm}^3 \text{ kg}^{-1} \text{ H}_2$, $\text{O}_2 < 10$ ppb)
- Added LiOH+ H_2 (0.5 ppm Li, $30 \text{ cm}^3 \text{ kg}^{-1} \text{ H}_2$, $\text{O}_2 < 10$ ppb)

Simulated HFT was carried out at $286\text{-}292^\circ\text{C}$ for 600 hours. At which point, some of the specimens were removed to examine the surface oxide formed, while the others were subjected to corrosion tests out to 3000 hours under simulated conditions for power operation (i.e., $\text{H}_3\text{BO}_3/\text{LiOH}/\text{H}_2$ addition and 307°C). The amount of metal lost was measured after each test.

Overall, LiOH+ H_2 was found to be the most effective HFT chemistry. It provided the best suppression of Alloy 600TT corrosion during simulated HFT, and produced the thinnest, most Cr-rich oxide film. This was rationalised in terms of the Cr-rich oxide film, which is more stable in a reducing environment, being formed by H_2 addition, and dissolution from the oxide film being minimised by LiOH addition. These differences were maintained during the simulated power operation, in that the amount of metal released was lowest for those Alloy 600TT specimens that had been treated with the LiOH+ H_2 chemistry. The results for the Alloy 690TT specimens showed a similar pattern, although the releases were lower than for Alloy 600TT because of the higher Cr-content and improved corrosion resistance of Alloy 690TT. A LiOH+ H_2 HFT chemistry was successfully employed for Tomari Unit 1, and was credited with a $\sim 20\%$ reduction in dose rates at the first annual inspection compared to other plants where HFT had been carried out with the conventional chemistry.

10.4.2. EDF Experience with SGR

Early examples of Alloy 690 replacement SGs for EDF plants showed encouraging passivation behaviour, with oxidation rates falling so low that little nickel is released, and this was despite no HFT passivation procedure being employed [52]. However, it was recognised that the initial oxidation makes a large amount of oxidised nickel available for subsequent release into the primary circuit. This release may be delayed, depending on the operational conditions, but not prevented by normal chemistry. Hence, the benefit of a nickel clean-up step during early operation was identified, and this was to follow an initial 'pre-oxidation' of the tubes [207]. Based on understanding at the time, it was proposed that an alkaline-reducing chemistry would be the best choice for the pre-oxidation step, and then a period with acid-reducing chemistry conditions at 170°C to remove nickel. The pre-oxidation step was intended to form a stable and protective oxide layer to minimise future nickel releases, and so it was important that the cleaning step should dissolve nickel oxides from the outer layer while preserving the inner (chromium-rich) layer.

The first implementation of such a procedure was at Bugey 3 after the SGR in 2010 [208]. It was intended to apply a two-stage HFT process, as follows:

- Oxidation at 285°C for 300 hours under alkaline and reducing conditions ($2.2 < [\text{Li}] < 3.5$ ppm, $[\text{B}] \approx 2000\text{-}2500$ ppm, and $10 < [\text{H}_2] < 35$ cm³ kg⁻¹).
- Cleaning at 170°C for 200 hours under acidic and reducing conditions (as per oxidation but with $[\text{Li}] < 0.5$ ppm).

However, due to operational constraints, it was necessary to limit the oxidation step to 136 hours during HFT (it continued at power), delay the cleaning step by 7.5 months, and perform the cleaning at 190°C rather than the intended 170°C. Furthermore, it was decided that the cleaning procedure would only be efficient with the nickel concentration above a minimum of 1 ppm. Therefore, the cleaning step was terminated after 36 hours when the nickel concentration did not exceed 190 ppb and stabilised at 130 ppb. A specific monitoring programme (metal concentration measurements, circulating and deposited activities, and plant dose rates) was performed in real time to evaluate the procedure, but was unable to identify any significant positive impact. This underlined the need for further R&D.

Experiments were conducted using EDF's Boreal loop [209]. The effects of different pre-oxidation conditions (at 300°C for 300 hours) were studied: reducing and alkaline in Test A, deaerated and alkaline in Test B, and deaerated and acidic in Test C. Each of the three tubes was then cleaned under acid-reducing conditions (at 170°C for 200 hours) before being exposed to simulated (alkaline and reducing) operational conditions at 325°C for a further 300 hours. The various conditions were obtained by using appropriate combinations of boron (1000 or 2000 ppm), lithium (0 or 2 ppm), hydrogen (0 or 30 cm³ kg⁻¹) and oxygen (0 or <5 ppb) concentrations.

At the end of the pre-oxidation step, Test A (reducing and alkaline conditions) showed the lowest corrosion release, equivalent to a depth of 12 nm, whereas Tests B and C (deaerated conditions) resulted in higher pre-oxidation releases of 27-30 nm, although there was little difference between them (for alkaline versus acid conditions). Despite the higher pre-oxidation metal releases for Tests B and C, no further release was then measurable for these two tubes during the cleaning step, whereas the release for Test A increased to a depth of 45 nm. The recirculating Ni concentration increased markedly during the cleaning step for Test A due to simultaneous oxide dissolution and continued corrosion. Some nickel was also dissolved during the cleaning step for Tests B and C, but without further oxidation and dissolution of the (inner) protective layer. For the simulated operational conditions, a further 4 nm of metal was released for Test A,

and a further 5-6 nm was released for Tests B and C. Hence, for the whole procedure, the total corrosion releases amounted to 49 nm, 32-33 nm and 35-36 nm for Tests A, B and C, respectively.

The results validated the beneficial effect of performing a HFT procedure for replacement SGs, as the release rates sustained during simulated operational conditions were low in all three cases. It was apparent that the pre-oxidation conditions had only a slight effect on the release rate after the cleaning step, although the oxide-layer thickness differed and decreased in the order Test A>Test B>Test C. Overall, it was not obvious that maintaining reducing conditions (i.e., the presence of 30 cm³ kg⁻¹ hydrogen) during the pre-oxidation step was optimal for limiting further release. While this led to a very low initial corrosion rate, the oxide layer formed was not sufficiently protective and so corrosion continued during the cleaning step (for Test A). On the other hand, a protective chromium-rich layer was formed during the pre-oxidation step under deaerated (<5 ppb O₂) conditions (for Tests B and C), and so no further oxidation took place during the cleaning step. By the end of the cleaning step, a protective oxide had been formed for all three tests. This was thickest for Test A and thinnest for Test C. Hence, it is not necessary to build-up a thick (chromium) oxide layer to protect the underlying metal and to control the corrosion release. Instead, it is the oxide structure and composition that is most important.

10.4.3. HFT with Zinc Injection

Following the improved HFT chemistry conditions employed by Sizewell B in the mid-1990s, the next major change was to inject zinc during HFT, and the first PWR to do so was Tomari Unit 3, which started commercial operation in December 2009. Tomari Unit 3 is a 3-loop PWR designed by MHI. The SGs are tubed with Alloy 690TT. HFT lasted ~1000 hours (~41 days) during which the temperature was ~290°C, lithium was controlled to a target of 0.5 ppm and dissolved hydrogen was 25-35 cm³ kg⁻¹ [210]. No information is provided about the boron concentration during HFT, and there is no indication that boric acid was added. With no pre-existing oxide film on the RCS surfaces, zinc was detected in the primary coolant just after starting injection, and reached 1 ppb after 37 hours, and 5 ppb after ~100 hours. The target concentration (for power operation) is 5±3 ppb zinc [210].

A Type 304 stainless steel insert plate was removed from a SG during HFT after 700 hours and compared with an equivalent plate removed previously from Tomari Unit 1, where Tomari Unit 1 did not inject zinc during HFT [210]. The corrosion mass accumulated for the Unit 3 plate was 75% lower than for the Unit 1 plate, indicating that zinc had suppressed initial corrosion. TEM and X-ray diffraction confirmed that zinc injected during HFT had been incorporated deep into the oxide film, forming an inner layer of stable zinc chromite. Plant dose rates for Tomari Unit 3 during the first two refuelling outages (RF01 and RF02) were compared with those of another unnamed Japanese 3-loop PWR that did not inject zinc during HFT [211]. Dose rates for the SGs, reactor vessel and main coolant piping were ~50% lower for Tomari Unit 3 than for the unnamed PWR at RF01, and ~80% lower at RF02. There was less benefit for some of the surrounding components (e.g., the RHR heat exchanger and pressuriser sprays) at RF01, but the dose rates of these components then fell sharply for Tomari Unit 3 at RF02.

The amount of nickel removed from the primary circuit followed a similar pattern to the plant dose rates, consistent with Co-58 being the main source of out-of-core radiation fields during early operation. The amount of nickel removed from Tomari Unit 3 during RF01 was 20% less than for the unnamed plant with zinc injection, and 80% less during RF02 [211]. It was considered that although a stable oxide film, including zinc, was present on the inner surface of the primary components during the first cycle, this was relatively thin and so nickel was still

released into the coolant from the base metal. However, it had likely become thicker during the second cycle and so the corrosion suppression effect of zinc was clearer. Analysis based on the amounts of nickel removed from the circuit and the circuit Co-58 inventory (from in-situ γ -spectroscopy) suggested that the beneficial effect of zinc was attributable mainly to suppression of Co-58 uptake into the oxide film for Cycle 1/RF01, whereas suppression of corrosion release was the dominant factor for Cycle 2/RF02. No subsequent data are currently available because Tomari Unit 3 has been shut down since May 2012.

The 4-loop PWRs Grafenrheinfeld (Germany) and its sister plant Angra-2 (Brazil) also provide valuable operating experience of zinc injection with bare metal surfaces in the RCS [212], either during initial commissioning or after a full-system decontamination (FSD). Both units are of the Siemens/KWU design with Alloy 800 SG tubes. It has been shown that the corrosion rate of Alloy 800 is relatively high for 100-200 hours of exposure, before reducing.

Grafenrheinfeld began commercial operation in 1982 but performed a successful decontamination of the whole primary circuit in 2010. This was intended to reduce personnel dose rates during a planned large-scale refurbishment programme. Having achieved an average decontamination factor of 60.5, attention then switched to achieving low circuit recontamination during subsequent operating cycles. To achieve this, a dedicated passivation process was performed with the core loaded and hot, but subcritical. Addition of lithium, hydrogen and zinc commenced after disconnection of the RHRS at 170°C to achieve target concentrations of 6.3 ± 0.3 ppm Li, >2 ppm H₂, and 5-15 ppb Zn for 120 hours at 260°C. In the first outage after the FSD, the average contact dose rate of all the measuring points at the main loops was ~ 0.8 mSv/h, less than half of that measured in the plant's first outage in 1983, and less than 30% of that before FSD. Recontamination remained low after five years of operation post-FSD, as evidenced by average main coolant pipe dose rates of ~ 1 mSv/h.

Angra-2 did not begin commercial operation until 2000. Zinc injection was started during the commissioning power tests, 2 days after first criticality. An initial daily amount of 25 g of zinc was injected (as depleted zinc acetate) and zinc was immediately detectable in the primary coolant at the start of zinc injection. The target concentration of 5 ppb zinc was achieved ~ 4 weeks after zinc injection started. No other aspects of a dedicated HFT passivation programme were envisaged for the commissioning phase, but average contact dose rates were kept low (mainly <0.2 mSv/h) during the following 15 years of operation.

Despite being sister plants, the dose rates at Grafenrheinfeld after FSD were higher than those at Angra-2 after commissioning because the passivation treatment of Grafenrheinfeld was carried out with core internals that were already activated after 27 years of operation, and this initially resulted in high coolant concentrations of Co-60, some of which was incorporated in the establishing oxide layers. Also, the measured contact dose rate of the main coolant piping is extenuated by the higher wall thickness at Angra-2 (76 mm), compared to the 49 mm at Grafenrheinfeld.

10.4.4. AP1000 HFT Chemistry

The Westinghouse AP1000 HFT chemistry protocol was developed to release and remove sufficient nickel and iron from Alloy 690TT and 304H stainless steel components to allow for the formation of a chromium-rich oxide with zinc incorporated at the metal-oxide surface, thereby minimising both corrosion and plant radiation fields during subsequent operation. The expected benefits of the protocol have been demonstrated using an autoclave test programme and by examining installed coupons that were present during HFT of Sanmen Unit 1 and Haiyang Unit 1 in 2016 [213].

The AP1000 HFT chemistry regime has three main phases. The alkaline-reducing phase (Phase 1) starts with the addition of LiOH during the 177°C plateau, followed by hydrogen and zinc addition during the heat-up to normal operating temperature of 292°C. Near the end of the normal temperature plateau, lithium is removed and boric acid is added to establish acid-reducing conditions (~500 ppm boron). This is Phase 2, which is intended to promote the release of corrosion products. After cooldown and hydrogen degassing, acid-oxidising conditions (>1 ppm O₂) are established in Phase 3 by adding hydrogen peroxide. Phase 3 is intended to release soluble nickel. For Sanmen Unit 1 and Haiyang Unit 1, the time in Phase 1 (normal operating temperature) was 15-16 days and the average concentrations of the chemistry additives were 0.4-0.7 ppm Li, 25-29 cm³ kg⁻¹ H₂, and 53-65 ppb Zn. The pH_T was 7.1-7.3. Westinghouse justifies the use of an elevated zinc concentration for HFT on the grounds that there is no fuel in the reactor at the time.

Autoclave testing was conducted to compare the AP1000 HFT chemistry protocol with the traditional HFT chemistry used by Westinghouse PWRs that started operating in the 1980s (i.e., deoxygenated water with only LiOH added). Coupons were installed within the autoclave on two support rods, one with nine Alloy 690 coupons and the other with nine stainless steel coupons. Liquid samples were removed periodically for both the NOT and cooldown phases of each test and were analysed, after acidification, for metal content using ICP-MS. Nickel and iron concentrations were initially stable and low (<5 ppb) at NOT conditions for both tests, although nickel trended higher for the traditional chemistry (~4.3 ppb) than for the AP1000 chemistry (~0.6 ppb). However, the levels of nickel and iron began to increase with the transition to an acidic pH and with cooling for the AP1000 chemistry, indicating a release from system surfaces. The nickel concentration spiked when hydrogen peroxide was added. During cooldown, the average nickel and iron concentrations were both ~600 ppb for the AP1000 chemistry compared to 0.01-0.3 ppb for the traditional chemistry. This shows that the AP1000 HFT chemistry protocol was able to successfully release corrosion products from the metal surfaces.

A selection of the autoclave test specimens was investigated using SEM and XPS. For the stainless-steel coupons, those exposed to the AP1000 chemistry showed a significant chromium enrichment in the oxide as compared to those that experienced the traditional chemistry, whereas both chemistries resulted in chromium-enrichment (and surface nickel depletion) for the Alloy 690 coupons. Zinc was incorporated in the oxide layer of the stainless steel and Alloy 690 coupons exposed to the AP1000 chemistry, with a maximum concentration at the oxide surface.

Returning to the in-reactor test programme, 10 coupons were installed in each of the Sanmen Unit 1 and Haiyang Unit 1 reactor vessels: five each of Alloy 690TT and 304H stainless steel. These were mounted on the underside of the full flow restrictor, which is attached to the upper core plate during HFT. For both units, total coolant concentrations of nickel and iron were low during the initial heat-up and NOT plateau, before increasing with the transition to acid-reducing chemistry. Iron peaked during the subsequent cooldown whereas nickel peaked later when hydrogen peroxide was added. Five coupons from each plant (including examples of Alloy 690 and stainless steel) were examined using SEM and XPS. Several coupons of both materials appeared to have an amorphous layer overcoating the crystalline particles, and Westinghouse notes that similar has been observed previously for zinc plants. Overall, it was evident that the oxides were enriched with chromium and zinc. The zinc concentration was typically highest at the surface and trended down through the oxide depth. Oxides of both materials appeared to have a duplex structure that was iron and nickel rich in the outer surface (from hydrothermal deposition) and enriched in chromium in the inner layer, which was grown-in-place. There was less iron in the oxide layer than in the base metal for the stainless-steel coupons, and the oxide layer was similarly depleted in nickel, compared to the base metal, for the Alloy 690 coupons.

The oxide thickness was similar for both materials at ~100-200 nm.

10.4.5. EPR HFT Chemistry

EDF's approach to HFT for Flamanville 3 EPR is summarised in [214]. Plant components are exposed to high-temperature water for the first time during HFT, and this temperature increase can affect corrosion and passivation of materials, as well as the transport of impurities and corrosion products. Therefore, particular attention was paid to the chemistry conditioning to be applied during HFT. Several workstreams were undertaken to inform the decision-making and these can be summarised as follows:

- A review of relevant published literature.
- R&D works enabling the identification of optimum HFT conditions.
- Analysis of EDF fleet OPEX, including commissioning, operating cycles, and SGR.
- Common work between EDF and AREVA chemistry and commissioning teams.

In addition, it was necessary to balance the benefits, risks and commissioning constraints associated with the various options for chemistry conditioning to determine the optimal and feasible procedure for HFT. The final selection was established based on ALARP-TOR (As Low As is Reasonably Practicable-Tolerability of Risk) principles.

It was concluded that neither source term nor plant dose rates are directly correlated to the chemical conditions applied during HFT, and that SG tubing manufacturer is the most significant factor affecting the long-term shutdown release. That said, EDF considered HFT conditioning to be essential towards creating optimal conditions at the beginning of plant operation (see Section 10.4.2). Even if the positive effects of zinc, lithium and boric acid can be argued as being either more or less significant, no detrimental impacts were identified and so it was decided that all three would be added during HFT (and subsequent pre-critical tests and power ascension). It was also decided that a HFT temperature plateau at 300°C would be followed by a cleaning phase, during which the boric acid concentration would be increased during cooldown before adding hydrogen peroxide.

On the other hand, EDF concluded that the potential benefits of hydrogen injection during HFT were not sufficient compared to the associated risks, although hydrogen injection would be required later for pre-critical tests with fuel in the reactor (to limit radiolysis in the primary coolant). The main concerns about hydrogen injection during HFT were regarding the formation of explosive gas mixtures and nitrogen asphyxiation from the required nitrogen flushing. It was noted that while some experiments showed that hydrogen contributes to minimising corrosion product release ([215] and references therein), its effect is not dominant under all conditions (e.g., the effect is less clear for Alloy 690 when using correctly deaerated water, [209]). It was also stated [214] that:

- An EDF/CEA analysis [45] does not show any correlation between hydrogen injection during HFT or SGR start-ups and Co-58 releases or dose rates during normal operation.
- EDF units without hydrogen injection during HFT or SGR present comparable [dose rate] results with units having injected hydrogen [216].

The HFT sequences for passivating the Flamanville 3 primary circuit and removing the resulting surface contamination took place between September 2019 and February 2020 [217] [218]. These were characterised by operation at a nominal temperature and pressure of 303°C and 155 bar. Chemical conditioning of the primary circuit (i.e., injection of LiOH, EBA, and zinc acetate) was initiated during heating from ca. 120°C to 300°C with the objectives of achieving 40-60 ppb zinc and $\text{pH}_T \geq 7.2$ for the 300-hour duration of the stable (300°C) plateau. Lithium

and boron were 2.5-3.0 ppm and 460-520 ppm, respectively, for the period at 300°C. The feasibility of zinc injection at higher concentrations than in normal operation was accepted due to the absence of fuel. The primary coolant was acidified ~24 hours prior to cooling (for the S4 shutdown) by boric acid injection to achieve a concentration of ~1150 ppm boron, and then by the removal of lithium. When the temperature was below 80°C, the primary circuit was oxygenated with 35 litres of hydrogen peroxide. Acidifying the coolant appeared to have more effect on the solubilisation of nickel, iron and chromium corrosion products, whose concentrations peaked at ~10-12 ppb, than did the hydrogen peroxide addition.

Flamanville 3 (FA3) was the third EPR to undergo HFT, after Taishan 1 (TSN1) in China [219] and Olkiluoto 3 (OL3) in Finland [220]. HFT at TSN1 took place between March and December July 2017, shortly before HFT at OL3, which ran from December 2017 to May 2018. TSN1 HFT was interrupted by the need to repair leaks on a CVCS heat exchanger, but it was possible to complete the passivation step beforehand. HFT of TSN1, OL3 and FA3 was similar in many respects. In all three cases, there was a 300-hour pre-oxidation phase at nominal temperature and pressure to passivate the system surfaces, followed by a cleaning phase to remove the non-protective outer oxide formed during the pre-oxidation phase. Cleaning was achieved in two stages: acidifying the coolant prior to cooldown (by adding boric acid and removing the lithium), followed by forced oxidation with hydrogen peroxide when the temperature was <80°C. However, there were also some significant differences, mainly regarding the chemistry regime used for the pre-oxidation step.

While all three units used deaerated water (<10 ppb O₂) and maintained alkaline conditions during the pre-oxidation phase (by adding ⁷LiOH), hydrogen was also added to produce reducing conditions (~17-35 cm³ kg⁻¹ H₂) at TSN1 and OL3, but not at FA3. On the other hand, zinc was injected during the pre-oxidation phase at FA3 (depleted zinc acetate) and OL3 (depleted zinc oxide), but not at TSN1 because the latter was not equipped with a dedicated zinc-injection line available during HFT. That said, the target concentration during HFT was lower at OL3 than at FA3 (5-10 ppb Zn versus 40-60 ppb Zn), although the OL3 zinc concentration was unstable and more like 5-40 ppb in practise. Finally, it is noted that while FA3 added enriched boric acid to a concentration of 460-520 ppm boron during the pre-oxidation phase, the corresponding target concentration was just 20 ppm at TSN1 and OL3. With broadly similar lithium concentrations (ca. 2-3 ppm), this resulted in a higher pH_{300°C}=7.7-7.9 for TSN1 and OL3 than for FA3, where pH_{300°C} was 7.2-7.4. TSN1 and OL3 maintained a low concentration of boron to avoid caustic SCC of pressuriser heaters, which had been observed for the French PWR fleet after one cycle of operation, and for which commissioning in a caustic environment with only lithium present, especially during HFT, was identified as a contributory factor.

Soluble nickel concentrations were highest during the cleaning phase for all three units, peaking after acidification and cooling, but prior to peroxide addition. Peak nickel concentrations decreased in the order TSN1(~1100 ppb)>OL3(~450 ppb)>FA3(~11 ppb), which suggests that zinc addition during the pre-oxidation phase (at OL3 and FA3) had a much larger effect on stabilising the inner oxide and reducing the corrosion release than did adding hydrogen (at TSN1 and OL3). Towards the end of commissioning, surveillance coupons present in the reactor vessels of TSN1 and OL3 during HFT were removed for examination. The results for TSN1 were not available at the time of [219], but examination of the Alloy 690TT and 304L stainless steel coupons from OL3 showed a zinc-containing oxide layer that was thin, continuous, and homogenous, with Cr-enrichment of the inner layer [220]. This confirmed the success of the pre-oxidation chemistry strategy.

10.5. Ultrasonic Fuel Cleaning

As mentioned in Section 7.1.2, Callaway experienced CIPS from the outset of Cycle 10 after being affected by severe CIPS in Cycle 9. Analysis of in-core flux traces indicated that the CIPS behaviour at the start of Cycle 10 was driven by residual crud on the once-burned fuel assemblies that were reloaded at the end of Cycle 9 (i.e., by the fuel assemblies in their second cycle of operation). The normal shutdown practises during Refuelling Outage 9 had not removed the tenacious fuel crud formed during the previous cycle. This is not surprising because PWR shutdown chemistry guidance was developed to manage releases from fuel crud comprised mainly of nickel ferrite, whereas high-duty cores with SNB tend to produce nickel-rich fuel crud containing species such as NiO and bonaccordite.

While it is possible to modify the shutdown chemistry for such plants to reduce particulate contamination of out-of-core surfaces and to achieve coolant activity clean-up criteria more quickly (e.g., by stopping the RCPs before hydrogen peroxide addition and/or reducing the system clean-up volume), this carries a risk of leaving more crud on the fuel (see Section 9.4). In any case, tenacious fuel crud species (such as NiO and bonaccordite) are not removed effectively by the shutdown chemistry, as evidenced by their abundance in crud scrape samples (see Section 7.1).

This led Callaway and EPRI to co-sponsor Dominion Engineering to design, construct and qualify a UFC technology for deployment in the Spent Fuel Pool (SFP). The programme commenced in 1997 and the primary objective was to remove fuel deposits, especially from once-burned fuel, and minimise crud carryover on reload fuel. This, in turn, would reduce the corrosion product inventory available for boron hideout, either on the reload fuel directly, or transported from the reload fuel to feed fuel, thereby postponing or eliminating the occurrence of CIPS in subsequent cycles.

10.5.1. Laboratory Tests

Using ultrasonic energy to dislodge fuel deposits had been considered previously, but it was found that the energy did not penetrate effectively into the interior of complex volumes like PWR fuel assemblies. In which case, the exterior rods would be over-energised, potentially causing damage, while the inner rods would not be efficiently cleaned. However, laboratory tests using a mock-up of a PWR fuel assembly with simulated deposits showed that technological advances made with novel ultrasonic transducers, used to produce high-frequency pressure pulses (advanced push-pull ultrasonics), were sufficient to overcome this problem [221]. In addition, flat plate reflectors were found to be effective for improved cleaning.

As well as dislodging deposit, the ultrasonic energy subjects the fuel rods to vibrational excitation modes. The translational magnitude of these vibrations must be benign with respect to potential fuel pellet and cladding damage. Therefore, vibrational measurements were conducted for the laboratory mock-up and analytical methods were employed to extend the observations to a full-length fuel assembly. Engineering calculations showed that vibrational displacements were within those expected for flow-induced vibration (FIV) when a fuel assembly is in an operating PWR core [222]. In addition, exposure to ultrasonic cleaning was anticipated to be for minutes compared to the (up to) 18-month duration of a fuel cycle. Hence, any impact on fuel integrity was expected to be well within the design limits anticipated by the fuel vendor.

10.5.2. Field Demonstrations

Full scale testing and demonstration of the cleaning apparatus took place in the Callaway SFP during April and August 1999 using discharged fuel assemblies [221] [223]. Briefly, the (first generation) equipment is comprised of a cleaning module and a waste-collection module, with the two systems connected by a flexible hose (see Figure 40). The cleaning chamber consists of a rectangular channel encompassing the fuel assembly to be cleaned, which is supported by the fuel grapple and surrounded by a matrix of ultrasonic transducers. Pool water is drawn into the open top of the cleaning chamber, carrying away the dislodged fuel crud to the bottom, through the flexible hose, through a bank of disposable filter cartridges, and back to the pool. The pump providing flow for the water is mounted between the flexible hose and the filter bank. Progress with fuel cleaning is monitored using gamma detectors tuned to Co-58 and Co-60 at the pump inlet and near to the filter cartridges, and operations are controlled using consoles on the pool deck.

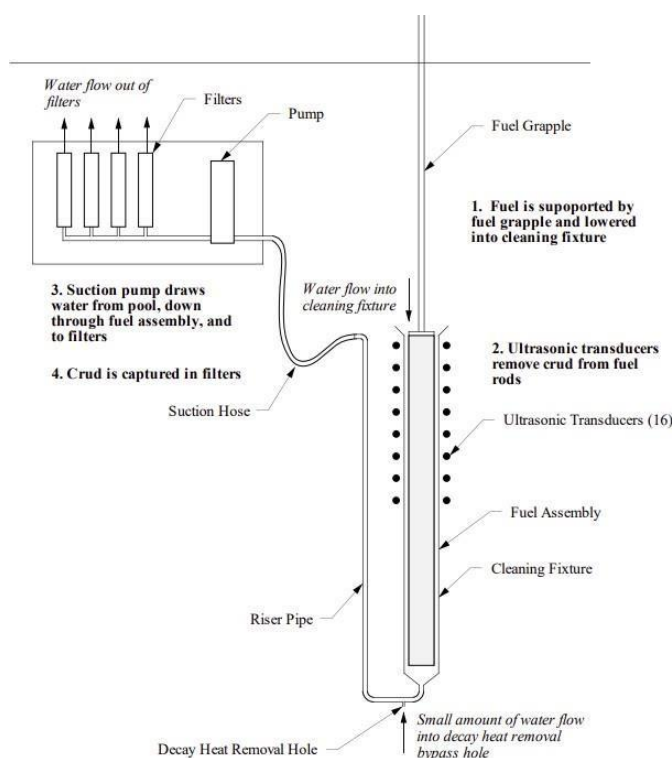


Figure 40: Schematic of Callaway (First Generation) UFC Equipment (From [221])

Five fuel assemblies were cleaned in April 1999 including G32, which was known to be affected by severe deposition based on crud scrapes obtained several years previously (it had been stored in the SFP for 6 years since being discharged). Experience with cleaning G32 showed that a large amount of crud was removed during the first two minutes, and that measurable cleaning was still taking place at a slower rate after 6-7 minutes. Comparison of video images before and after cleaning (e.g., Figure 41) confirmed that a significant amount of crud was removed, and the cleaning efficiency was estimated to be ~50%. In contrast, cleaning of the other four fuel assemblies (J13, J36, K75 and K96) appeared to be much less dramatic than for G32. The power histories of the assemblies showed that they all experienced low power operation in their last fuel cycle, whereas G32 did not. It was hypothesised that crud was lost from the fuel assemblies during this low power operation. Accordingly, criteria were developed to select more suitable spent fuel assemblies for additional process optimisation tests in August 1999.

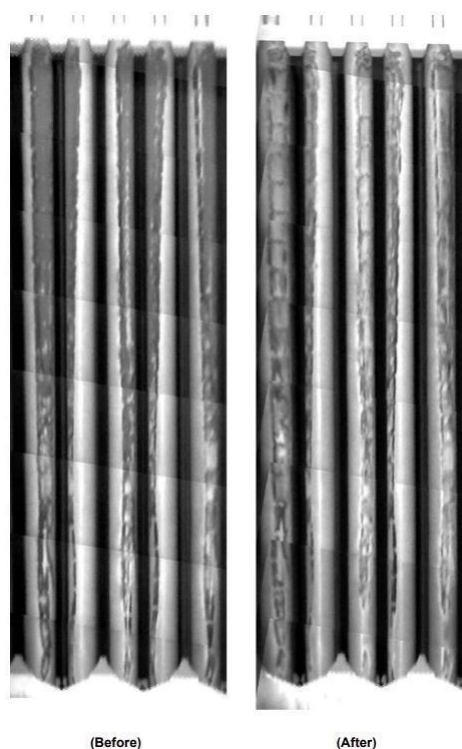


Figure 41: Images of Callaway Fuel Assembly G32 Before and After Cleaning (From [221])

A key observation from the August 1999 demonstration was that the video images showed more effective cleaning for the North and South sides of fuel assemblies, and less effective cleaning for the East and West sides. Ultrasonic transducers were present only on the North and South faces of the Callaway cleaning fixture and so the production cleaning procedure was modified to include an optional second round of cleaning after rotating the fuel assembly by 90° about the axis of the fuel handling tool.

10.5.3. Production Cleaning

The first ultrasonic cleaning of reload fuel took place at Callaway during October 1999 for a batch of 16 once-burned fuel assemblies [221]. These fuel assemblies were in-core in Cycle 10 and then reloaded, after being cleaned, for Cycle 11. Fuel cleaning was not on the outage critical path and so additional time was spent performing video inspections and obtaining crud scrapes for the reload fuel. All 16 reload fuel assemblies were inspected by video camera and crud scrapes were obtained for three of the assemblies. These activities were carried out both before and after cleaning to afford comparison. A total elapsed time of 16 hours was required to clean, inspect, and scrape the fuel.

Activity levels accumulated on the filters during fuel cleaning were less than expected based on the high axial-offset deviation observed for Cycle 10, and this was attributed to a reactor trip seven weeks prior to the outage. The associated thermal transient led to a large crud burst that dispersed loosely adherent fuel crud throughout the primary circuit. Video inspection showed that a very high percentage of fuel crud was removed by the ultrasonic cleaning. An average figure of ~70-80% removal was estimated using the crud scrapes for fuel assemblies M89 and M91, and the video inspections and crud scrapes were consistent for these two cases. Video inspections of M78 suggested a similar degree of cleaning for this fuel assembly, but analysis of the crud scrapes resulted in a much lower efficiency (~20% removal). It was concluded that the crud scraping technique was not wholly suitable for the purpose of estimating cleaning efficiencies.

Following the success in cleaning the 16 lead test assemblies reloaded in Cycle 11, all 96 fuel assemblies reloaded for Cycle 12, and then all 97 fuel assemblies reloaded for Cycle 13, were cleaned ultrasonically, amounting to >55,000 fuel rods [224]. This was described as full-core application.

10.5.4. Second Generation Equipment

The first-generation UFC equipment was not designed to be mobile and was retained in the Callaway SFP between uses. The next units to deploy UFC were South Texas Project (STP) 1 and 2. This was principally for CIPS mitigation, because Unit 1 had recently undergone SGR, and SGR was planned for Unit 2. Higher corrosion product releases were anticipated for the bare metal surfaces, potentially leading to worse deposition in core. In addition, fuel cleaning was viewed as an enabler to designing a more efficient core requiring four fewer fuel assembly purchases. Several enhancements were introduced for the second-generation fuel cleaning equipment [224] that was first used at STP 1 and 2 in April 2003 and October 2002, respectively, and they are summarised in Table 4. The upshot was improved availability and increased throughput. Figure 42 provides a schematic diagram of the second-generation equipment.

Table 4: Comparison of Ultrasonic Fuel Cleaning Technologies

Criterion	Ultrasonic Fuel Cleaning Equipment	
	1 st Generation	2 nd Generation
Number of chambers	One cleaning chamber.	Two cleaning chambers.
Seismic support	Fuel assembly to be cleaned must be supported by fuel handling tool connected to spent fuel bridge.	Free standing on SFP floor in area free of spent fuel racks.
Ultrasonics	16 horizontally mounted transducers, 8 on each of two sides of the cleaning chamber. Cleaning effectiveness is improved if fuel assembly raised, rotated by 90°, and reinserted for additional cleaning.	Each chamber has a transducer basket installed within a reflector housing, with vertically mounted transducers on all four sides of each cleaning cell. Only 10 transducers per cell required to give greater power density than previous design.
Availability and throughput	Cleaning possible only after core offloaded and not while fuel being transported from reactor to SFP. 2-3 fuel assemblies per hour.	Cleaning possible while core offloading is in progress. Can clean one assembly while spent fuel bridge is in use to return/fetch another. 4 fuel assemblies per hour.
Storage and maintenance	Remains in wet storage in SFP.	Transducer baskets removable for dry storage and maintenance when not in use.

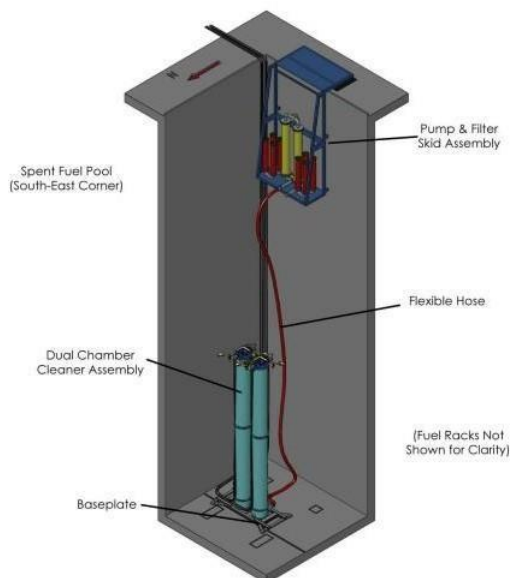


Figure 42: Schematic of STP 1 and 2 (Second Generation) UFC Equipment (From [224])

10.5.5. Benefits, ALARA and LLW Impacts

While the main objective of UFC is to mitigate the risk of CIPS, there is an ancillary benefit of reducing the total inventory of activated corrosion products in the primary circuit, which can migrate to out-of-core surfaces where they increase shutdown radiation fields, resulting in ORE. In addition, it has been suggested that cleaning fuel prior to casking for transport may prove beneficial in minimising radwaste and dose generated by fuel crud deposits dislodged during transport and left uncontained in the cask [222]. One advantage of UFC is that it generates no wastes other than the dislodged deposits. However, the removed crud must be disposed of, and the handling, collection and removal of crud impacts site ALARA and LLW programmes.

Owing to the premium put on time during a refuelling outage, a detailed assessment of UFC efficiency was carried out 'offline' at Callaway in October 2021 [225]. The downside of this approach is that only discharged fuel assemblies that had experienced multiple fuel cycles were available, whereas measurements on once-burned fuel as it is cleaned in preparation for reinsertion would have been ideal, especially in the case of fuel assemblies affected by CIPS. Two fuel assemblies, neither of which had been cleaned previously, were selected as candidates:

- L-region assembly L80, which was in-core for Cycles 9 and 10. It experienced high axial-offset deviation in Cycle 10 and cursory inspection of crud scrapes at the end of the cycle showed flakes up to $\sim 75 \mu\text{m}$ in thickness with a needle-like phase believed to be bonaccordite. On the downside, this assembly had been in the SFP since October 1999, and it is known that this can affect residual fuel crud.
- M-region fuel assembly M74, which was in core for Cycles 10 and 11. This was a high-power fuel assembly in Cycle 10 and was borderline in terms of CIPS. Therefore, crud should have been present. The high-power operation in Cycle 11 would then be expected to minimise crud removal in that cycle. An advantage of this fuel assembly is that it had spent less time in the SFP than had L80.

Visual inspection suggested that the amount of crud on both fuel assemblies was significantly less than when they were originally discharged, but cleaning nonetheless readily removed the remaining deposits with no distinction between loose and tenacious deposits. A programme of crud scrapes was devised for each assembly based on pairs of peripheral rods. Samples were

collected from one rod of each pair at the spans with the greatest amount of deposit. The fuel assembly was then cleaned before the scraping fixture was returned to collect samples from the paired rods. Samples were analysed chemically and radiochemically to establish the crud mass and activity per unit area. Comparison of deposit loadings and isotopic activities before and after cleaning provided information on the fraction of crud removed. It was found that, on average, UFC removes 85% or more of corrosion products from irradiated PWR fuel assemblies.

After experiencing CIPS in Cycles 4-10, Callaway Cycle 11 also experienced core wide CIPS [224]. There was no evidence that the 16 once-burned fuel assemblies cleaned at the end of Cycle 10 and reloaded for Cycle 11 were affected by axial flux depressions, but only two of them were instrumented. Neither Cycle 12 nor Cycle 13, for which all the reload fuel assemblies were cleaned, experienced CIPS. It is reasonable, therefore, to conclude that UFC of reload fuel was beneficial in mitigating the occurrence of CIPS for Callaway, although there is uncertainty regarding its precise contribution because other countermeasures were implemented at around the same time. After operating with various pH_T regimes for Cycles 6-10, in which the pH_T varied during each cycle, Callaway operated Cycles 11-13 with a high and constant $pH_T=7.2$. In theory, such a change should be beneficial in reducing the corrosion product release and its propensity to deposit on fuel, but there was no evidence of consistent benefit for several PWRs that had implemented a similar change. Probably of more significance is the fact that T_{ave} was lowered by 2.2°C (from 309.1 to 306.9°C) in mid-Cycle 10 to reduce SNB and, hence, the build-up of fuel crud. T_{ave} remained at 306.9°C for Cycles 11 and 12, before being raised by 1.1°C to 308.0°C for Cycle 13. The amount of crud that builds up on the fuel is directly related to the total core sub-cooled nucleate boiling area, and the feed assembly boiling area was generally lower for Cycles 12 and 13 than for Cycles 6-11, and especially so for the early parts of the cycles.

An initial assessment of the dose benefits arising from fuel cleaning were carried by EPRI using the CORA activity transport code; a mathematical model simulating various corrosion product generation and transport mechanisms [226]. Parametric evaluations of Co-58 and Co-60 activity concentrations on SG and loop piping surfaces, converted to dose rate approximations, were generated using baseline models for Callaway and Diablo Canyon 1 – two PWRs with significantly different operational histories – assuming different levels of cleaning effectiveness (between 25 and 100%) and different frequencies of fuel cleaning (every cycle, every other cycle, and every fifth cycle). For a conservative assumption of 50% cleaning effectiveness, cleaning the reload fuel for every cycle was predicted to result in a 39% dose rate reduction for Diablo Canyon 1 and a 23% reduction for Callaway. The predicted benefits were found to shrink and become more variable with reducing cleaning frequency. At the time (December 2001), Diablo Canyon 1 had operated with zinc injection for several cycles and the zinc effect on dose rates was included in the CORA model. A key conclusion was that UFC could greatly enhance the impact of zinc injection on plant radiation fields. Conversely, there were limitations of modelling the Callaway CIPS history, resulting in greater uncertainty.

The dose benefits for Callaway were subsequently borne out by operating experience [224] [227]. The ALARA impacts of UFC were assessed to be a ~30% reduction in SG channel head dose rates over three refuelling outages (11-13), a ~50% reduction in loop dose rates over the same period, and a 50-70% reduction in cumulative exposure per hour worked in the radiation-controlled area. Focussing on tasks with a similar work scope from outage to outage, the average dose per man hour fell by 41% from Refuelling Outage 11 to Refuelling Outage 12 for SG nozzle dam insertion, and the average dose per man hour fell by 24% for reactor vessel head assembly/disassembly. At power, radiation fields at the CVCS heat exchanger outlet dropped from an average of ~300 mR/h for Cycle 10 to ~100 mR/h for Cycle 13, after successive fuel cleaning campaigns. The STP units also experienced significant radiation field reductions, with UFC contributing, at least in part, to their second lowest refuelling outage cumulative dose,

recorded for Unit 2 during Refuelling Outage 10, which took place after SGR.

Table 5, which is reproduced from [227], summarises the impacts of UFC on LLW generation at Callaway, STP 1 and 2, and Vogtle 1 and 2 (Vogtle was the next site to implement fuel cleaning after STP). The dose rate cut-off for changing filters varied from 40 R/h at Vogtle to 130 R/h at Callaway and 150 R/h at STP, and this correlated with the number of fuel assemblies cleaned per filter (7-9 at Vogtle, 12 at Callaway and 16 at STP). The LLW impacts were minimised by noting that Co-58 is initially the primary radionuclide present, and its activity decays away after storage for two years. At the time of reporting (December 2004), only the STP filters had been shipped for disposal. By then, Co-60 accounted for 80% of the radiation fields, and these were 1-5 R/h at 1 foot. The generation of LLW was easily manageable.

Table 5: Summary of UFC LLW Generation at PWR Stations

Parameter	Callaway	South Project (Both Units)	Texas	Vogtle (Unit 1/Unit2)
Assemblies cleaned per outage	~100	128		117/113
Filters used during each cleaning	12	8		16/12
Dose rate cut-off for filters during cleaning	130 R/h	150 R/h (at 18 inches)		40 R/h
Dose rate at shipping time (after two years storage)	NA	1-5 R/h at 1 foot		NA

Notes: This Table is reproduced from [227].

EPRI identified three scenarios [224] for which consideration should be given to ultrasonically cleaning reload fuel, to reduce the reintroduction of corrosion products at the beginning of each cycle:

- A plant that has experienced CIPS.
- Prior to the cycle of starting zinc injection.
- A plant with high dose rates.

Following early experience with UFC, licenses were issued to Westinghouse, AREVA, ENUSA and KNF [228]. By the end of 2020, ~200 PWR applications had been carried out, predominantly in the US, but also in Spain (Asco 1 and 2, and Vandellos 2), Sweden (Ringhals 2, 3 and 4), and several South Korean plants. The application of UFC to Ringhals PWRs is discussed in [229, 230], and South Korean experience is documented in [231] [232] [233]. The first PWR campaign of high-efficiency ultrasonic fuel cleaning (HE-UFC) was carried out in 2011. It is understood that EPRI is currently investigating combining UFC with a chemical treatment. UFC is also performed for BWRs using similar equipment [234] [235].

10.6. Plant Monitoring to Identify Crud Related Problems

Flux monitoring will detect occurrences of CIPS, and detailed fuel examinations may be performed to confirm instances of CILC. However, the objective of routine monitoring must be to provide early warning of an increased risk of such phenomena before they occur. Visual inspection of fuel assemblies during routine handling is important but has its limitations. In terms of fuel crud, such inspections may not detect subtle changes that take place gradually over

multiple cycles.

It is routine for PWRs to monitor the primary coolant concentrations of gamma-emitting radionuclides, including the main activated corrosion products, during normal operation and reactor shutdowns, including refuelling outages. Precautions are taken to obtain representative results for soluble and particulate fractions. All such data should be trended, but Co-58 concentrations will be of most interest in terms of fuel crud and CIPS risk, because of the nickel source that is common to both. Based on the operational experience and laboratory work reviewed in this report, the Co-58 shutdown oxygenation peaks are likely to be the best indicator of changes in nickel release rates and the amount of nickel deposited as fuel crud. Integrated shutdown activities provide a similar indication, and the effort required to calculate them from routine data is worthwhile.

Component dose rates are also monitored routinely. It may be possible to correlate the dose-rate behaviour with Co-58 trends, although other radionuclides such as Co-60 will often dominate the radiation fields. Another useful parameter is the split between soluble and particulate fractions for the cobalt radionuclides during normal operation. For plants with low levels of fuel crud, the activity may be equally distributed, or soluble activity may dominate, whereas cycle data for plants with high levels of fuel crud often exhibit characteristic increases in particulate activity at the beginning and end of cycles.

Some PWRs undertake additional monitoring that is not routine across the industry. Instead, it may be intended specifically to understand the impact of plant changes on fuel crud and CIPS risk, or to assess the effectiveness of mitigations. This should be regarded as optional best practice. Gamma spectrometry of ex-core components is of value because it determines deposited activities of individual radionuclides. Plant surveys of this type are a substantial undertaking, but EDF experience suggests that use of a CZT-device may provide a workable compromise. Consideration may also be given to monitoring the coolant concentrations of elemental corrosion products, such as nickel, cobalt, and iron, etc. These are typically highest, and most easily quantifiable, during shutdowns and start-ups, and may be used with radionuclide concentrations to determine specific activities, such as Co-58/Ni. The specific activity of Co-58, for example, can be used to assess whether activity releases are coming from fuel crud or ex-core surfaces. However, collection of elemental concentrations may require additional outlay for suitable analytical equipment as well as technician effort during a busy time on plant.

For all the parameters discussed here, the focus should be on long-term trending to detect changes in behaviour. In most cases, the trends will likely be more revealing than the magnitude of individual parameters.

11. Impact of Fuel Crud under Accident Conditions

11.1. Consideration of Relevant Accident Conditions

There are at least two ways of considering the impact of fuel crud under accident conditions.

First, where fuel crud initiates the accident through any one of several possible mechanisms, such as CIPS.

Second, where an accident arises from whatever cause (e.g. LOCA), and the subsequent influence of fuel crud on the evolving situation.

Furthermore, it has to be recognised that “accident conditions” covers a range of circumstances and severities. Some of these will be within the scope of a Design Basis Accident (DBA) which has been established for the plant, and the plant should be able to recover from those conditions; however others will be Beyond DBA (BDBA) and plant recovery is by definition less certain.

In this section we consider these two aspects of the impact of crud on reactor accidents, in turn.

11.2. The Adverse Consequences of Fuel Crud

Fuel crud in PWR reactors may have the potential to relate to one of three principal consequences which have relevance to nuclear safety.

- CIPS could in principle compromise core reactivity control, due to the possibility for uncontrolled reactivity insertion that could exist in extreme cases of thick fuel crud with extensive boron hideout. Consequently this is considered the most significant nuclear safety concern relating to fuel crud.
- If thick fuel crud were subject to short-term redistribution due to a chemical and thermal-hydraulic transient, resulting in restriction of flow paths within the core, the possibility for compromise of core cooling must be considered.
- CILC can lead to fuel failures, although even with a severe manifestation of this mechanism, it is not clear if rate and extent of these, whilst highly undesirable, could constitute an accident scenario. However, the possible challenge to containment of nuclear and radiological inventory should be recognised.

These matters are discussed in turn in the following section.

11.3. Role of Fuel Crud as a Transient Initiator

In this section we summarise the mechanisms by which a hypothetical accident could derive from the presence of fuel crud. It should be noted that these all relate to thick fuel crud.

As has been discussed at length in earlier sections, the build-up of thick crud incorporating boron may under certain specific conditions eventually produce the consequence of CIPS. Core reactivity control is a primary concern and historically was the initial driver for understanding and controlling fuel crud, to address the severe operational penalties that resulted from cycle de-rating to avoid violating technical specifications. The current industry focus is on minimizing crud build up to levels far below those that would produce significant CIPS. In this respect, the possibility for CIPS to develop to the extent that it could cause a reactivity transient should not exist, but nonetheless this is the extreme manifestation of the mechanism. It should also be recognised that is normally expressed as an axial offset in power, although it could also be a

radial shift (core tilt) if some crud-laden fuel has been (as is normal) shuffled in an end-of-cycle refuelling outage. The impact of crud on reactivity control is usually to transfer reactivity away from the upper spans of the fuel assembly, since that is where crud predominantly deposits (by nucleate boiling). The widely used practice of fuel shuffling at end of cycle often involves fuel which has been irradiated at the centre of the core (and has thus seen highest SNB duty) relocated to the outer regions of the core for re-irradiation. This provides a source of crud in the outer part of the core, but this crud inventory is commonly observed to decrease with time after the start of the next irradiation cycle.

The pressure differential between the top and bottom of the PWR core is a performance metric, and the possible role of crud in adding resistance to the flow path (so increasing the pressure differential) is a concern. This is most acute at constriction points such as nozzles and grids, but also has some relevance to the general surface of the fuel rods. The flow path of water through the fuel rod assembly consists of multiple instances of a "rounded cruciform" cross section, with the fuel rods almost touching at their nearest point of contact; the gap between rods is actually only one or two millimetres depending on fuel assembly design, so under the conditions of extremely high flow rate typical of PWR core, even very small restrictions can result in a reduction of flow rate. In turn this could reduce the overall ability of the coolant to remove heat from the fuel, recognising that the actual thermal hydraulic response will be complex. In a heavily crudded core, if a rapid chemical and thermal hydraulic transient caused rapid redistribution of deposits, then the possibility for a compromise in circuit heat removal capacity should be considered. Earlier sections have presented OpEx where an increase in core pressure differential appears to have occurred to a measurable extent, although this does not appear to have affected heat removal. Although details are limited, it appears that this has been associated with chemistry changes that would not be considered under current practices.

Reference [17] describes a number of crud related effects. Bosma et al note that thick crud deposits on the fuel rods increase the potential for fuel damage. Although porous, a thick crud deposit can reduce the thermal conductivity providing an insulating barrier to cooling. This can lead to excessive temperature increases at the clad surface, including dryout, as the Axial Offset moves positive toward End Of Cycle. This could be considered as an exacerbation of the CILC failure mechanism resulting from concentrating chemical species within the deposit. In any case fuel failures are highly undesirable, although limited instances are typically tolerable in an operating PWR core. It seems unlikely that a crud related mechanism alone could produce rapid and widespread fuel failures that could not be managed through normal control measures (including shut down), without further initiating events, but this should not be categorically discounted.

In [17] (Section 5.3) it is noted that Three Mile Island (TMI) Unit 1, Seabrook, and Palo Verde Unit 2 all experienced crud-influenced fuel failures on feed fuel assemblies that were attributed to CILC. However, there is no detail provided on the circumstances or nature of these fuel failures. Reference [17] does indicate that there were a number of mid-cycle shut-downs at Seabrook, particularly, associated with CIPS transients.

11.4. Reactor Accidents where Fuel Crud Influences the Progression

In instances of Loss of Coolant Accidents (LOCA) it must be recognised that there are both large and small break LOCAs. When LOCAs occur one of the considerations is the power shape of the core [17] (Section 5.4 therein), in terms of energy distribution (and available coolant to take the heat away). There will be (for each reactor) a range of LOCA power shapes bounded by the allowable axial power operating limits. When in a LOCA situation a plant will have its allowable power shape defined in terms of absolute axial power difference, and the plant must continue to operate within the allowed range in the presence of CIPS. This means allowable power shapes must remain valid whatever type of LOCA occurs, but CIPS may have an effect on how the plant actually performs. For example in a DBA it is likely that boron may be returned to the coolant as a result of a crud burst or crud dissolution (and thus affect reactivity) and that additionally lithium would also likely be returned and affect coolant pH.

The evaluation of the LOCA events must also consider potential reactivity effects due to the presence of boron-rich crud on transient response. The severe thermal and hydraulic transients associated with LOCA events may result in a crud burst. The conservative assumption is to conclude that a burst will occur sometime during the event and thus, the reactivity effects must be considered. For the small break LOCA, an evaluation of reactivity associated with a crud release prior to rod insertion due to reactor trip should be considered. For the large break LOCA, this same reactivity effect due to a crud release should be considered however, it is likely that the small positive reactivity insertion due to a crud release with CIPS present will be insignificant as compared to the large negative reactivity insertion associated with a voided core.

The evaluation of the LOCA events must also consider potential reactivity effects due to the presence of AOA on the post-LOCA sub-criticality analysis.

Following a design basis event, any boron held in the crud layer will eventually be returned to the RCS, either through a crud burst or by dissolution. As lithium can be expected to return as well, the effect on coolant and sump pH should be considered in the appropriate accident safety evaluation.

11.5. Review of Fuel Failures

The occurrence of fuel failures on a world-wide basis has been reviewed by the IAEA, in a series of documents. First in a survey of fuel between 1987 and 1994 [236], second a survey between 1994 and 2006 [237] and thirdly a survey between 2006 and 2015 [238]. Whilst a limited amount of fuel failure does not necessarily constitute an accident, it is far more likely that an accident will involve fuel failure. Therefore, a subset of the recorded fuel failures will point to accident situations, usually in the context of severe degradation. Furthermore, as for present purposes we are interested only in PWR fuels, the cases of interest are an even smaller subset.

The causes of generic fuel failure are outlined in [236] and tabulated, presented here in Table 6. This excludes causes which are specifically non-PWR.

Table 6: Causes of fuel rod failures (from [236])

Fuel Rod Failure Causes	
Manufacturing defects	In clad, end plug, or weld
Hydriding	By moisture or other contamination in pellets/ rods
Pellet Clad Interaction / Stress Corrosion Cracking	By high power ramps, or assisted by clad / pellet imperfections
Corrosion	With large variety of different root causes and contributing factors
Clad collapse	By axial gaps in the fuel column due to fuel densification
Grid-rod fretting	With large variety of different root causes and contributing factors
Debris fretting	From metallic debris circulating in the coolant
Rod bow	From several root causes, can lead to exceeding design limits but has not caused fuel failure except in one early case
Baffle jetting	By cross-flow from defective core baffle joints
Damage to the assembly structure	
Assembly bow	From several root causes, can lead to handling damage or other problems
Other deformation	By Zr alloy growth leading to structural misfit
Fretting wear	From a large variety of phenomena with different root causes
Zr alloy hydriding	Only one case of excessive hydrogen take-up in guide tubes

The IAEA review [236] makes the point that historical cases of fuel failure must be put in the context of early PWR fuel designs (typically fuel rods with diameter 10.7 to 11.2 mm, configured as assemblies of 14x14 or 15x15 rods (and 16x16 in some Siemens plants)) as compared with later fuel designs with fuel rod diameters in the range 9.1 to 9.8 mm, configured as assemblies of 16x16, 17x17 or 18x18 fuel rods. Common features of the newer fuel designs include the use of advanced Zr alloy spacer grids, some debris catcher to prevent debris fretting failures and advanced cladding materials with improved corrosion resistance. It should also be recognised that historically, fuel burnup was significantly lower than is commonplace now, burnup was frequently below 40 GWd/teU prior to 1994. Alongside these root causes are the measurements which may indicate fuel failure. For PWRs this is the "fuel reliability indicator" (FRI) which is the steady-state coolant concentration of ^{131}I , after correcting for tramp uranium which may have been present anyway and may have released ^{131}I .

There are also various approaches to calculating generic fuel rod failure rates, but subject to some uncertainty as one of the input terms in the calculation is the number of failed rods (not assemblies) across all reactors in operation, for the year in question. Too often that number is unknown, as it may involve PIE and assembly dismantling, and is not an easily obtained piece of information.

The underlying causes of fuel failures between 1987 and 1994 has been subdivided at pre-and post-1991, when a number of fuel designs changed. Whilst the clearly understood causes of failure changed distribution between the various mechanisms, there remained nearly half of the fuel failures which were for "unknown" reasons.

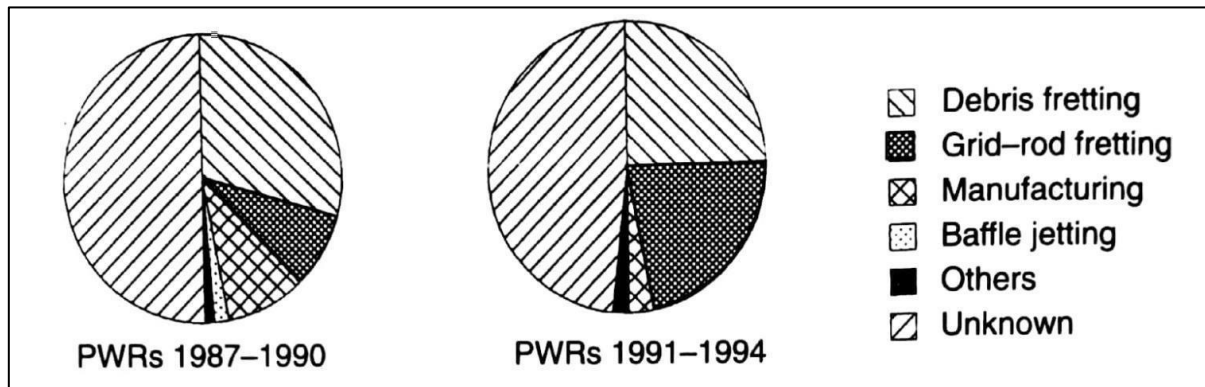


Figure 43: Distribution of fuel failure causes between 1987 and 1994 from [236]

In relation to the term “accident” a more helpful category of incident is listed by the IAEA in regards to events involving failure of ten or more fuel assemblies. This category more readily aligns with the concept of a reactor accident. Incidents of such multiple failures are tabulated below, segregated to only refer to PWR incidents. The vast majority of such incidents involve the failure of no more than 30 rods per assembly, recognising there are between 196 and 324 rods per assembly, depending on design.

Table 7: PWR fuel failures in incidents involving more than ten assemblies, 1989-1994 (from [236])

Year	Plant	Main failure mechanism
1989	1 PWR – USA	Grid-rod fretting
1989	Connecticut Yankee (USA)	Debris fretting
1989	1 PWR - USA	Debris fretting
1991	1 PWR - USA	Grid-rod fretting
1992	1 PWR - USA	Debris fretting
1992	1 PWR - Asia	Grid-rod fretting
1992/93	Angra-1 (Brazil)	Grid-rod fretting
1993	Beaver Valley 1 (USA)	Grid-rod fretting
1993	1 PWR - USA	Grid-rod fretting
1993	1 PWR - USA	Grid-rod fretting
1994	1 PWR – USA	Grid-rod fretting

The worst event over the 1989-94 period was at Connecticut Yankee in 1989, which at the time was still using stainless steel clad fuel, which suffered damage to around 100 assemblies comprising 450 damaged fuel pins.

The IAEA [236] note that following fuel pin failure, it has often been possible to repair and reconstitute damaged fuel. There are clearly some potential concerns with re-using previously damaged fuel, in light of the “zero defect strategic objective” however more pragmatic considerations on the use of partly burned fuel with only a few, or even one, damaged rod have been an argument for some re-use. EDF had (by 1996) developed a set of criteria relating to the size of the damage feature and the expected release of fission products if a repaired or reconstituted fuel assembly is re-irradiated. However, this practice was discontinued from 2002.

The IAEA review of fuel failures between 1994 and 2006 [237] provides an update on the topic. The trend in fuel burnup is a continuous (but not linear) increase over the reporting period.

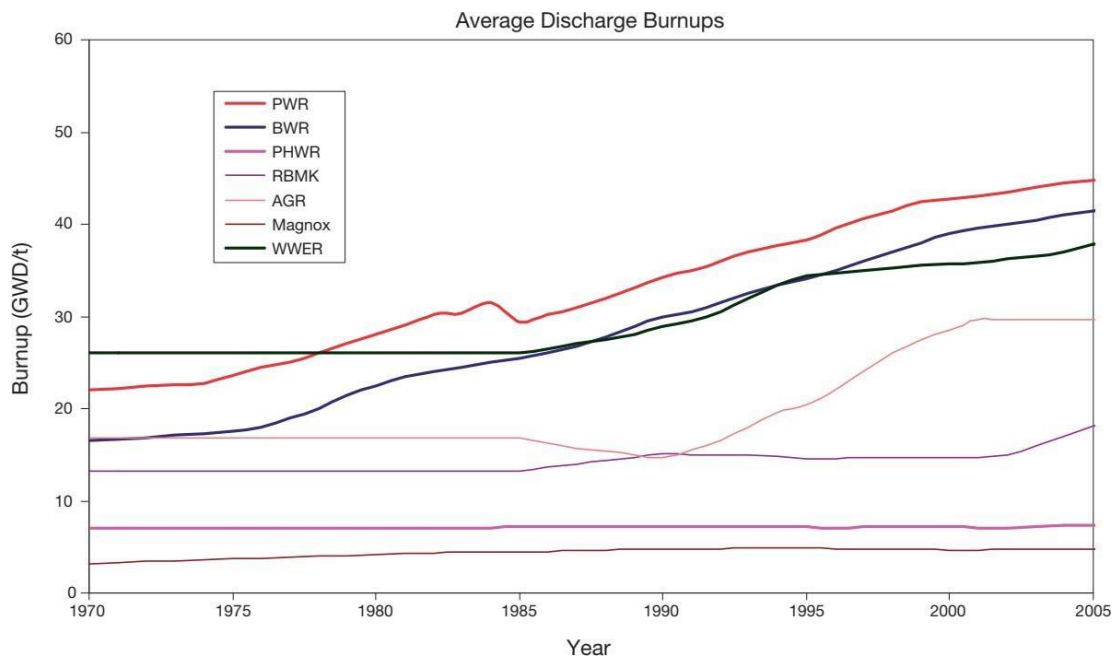


Figure 44: Trends in fuel burnups between 1970 and 2005 [From [237]]

It is noted [237] that newer fuel designs have included improved debris filters, and also stiffer control rod guide tubes (to counteract bowing of earlier designs of control rod guide tubes, which had some tendency to bow and therefore obstruct free movement of the control rods, leading to friction and some metal spalling). A further improvement has been in regard to failure of screws attaching springs to the top nozzle of fuel assemblies; more modern fuel designs improve on the way that springs are retained, and have eliminated this problem. The design of fuel, in terms of the number of rods per assembly, has moved on slightly from the 1994 review, with more of the smaller-diameter fuel coming into use.

The IAEA survey of fuel failures from 1994 to 2006 clearly sets out that reactor accidents are outside of the scope of that document. The distribution of fuel failure mechanisms is similar to that illustrated in Figure 43, although the overall number of failures is reduced and the distribution of mechanisms varies slightly. An update is provided on instances of multiple fuel assembly failures (>10 assemblies in one cycle) and that information is presented in the following table.

Table 8: PWR fuel failures in incidents involving more than ten assemblies, 1995-2005 [237]

Year	Plant	Main failure mechanism
1994	1 PWR – USA	Unknown
1995	1 PWR - USA	Manufacture
1996	1 PWR - USA	Grid – rod fretting
1998	1 PWR - USA	Grid - rod fretting
2000	1 PWR - USA	Grid – rod fretting
2001	1 PWR - USA	Grid - rod fretting
2001	1 PWR - France	Fretting at bottom grid
2002	1 PWR - France	Fretting at bottom grid
2003	1 PWR - USA	Unknown
2006	1 PWR - USA	Grid - rod fretting

It is immediately apparent that the major cause of failure in these 10+ assembly failure events is fretting of one type or another. According to the IAEA survey no instances have been reported where fuel crud is identified as a contributory factor. At worst fuel crud may be responsible for the two “unknown” failure mechanisms, but even that is hypothetical.

The most recent update from IAEA regarding fuel failures is [238]. This covers fuel failures reported over the timeframe 2006 -2015. Again, data received in response to a questionnaire was not consistent across all responding countries, some responding reactor by reactor, or station by station, or reactor type groupings. Over the study period the trend has been that leaking fuel assemblies continue to be less abundant. No new mechanisms for fuel failure have been identified, and in the latest data (2011-2015) the main cause is fretting wear, followed by debris – initiated failure. The kind of data reflected above in Tables 8.1 and 8.2 is not replicated for this time period, as there was only one PWR incident where >10 Fuel Assemblies were failed a one time. That occurred in an unnamed reactor in the USA in 2006, the exact number of failed fuel assemblies is not provided. Over the same time period there were nine incidents where somewhere between five and nine PWR fuel assemblies were failed at each instance. The causes, in all instances, were either fretting wear or fabrication deficiencies. Nevertheless, EPRI [17] have recorded a small number of CILC fuel failures; these are clearly very minor contributors to the overall incidence of fuel failure.

11.6. Major Reactor Accidents

11.6.1. Reactor Safety Post-Three Mile Island (1979)

The Three Mile Island accident relates directly to the PWR reactor type, but the accident did not involve fuel crud. The Three Mile Island reactor accident is comprehensively explained in an EPRI document [239] prepared for IAEA, which presents the progression of events and the responses of the power station staff in reaction to the events. Because TMI-2 was known to suffer from fuel crud, and the accident related to fuel performance, it is considered relevant to examine the possible role of crud in the accident progression. The fundamental cause of the accident on 28 March 1979 was a stuck relief valve on the pressuriser which remained open when it should have been closed. The consequential series of events, in loss of coolant and core boiling, pump trips and emergency procedures have all been analysed in detail, even if there were some

shortcomings in the availability of some data (such as the pressure within the pressuriser relief drain tank – the gauge was “round the back of a cabinet” and not apparent to operators at the main console). There were undoubtedly some lessons to be learned.

In terms of fuel involvement in the accident, a point was reached where the core was overheating and the water therein was not being replaced or circulated, and a steam bubble formed within the core. This combination of high temperature and steam availability initiated the Zircaloy-steam reaction, which both accelerated the oxidation of zirconium and generated hydrogen. Some of the hydrogen escaped through the (stuck open) pressuriser relief valve and eventually, via the pressuriser relief drain tank, made its way into the containment, where it combusted. The resultant pressure pulse was within the design limits for the containment building.

There is no suggestion that fuel crud had any effect on this sequence of events. Even recognising the potential for fuel crud to impair heat transfer it is doubtful whether the presence (or not) of fuel crud could have had any meaningful effect on the rate of fuel temperature rise and almost certainly had no effect on the overall outcome of the accident. Reference [239] mentions fuel crud several times, but makes no connection between the presence of crud (which is merely commented on in the context of describing normal reactor coolant cleanup) and any involvement in the accident.

The safety of nuclear reactors in accident conditions had been previously (1975) considered in the US NRC document NUREG 75/014, also known as WASH-1400 or the Rasmussen report [240]. Rasmussen and co-workers had attempted to lay out the probability of large accidents involving nuclear power plant and the consequences in terms of loss of human life. That report was controversial at the time, and even more so in the light of the Three Mile Island accident four years later. That document mentions “fuel” many times, but there is not a single mention of the term “crud” or “fuel deposit”. This serves to confirm the enduring perception that fuel crud is not likely to be an underlying cause of any reactor accident.

Some 40 years later, in 2016 the USNRC report NUREG/ KM-0010 [241] explored in great depth the probabilistic safety arguments surrounding reactor accidents. Throughout that document, the term “crud” is not mentioned once, again indicating the absence of any clear link between fuel crud and any direct role in reactor accidents. Interestingly, KM-0010 finds that the original WASH-1400 report would not have helped at TMI because the probabilistic fault sequence studied in WASH-1400 was for a Westinghouse reactor whereas TMI was a Babcock and Wilcox reactor with different system features.

11.6.2. The Paks Fuel Accident (2003)

This was an unexpected event, but worth mention because in this case, an operation intended to deal with fuel crud was the cause of an accident. Some 30 VVER fuel assemblies were badly damaged in an event associated with cleaning fuel during a reactor outage. The IAEA account of the event is presented in [242].

The background to the event was that during the 1990s the four VVER-440- reactors at Paks began to experience increasing levels of fuel crud deposition. Reference [242] indicates that the most probable causes of this was the use of chemical cleaning reagents on the primary coolant circuit, necessitated by the problems being experienced in the SGs which required man-entry into the SG structures during outage. In order to minimise radiation dose exposure to these workers, it was considered reasonable to also decontaminate the primary side of the SGs (apart from reactor 4, which used physical shielding methods to reduce dose to operatives). In turn, traces of the organic cleaning reagents persisted in the primary circuit of reactors 1-3 and enhanced the amount of magnetite deposition on the fuel cladding. Consequently, it had become a frequent problem that whole cores of fuel needed to be replaced, instead of the more economic

approach of fuel shuffling and a partial fuel reload. In order to mitigate this uneconomic situation, it was decided to adopt the practice of fuel cleaning at outage, and a large tank for ultrasonic cleaning of fuel was installed within the fuel handling pit adjacent to the reactor (which would be flooded at outage) – see Section 10.5.3. Fuel was cleaned in batches of 30 fuel assemblies whilst the fuel was cooled by a high mass flow pump (250 t/h), which would remove the residual heat from the fuel; on 10th April 2003 the sixth batch of fuel had finished its cleaning process, but was not removed from the cleaning tank because the crane was in use for other purposes. As an interim measure, the fuel was cooled by a submersible pump with lower mass flow rate (20 t/h) than that used during cleaning. Unfortunately, the submersible pump had too low a mass flow rate and was not able to remove heat from the fuel at an adequate rate. Due to the complexities of the design of the fuel and of the cleaning tank, some thermal convection currents were set up which stratified the cooling water, whilst the pump was ineffectual. Eventually coolant temperature reached saturation in the upper part of the cleaning tank and boiling occurred. The formation of steam pushed coolant out of the tank and worsened the situation (both inlet and outlet pipe connections to the cleaning tank were at the base of the tank). The fuel heated up to over 1000 °C and all assemblies were badly damaged. There was some discharge of radioactive noble gases to the reactor hall and to the environment.

The lid of the cleaning tank was removed (as was normal practice for getting the fuel in and out) at that point it became evident that most of the fuel was badly damaged. Recovery of the situation was carried out in a controlled way and the only environmental release was radioactive noble gases. The fuel, in the recovered tank structure, remains at Paks.

In the ensuing investigation and enquiry, it was advised by the Russian company Hydropress (which investigated the safe working limits of VVER-440 fuel burdened with significant fuel deposits) that a safe working limit for VVER-440 fuel would be 355 °C. This accident was occasioned because of the effect of fuel deposits on the economics of reactor operations, but this was not the primary cause of the event. The singular cause was the use of a substantially inadequate heat removal provision to cool a batch of 30 irradiated fuel assemblies.

11.6.3. Reactor Safety Post-Fukushima (2011)

The safety and reliability of reactors and specifically reactor fuel received a significant impetus in the light of the Fukushima accident. The IAEA convened an International Experts Meeting (IEM) to consider the onward implications of the Fukushima accident on future reactor operations; their findings were published in an IAEA report [243]. The conclusions point to ways forward for improving reactor safety; however, none are overtly concerned with avoiding or mitigating fuel crud build up.

The point is repeatedly made that the necessary Defence in Depth approach is directed to ensure that DBA (those tolerable within the intended design basis) do not escalate to become BDBAs. A further output of the IEM was that Severe Accident Management Guidelines (SAMGs) should be developed for all the facilities along the fuel route, including storage pools. In an oblique reference to fuel performance, it was recognised that a knowledge gap existed in terms of the evolution mechanisms of spent fuel in storage, which included cladding properties evolution. Logically, it would be unlikely that significantly more fuel crud would deposit, but further corrosion of the fuel (particularly cladding underneath existing crud deposits) would be a topic for further investigation. The specific terms “crud” and “deposit” are not found within the review document, as they were not causal aspects of the Fukushima accident. One consequence of the Fukushima accident has been a global impetus to provide accident tolerant fuels (ATF) with accident safety as an inherent characteristic. From that may stem a future requirement to understand the performance of ATFs in supporting crud formation and resisting CILC.

11.7. Operational Experience Feedback

In the event of any untoward incidents with facilities connected to the nuclear fuel cycle, the IAEA have an expectation that facilities within member countries will engage with their operational experience feedback system, FINAS [244]. This provides an international focal point for improving safety and covers both technical and human factor causes of events that have a bearing on safety. Access to FINAS is restricted, meaning that member organisations can circulate information within their own organisation, but external search and copying of data is not permitted.

It is for this reason that [IAEA Specific Safety Guide No. SSG-50] gives detail of “how to” provide feedback, but contains no actual case information.

Consequently, a detailed search of FINAS for instances where fuel crud has been implicit in any accident, is not possible.

11.8. Summary of Accidents featuring Fuel Crud

In this survey of fuel crud involvement in reactor accident conditions, some clear indications have been identified.

- a) There have been numerous incidents in which more than ten fuel assemblies at a time have been damaged. These incidents have not been formally assigned as accidents. The great majority of these incidents have been caused by fretting wear of the fuel cladding, or manufacture issues, none are overtly caused by corrosion deposits.
- b) There have been a number of investigations into the probability of reactor accidents, two of which have been commented on above. In neither case does fuel crud present as a mechanism of concern in quantifying reactor accident risks.
- c) There have been two major accidents involving LWR reactors where some crud is likely to have been present on the fuel surfaces at the time of those accidents (Three Mile Island and Fukushima Daiichi). In the subsequent detailed investigations, there has been no suggestion that fuel surface corrosion deposits exacerbated the development of the accident in any meaningful way.
- d) In a minor accident involving the cleaning of fuel carrying surface deposits, the actual cause of the accident was insufficient decay heat removal from irradiated fuel after it had been cleaned. The corrosion deposit itself was not responsible.

In summary, there have been no instances where corrosion deposits have been the cause of an accident.

12. Crud Implications for Spent Nuclear Fuel Storage

12.1. PWR Spent Fuel

The storage of spent PWR fuel is not overtly influenced by the presence (or absence) of fuel crud. It is normal practice to store spent fuel at the station pond until the fuel is cool enough (both radiologically and thermally) to be placed in long term storage (or in France, sent for reprocessing). Whilst the fuel is in interim storage, and as its surface temperature decreases with time, there is a possibility that fuel crud may spall off the fuel surface (in both wet and dry storage environments) and so create a secondary intermediate-level waste stream that will need to be safely managed, either by being packaged with the fuel for final disposal or by being separately packaged and managed.

In the UK, in the absence of fuel reprocessing, the assumption is that PWR fuel will be stored until a Geological Disposal Facility (GDF) is available to accommodate the fuel for final disposal. Currently the practice at Sizewell B PWR is for dry storage, once the fuel has cooled sufficiently. The best practice for drying the fuel is outlined in an ASTM standard method [245] which recognises that crud may impede or delay the fuel drying process. The method relies on successive periods of vacuum suction to remove all gas plus water vapour, followed by periods of warming using an inert gas at elevated temperature; the vacuum and warming cycles are alternately repeated until a vacuum rebound test can be successfully demonstrated. This involves isolating the container holding the fuel assembly, under vacuum, and monitoring the increase in pressure (rebound). If sufficiently dry, the loss of vacuum by water evaporation will take longer than the test criterion. The need for repeated vacuum / warming cycles concerns the possibility of water turning to ice under vacuum conditions, in which case it will not readily evaporate. Each warming cycle is intended to thaw any ice and evaporate water, making the water vapour amenable to removal by vacuum pumping.

If any thick crud is present, it could represent a location for water hold-up (both physisorbed and liquid in any pores, crevices or steam chimneys) which would require more cycles to be performed in order to achieve sufficient dryness. Relatively short-cooled fuel would have its own thermal output which further minimises the likelihood of ice forming, and increases the likelihood of water evaporation. Conversely, long-cooled fuel without much thermal output will be more difficult to vacuum-dry, although spalling of crud may mitigate water retention in long cooled fuel. An important point is that vacuum drying of spent fuel is primarily intended for intact fuel. Failed fuel (with any number of failed fuel rods per assembly) may be dried but only when the nature of failure is understood, and whether the fuel has become internally waterlogged. The definition of "failed fuel" is proposed by ASTM as meaning fuel which could be dried for short or interim storage, but whose long-term performance (as in geological disposal) is unpredictable because of some failure feature. A particular concern is that vacuum drying of failed fuel could have the effect of drawing out any volatile fission products and attendant problems of equipment contamination and very slow arrival at a point of passing a vacuum rebound test.

The acceptance criterion for a rebound test [245] is dependent upon the intended storage regime and whether the remaining amount of water is acceptable (e.g., with regard to corrosion of the storage cask, or potential hydrogen inventory). This is important because once in dry storage any residual water will be radiolysed and converted into hydrogen (stoichiometric oxygen will become further oxide corrosion product). ASTM indicate that for commercial PWR fuel a typical minimum acceptance requirement would be maintaining a 4×10^{-4} MPa (3 Torr) pressure for 30

minutes, which indicates that less than one mole of residual gas (released from trapped or physisorbed water, or ice) is inside the cask.

Additional hydrogen (from additional water carry over within crud pores) may potentially add to the fuel cladding inventory of zirconium hydride, a species of concern, although zirconium hydride formation is temperature dependent and at dry storage cladding temperatures the effect is simply a possibility. The presence of zirconium hydride is significant since within the cladding any crystals of zirconium hydride provide a "path of least resistance" to propagate delayed hydride cracking (DHC) – which in principle could lead to fuel cladding failure. There will anyway be some zirconium hydride present from the corrosion of the cladding during reactor operations. This matter has been widely studied over the past few decades, for example an early general study [246] and a recent study probing the phase distribution of the hydride crystallites [247]; there have also been efforts to model the process [248]. Additionally, the IAEA have provided a general survey [249]. Additional hydrogen derived from water carry-over may be lessened in impact as the solubility of hydrogen in zirconium decreases almost exponentially with decrease in temperature; the temperature of the stored fuel then becomes an important parameter. The orientation of the zirconium hydride crystals is important, they normally arise in a circumferential orientation, aligned with hoop stress in the tubular cladding metal, but can potentially re-orientate towards a more radial configuration, leading to a weakness in the fuel cladding (which will be under stress due to pellet-clad interaction). Such re-orientation is facilitated by changes or cycles in temperature, precisely the treatment in the vacuum / hot gas cycling drying method. Therefore, it is advisable to minimise the number of thermal cycles in the process and to minimise equilibration time in a hot condition. But this may not be possible if crud makes drying difficult by requiring longer treatment steps or requires additional numbers of vacuum / hot gas cycles. The significance of any DHC is also conditional upon the status of the dry fuel container. If it is a designated disposal container, never to be opened, (or part of an approved disposal system where it will be overpacked) then the condition of the fuel within should have no safety consequence. However, if it has to be re-opened and the fuel re-packed prior to GDF emplacement, then any fuel failure due to DHC would require additional safety management arrangements.

A further matter which may require regulatory attention is the nature of any medium-term dry storage facility, by way of design and compatibility with transportation of fuel away from the reactor site to a GDF. It is reasonable to assume that a dry storage facility would be constructed at the reactor site, and that it would be possible to construct more storage capacity until the reactor's lifetime mission had been completed. Subsequently, the removal of fuel to a GDF should ideally be readily engineered using at least the innermost containment of the dry storage system, so the fuel never needs to be repacked into another container. Therefore, regardless of crud and any conceivable crud-related mechanisms, failure of the fuel (or spalling of crud from long-cooled fuel) need not be a concern in the onward steps of the fuel life cycle. It is widely recognised that this forward thinking has not been evident particularly in the USA, where the particular arrangements for ultimate geological disposal rest with the State, and the Utilities are only responsible for interim storage; the Utilities have no inducement to provide an engineered storage system compatible with transport, and some of the storage systems deployed are evidently not transportable. With or without crud, repacking of fuel after possibly several decades of dry storage would require extensive and expensive remote-handling shielded facilities in a possible scenario where the station has ended its power production and has been partly decommissioned. Significant experience from long term storage of heavily crudded early US assemblies will inform subsequent assessments of repacking operations and there are programmes underway in this area. Contemporary plants with much lower crud inventory fuel should be bounded by this behaviour.

12.2. UK Experience

UK experience of fuel storage is centred around the long-term storage of Magnox and AGR fuels, in appropriate ponds at Sellafield, Cumbria. Evidently, neither of these fuels will have corrosion product deposits in the form of crud on the fuel surface (although AGR fuel may have carbonaceous deposits on the cladding surface). Since the cessation of fuel reprocessing at Sellafield the expectation is that fuel will be stored for a long duration (possibly several decades) until a GDF is available to receive intact fuel. For AGR fuel, that fuel is already in a dismantled condition and individual pins (in groups of 108, representing three fuel elements) are stored in "slotted cans" in the THORP receipt and storage pond. In order to prevent corrosion of the stainless steel fuel cladding, some of which (the lower elements in a stringer) has been sensitised, the fuel pond has to operate at high pH, with a target of pH 11.4. It is apparent that AGR (and any residual Magnox) fuel will need to be dried before disposal, therefore there is some commonality of technology anticipated some decades in the future.

A dry fuel store based on the widely deployed Holtech International "HI-STORM" cask system was commissioned at Sizewell B in 2016, although relatively little technical information is available in the public domain. Further, the UK has also had in storage some LWR fuels imported to Sellafield for reprocessing (from Japan and continental Europe). The Multi-Element Bottles (MEBs) used for their pond storage at the Thorp Receipt and Storage plant were of two different designs, namely those for Japanese fuels (the BNFL design MEB) and those for European fuels (the NTL MEB). Nuclear Transport Ltd (NTL) was an erstwhile joint venture between BNFL and COGEMA and operated across Europe. The MEB designs differ in that NTL pattern MEBs have exposed aluminium metal, internally, as part of the Boral neutron absorber and criticality control system, whereas in BNFL pattern MEBs the Boral (which is still present) is sheathed in stainless steel and the aluminium surface is not exposed. It would not be advisable to expose aluminium to high pH pondwater, therefore the NTL pattern MEBs have had to be removed from pond due to their incompatibility with the high pH now required for safe storage of AGR fuels for the coming decades. It is thought likely that (broadly speaking) the European – origin LWR fuels have been reprocessed, and that the Japanese -origin LWR fuels have not been reprocessed, since the BNFL pattern MEBs are compatible with the new pondwater chemistry regime. Nevertheless, the fuels themselves, all clad in zirconium alloys, will also be exposed to pond water at pH >11, as the MEBs are normally operated fully flooded and not sealed, to avoid radiolytic hydrogen buildup. However, zirconium corrosion rates are expected to be very low at pond / ambient temperatures. Again, there may be some commonality of technology anticipated some decades in the future, if or when such LWR fuels have to be dried before emplacement in a GDF. For these fuels, particularly, the presence of crud and the absence of intrinsic thermal heat (for long-cooled fuel) may exacerbate the length of time (or number of vacuum–heating drying cycles) necessary to pass a pressure rebound test.

12.3. Other fuel types - CANDU

Regarding other types of reactor fuel, all Canadian CANDU fuel is cooled (short term) in the station cooling ponds pools and then transferred to a dry storage environment for interim storage until such time as a geological disposal facility becomes available. The interim storage arrangements vary, station to station, and some are more problematic than others in terms of retrievability, but none are designed with any regard for crud adhering to the fuel. It should be noted that delayed hydride cracking (discussed above) is also relevant to CANDU fuels and has been observed / measured in CANDU zirconium alloy pressure tubes [250].

At Gentilly (which is now in decommissioning) the fuel elements have been dried and placed in a stainless steel cylindrical basket, the basket purged with helium, and the lid welded on. It is not known if some vacuum drying procedure has been used within the process. The baskets were transferred to the modular vault dry store (known variously as a MACSTOR or CANSTOR) where they were loaded one on top of another in a carbon steel tube containing up to eight baskets; twelve such carbon steel tubes are pre-located in each module of the store. The modules are constructed of massive reinforced concrete with passive air-cooled channels. The storage tubes are sealed off with a massive steel and concrete cap and a weatherproof plate. There is no intention to reprocess such fuel, and the stainless steel baskets are not intended to be re-opened. Retrieval of the fuel baskets is possible using shielded flasks positioned above the sealing caps, fitted with a gamma-gate. The whole facility is serviced by Goliath cranes which straddle the modular store. Gentilly power station is now shut down and it is probable that all the fuel is now either in the station pond or the modular store.

Broadly similar arrangements apply at Point Lepreau and at Chalk River where, instead of a modular store, each carbon steel tube exists within its own concrete shell (a "concrete canister" store). Again, there are up to eight baskets per storage tube. These fuels are retrievable, basket by basket, provided a suitable crane and gamma-gated flask are available. Because the stainless steel baskets are never intended to be opened, the condition of the fuel within is deemed irrelevant, and so the effects of any crud on the fuel, hypothetically causing overheating and failure, are irrelevant anyway. In practice the fuel is sufficiently well cooled before emplacement in a basket.

More problematic is the situation at Pickering and Bruce power stations, where (in an underwater, pond operation) fuel has been loaded into stillages which in turn have been loaded into storage containers with thick shielding walls. Each container and its contents are recovered from the pond, drained and dried, and the thick container lid welded on (in a multi-pass automated weld). The problem is that these containers are not qualified as disposal containers and it is possible that the fuel will need to be unloaded prior to geological disposal. If, in the meantime, fuel crud has influenced heat rejection and any localised overheating or cladding failure, that remains a potential concern. In mitigation, the fuel is adequately cooled before emplacement in a storage container. There is an argument to the effect that the interim storage containers should be designated as disposal containers, perhaps with an overpack. It would be operationally very difficult to unload the interim storage containers (which involves undoing a very large multi-pass weld, followed by underwater operations), particularly if the reactor station has closed down and the fuel handling pool is no longer available.

12.4. Other fuel types - SCWR

Super-critical water reactors are as yet still in the design phase, although some test loops under supercritical conditions have been operated at Beloyarsk [251]. The cladding material for SCWR fuel is not yet settled, there is a strong possibility that stainless steel may be used (as at Beloyarsk) and since the operational temperature of a SCWR must, by definition, be above T_{crit} which is 374 °C, there is a significant possibility that a stainless steel fuel cladding may be radiation-sensitised (in common with AGR fuel). That in turn leads to complications with spent fuel storage, which, if in a pond, has to be at pH 11.4 – in the case of AGR fuel, as implemented at Sellafield. There is no evidence that crud influences the safe storage of SCWR fuel, but since such evidence would be limited to Beloyarsk loop fuel, and that aspect has not been reported on, the influence of crud remains effectively unknown.

12.5. Summary of Crud Implications for Spent Fuel Storage

There have been no reported instances of fuel crud influencing the safe storage of spent nuclear fuel. The obvious concern with crud inhibiting heat ejection under dry storage conditions is usually mitigated by only dry-storing fuel which is sufficiently long-cooled and which would not overheat even with a substantial crud layer. The mechanism for dry-storage preparation (vacuum drying / hot gas treatment) has been described, as has the vacuum rebound test to verify an acceptable degree of dryness. It is noteworthy that only intact fuel is normally dried in this way; failed fuel remains problematic.

The matter of delayed hydride cracking has been identified, with recognition that fuel crud may represent a means of water hold-up within the crud which requires additional or extended process cycles in the standard vacuum / hot gas treatment process. Increased time at temperature and increased number of temperature cycles are factors which may contribute to zirconium hydride crystal reorientation from circumferential to radial, and thus develop cladding weakness leading to failure.

UK experience has been summarised, picking up the detail that there will be some overseas-origin LWR fuel in storage at Sellafield, where crud is likely to be present, but in pond storage this does not cause a problem apart from management of any potentially mobile radioactive particulate arising from detached or spalled crud. Other fuel types (CANDU and SCWR) have been commented on, again there are no specific crud-related problems but there may be additional concerns which are noteworthy.

13. Fuel Crud in non-PWR systems

It is a matter of historical dispute whether the term crud originally derived its meaning from anomalous deposits first found on fuel at the Chalk River prototype CANDU reactor (Chalk River Unidentified Deposit) or whether the term arose as (or has evolved into) a more generic Corrosion Related Unidentified Deposit, as some would argue. Alternatively, there is a view that there has long been a vernacular English language usage of “crud” as a term for an undesired dirty or unpleasant substance, as in the phrase “Those fuel elements have some sort of crud on them”, which was then retrospectively adopted as an abbreviation to lend technical credibility. Semantics apart, the point is made that CANDU reactors were one of the early manifestations of this phenomenon.

In this section we explore the literature and historical accounts of crud arising in four water-cooled reactor systems, namely Boiling Water Reactors (BWR) Pressurised Heavy Water Reactors (PHWR), VVER, and Supercritical Water Reactors (SCWR).

The following graph [252] illustrates the trends in fuel discharge burnup across the reactor fleets of all kinds, as of 2005, and the trend is clearly increasing for all types. Currently PWR average discharge burnup is around 50 GWd/te so the trend has plateaued to some extent in recent years for PWR and similar is likely for other types such as BWR and VVER.

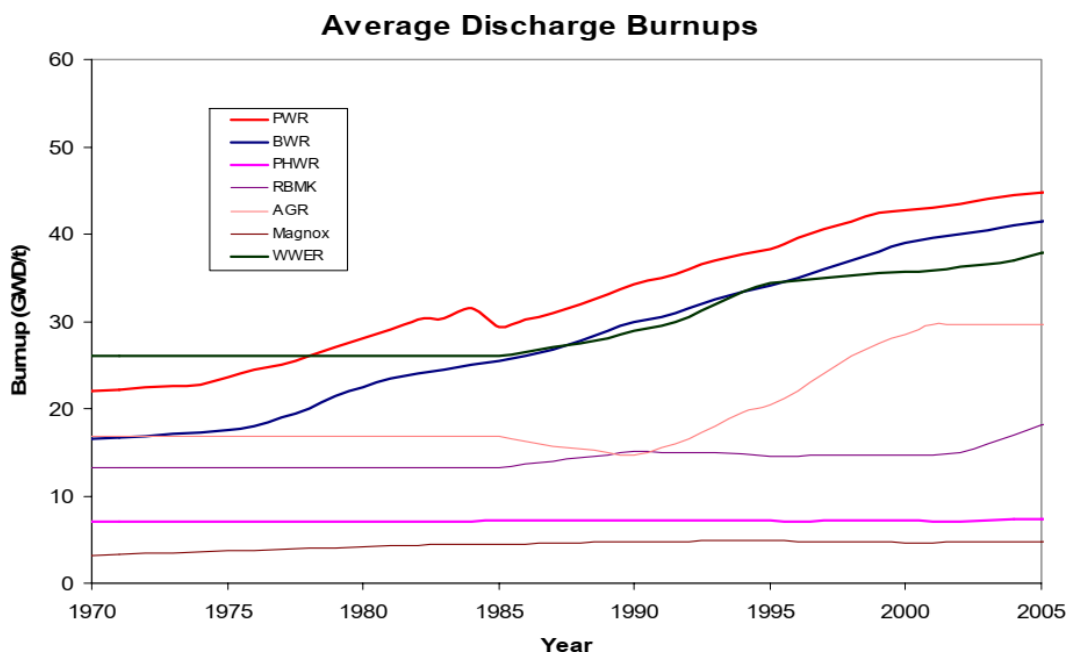


Figure 45: Average discharge burnup data (2005) across all reactor fleets (From [252])

There follows, for each reactor type, a summary of the crud-related technical material of relevance.

13.1. Crud in Boiling Water Reactors

13.1.1. Introduction to BWR Reactor Cooling Systems

It is evident that in BWRs the primary purpose is to make water boil on the surface of the fuel, and the steam so formed goes directly to the turbine without need for a SG. Therefore, there is unavoidably boiling, and associated steam bubbles, on the fuel surface. Any minor impurity in the water (although the water quality is specified to very high cleanliness standards) will unavoidably deposit on the fuel. It is frequently observed that BWR fuel, on discharge from reactor, appears very heavily affected by corrosion product deposits.

Additionally, these deposits become activated and are subsequently detached or dissolved and find their way throughout the primary circuit. Accordingly, dose to maintenance staff during shutdown operations can be appreciable. Consequently, efforts have been made to reduce this man-dose exposure.

In regard to iron, it is notable that some (older) plants used carbon steel in the Heater Drains from the condenser system and this gave rise to a measurable iron content in the feedwater chemistry. More recent plants use materials such as chrome-containing steels and these produce far less iron in the feedwater. Thus, BWRs divide into high-iron and low-iron plants. However, to mitigate various aspects of corrosion around the flow path, some iron in the feedwater is desirable, and therefore deliberate injection of iron into the feedwater is sometimes adopted.

An excellent review of BWR operational chemistry (applied to Advanced Boiling Water Reactors (ABWR), but relevant to all BWR plants) is provided in [253]. Consequently, this document only picks up some highlights which amplify certain matters of interest.

A successful approach to radiation dose reduction has been zinc injection, which was developed first for BWR reactors. It had been noted that BWR reactors with condensers containing brass tubing (and therefore containing zinc) were less prone to develop heavy crud formation all around the primary circuit, including on the fuel. This realisation was applied to BWR reactors not having brass-tubing condensers by deliberately injecting zinc obtained by the dissolution of zinc oxide; a process patented by GE™. Although the solubility of zinc oxide is quite low, the few ppb zinc generated that way was sufficient to mitigate heavy crud formation. Zinc appears to work by occupying tetrahedral sites in the iron oxide (magnetite) spinel structure and blocking the channels through the spinel to other metals (such as cobalt) and restricting the growth of the spinel. This in turn means a thinner layer of crud and lower uptake of cobalt, whereby the uptake of Co-60 in out of core surfaces is mitigated. The same approach has been extended to PWR reactors (see Section 10.3). For completeness, it should be noted that copper (originating from brass condensers) has also been found [254] to be responsible for CILC leading to fuel failures, leading to a widespread programme of brass condenser tube replacement with stainless steel or titanium.

A further issue with BWR reactors is the radiolysis of water in the reactor core, and the operating chemistry (as pure water as possible) meaning the pH_{25} is neutral. At nearer 300°C the pH_T is slightly acidic, and this coupled with the high abundance of H_2O_2 from radiolysis (H_2 from radiolysis will promptly exit the coolant as gas, in the steam phase) has led to the aggressive corrosion (cracking) of the core shroud, a cylindrical plate which separates the incoming water

(descending just inside the pressure vessel wall) from the fuel channel water (rising through the core in the centre of the pressure vessel). The cracking of the core shroud was considered a particularly severe problem, and two solutions are widely adopted, either individually or in combination.

The first of these solutions is to add a small amount of hydrogen to the system, just enough to inhibit radiolysis and prevent the concentration of hydrogen peroxide from approaching levels where corrosive damage might arise. This is termed "hydrogen water chemistry" and is deployed in a number of BWRs.

The second solution which has been widely adopted is noble metal chemical addition (NMCA) (proprietary versions known as NobleChem™ or online NobleChem addition - OLNC) which was developed by GE. In this treatment, colloidal noble metals such as platinum and rhodium are added to the coolant and the colloidal particles act as active sites for reaction between H₂O₂ and H₂, effectively catalysing the re-formation of water. Whilst this approach has been successful in overcoming the primary problem of core shroud cracking, it inevitably leads to some (relatively small amount) of noble metal deposition on fuel surfaces. There is a down-stream concern, however, which is that the noble metals are cathodic relative to zirconium, and could serve as corrosion site initiators. There is no observed evidence for this during the operational life of the fuel, a matter of up to several years: but over a longer time period (such as wet storage of spent fuel pending geological disposal - possibly several decades, or in a geological disposal facility after resaturation) then the life of the cladding as primary containment could be shortened. Thus, any NMCA deposits on the fuel surface may have implications long beyond the operational life of fuel in the power station.

13.1.2. Fuel Deposits in BWRs

In a review by IAEA [255], it was noted that the composition of fuel deposits differs between BWR and PWR reactor types. PWR reactor systems tend to produce fuel deposit composed of nickel spinel complexes; these are tightly bound to the fuel assembly. However, BWR reactor systems tend to produce fuel deposit based on iron oxide based which tends to be loosely bound to the fuel assemblies.

An early (1986) assessment of BWR fuel crud was provided by Nagao et al [256] with the recognition that BWR plants can divide into "high crud plants" and "low crud plants". The distinction appears to correlate with the presence (or not) of Condensate Prefilters, which would support the default Deep Bed condensate polisher equipment. They analysed fuel deposits from both types of plant and realised that in low crud plant, the thin crud layer was relatively rich in nickel, but this was in response to the much-reduced presence of iron. Their results are presented in Table 9. The two plants identified here are 2F1 (Fukushima Dai-ni Reactor 1) and 1F3 (Fukushima Dai-ichi reactor 3).

Table 9: BWR Fuel crud scraping analysis results (from [256])

Plant	EFPY	Fe Composition (%)						
		(g/cm ²)	Fe	Co	Ni	Cr	Cu	Zn
2F1	1.27	150	65.1	0.30	31.3	3.1	0.04	0.2
	2.18	240	77.4	0.20	23.9	1.2	ND	0.2
1F3	1.37	13,000	97.6	0.075	1.3	0.33	0.32	0.40
	1.93	15,000	97.8	0.042	1.1	0.59	0.27	0.25

From X-ray diffraction measurements the structure of the fuel deposit at 2F1 at 1.27 Effective Full Power Years (EFPY) was almost stoichiometric nickel ferrite. At 2.18 EFPY this remained mostly nickel ferrite with a small amount of haematite. This difference was thought to reflect a slight increase in iron in the feedwater, and a reduction in nickel release due to ageing effects and a semi-protective oxide building up on the nickel-bearing surfaces.

In 1990 Lin [257] prepared a study on BWR chemistry arrangements in "foreign" reactors, under EPRI auspices; thus "foreign" means non-USA. This was aimed at controlling radiation field build up, predominantly in out-of-core components, although evidently the deposition and activation and release of crud on fuel surfaces is an integral part of the activity transport mechanism. Interwoven in this is the (then) topical issue of cobalt reduction in primary circuit components, chiefly by avoiding stellite hard-facing surfaces in valves, a matter which is presently considered best practice and cobalt from that source no longer an issue. Lin notes that activity buildup is decreased in plants having condensate filtration to remove iron, and achieve better water purity; however, some plants found that too low an iron content reversed such gains. Also, modest changes in operating pH and some shutdown procedures were also helpful in reducing activity release.

In 1991 the fuel crud deposits at the Tokai-2 BWR were discussed in a conference paper [258]. The fuel deposits were removed first using a nylon brush, to detach the loose outer oxide, then an alumina stone for abrading the adherent inner deposit. The amount of deposit for each fuel assembly span was measured, along with analysis of every sample obtained. The results are shown in []. These results indicate that more crud was deposited in the lower spans of the fuel assembly than the higher spans, both as loose and adherent crud. This is perhaps counter-intuitive, as it would be expected that more boiling would occur in the upper spans as coolant temperature increases, however raises the argument that fluid flow velocity varies along the fuel assembly, and is slower in the lower spans with less void content (i.e. the upper spans should have oxide deposits restricting flow path) and this affects the shear forces causing release of deposits from fuel surfaces. The slower the flow, the less release of deposit. The analyses refer to fuel assemblies selected after a number of operational fuel cycles (that is, in the operational history of the reactor, not that fuel was subjected to 9 irradiation cycles). The chemical analysis indicates that with progressing cycles the iron content of the fuel crud increases until after 10 cycles it is all essentially iron and nickel, everything else is <1%.

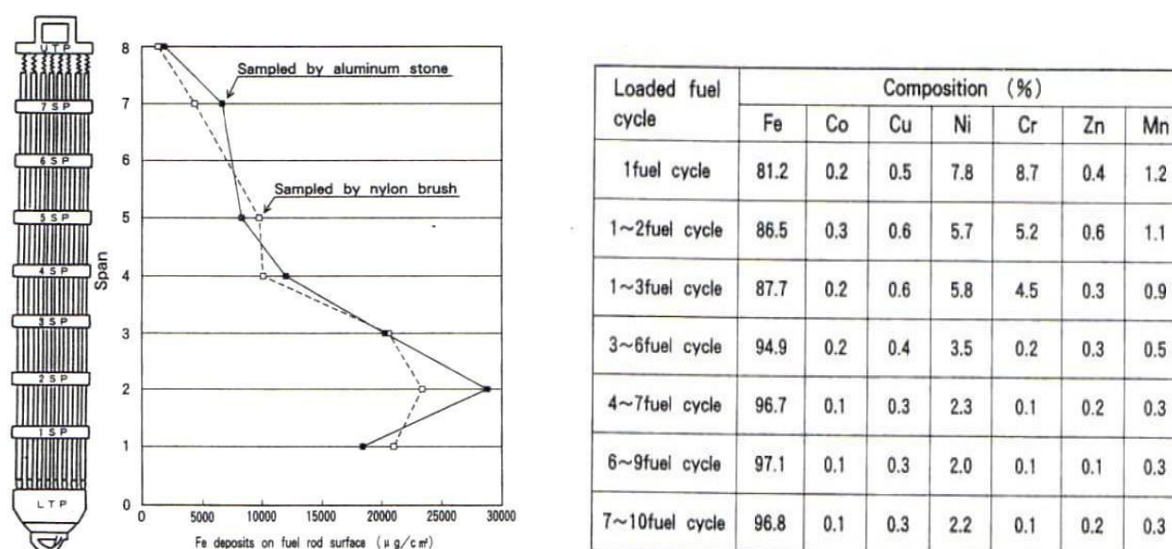


Figure 46: Fuel crud arisings and analysis at Tokai-2 BWR (From [258])

The optimised chemistry of BWRs has been reviewed by Lin et al in 1994 [259]. Besides presenting a summary of the chemistry and radiolysis within the BWR coolant system, Lin et al explain that the feedwater iron is influenced by the corrosion of "balance of plant" carbon steel components in the steam / condensate and feedwater systems, delivered to the reactor by the feedwater. The iron plays an important role in primary circuit transport of cobalt-60 and its deposition on fuel surfaces (along with other transition metals). However excess iron in the feedwater enhances release from fuel surfaces when fuel deposits contain excessive iron. Also, coolant with a high dissolved iron content is prone to enhanced corrosion product deposition in zones of low flow rate, thus creating radiation hot spots. Therefore, iron may be deliberately added to the feedwater flow in order to minimise corrosion at the carbon steel components, even though it may contribute to additional deposits on the fuel surfaces.

In 2000 Kelen et al [260] reported a survey of BWR fuel failures and fuel corrosion. Here there is a complication between the naturally occurring corrosion of zirconium alloy in high temperature water and any deposition of corrosion products derived from elsewhere in the reactor coolant circuit. The measured "oxide thickness" may be a combination of both these sources, particularly from times before the wider introduction of "hydrogen chemistry" in BWRs, when circuit chemistry was comparatively more oxidising. The oxidation of zirconium is of itself a complex field with different oxide crystal structures co-existing and evolving on the same metal substrate. Kelen et al draw attention to different forms of corrosion of BWR fuel, notably "shadow corrosion" and "enhanced spacer shadow corrosion", which exhibit significantly thicker oxides than the more typical "midspan corrosion" of fuel away from spacer grids – also known as general corrosion in the absence of crud deposits. Whilst their data was anonymised, the common factor in this study was that all stations used Atom (manufacturing source) fuel. The relative significance of these differing corrosion mechanisms is illustrated in Figure 47.

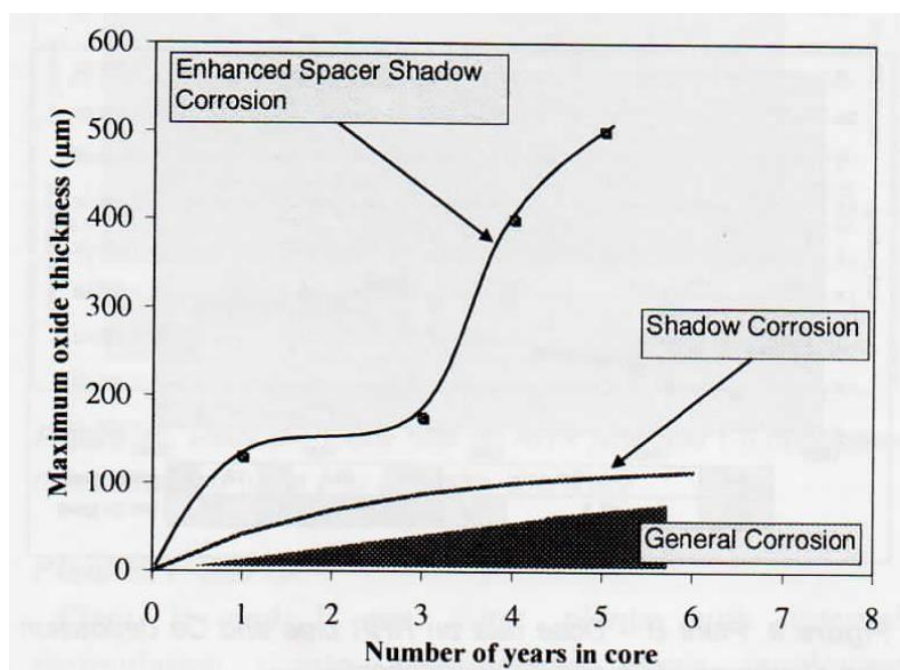


Figure 47: Differences between midspan (general) corrosion, shadow corrosion and enhanced spacer shadow corrosion (From [260])

In 2002 Hermannsson reported [261] on a series of studies on BWR fuel crud phases from Swedish reactors using laser Raman spectroscopy. The fuels were from Ringhals 1, Barseback 2, Forsmark 3 and Forsmark 2. Those studies revealed that the underlying oxide is always a monoclinic ZrO_2 layer of between 25 and 50 microns thickness. Overlying this is the deposited crud consisting of some larger octahedral crystallites but with a much finer "porridge-like" grey deposit in between and around the larger crystallites, mainly consisting of trevorite and haematite with occasionally some amorphous $FeOOH$. The deposit thickness varied between "very thin" and 15 microns.

In 2009 Lin prepared a review of corrosion product transport and radiation field buildup in boiling water reactors [262] in which he noted that the level of total fuel deposit loading and its chemical composition may vary significantly, depending on core location and the number of fuel cycles of exposure. The disposition of the crud is usually as two layers, a softer outer layer which is easily removed by brushing, and a more tenacious inner layer which must be removed by scraping or abrading. The solubilities of the various corrosion product oxides are discussed, noting that deposited materials are also subject to release, so the amount of deposit on a fuel surface is in dynamic equilibrium with the applied environment (be that normal chemistry, hydrogen water chemistry, zinc chemistry, etc). Sampled fuel crud from three different fuel assemblies (from the same plant, which operated a deep bed water cleanup regime) all showed more deposition in the lower spans of each fuel assembly, and that the iron and cobalt were predominantly found in the outer (easily removed) oxide.

The mechanism of transport of crud around the BWR circuit was reported by Hermansson and Haag in 2010 [263]. By examining filter-paper based particulates and radioactivity at five Swedish power plants (Barseback 2, Forsmark 2, Oskarshamn 2, Oskarshamn 3, Ringhals 1) operating with different chemistry regimes, the study was able to identify a difference between NWC and HWC plants, in that the circulating particulates were smaller under HWC and were chiefly composed of haematite, which it was inferred as being freshly precipitated from solution given the electrochemical impact of HWC on the iron rich feedwater. Similarly, Trevorite was less widely observed under HWC.

An analysis of the precipitation of fuel crud using a Gibbs Energy Minimisation approach was reported by Orlov et al, [264]. Using data from the Liebstadt reactor (Switzerland) they calculated the energy levels of the different complexes and precipitates at fuel cladding temperatures, they concluded that under BWR conditions and with boiling, the predominant dissolved species are $Fe(OH)_3$ and $FeOO^-$ and that precipitation of haematite (Fe_2O_3) occurs even without boiling. Furthermore, the nature of the crud depends on the temperature and boiling regime. In a no-zinc NWC regime a Ni-ferritic spinel will only be formed when the steam to water ratio is $>95\%$, so near the top of the fuel rod; but with zinc present franklinite deposits if the steam to water ratio is $>50\%$, so over a wider area of the fuel rod.

Subsequently in 2011 Sawicki [265] amplified some aspects of this, noting that sampled fuel rods are often stored (wet or dry) for some time before sampling, whilst out of reactor core, and that this time provides opportunity for the deposited oxides to change morphologically, due to the action of oxidising species in the pond water. Sawicki proposes that under hydrogen water chemistry the oxide deposit is composed of a thinner and less well-structured oxide crystalline layer, compared with normal water chemistry.

The potentially complex interaction of multiple chemistry regimes (HWC, zinc injection and OLNC) being applied simultaneously is reported by Oliver et al [266] who found that sometimes the Liebstadt BWR plant did not always respond in the way anticipated. Since around 2004 the plant had been injecting zinc, with a stable reactor water concentration around 5 ppb Zn. In

2008 the plant began using Hydrogen Water Chemistry (HWC) and implementing OLNC via annual injections. However, following the first (2008) OLNC injection the reactor water Co-60 spiked, and mitigation was attempted by injecting more zinc. This didn't have the desired effect, instead mass balance calculations suggested that more zinc was depositing on surfaces (including fuel). This coincided with increased observations of fuel crud spalling. Post irradiation fuel observations indicated that crud spalling was greatest at axial elevations where crud load is typically higher. But there was a mixed picture, not all elements spalled in a consistent pattern. The crud deposition pattern was shown to be initially greatest on the lower fuel rod spans, for some fuel assemblies. However, after four cycles of ONLC the crud growth was predominantly in the upper half of the fuel rods and significantly more than before OLNC. The deposition of Pt particles on the fuel surface was also investigated. There had been some concerns that Pt particles could be cathodic to the metal zirconium alloy cladding and could thereby accelerate cladding corrosion. But because the OLNC injection had been made after the fuel had been in-core for some time, and a good thickness of ZrO_2 had developed, measurements showed that the Pt was mainly attached to the outer deposited crud, and not on the inner oxide and close to the metal of the cladding material. It is therefore important to recognise that OLNC injections should not be made on fresh metal fuel surfaces, with no oxide covering.

The effect of Pt deposits on BWR fuel simulants has been further investigated by the Liebstadt team, with a view to investigating hydrogen pick-up in the zirconium cladding [267]. They found that there was no clear relationship between the timing of OLNC injections and hydrogen pick up in the alloy, although caveated by the short timescale nature of their tests. The surface concentration of deposited Pt was found to be greater in tests with boiling at zirconium alloy surfaces, than in non-boiling control tests. Even though the initial surface oxide was quite thin in these tests, no adverse effects of OLNC were observed.

Post-irradiation examination of failed BWR fuel rods from the Forsmark BWR station (Units 1, 2 and 3) over the period 2003-2018 have been reported by Olsson [268]. In total 103 fuel pin failures occurred over the study timeframe (of which 43 were examined in detail) and predominantly were associated with debris fretting (typically at 2 to 3.5 metres axial elevation). Some secondary degradation was usually seen some 2 metres higher up the fuel assembly; fuel failures were more common amongst fuel assemblies of lower burnup. A feature of the Forsmark BWRs (Asea Atom design) is that there are no major pipework connections below core level, this has safety advantages but means that any debris entering the core has greater difficulty in leaving. Thus, debris may accumulate in the core. The debris is thought to be mainly metal scrap caught between a fuel rod and a spacer. In total 103 fuel rods have failed in this way. There is no suggestion of spalled fuel deposit material contributing to the debris inventory, but neither is there any discussion of the source of the debris (other than the comment "it is thought to be scrap" and recognising that fretting wear, amongst others, is a possibility). The point that the damage appears at some well-defined axial elevations could be due to growth of fuel deposits at certain temperatures, or to buoyancy of small suspended solids. The key point here is that "safer" reactor designs with no major pipework connections below core level may need to be assessed with a view to accumulated debris and fuel failure.

A summary review of all BWR fuel failures and their causes has been prepared by the IAEA in 2010 [237] with an update in 2019 [238]. Their data is presented graphically in Figure 48 and numerically in Table 10.

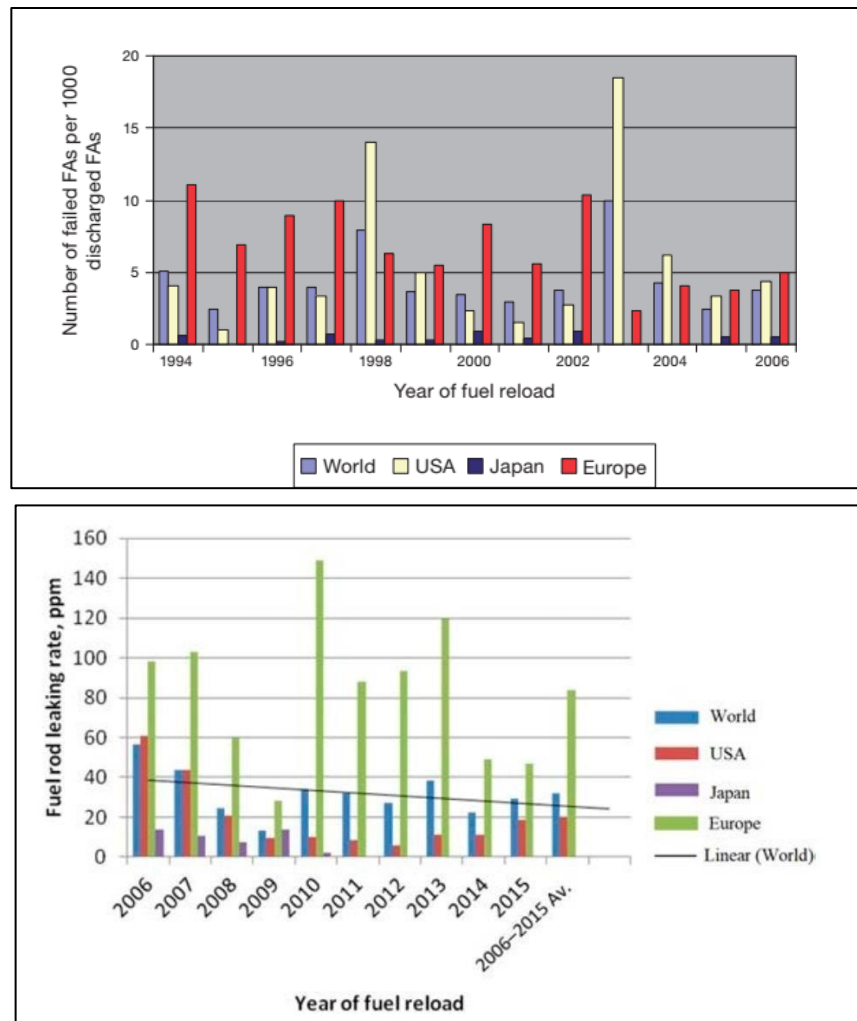


Figure 48: Number of leaking BWR fuel bundles per 1000 discharged bundles and leaking rods per million rods. (From [237] and [238])

Note that in the two graphics, the basis of calculation differs between the early (up to 2006) approach of leaking fuel assemblies per 1000 fuel assemblies (regardless of how many rods per assembly were actually leaking) and the more recent approach (since 2006) of calculating leaking rods per million rods. Whilst there are clear patterns, and European reactors do not compare well with the rest of the world, the overall world trend (up to 2015) is to see a continuing reduction in fuel failures in BWR reactors.

The data in Table 10 indicates that crud or corrosion was (historically) a major contributor to fuel failures but in more recent times it has become a tertiary issue whereas debris fretting has become much more significant, against the backdrop that failure rates are generally falling in total.

As described in detail above, the addition of noble metals such as colloidal platinum or palladium to reactor coolant water has become established in BWR technology. Spent fuel assessments should consider any possible differences in behaviour for fuel with some noble metals embedded in any crud. Such metals would be electrochemically cathodic to zirconium, and in an extended wet storage regime it would follow that potentially there could be enhanced corrosion of the zirconium cladding. A counter argument to this is that the noble metal atoms would not be in immediate contact with the zirconium metal, but would be separated by an insulating layer of oxide: thus, no current would flow. However, the zirconium oxide is known to be highly flawed

with multiple morphologies and grain orientations. The detail of this with respect to corrosion during extended wet storage remains to be established.

Table 10: BWR Fuel failure analysis results (from [238])

	Fuel failure cause (%)						
	1987–1990	1991–1994	1995–1998	1999–2002	2003–2006	2007–2010	2011–2015
Debris fretting	17.5	50.5	39.6	53.4	32.2	58.6	66.0
Crud or corrosion	42.3	4.4	46.8	23.1	52.9	3.9	13.2
PCI/SCC	27.7	34.1	9.9	11.5	14.2	36.2	18.9
Fabrication	10.1	11.0	3.7	11.5	0.7	1.3	1.9
Handling	2.4	0	0	0	0	0	0
Unknown/ undetermined	1.62	32.5	24.0	27.8	13.6	29.2	26.4

13.1.3. Summary considerations on BWR designs

BWR fuel deposits differ from PWR fuel deposits in that they are usually more abundant, and comprise two layers, a soft outer layer which may be easily brushed away, and a tenacious inner layer. All layers are rich in iron, and the growth of deposits and simultaneous release of activated radionuclides is a dynamic equilibrium, although the growth of deposit increases relatively monotonically. Due to the relatively more oxidising conditions in a BWR (compared with PWR) the underlying zirconium alloy fuel cladding is likely to have developed a thicker oxide layer, on which the deposits have been added.

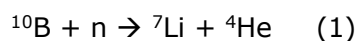
The various endeavours to reduce out of core radioactivity and core shroud cracking by reducing corrosion and fuel crud (zinc injection, NMCA, hydrogen water chemistry) have been widely successful and currently BWRs are less vulnerable than once they were. However, the experience from Liebstadt indicates that simultaneous use of multiple approaches may lead to complex interactions.

There are reports of fuel failures due to localised overheating underneath fuel deposits, and reports of fuel failures due to debris fretting, attributed to extraneous material other than fuel deposits but without any convincing argument to isolate the origin of the core debris.

13.2. Crud in VVERs

13.2.1. Introduction to VVER Reactor Cooling Systems

The Voda-Vodyanou Energeticheski Reaktor (VVER, meaning water cooled, water moderated energetic reactor) originated in the Soviet Union and is prevalent in modern day Russia, eastern Europe, other historic regions of Soviet influence and more recently has been exported from Russia particularly in Asia. The reactor type is essentially a PWR, although chemistry is different, in that the coolant pH is stabilised using potassium hydroxide rather than lithium hydroxide. Boric acid is also added to the coolant and its concentration is greatest at the start of each fuel cycle (exactly the same as in a PWR) and is decreased through the fuel cycle to control fuel reactivity. There has to be a balance between the potassium concentration and the boric acid concentration, in order to arrive at a high-temperature pH within acceptable constraints. Nonetheless, the choice of using potassium has its benefits in providing a stable pH which is only marginally affected by boron radiochemistry through each fuel cycle, as in the following reaction.



Equation 2: Neutron capture by boron

A discussion of whether to use lithium or potassium for pH regulation is provided in [269], focusing on global supply issues which surround the availability of startup chemistry and isotopically enriched chemicals such as ^{10}B . The choice of whether to use lithium or potassium for pH control also has potentially wider implications for some Generation-4 designs of reactor, which may be proposed for regulatory approval.

The general design of VVER reactors follows the evolution through a Generation 1 (VVER440) to Generation 2+ plant (VVER1000), with differences particularly in safety considerations. The reactor pressure vessels are, like PWRs, generally a ferritic steel body internally clad with austenitic stainless steel [270]. The RPV body is typically a low alloy steel, with some variation on grade of steel from site to site, and the cladding consists of two layers, the inner layer being an unstabilised austenitic stainless steel, and the outer (wetted) layer being a niobium-stabilised stainless steel roughly equivalent to AISI 347. The early VVER440 reactors had a small RPV and a resulting small water gap between the fuel and the RPV wall; the consequential neutron bombardment of the vessel has been intense and may lead to brittleness. A significant surveillance programme has been initiated in east European reactors now subject to Western safety standards. There are also differences between VVER440 plants based on safety systems, design basis and design lifetime, the 440/213 series having a 30 year design life and the 440/230 series a 50 year design life. A number of Russian and East European plants of both designs are already shut down, but there are also economic drivers to extend the lives of reactors of both types.

Some of the key aspects of VVER reactors are summarised in Table 11, and compared with a broadly similar PWR plant. Note, some data is from 2011 [271].

Table 11: A comparison of key parameters for VVER-440, VVER-1000 and typical PWR (from [270] and [271])

	VVER-440 (Paks 4)	VVER-1000 (Novovoronezh-5)	PWR (Sizewell B)
Number of Steam generator loops	6	4	4
Peak Fuel Burnup	37 GWd/teU	26 - 40 GWd/teU	33 GWd/teU
Fuel Assembly Profile	Hexagonal	-	Square (17 x 17)
Coolant Pressure	12.3 MPa	15.7 MPa	15.5 MPa
T _{in}	266 °C	289 °C	292 °C
T _{out}	297 °C	324 °C	323 °C

One particular feature of VVERs is that the SGs are configured horizontally, not vertically as in PWRs as shown in Figure 49 (featuring nuclear reactor (NR) coolant pumps 1 to 4 and SGs 1 to 4 and pressuriser P). VVER-440 plants have six loops, whereas VVER-1000 plants have four loops, as shown. This SG arrangement brings several advantages, including reduced vibrations and absence of sludge at the tube sheet. The materials of construction of the SGs are typically austenitic stainless steels, rather than the nickel alloys used in PWRs; details are provided in Table 12.

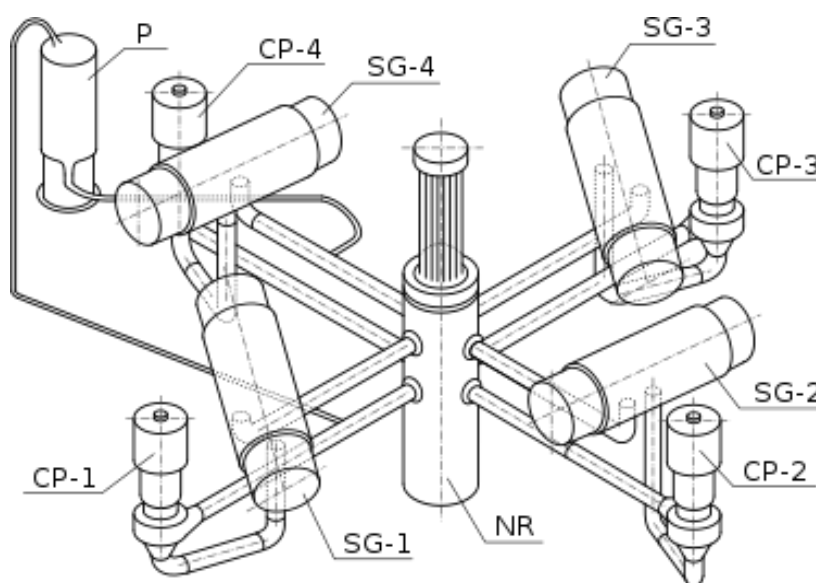
**Figure 49: Layout of VVER-1000 reactor cooling loops (From [272])**

Table 12: A comparison of SG materials in VVER-440, VVER-1000 and typical PWR (from [270])

	VVER-440	VVER-1000	PWR
Heat exchange tubes	08H18N10T	08H18N10T	Alloy 600, 690 or 800
Tube sheet, collector	08H18N10T	10GN2MFA, 08H18N10T cladding	and Low alloy steel and cladding
SG vessel	22K	10GN2MFA	Low alloy steel
Tube grid	08H18N10T	08H18N10T	Carbon or stainless steel

*Note: these VVER materials grades are Soviet – era Russian specifications.

13.2.2. Fuel Deposits in VVER reactors

At the outset, it must be stated that very few direct references to fuel deposits on VVER fuel exist in the open literature. This is understood to include reasons of public perception under the former Soviet regime, when many early VVERs were constructed. Consequently, the extent of fuel deposits must largely be inferred from radioactivity elsewhere in the primary circuit which owes its existence to activated fuel deposits which have been partially re-suspended or dissolved and redistributed.

The primary coolant chemistry experience of VVER reactors has been reviewed by Kysela [273] who (in 1992) pointed out that VVER 440 power stations tend to be high load factor stations (>75%). That paper reviewed personnel dose exposures at several East European reactor stations (implicitly, the amount of activated fuel deposit that had been re-distributed around the primary circuit). The VVER standard chemistry uses ammonia to provide H₂ in solution, through the radiolytic degradation of NH₃, this is sometimes augmented by addition of hydrazine (N₂H₄) and Kysela describes the hydrazine addition rationale and pattern. Overall pH control is established by addition of KOH with a target pH₃₀₀ of 7.2. There is significant scatter in radiation dose rate out of core, however there is also recognised some significant differences of cobalt content of structural materials used in different countries. In a related paper by Burclova [274] it is implicit that some fuel failures must have occurred for ¹³¹I to be measurable in Bohunice and Loviisa plants, although no remarkable surface activity of fission products was measured. The variations in plant-to-plant chemistry for Paks, Bohunice and Kola power stations indicated significant variations in Fe in coolant water, with Kola having the highest loadings. However, as Kysela also noted, there are also variations in sampling methods between stations; we imply significant error bars in the absolute measurement of corrosion product concentrations.

An early (1992) study by Zmitko [275] showed how corrosion product particles sampled from the coolant flow of two VVER power stations (Dukovany, Rheinsburg) indicated mobile particles derived from fuel deposits where the chemistry was predominantly magnetite with some nickel ferrite. Examination of oxidised out of core stainless steel surfaces revealed that chromium remained in the surface oxide, by composition up to 28% Cr in the adherent surface oxide, which is well above the Cr percentage in the parent metal; in contrast the mobile corrosion product is depleted in Cr.

A further review was provided by Zmitko, Kysela et al in 1996 [276]. They point out that in VVER all non-fuel surfaces are made of or sheathed with stainless steel 08H18N10T (austenitic, titanium stabilised, similar to AISI 321), whereas the fuel is clad with a Zr-1% Nb alloy, and with Zr or stainless steel spacer grids. Stellites are absent. Harmonisation of VVER 440 reactor chemistry was being introduced since the "Standard Water Chemistry" (ammonia pH control) was being replaced by the "Modified Water Chemistry" whereby a constant pH_T (7.1 to 7.3) and stable conditions are prioritised. Nonetheless, the concept of using hydrogen-injection chemistry was also being investigated. There remain differences, plant to plant, on maximum permissible potassium concentrations. Out of pile dose rates, and activity in particulate corrosion products (indicating spalled fuel deposits) are dominated by ^{58}Co , which derives from nickel in the stainless steel. Data from Dukovany confirmed that the Cr content of surface oxides in the hot and cold SG collectors was in the range 17 to 34%, compared with 17 to 19% in the equivalent parent material (AISI 321).

In 2000 Smiesko et al [277] examined data from three Czech and Slovak VVER stations, again with the primary focus of considering out of core dose rates, but which are unavoidably linked to detached or dissolved fuel crud. They report some correlation (shown in Figure 50) between radio-iodine (which can only arise from fuel failures) and SG dose rates at two different power stations – Bohunice (EBO) and Dukovany (EDU). Note there were four reactors at each plant, although some are now shut down.

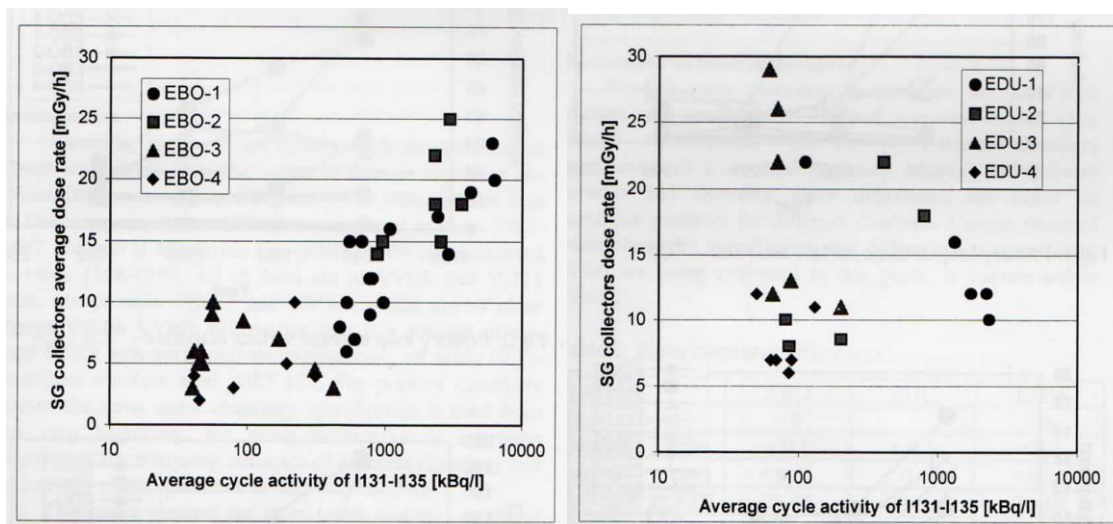


Figure 50: Fuel integrity and SG dose rate correlation for two VVER-400 reactors (From [277])

For the Bohunice plant there appears some correlation between SG dose rate (derived from re-attached crud or deposit) and the extent of fuel failures as inferred from radio-iodine. Whilst fuel failures may occur for a number of reasons, one possible explanation for this correlation is that fuel crud has built up, then partially detached or dissolved and spread through the primary circuit, whilst the fuel then suffers overheating and failure. The lack of such correlation at Dukovany (EDU) is heavily swayed by data from EDU-3 reactor, which Smiesko et al note has a generally much better fuel integrity record and has significant scatter due to having mixed (country of origin) SGs installed.

An update review of VVER coolant chemistry and corrosion product has been provided by Kysela et al in 2011 [278]. They conclude that crud in VVER reactors originates from a completely different source to that in PWRs and instances of worst crud deposits are principally due to organic substance contamination due to clean-up at outages and specifically SG decontamination. Whilst the exact deposition mechanism is not understood, it is influenced by organic substances. Loop tests simulating a clean VVER primary circuit developed crud featuring steam chimneys etc, much like PWRs. Tests involving a deliberately organic-contaminated loop were still to yield results. Plant observations indicate that fuel deposits (at that time) were limited to VVER400 plants, and that the following conclusions could be drawn.

- The formation of deposits was accompanied by a loss of pressure drop across the active zone of the fuel.
- The formation of deposits was not correlated with system pH in the plant, there appeared to be no mechanistic reason (and thus no model) to account for the incidence of fuel deposits.
- Crud deposits appear to affect both fuel pins and grid supports in the fuel assembly, sometimes growing out from the grids in a direction directly into the oncoming water flow. The deposits are frequently crystalline, suggesting that the deposition mechanism might include crystallisation as a process.
- Fuel failures as a result of crud deposition have been observed, but one plant (Paks) has not suffered fuel failure despite having fuel deposits. The exact morphology of the deposits appears to be unique to each station and reflects the chemistry history of that station, an apparent memory effect.
- Pressure loss indications are the only warning available that deposition is occurring. There is no correlation with feedwater iron concentration. Once a pressure loss measurement has been observed, it is not possible to reverse it; such observations only occur once deposition has exceeded a certain threshold value.

Kysela et al [278] further report that plant experience has shown that SG decontamination using organic reagents such as oxalic and citric acids, has a significant effect on corrosion when the plant is subsequently operated, to the extent of clogging of fuel assemblies and forcing plant shut-down. Examination of the deposits has revealed that from un-decontaminated plant the oxide is a relatively thin (1-2 μm) compact protective inner layer of mixed spinel oxides and an outer layer of loose crud composed mainly of magnetite and/or hematite. However, plants which have been decontaminated showed considerably thicker non-protective deposits of crud, which was found to have increased mobility around the primary circuit. Furthermore, at various locations high concentrations of elementary carbon were found, with no satisfactory explanation for its presence. The possible sources of carbonaceous material have been considered: besides the decontamination reagents there are also ion exchange resin beads which may have infiltrated the coolant circuit, lodged in the grids, and remained there until destroyed by thermal or radiolytic degradation. Other possible sources of organic contaminant include graphite and glycerine and other materials.

Katona [270] states that the principal failure mode for VVER-400 reactors is SG tube cracking from the outer wall (secondary circuit side) where the grid structure supporting the tube bundle gathers deposit rich in corrosive species. Moreover, on VVER-440 plant, the SGs are not practically replaceable, and have to be decontaminated instead. Another mitigation has been to replace the secondary circuit condenser using stainless steel, rather than brass condenser tubes, and so allowing the secondary circuit to operate at a higher and more protective pH.

A study at Paks reactor concerning corrosion particles circulating in the coolant flow was reported in 2010 [279]. It was established that corrosion particles in circulation were of significantly

different specific activity from those attached to SG tube walls, and that following startup particle residence in the core was typically in the range 14 to 34 days. Whereas after a shutdown the residence time was much reduced to between 1 and 28 days. Clearly, at shut down there would be a crud burst and this influences the retention timescale of particles in the core.

In 2010 Kritsky and Berezina presented [280] their work on corrosion of zirconium fuel cladding on VVER fuel subjected to very high burn up (up to 80 GWd/teU, over 6 cycles). At the very least this informs that VVER fuel in Russia is likely to be pushed to very high burnup levels and that the underlying zirconium corrosion consequences have been analysed and deemed acceptable. The greatest thickness of oxide corrosion product is expected on the spacer grids (up to 200 microns). A formula to predict corrosion depth has been developed which considers most of the physical parameters. It is proposed that the methodology, which includes calculation of the activation energy of the oxidation process, could be applied to the corrosion of any type of LWR fuel.

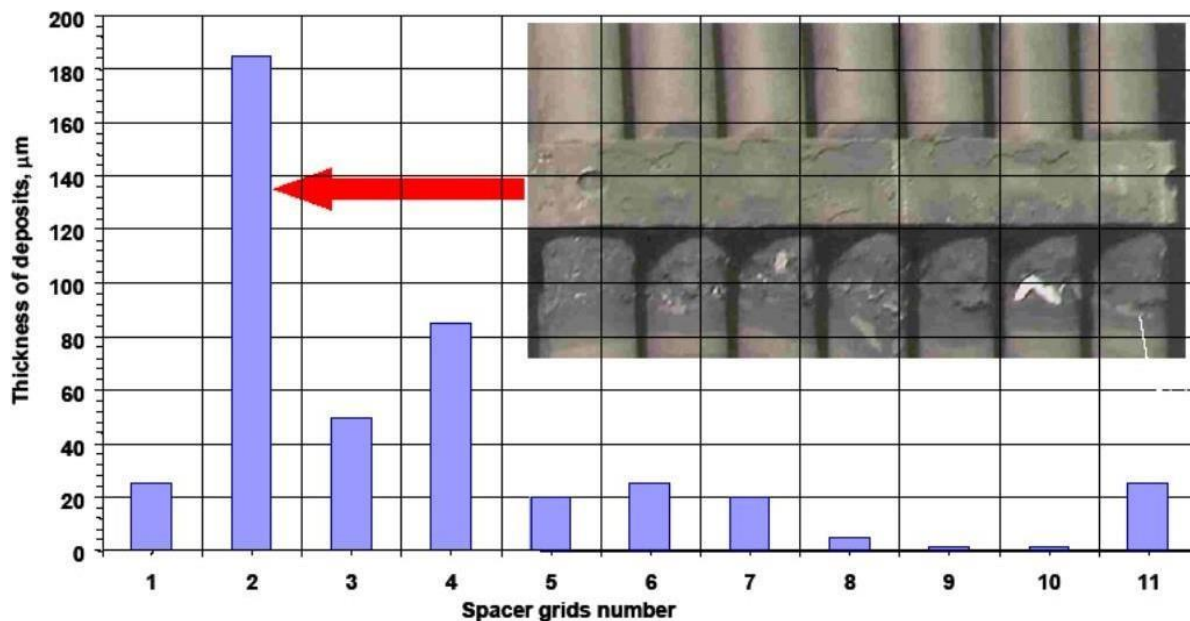


Figure 51: The amount of deposit and acceleration of cladding corrosion along fuel rod N7 under spacer grids plates of fuel assembly after 4 years operation (From [281])

In a study concerning VVER-440 reactor coolant flow and the influence of pressure drop (caused by the growth of deposits on fuel, amongst other things) Kritsky et al [281] develop a method for predicting pressure drop based on corrosion product mass transfer. The approach is based on plant observations, see Figure 51 for a visual illustration of corrosion product deposition on VVER-440 fuel pins just below the second spacer grid. The reactor which this fuel is from is not identified. The observation is also made that these deposits assist in bringing about nucleate boiling and thus accelerated deposit formation. The numerical methodology may find application in a model of VVER activity transport.

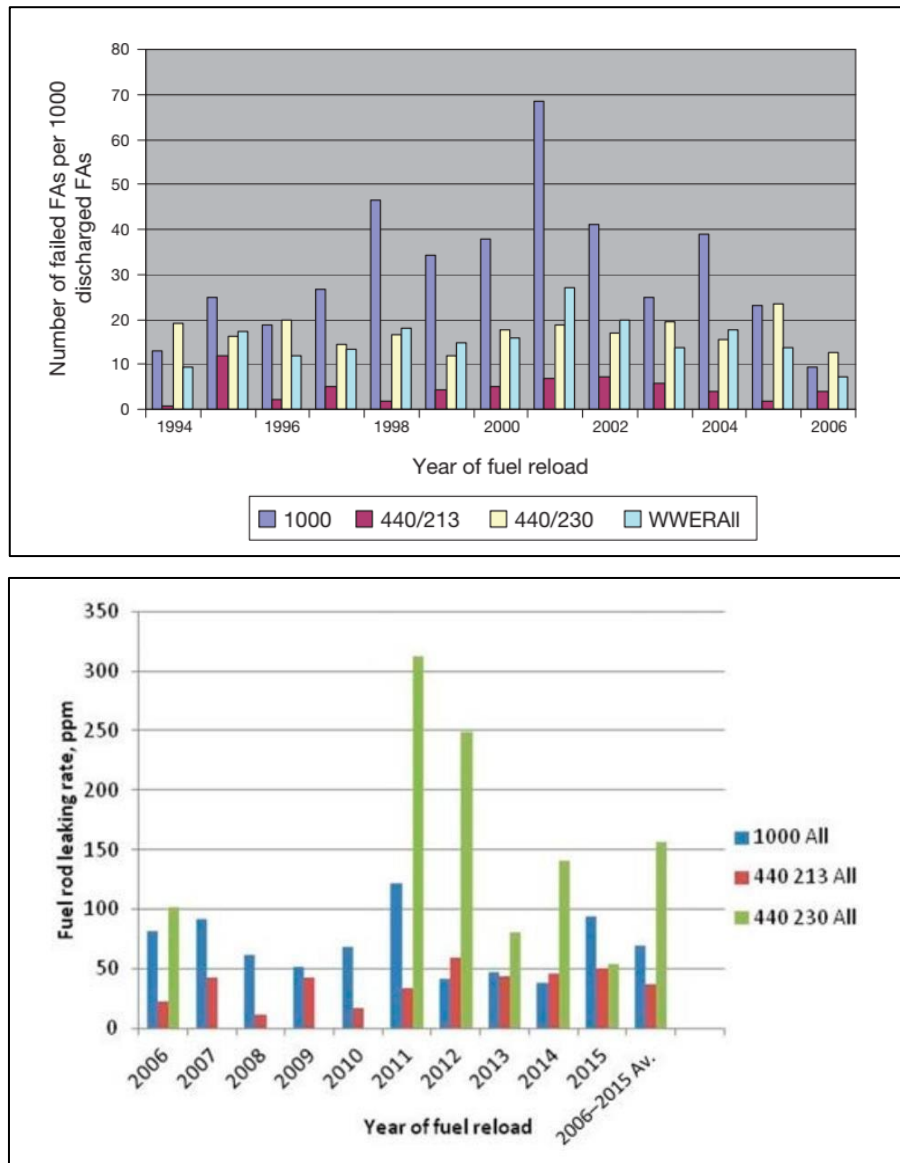


Figure 52: Number of leaking VVER fuel bundles per 1000 discharged bundles and leaking rods per million rods. (From [237] and [238])

As a matter of record, in 2015 the Loviisa VVER-440 plant reported [282] “abnormal primary coolant solids”, which were investigated during a subsequent outage and found to be based on particles derived from grinding wear on a primary coolant pump, which released some 3.5 kg of solids into the primary coolant. Incidentally some fuel crud was disturbed by this solid material and coolant samples recorded elevated levels of Zr-95 and Nb-95, in both solids retained on the sample membrane filter and in the liquid coolant sample. The point is simply that fuel clad deposits may be disturbed by extraneous solids which appear in the coolant.

A summary review of all VVER fuel failures and their causes has been prepared by the IAEA in 2010 [237] with an update in 2019 [238]. Their data is presented graphically in Figure 52. The data is subdivided into VVER-1000 fuel and VVER-440/230 fuel and VVER-440/213 fuel. The WWER-All information is then number-averaged to account for the actual numbers of power stations of these respective types. In [238] it is stated that the major cause of VVER fuel failure is fretting wear damage.

13.2.3. Summary of Considerations on VVER Designs

In the main, VVER reactors do not generate large amounts of fuel deposits, nevertheless there are some deposits and these behave in a similar manner to PWR deposits. VVER fuel is liable to fail, occasionally. The most frequent cause of fuel failure is fretting wear damage. The most vulnerable part of a VVER-440 reactor as a whole is the SG (which is not replaceable) and the secondary circuit is a priority for corrosion inhibition chemistry and occasional chemical cleaning of the metal surfaces on both sides of the SG tubes. The organic reagents used in the primary circuit may then remain as trace contaminants in primary chemistry. Modelling of fuel deposit formation has been developed, in parallel with PWR models but no comprehensive systematic model appears to be available. Models address different aspects of the matter independently. There appears to be a push towards very high burnup fuel usage for VVER-440s, with burnup in the range 80 to 100 GWd/teU after 5 or 6 irradiation cycles; this requires highly reliable fuel in order to avoid widespread fuel failures (extrapolating the extent of fretting wear to extended timescales).

13.3. Crud in Pressurised Heavy Water Reactors

The Pressurised Heavy Water Reactor (PHWR) category is dominated by the Canadian-designed CANDU reactors and the Indian-design IPHWR fleet. By design, the coolant and moderator are physically separated, and do not mix. Both coolant and moderator are heavy water. There is no boron added for reactivity control, and pH control is achieved using lithium hydroxide. Hydrogen may be added to suppress the radiolytic production of oxygen or oxidising species. Generically, the fuel cladding is a Zirconium -based alloy, the SG tubes are of an Inconel alloy and the remainder of the primary circuit (pipework etc) is carbon steel. This is in marked contrast to PWRs where the primary circuit pipework is stainless steel.

13.3.1. Operating PHWR Reactors

The world's CANDU reactors are chiefly located in Canada; there are multiple units at each site in Pickering, Bruce, Darlington, Point Lepreau, a shut-down generating station at Gentilly, and early (prototype) reactors at Chalk River and Whiteshell. There are also exported CANDU units operating in Argentina (Atucha and Embalse) and Romania (Cernavoda) and China (Qinshan phase 3) and South Korea (Wolsung-1) and one now decommissioned unit in Pakistan (Kanupp K1 – permanently shut down in 2021). Additionally, there are numerous PHWRs operating in India using the IPHWR-220 and -700 designs. There are 12 IPHWR-200 reactors (not including two units at Kalpakkam, which are barely changed from their original CANDU configuration). In addition the IPHWR-700 fleet includes one in operation, five under construction, and ten more which are planned.

A worldwide summary of fuel clad deposition and failure, across all water chemistries, was provided in an IAEA conference held in Ukraine, 2010 [283]. This reference contains several presentations covering a number of national perspectives across various reactor types, but which is particularly helpful for PWRs.

In [283] a team from Cernavoda presented their expectations that CANDU stations would be expected to increase water temperature, fuel residence time (burnup) and heat flux. Using a bypass (test autoclave) loop of the Cernavoda plant (and other ex-reactor test facilities) they report that PHWR fuel crud is porous, enabling lithium hideout, and consists of two layers, an outer "loose crud" and an inner "adherent crud". The reactor inlet temperature T_{in} was 260 °C

and outlet temperature, T_{out} was 310 °C. Under these conditions and with normal water chemistry fuel surface deposits (on surrogate coupons) was greater under inlet chemistry conditions, possibly because the coolant was saturated in Fe from the circuit pipework. The outlet conditions produced less deposition. The deposits were primarily magnetite, observed after an exposure of 828 days. The corrosion rate of the Zircaloy-4 substrate was in the range 0.276–0.313 $\mu\text{m}/\text{dm}^2\cdot\text{day}$. Note that at Cernavoda the SG tubes are made of Inconel-800 (for composition see Table 13, data taken from [284]). Whilst this is not a majority-nickel alloy, there is a still significant nickel component and therefore some nickel component in the fuel crud would be expected. Parallel experiments in a TRIGA (academic) reactor used a dedicated loop / autoclave with abnormal water chemistry, at pH \sim 10.5 (using Li^+) and / or O_2 at >200 ppb, and these showed abundant corrosion and deposits on simulant fuel surfaces. The deposits contained a range of elements and were 60 to 110 microns thick. Those authors suggest that the thermal insulation properties of adherent crud cause an enhancement of 1 °C per micron of deposit thickness, for a heat flux of around 1 MW/m^2 . Consequently, the additional 60 to 110 °C served to enhance waterside corrosion of the fuel cladding. The resulting nodular corrosion on the fuel simulant surface (after removal of the adherent deposit) is shown in Figure 53. The nodules consisted of white ZrO_2 circles with diameter up to 4 mm.

Table 13: Composition of Inconel 800 series Alloys (from [284])

Incoloy alloys	800	800H	800HT
UNS designation	NO8800	NO8810	NO8811
Nickel	30.0 – 30.5	30.0 – 30.5	30.0 – 30.5
Chromium	19.0 – 23.0	19.0 – 23.0	19.0 – 23.0
Iron	39.5 min	39.5 min	39.5 min
Carbon	0.10 max	0.05 – 0.10	0.06 – 0.10
Aluminium	0.15 – 0.60	0.15 – 0.60	0.25 – 0.60
Titanium	0.15 – 0.60	0.15 – 0.60	0.25 – 0.60
Al + Ti	0.30 – 1.20	0.30 – 1.20	0.85 – 1.20



Figure 53: Nodular corrosion (after crud removal) on CANDU fuel rod Zircaloy-4 cladding tested 90 days in TRIGA reactor using irradiation capsule. (From [283])

The authors of [283] also claimed (referring to an internal Romanian document) – but also echoed in [278] that the quantity of adherent corrosion products on a Zircaloy-4 surface was dependent on the thickness and physico-chemical characteristics of the initial ZrO_2 surface film. Consequently, for oxidation at 310 °C only small amounts of surface deposits were observed (1 to 1.5 microns thick). However, on surfaces oxidised in steam at 400 °C much thicker and more porous corrosion products were formed, being 8 to 12 microns thick. These were adherent to the surface, and subsequent examination by microscopy and gravimetric analysis indicated that the adherence of corrosion deposits increased with the thickness and particularly with the porosity of zirconium oxides. It was found that a significant proportion of the corrosion deposits are incorporated in pores and lateral cracks of the surface oxides. Should it prove to be the case that operationally, water temperatures and fuel burnups are increased (as of 2010 levels), this may raise further concerns regarding fuel deposits and Zircaloy-4 corrosion.

Also in [283] a team from Kalpakkam power station (India) reported that for Indian PHWRs the chemistry control bands are normally in the following ranges: pH >10.2 to <10.5, dissolved oxygen <10 ppb, dissolved hydrogen >2 to < 10 ml/kg. This pH range is high in comparison to PWRs where the system pH is maintained at close to $pH_{25} = 7.4$ due to the corrosion susceptibility of Zircaloy at high pH; it may be that these authors are referring to pH_T at some other temperature. The circuit materials are Zircaloy, carbon steel, and Inconel / Monel (note; no stainless steel). As carbon steel is the majority structural material, magnetite dominates the corrosion product composition. There is a key necessity to control pH to optimise carbon steel corrosion (and hence the need for a high pH), recognising the possible role of Flow Assisted Corrosion (FAC). However, the pH limit for zirconium alloy safe operation should also constrain the upper limit of this range. The stoichiometry of corrosion product formation in D_2O (heavy water coolant / moderator) results unavoidably in the formation of some molecular D_2 as a by-product of corrosion.

Some points of particular interest from the Indian experience are that the incidence of FAC at bends, particularly in feeder bends and elbows, is governed by a known pH dependence of FAC which shows a minimum in the temperature range 150 to 190 °C. Clear evidence is not available at around 310 °C, nevertheless this pH dependence is inferred at higher temperature and prevents dosing the plant chemistry to high pH, which would provide for a cleaner core with less magnetite. Also, that plants report fuel surface deposits containing some antimony (^{122}Sb and ^{124}Sb) which is thought to originate with primary coolant pump seals and bearings. The chemical speciation of the antimony is not known.

The rate of oxidation of the carbon steel surfaces in PHWR feeders and headers has been investigated [285] with reference to the hot pre-treatment of the steels and their carbon content. It was found that the rate of magnetite formation (and thus release of magnetite to the primary coolant circuit) varied somewhat, with high carbon content steels initially oxidising more rapidly than the low carbon variety, under PHWR HFT conditions. After a period of 72 hours the differences narrowed down to give similar corrosion rates.

The failure rates of PHWR fuel have been summarised by the IAEA [237] and [238] and the trends from 1994 to 2006 then 2006 to 2015 are presented graphically in Figure 54. Note that the basis of accountancy changes from leaking bundles per 1000 bundles to leaking rods per 1,000,000 rods.

It is obvious that Indian PHWR designs are much more liable to experience leaking fuel than Canadian design CANDU reactors. Reasons for this are not explicitly stated, although in overall terms the causes of PHWR fuel failure have been attributed to the following reasons:

- Debris damage (particularly in early cores, Indian reactors)
- Fabrication flaws (e.g. end cap welding and hydriding near the end caps)
- Power ramps
- Unknown

There is clearly (for CANDU reactors) an improving trend year on year, as seen in Figure 54. There is no attributable linkage between fuel failure and corrosion deposits, in the view of IAEA, unless that comes under the "unknown" category. That 2006 IAEA report commented that there have been no corrosion-related fuel failures in VVERs or CANDUs, only in infrequent abnormal operations.

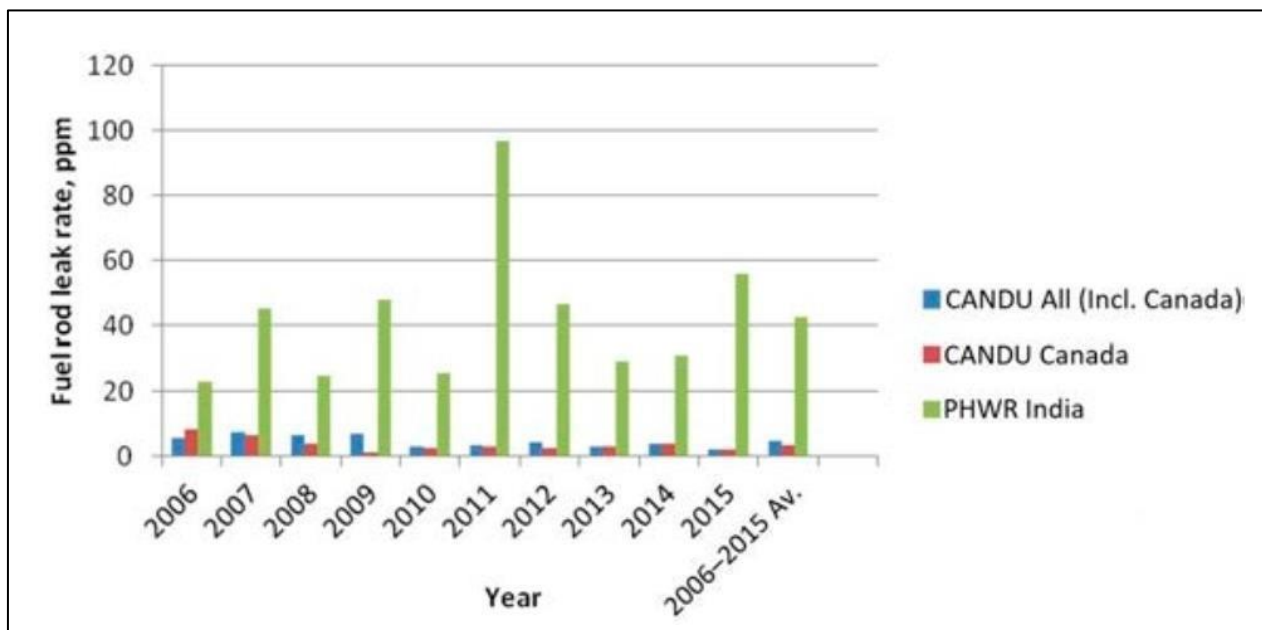
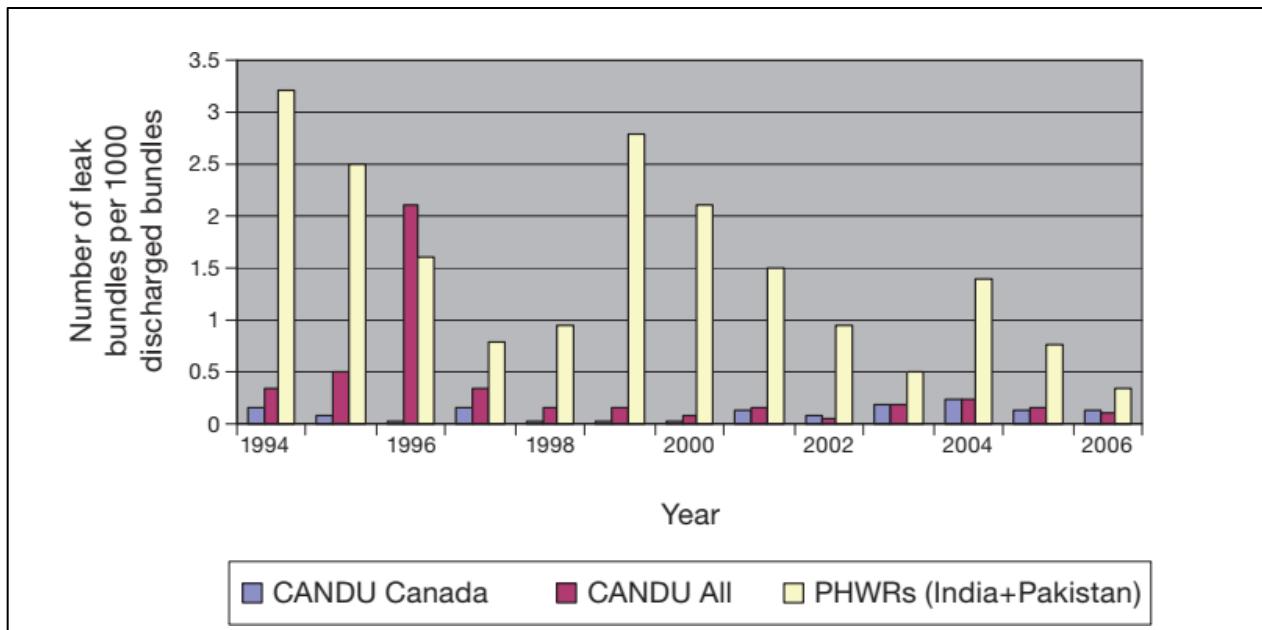


Figure 54: Number of leaking PHWR fuel bundles per 1000 discharged bundles. (From [237] and [238])

13.3.2. Crud and Spent CANDU Fuel

All Canadian CANDU fuel is cooled (short term) in the station cooling ponds and then transferred to a dry storage environment for interim storage until such time as a geological disposal facility becomes available. The interim storage arrangements vary, station to station, and some are more problematic than others in terms of retrievability, but none are designed with any regard for crud adhering to the fuel.

13.3.3. Summary of Considerations on PHWR Fuel Deposits

There are a significant number of PHWR power stations around the world, and they commonly have some carbon steel components such as feedwater headers exposed to the primary coolant and these surfaces are the primary source of magnetite which deposits on fuel surfaces. The resulting fuel crud is magnetite -based and overlies zirconium oxide arising from the zirconium alloy fuel rod cladding. Nodular morphology has been observed but may not be exclusive. The interface between the magnetite deposit and the underlying zirconium oxide may include magnetite depositing in the pores and cracks of the zirconium oxide surface, so the magnetite may be highly adherent, although there is also an outer loose layer of deposit. In order to mitigate carbon steel corrosion the coolant is conditioned to a high pH (>10.2 to <10.5). This is relatively high, in comparison to PWR coolant, and the high pH corrosion of zirconium alloys must be taken into consideration. Fuel failures are known to have occurred and may be connected to hot spots under oxide deposits, although debris damage is a more prevalent cause of fuel failure.

Based on all the above information, it can be seen that PHWR fuel may be subject to fuel deposits in much the same way as PWR fuel and consist of magnetite deposited on an underlying zirconium oxide. Nodular corrosion has been observed, as well as deposits rooted into pores in the underlying oxides.

13.4. Crud in Supercritical Water Reactors

Supercritical water reactors (SCWRs) are a Generation 4 concept for new nuclear power plant designs. Whilst there are no operating SCWRs the theory behind them has been developing over several decades and designs have been produced in the past decade or so. There are currently recognised to be five designs of SCWR, proposed by Japan, China, Russia, Canada and the European Union. The Japanese and European designs both feature a pressure vessel system enclosing the hot (light-water) coolant, with a heavy-water moderator fluid at lower temperature and pressure also flowing through the pressure vessel. A survey of current SCWR concepts is presented in [286].

13.4.1. The Canadian Design of SCWR

As one of the more completely documented SCWR types the Canadian design is now considered as an exemplar of the type of design and technology to be expected.

The Canadian design leans on the CANDU reactor design and features an arrangement with pressure tubes, again using light water for the fuel coolant (and heavy water for the moderator) [287]. The concept design and flow routes for the Canadian design are shown in Figure 55. Using the Canadian design as a working example, the following details are known. In summary, in the Canadian design the light water flow over the fuel first travels downwards through the centre of the assembly, reaches the bottom of the assembly then returns up the annular outer path of the assembly. The fuel itself is annular, located between the downwards and upwards coolant flow paths. In the outlet plenum (red in Figure 55 (A)) the coolant temperature is intended to be 625 °C at 25 MPa, whilst the inlet is at 350 °C and 26 MPa. The inlet plenum is proposed to be made of forge SA508 steel, overlaid with austenitic stainless steel to reduce corrosion. The outlet plenum is proposed to be a creep-resistant Ni-based alloy. At some point along the length of the fuel pins the coolant undergoes transformation from liquid water to supercritical fluid; the solubility of corrosion products in supercritical fluid is poorly known and the possibility of corrosion product deposition should be considered.

Some caution is necessary concerning the austenitic overlay for the inlet plenum, since austenitic stainless steels, such as the 20/25/Nb stainless used for AGR fuel cladding are well known to undergo Radiation-Induced Sensitisation (RIS), with an optimum temperature of around 420 °C. RIS leads to chromium depletion from grain boundaries, with the resulting effect that the steel is no longer “stainless” and corrodes readily (as evidenced by AGR fuel in neutral-pH storage ponds) unless measures are taken to increase the pH and thereby passivate the fuel cladding. A pH in excess of 11 is used in AGR storage ponds and an equivalent pH_T will be needed for the inlet plenum. However direct radiolysis of high pH water is recognised to produce abnormally high radiolytic product yields of molecular hydrogen [288]; whilst the fate of the stoichiometric oxygen-containing products is less certain, the oxygen must go somewhere and in a metallic system the probable fate is as additional corrosion product.

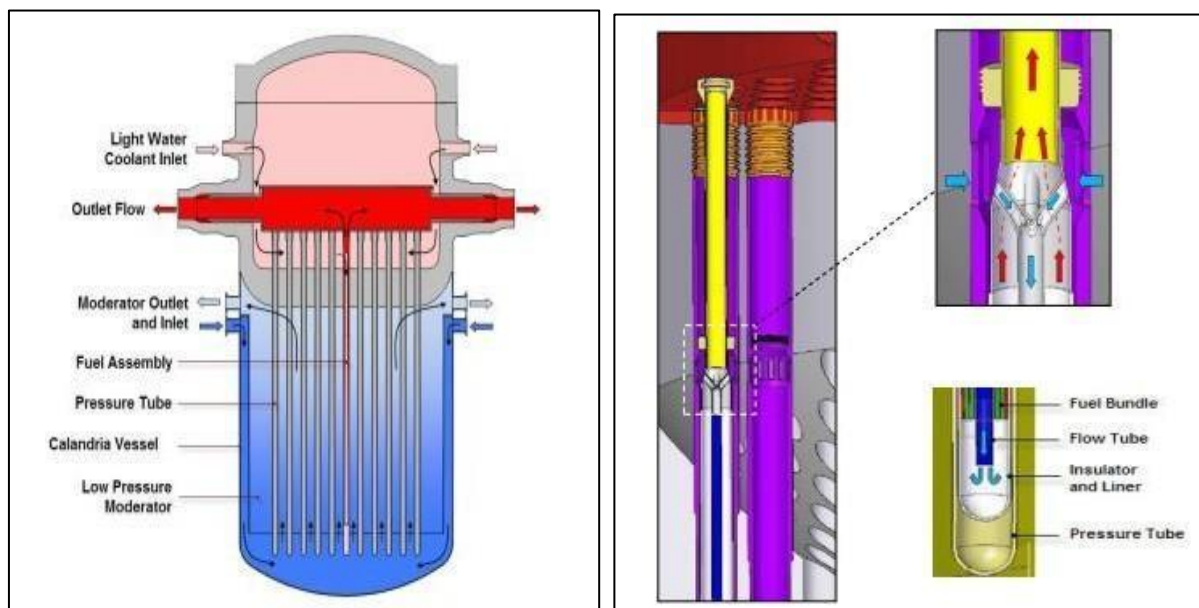


Figure 55: (A) Canadian SCWR core schematic and flow streams and (B) fuel channel schematic and flow streams (From [287])

The Canadian design intends to use for the pressure tube a zirconium-based alloy named Excel, developed in the 1970s, favoured due to its' low neutron cross-section [289]. However, a contemporary IAEA survey of SCWRs gave the opinion that zirconium-based alloys were unsuitable [290]. The fuel channel design has a diameter of 181 mm. The pressure tube is in direct contact with the heavy-water moderator (see Figure 56) and the pressure tube is internally coated with a stabilised yttria-zirconia ceramic insulator to facilitate the large temperature difference between the light water coolant and the pressure tube. The insulator is internally clad with a liner tube, to prevent any ceramic from detaching and entering the coolant flow. Between this liner and the inner tube (the inward coolant flow tube) are the fuel pins formed of multiple thin tubes containing UO₂; the hot coolant flows between these fuel pins within the annulus between the liner and the inner (cold coolant) tube. There is no detail on what material the fuel cladding will be, it is presumed to be a steel of some grade.

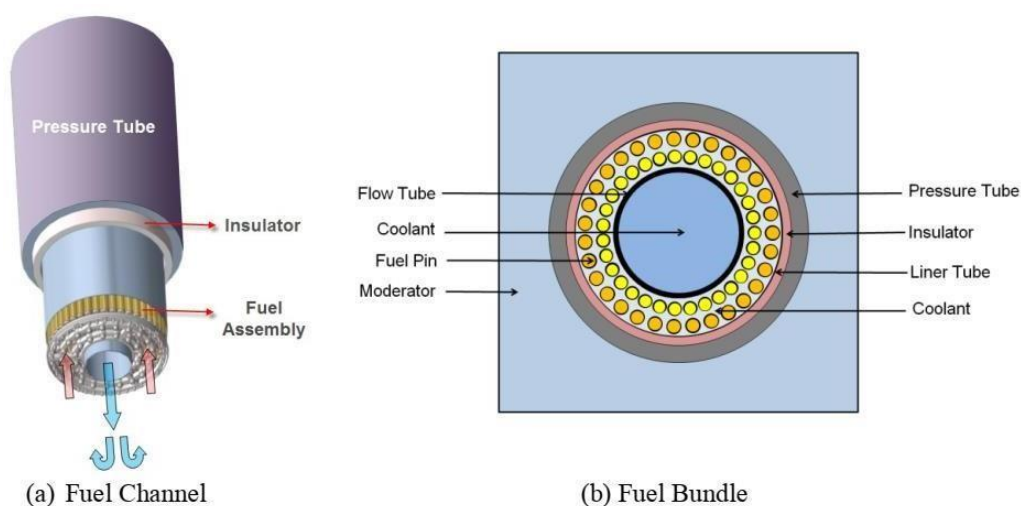


Figure 56: (A) Canadian SCWR fuel channel schematic and (B) fuel bundle schematic. (From [287])

13.4.2. Other designs of SCWR

The other designs of SCWR are only designs, on paper, there are no built working examples. Moreover, the materials specifications are often vague, even the generic type of metal is often not indicated. There is no design where the grade of each alloy is defined. The tendency of any plant to produce corrosion deposits on fuel pins will depend on the materials in the primary coolant system and their tendency to corrode. In this respect the Canadian design is the most advanced, at least stating the broad type of metal for certain plant locations, which is why it was selected for more detailed consideration, above.

In 2010 Yurmanov et al [251] reported on developments of SCWR technology in Russia, noting that the Belyarsk stations 1 and 2 had been operating with supercritical water for many years (as loops attached to VVER reactors). They provided a reasonably detailed description of crud / deposits arising in out of core locations, but did not provide detail for deposits on fuel surfaces.

The surface deposit loading was 2 mg/cm² in the water section, in the steam/water regime 0.6 mg/cm² and in the supercritical steam section 0.5 mg/cm². The feedwater pH was in the range 9.2 to 9.5, and they also reported that fuel rods clad in EI-847 steel and in iron-nickel alloy EP-753 had been successfully tested up to 17 GW·day/kg U.

A wider review of the materials which could be utilised in SCWR reactors and fuels is provided in [291]. They note that up until 2020 most research effort had been directed towards in-core materials, although out of core materials exposed to supercritical fluid will need thorough underpinning also. The combination of intense radiation and higher temperatures will combine in the consequences of radiation-driven phenomena such as defect migration in metals and void swelling from trapped hydrogen (thermalised protons). Some advanced materials are proposed, including steels which are alumina-stabilised or oxide-dispersion strengthened steels. However [291] notes two specific knowledge gaps.

- a) The data for the performance of these materials at SCWR conditions is scarce and that knowledge gap needs to be improved on.
- b) The radiation chemistry of the SCW regime is not adequately understood in terms of its corrosivity.

Other designs will be evolving even as this document is written and this present document is simply a snapshot in time.

13.4.3. Summary considerations on SCWR designs

There are a number of considerations that merit the attention of regulators were a SCWR to be proposed for generic design approval in the UK.

Since there is no SCWR plant in operation (other than the VVER loops at Beloyarsk) there are no data from plant observations. However, from the above discussion it should be recognised that there are specific points for regulator concern.

- The transition of coolant from liquid water to supercritical fluid at some point along the length of the fuel pins (corresponding to increase in temperature) may be accompanied by a change in corrosion product solubility and thus facilitate deposition on the fuel pin cladding. However, this is not borne out by the Beloyarsk information.
- The alloy specification for the SG tubing is not known; but since (in the Canadian design) the outlet plenum is a nickel-based alloy subject to 620 °C supercritical fluid, some nickel corrosion is inevitable and may (with any other nickel-bearing alloys such as stainless steels) contribute to deposits including nickel and iron oxides or mixed nickel / iron spinels. Various other alloys and materials are proposed including alumina-forming steels and oxide dispersion strengthened steels, and the Russian alloys EI-847 and EP-753 have already undergone some in-core testing.
- In PWR systems the coolant pH is equivalent to an ambient temperature pH of around 7.4. In a SCWR system the coolant pH may well be much higher, with attendant consequences of high radiolytic hydrogen and oxidant production.

SCWR fuel cladding material will need to be carefully selected in order to minimise the incidence of RIS or to be compatible with a very high coolant pH. Whilst specific details of materials are still in outline development, the general scheme design for the Canadian SCWRs is as some development of the PHWR reactor, having a calandria type core with fuel channels surrounded by a tank of heavy water moderator.

If the coolant system included a high-pH environment, the corrosion of the primary circuit materials by coolant would be expected to be minimised, although the very high temperature (often >600 °C at core outlet) could enhance corrosion rates. The presence of a nickel-based alloy in the outlet plenum would give rise to some nickel in the corrosion products, but in terms of relative surface area the fuel pin cladding and the SG tubing surfaces are expected to dominate.

14. References

- [1] J. Glover, M. Redmond and J. Culshaw, "Regulating Chemistry for New Nuclear Power Stations in Great Britain," in *20th Nuclear Power Chemistry International Conference*, Brighton, 2016.
- [2] Health and Safety Executive, "Safety Assessment Principles for Nuclear Facilities: 2014 Edition Revision 1 (January 2020)," Health and Safety Executive, Bootle, 2020.
- [3] ONR, "NS-TAST-GD-088 (Revision 3) "Chemistry of operating civil nuclear reactors",", Office for Nuclear Regulation, Bootle, 2019.
- [4] Office for Nuclear Regulation, "Chemistry Assessment NS-TAST-GD-089 Issue 1.1," Office for Nuclear Regulation, Bootle, 2022.
- [5] ONR, "NS-TAST-GD-075 (Issue 3.1) "Safety of Nuclear Fuel in Power Reactors",", Office for Nuclear Regulation, Bootle, 2022.
- [6] Office for Nuclear Regulation, "Safety Aspects Specific to Storage of Spent Nuclear Fuel: NS-TAST-GD-081 (Issue 4.1)," ONR, Bootle, 2022.
- [7] IAEA, "IAEA Safety Standards: Design of the Reactor Core for Nuclear Power Plants: Safety Guide NS-G-1.12," IAEA, Vienna, 2005.
- [8] IAEA, "IAEA Safety Standards Series: Design of the Reactor Core for Nuclear Power Plants: Specific Safet Guide SSG-52," IAEA, Vienna, 2019.
- [9] C. A. English, J. M. Hyde and R. J. Taylor, "Sustaining Expertise in Specific Aspects of Nuclear Technology," in *16th Environmental Degradation of Materials in Nuclear Power Systems - Water Reactors*, Asheville, North Carolina, USA, 2013.
- [10] W. S. Walters, J. D. Page, A. P. Gaffka, A. F. Kingsbury, J. Foster, A. Anderson, D. Wickenden, J. Henshaw, M. Zmitko, V. Masaric and V. Svarc, "The effect of zinc addition on PWR corrosion product deposition on Zircaloy-4," in *Chimie 2002*, Avignon, 2002.
- [11] R. Reiss, "Chemistry Experience in the Primary Heat Transport Circuits of Kraftwerk Union Pressurized Water Reactors," *Nuclear Technology*, vol. 29, no. 2; DOI: <https://doi.org/10.13182/NT76-A31574>, pp. 153-159, 1976.
- [12] R. F. Hazelton, "Characteristics of Fuel Crud and its Impact on Storage, Handling, and Shipment of Spent Fuel," Pacific Northwest Laboratory Report , PNL-6273; DOI: <https://doi.org/10.2172/6164184>, 1987.
- [13] J. W. Roe, "Effects of Crud Buildup and Boron Deposition on Power Distribution and Shutdown Margin," US NRC, Information Notice No. 97-85. <https://www.nrc.gov/docs/ML0310/ML031050032.pdf>, 1997.
- [14] P. L. Frattini, "Axial Offset Anomaly: Coupling PWR Primary Chemistry with Core Design," in *International Conference on Water Chemistry of Nuclear Reactor Systems*, Bournemouth, 2000.
- [15] K. G. Turnage, "Interactions of Fuel and Water Chemistry," in *International Conference*

on Water Chemistry of Nuclear Reactor Systems, San Francisco, USA, 2004.

- [16] W. A. Byers, J. Deshon, G. P. Gary, J. F. Small and J. B. Mcinvale, "Crud Metamorphosis at the Callaway Plant," in *International Conference on Water Chemistry of Nuclear Reactor Systems*, Paper Number 7-3. Jeju, South Korea, 2006.
- [17] "PWR Axial Offset Anomaly (AOA) Guidelines, Revision 1," EPRI, Report: 000000000001008102, 2004.
- [18] EPRI, "Characterisation of Corrosion Products on the Callaway Cycle 9 PWR Core," EPRI, Report: 1003129, 2001., 2001.
- [19] A. Tigeras, J. L. Bretelle and E. Decossin, "EDF AOA Experience: Chemical and Thermal Hydraulic Analysis," in *International Conference on Water Chemistry of Nuclear Reactor Systems*, San Francisco, USA, 2004.
- [20] W. Y. Maeng, B. S. Choi and D. K. Min, "The Status of AOA in Korean PWR and a Study on the CRUD Deposition on Cladding Surface," in *International Conference on Water Chemistry of Nuclear Reactor Systems*, Berlin, Gemany, 2008.
- [21] W. A. Byers and J. Deshon, "Structure and Chemistry of PWR Crud," in *International Conference on Water Chemistry of Nuclear Reactor Systems*, San Francisco, USA, 2004.
- [22] EPRI, "Rootcause Investigation of Axial Power Offset Anomaly," EPRI, Report: TR-108320, 1997.
- [23] EPRI, "Primary Water Chemistry, Fuel Rod Corrosion, and Crud Deposition in PWRs: A Comparison of European and U.S. Plant Performance," EPRI, Report TR-107255, 1996.
- [24] EPRI, "Steam Generator Reference Book, Revision 1: Volume 1," EPRI, Report TR-103824-V1R1, 1994.
- [25] IAEA, "Review of Fuel Failures in Water Cooled Reactors (2006-2015): An Update of IAEA Nuclear Energy Series No. NF-T-2.1," IAEA, NF-T-2.5, 2019.
- [26] B. Cheng and R. L. Yang, "Fuel Failure Experiences in US Light Water Reactors," in *International Conference on Global Environment and Advanced Nuclear Power Plants*, Kyoto, 2003.
- [27] D. Perkins, K. Ahluwalia, J. Deshon and C. Haas, "An EPRI Perspective and Overview of PWR Zinc Injection," in *International Conference on Water Chemistry of Nuclear Reactor Systems*, Berlin, Germany, 2008.
- [28] EPRI, "The Effect of Dissolved Zinc on the Transport of Corrosion Products in PWRs," EPRI, Report: NP-6975, 1990.
- [29] EPRI, "Source Term Reduction: Impact of Plant Design and Chemistry on PWR Shutdown Releases and Dose Rates," EPRI, Report: 1013507, 2006.
- [30] H. W. Rich, M. Lips and G. Meier, "27 Cycles of Primary Water Chemistry at Gosgen Nuclear Power Plant," in *International Conference on Water Chemistry of Nuclear Reactor Systems*, Jeju, South Korea, 2006.

- [31] J. C. Bates, K. Garbett, K. Hinds, G. Lancaster, M. Mantell and G. Renn, "Development of Corrosion Product Behaviour and Radiation Fields at Sizewell B PWR from 1995 to 2008," in *International Conference on Water Chemistry of Nuclear Reactor Systems*, Berlin, Germany, 2008.
- [32] F. Dacquait, H. Marteau, L. Guinard, G. Ranchoux, M. Wintergerst, J. L. Bretelle and A. Rocher, "The Impact of Steam Generator Replacement on PWR Primary System Contamination," in *International Conference on Water Chemistry of Nuclear Reactor Systems*, Quebec, Canada, 2010.
- [33] P. V. Sivaprasad, J. Frodigh and U. Stenlund, "Evaluation of Nickel Release and Oxide Formation on Alloy 690 Steam Generator Tubes in Simulated Primary Water Conditions," in *International Conference on Water Chemistry in Nuclear Reactor Systems*, San Francisco, USA, 2018.
- [34] E. Laney, M. Scrancher, B. Welsh, B. Osborne, M. Mantell and K. Garbett, "A Review of the Shutdown and Start of Cycle Primary Water Chemistry and Elemental and Radionuclide Behaviour at Sizewell B," in *International Conference on Water Chemistry in Nuclear Reactor Systems*, San Francisco, USA, 2018.
- [35] B. Bengtsson, P.-O. Aronsson, S. Larsson and P.-O. Andersson, "Experiences with Elevated pH and Lithium in Ringhals PWRs," in *International Conference on Water Chemistry of Nuclear Reactor Systems*, Berlin, Germany, 2008.
- [36] F. Carrette, F. Cattant, L. Legras, F. Bardet, M. Merrer and L. Guinard, "Impact of the Surface State of Steam Generator Tubes on the Release of Corrosion Products in Pressurized Water Reactors," in *International Conference on Water Chemistry of Nuclear Reactor Systems*, Jeju, South Korea, 2006.
- [37] S. Taunier, M. Wintergerst, O. de Bouvier, C. Pokor, F. Carrette, A. Toivonen, G. Ranchoux and J. L. Bretelle, "Corrosion Products Behaviour and Source Term Reduction: Guidelines and Feedback for EDF PWRs, Concerning the B/Li Coordination and Steam Generators Replacement," in *International Conference on Water Chemistry of Nuclear Reactor Systems*, Quebec, Canada, 2010.
- [38] L. Guinard, F. Cattant, S. Taunier, J. L. Bretelle, A. Rocher and B. Jeannin, "General Overview of the Evolution of International Collective Radiation Exposure and Associated Good Practices," in *International Conference on Water Chemistry of Nuclear Reactor Systems*, Berlin, Germany, 2008.
- [39] F. Dacquait, L. Guinard, F. Bardet, J. L. Bretelle and A. Rocher, "Low Primary System Contamination Levels in Some French PWRs," in *International Conference on Water Chemistry of Nuclear Reactor Systems*, Jeju, South Korea, 2006.
- [40] F. Carrette, S. Leclercq and L. Legras, "Characterisation of Oxides Formed on the Internal Surface of Steam Generator Tubes in Alloy 690 Corroded in the Primary Environment of Pressurised Water Reactors," in *International Conference on Water Chemistry of Nuclear Reactor Systems*, Paris, France, 2012.
- [41] A. Mazenc, S. Leclercq, A. Seyeux, A. Galtayries and P. Marcus, "Influence of Steam Generator Surface State on Corrosion and Oxide Formation," in *International Conference on Water Chemistry of Nuclear Reactor Systems*, Paris, France, 2012.

- [42] M. Clauzel, M. Guillodo and M. Foucault, "Correlation Between Ni Base Alloys Surface Conditioning and Cation Release Mitigation in Primary Coolant," in *International Conference on Water Chemistry of Nuclear Reactor Systems*, Quebec, Canada, 2010.
- [43] D. M. Wells, C. Marks, J. Dingee, C. Gregorich, J. Riddle and M. Bachet, "New Zinc-Based Passivation Technology for Reducing Corrosion Product Release," in *International Conference on Water Chemistry in Nuclear Reactor Systems*, San Francisco, USA, 2018.
- [44] A. Uehira and M. Kanzaki, "SG Tubes with SM-ART Technology for Reducing Metal Release in PWR," in *ISOE North American ALARA Symposium*, Fort Lauderdale, USA, 2011.
- [45] EPRI, "The Role of Coolant Chemistry in PWR Radiation-Field Buildup," EPRI, Report: NP-4247, 1985.
- [46] M. C. Song and K. J. Lee, "A Study on the Generation of Radioactive Corrosion Product at PWR for Extended Fuel Cycle," in *Proceedings of the Symposium "Technologies for the Management of Radioactive Waste from Nuclear Power plants and back End Nuclear Fuel Cycle Activities"*, IAEA-SM-357/75, 1999.
- [47] K. Fruzzetti and D. Perkins, "PWR Chemistry: EPRI Perspective on Technical Issues and Industry Research," in *International Conference on Water Chemistry of Nuclear Reactor Systems*, Berlin, Germany, 2008.
- [48] I. D. Dobrevski and N. N. Zaharieva, "Pressurized Water Reactor Fuel Performance Connected with Fuel Cladding Corrosion Process," in *International Conference on WWER Fuel Performance, Modelling and Experimental Support*, Albena, Bulgaria, 2007.
- [49] J. McElrath and K. Fruzzetti, "EPRI PWR Primary Water Chemistry Guidelines Revision," in *International Conference on Water Chemistry of Nuclear Reactor Systems*, Sapporo, Japan, 2014.
- [50] B. Fellers, D. Perkins, J. Bosma and J. Deshon, "Elevated-Constant pH Control Assessment at TXU's Comanche Peak Steam Electric Station," in *International Conference on Water Chemistry of Nuclear Reactor Systems*, Avignon, France, 2002.
- [51] J. Gardner, "Diablo Canyon Initiatives in Primary Water Chemistry," in *International Conference on Water Chemistry of Nuclear Reactor Systems*, San Francisco, USA, 2004.
- [52] J. A. Wilson, D. Morey, R. P. Walton, W. E. Allmon and J. M. Riddle, "Application of Zinc Addition and Elevated, Constant pH Control to a 24-Month Fuel Cycle at Three Mile Island Unit 1," in *International Conference on Water Chemistry of Nuclear Reactor Systems*, Jeju, South Korea, 2006.
- [53] F. Nordmann, "PWR and BWR Chemistry Optimization," *Nuclear Engineering International*, vol. 56, no. 689, pp. 24-29, 2011.
- [54] A. Graff and M. Bachet, "Complexation of Nickel Ions by Boric Acid or (Poly)Borates," in *International Conference on Water Chemistry of Nuclear Reactor Systems*, Sapporo, Japan, 2014.
- [55] A. Ferrer, F. Dacquait, B. Gall, G. Ranchoux and G. Riot, "Modelling of Crud Growth

Phenomena on PWR Fuel Rods Under Nucleate Boiling Conditions," in *International Conference on Water Chemistry of Nuclear Reactor Systems*, Paris, France, 2012.

- [56] J. Chen, "On the Interaction between Fuel Crud and Water Chemistry in Nuclear Power Plants," SKI, Report: 00:5, 2000.
- [57] J. Henshaw, J. C. McGuire and H. E. Sims, "The Chemistry of Fuel Crud Deposits and It's Effect on AOA in PWR Plants," in *International Conference on Water Chemistry of Nuclear Reactor Systems*, Jeju, South Korea, 2006.
- [58] S. H. Baek, H.-S. Shim and D. H. Hur, "Application of Acoustic Emission Technique for Interpretation of Crud Deposition Behaviour on Fuel Assemblies," in *International Conference on Water Chemistry in Nuclear Reactor Systems*, San Francisco, USA, 2018.
- [59] H. Kawamura and M. Furuya, "Effect of pH and Ni/Fe Ratio on Crud Deposition Behaviour on Heated Zircaloy-4 Surface in Simulated PWR Primary Water," in *International Conference on Water Chemistry of Nuclear Reactor Systems*, Berlin, Germany, 2008.
- [60] J. McGrady, The Effect of Water Chemistry on Corrosion Product Build-Up under PWR Primary Coolant Conditions, PhD Thesis, University of Manchester, 2017.
- [61] T. Grime and N. Stevens, "Modelling of Electrokinetic Deposition Mechanisms," in *International Conference on Water Chemistry in Nuclear Reactor Systems*, San Francisco, USA, 2018.
- [62] J. Wu, N. Stevens, F. Scenini, B. Connolly, L.-J. Pegg and A. Banks, "Finite Element Modelling of CRUD Deposition in PWR," in *International Conference on Water Chemistry in Nuclear Reactor Systems*, San Francisco, USA, 2018.
- [63] EPRI, "Modelling PWR Fuel Corrosion Product Deposition and Growth Processes," EPRI, Report: 1009734, 2004.
- [64] EPRI, "Modelling PWR Fuel Corrosion Product Deposition and Growth Processes: Final Report," EPRI, Report: 1011743, 2005.
- [65] B. Beverskog, "AOA Fuel Crud: A Theoretical Approach," in *Nuclear Power Chemistry 2006. Paper 7.2*, Jeju, 2006.
- [66] J. Chen, H. Bergqvist, D. Jadernas and B. Bengtsson, "Characterization of PWR Fuel Crud by High Resolution Transmission Electron Microscopy," in *International Conference on Water Chemistry of Nuclear Reactor Systems*, Quebec, Canada, 2010.
- [67] J. Chen, B. Bengtsson, H. Bergqvist and D. Jadernas, "On the Phase Compositions of Fuel Crud Formed in PWRs using Steam Generators Tubing Material of Alloy 600 and 690," in *International Conference on Water Chemistry of Nuclear Reactor Systems*, Paris, France, 2012.
- [68] J. Chen, F. Lindberg, D. Wells and B. Bengtsson, "EELS and Electron Diffraction Studies on Possible Bonaccordite Crystals in PWR Fuel Crud and in Oxide Films of Alloy 600 Material," in *International Conference on Water Chemistry of Nuclear Reactor Systems*, Sapporo, Japan, 2014.

- [69] W. Y. Maeng, M. H. Kim and U. C. Kim, "Crud Deposition Characteristics on Nuclear Fuel Cladding in High Temperature Water," in *International Conference on Water Chemistry of Nuclear Reactor Systems*, Paris, France, 2012.
- [70] S.-H. Baek, H.-S. Shim, K. S. Im, U. C. Kim and D. H. Hur, "Effect of Concentration Ratios of Ni/Fe Ions on the Fuel Crud Deposition," in *International Conference on Water Chemistry of Nuclear Reactor Systems*, Sapporo, Japan, 2014.
- [71] H. Kawamura and M. Furuya, "Effect of Water Chemistry on Crud Deposition Behaviour on Heated Zircaloy-4 Surface in Simulated PWR Primary Water," in *International Conference on Water Chemistry of Nuclear Reactor Systems*, Quebec, Canada, 2010.
- [72] H. Kawamura, "Effect of Low DH Concentration on Crud Deposition on Heated Zircaloy-4 in Simulated PWR Primary Water," in *International Conference on Water Chemistry of Nuclear Reactor Systems, Paris, 2012.*, Paris, France, 2012.
- [73] N. Doncel, J. Chen and H. Bergqvist, "Confirmation of Li₂B₄O₇ Presence in Fuel CRUD Formed under Simulated PWR Water Chemistry Conditions," in *International Conference on Water Chemistry of Nuclear Reactor Systems*, Jeju, South Korea, 2006.
- [74] N. Doncel, J. Chen, P. Gillen and H. Bergqvist, "On the Role of Nickel Deposition in a CIPS Occurrence in PWR," in *International Conference on Water Chemistry of Nuclear Reactor Systems*, Berlin, Germany, 2008.
- [75] R. A. Castelli, *Nuclear Corrosion Modelling - The nature of CRUD*, Oxford: Elsevier, 2009.
- [76] D. H. Lister, "Corrosion products in power generating systems: AECL report 6877," Atomic Energy of Canada Ltd, Chalk River, 1980.
- [77] N. N. Man'kina and B. L. Kokotov, "On the problem of the mechanism of formation of iron oxide deposits," *Teploenergetika*, vol. 9, p. 15, 1973.
- [78] W. E. Berry and R. B. Diegle, "EPRI Report NP-522 "Survey of corrosion product generation, transport and deposition in light water reactors"," Electric Power Research Institute, Palo Alto, 1979.
- [79] P. Cohen, *Water Coolant Technology of Power Reactors (Issue 1)*, Gordon & Breach Science Publishers Ltd, 1969.
- [80] A. M. Morillon, *Modelling of radionuclide transport in a simulated PWR environment. MSc Thesis.*, Massachusetts: Massachusetts Institute of Technology, 1987.
- [81] B. L. Chan, *Modelling of corrosion product transport in PWR primary coolant. PhD Thesis.*, Massachusetts: Massachusetts Institute of Technology, 1990.
- [82] M. Rafique, N. M. Mirza, S. M. Mirza and M. J. Iqbal, "Review of computer codes for modeling," *Nukleonika*, vol. 55, no. 3, pp. 263-269, 2010.
- [83] J. C. Robin, F. Coulet, P. Beslu, P. Ridoux and A. Long, "PACTOLE: A computer code to predict the activation and transport of corrosion products in PWRs," in *International symposium on activity transport in water cooled nuclear power reactors*, Ottawa, 1994.
- [84] IAEA, "IAEA TecDoc 667 V3 "Coolant technology of water cooled reactors"," IAEA, Vienna, 1992.

- [85] W. J. Marble, R. L. Cowan and C. J. Wood, "Control of Cobalt-60 deposition rates in BWRs", in *Water Chemistry of Nuclear Reactor Systems 4; British Nuclear Energy Society*, Bournemouth, 1986.
- [86] J. Henshaw, D. Hussey, S. Hanratty, J. McGurk, S. Dickinson, J. Westacott, M. Young, K. Epperson, C. Marks, G. Wang, M. Krammen and J. Fisher, "The Use of the Boron Offset Anomaly (BOA) Code for Understanding Material Transport and Chemistry in PWR Plants," in *The 21st International Conference on Water Chemistry in Nuclear Reactor Systems*, Brighton, 2018.
- [87] W. A. Byers, G. Wang and J. C. Deshon, "The Limits of Zinc Addition in High Duty PWRs," in *International Conference on Water Chemistry of Nuclear Reactor Systems*, Paper L13-4; Berlin, Germany, 2008.
- [88] J. P. Ferguson, H. Arcis and P. R. Tremaine, "Thermodynamics of Polyborates under Hydrothermal Conditions: Formation Constants and Limiting Conductivities of Triborate and Diborate," *Journal of chemical and engineering data*, vol. 64, pp. 4430 - 4443, 2019.
- [89] S. Sasidharanpillai, H. Arcis, L. Trevani and P. R. Tremaine, "Triborate Formation Constants and Polyborate Speciation under Hydrothermal Conditions by Raman Spectroscopy using a Titanium / Sapphire Flow Cell," *Journal of Physical Chemistry B*, vol. 123, pp. 5147 - 5159, 2019.
- [90] J. Henshaw, J. C. McGurk, H. E. Sims, S. Dickinson, A. Tuson and J. Deshon, "A model of chemistry and thermal hydraulics in PWR fuel crud deposits," *Journal of Nuclear Materials*, vol. 353, pp. 1 - 11, 2006.
- [91] E. L. Carlin, P. A. Hilton and Y. Sung, "Margin Assessment of AP1000 Loss of Flow Transient," in *Proceedings of ICONE14 International Conference on Nuclear Engineering*, Miami, 2006.
- [92] J. Deshon, D. Hussey, B. Kendrick, J. McGurk, J. Secker and M. Short, "Pressurized Water Reactor Fuel Crud and Corrosion Modeling," *Journal of Materials*, vol. 63, no. 8, pp. 64 - 72, 2011.
- [93] A. M. Elliott, *Multiphysics Modeling of Activity Transport and Evolution of CRUD and Steam Generator Oxides in Pressurized Water Reactors: MSc Thesis*, Massachusetts: Massachusetts Institute of Technology, 2018.
- [94] D. D. Macdonald, M. Urquidi-Macdonald, J. H. Mahaffy, A. Jain, H. S. Kim, V. Gupta and J. Pitt, "Electrochemistry of water-cooled nuclear reactors. Nuclear Energy Education Research (NEER) Final Technical Progress Report," Pennsylvania State University, 2006.
- [95] M. Jin and M. Short, "Multiphysics Modeling of Two-Phase Film Boiling within Porous Corrosion Deposits," *Journal of Computational Physics*, no. <https://www.elsevier.com/open-access/userlicense/1.0/>, 2016.
- [96] R. L. Williamson, J. D. Hales, S. R. Novascone, G. Pastore, K. A. Gamble, B. W. Spencer, W. Jiang, S. A. Pitts, A. Casagrande, D. Schwen, A. X. Zabriskie, A. Toptan, R. Gardner, C. Matthews, W. Liu and H. Chen, "BISON: A Flexible Code for Advanced Simulation of the Performance of Multiple Nuclear Fuel Forms," *Nuclear Technology*,

vol. 207, pp. 954 - 980, 2021.

- [97] D. R. Gaston, C. J. Permann, J. W. Peterson, A. E. Slaughter, D. Andrs, Y. Wang, M. P. Short, D. M. Perez, M. R. Tonks, J. Ortensi, L. Zou and R. C. Martineau, "Physics-based multiscale coupling for full core nuclear reactor simulation," *Annals of nuclear energy*, vol. 84, pp. 45-54, 2015.
- [98] C. Pan, B. G. Jones and A. J. Machiels, "Concentration levels of solutes in porous deposits with chimneys under wick boiling conditions," *Nuclear Engineering and Design*, vol. 99, pp. 317 - 327, 1989.
- [99] L. Di Pace and S. Sandri, "Evaluation of the Activated Corrosion Product (ACP) and Their Distribution in the Water Cooling Loop of the SEAFP Project," *Fusion Technology*, vol. 30, pp. 1485 - 1488, 1996.
- [100] R. E. Mesmer and C. F. Baes, "Review of Hydrolysis Behavior of Ions in Aqueous Solutions," *MRS Online Proceedings Library*, vol. 180, p. Article No. 85, 1990.
- [101] F. H. Sweeton and C. F. Baes, "The solubility of magnetite and hydrolysis of ferrous ion in aqueous solutions at elevated temperatures," *The Journal of Chemical Thermodynamics*, vol. 2, no. 4, pp. 479-500, 1970.
- [102] K. Mohajery, L. D. de Pierrefeu and D. H. Lister, "The dissolution rate constant of magnetite in water at different temperatures and pH conditions," in *Nuclear Power Plant Chemistry 2012*, Paris, 2012.
- [103] F. Dacquait, J. B. Genin and L. Brissonneau, "Modelling of the contamination transfer in nuclear reactors: The OSCAR code - Applications to SFR and ITER," in *1st IAEA Workshop on Challenges for Coolants in Fast Neutron Spectrum Systems*, Vienna, 2017.
- [104] D. L. Parkhurst and C. A. Appelo, "Users guide to PHREEQC (Version 2): A computer program for speciation, batch-reaction, one-dimensional transport and inverse geochemical calculations," US Department of the Interior / US Geological Survey Report 99-4259, Denver, 1999.
- [105] M. Wang, S. Perrin, C. Corbel and D. Ferron, "Electrochemical behaviour of 316L stainless steel exposed to representative chemistry in pressurised water reactors under proton radiation," *Journal of Electroanalytical Chemistry*, vol. 737, pp. 141 - 149, 2015.
- [106] Consortium for Advanced SIMulation of Light water reactors (CASL), *CASL Technotes, Volume 1, Issue 1.*, Oak Ridge, Tennessee: Oak Ridge National Laboratory, 2013.
- [107] P. J. Turinsky and D. B. Kothe, "Modeling and Simulation Challenges Pursued by the Consortium for Advanced Simulation of Light Water Reactors (CASL)," *Journal of Computational Physics*, vol. 313, pp. 367 -376, 2016.
- [108] J. Kysela, V. Svarc, K. Androva and M. Rucikova, "Crud deposition on fuel in VVER reactors," 2007. [Online]. Available: osti.gov/edweb/servlets/purl/21064726 . [Accessed 02 October 2023].
- [109] J. Wu, PhD Thesis "Finite Element Modelling of CRUD Deposition in PWRs", Manchester: University of Manchester, 2019.

- [110] H. H. Son, Y. S. Cho, N. Kim, S. J. Kim, B. G. Park, H. Lee and H. C. Shin, "Review of crud growth models compatible with thermal-hydraulics codes for multiscale simulation," in *Nuclear Power Chemistry 2018. Poster 10A*, San Francisco, 2018.
- [111] S. Seo, B. Park, S. J. Kim, H. C. Shin, S. J. Lee, M. Lee and S. Choi, "BOTANI: high - fidelity multiphysics model for boron chemistry in crud deposits," *Nuclear Engineering and Technology*, vol. 53, pp. 1676-1685, 2021.
- [112] J. T. Rizk, Thermochemical and continuum modelling to understand the chemical composition of PWR crud. PhD THesis., Knoxville, Tennessee: University of Tennessee, 2021.
- [113] Y. Liu, X. Liu, S. Du, J. Wang and H. He, "Multiphysics coupling model for thermal hydraulics and solute transport in crud deposits," in *Proceedings of the 23rd Pacific Basin Nuclear Conference, Volume 1. PBNC 2022*, Beijing and Chengdu, China, 2022.
- [114] X. H. Liu, K. Wang, Y. Lu, Y. N. Liu and X. Jin, "Study on simulation method of crud deposition behaviour on nuclear fuel," in *Proceedings of the 23rd Pacific Basin nuclear conference; Volume 2. PBNC 2022.* , Beijing and Chengdu, CHINA, 2022.
- [115] S. Seo, N. Chae, S. Park, R. I. Foster and S. Choi, "Model of deposition and erosion of crud on fuel surfaces under sub-cooled nucleate boiling in PWR," *Nuclear Engineering and Technology*, vol. 55, pp. 2591-2603, 2023.
- [116] D. Zaczorowski and J. Roland, "Radiolysis modelling in PWR core.," in *Nuclear Power Chemistry 2023. Specialists workshop on radiolysis and electrochemistry*, Antibes, 2023.
- [117] NEA, "Radiation Protection Aspects of Primary Water Chemistry and Source-Term Management," NEA, NEA/CRPPH/R(2014)2, 2014.
- [118] EPRI, "Radiation Field Control Manual," EPRI, Report: 1003390, 2004.
- [119] J. McElrath and C. Gregorich, "Incorporation of Co-58 and Co-60 into PWR Primary System Surface Oxides," in *International Conference on Water Chemistry of Nuclear Reactor Systems*, Brighton, UK, 2016.
- [120] EPRI, "Evaluation of PWR Radiation Fields and Out-of-Core Surface Activities," EPRI, Report: NP-858, 1981.
- [121] EPRI, "Application of the EPRI Standard Radiation Monitoring Program for PWR Radiation Field Reduction," EPRI, Report: 1015119. Non-proprietary version for U.S.NRC, 2007.
- [122] EPRI, "PWR Activity Transport and Source Term Assessment: Surface Activity Concentrations by Gamma Scanning," EPRI, Report: 1023027, 2011.
- [123] K. S. Kon, "Nuclide Analysis at Domestic Nuclear Power Plant with CZT Detector During the Overhaul," Transactions of the Korean Nuclear Society Autumn Meeting, Gwangju, South Korea, 2013.
- [124] EPRI, "Effects of Hydrogen Peroxide Additions on Shutdown Chemistry Transients at Pressurized Water Reactors," EPRI, Report: NP-692, 1978.

- [125] J. Trebilco, D. Deforge, M. Habert, J. L. Bretelle and M. Bachet, "Water Clarity Issues in Spent Fuel and Reactor Pools; An Analysis of French and International OPEX to find Preventative and Curative Solutions," in *International Conference on Water Chemistry of Nuclear Reactor Systems*, Brighton, UK, 2016.
- [126] M. Domae and K. Fujiwara, "Effect of Shutdown Chemistry on Corrosion Product Release from Oxide Film of Alloy 600," in *International Conference on Water Chemistry of Nuclear Reactor Systems*, Quebec, Canada, 2010.
- [127] EPRI, "PWR Shutdown Chemistry Practices, 1998 through 2001," EPRI, Report: 1007307, 2002.
- [128] EPRI, "Benchmarking Shutdown Chemistry Control Recommendations in the Pressurized Water Reactor Primary Water Chemistry Guidelines," EPRI, Report: 1011780, 2006.
- [129] S. Taunier, P. Varry, A. Tigeras, M. Bachet, L. Guinard, J. L. Bretelle and A. Rocher, "New Primary Shutdown and Startup Chemistry Guidelines Recently Developed for EDF PWRs," in *International Conference on Water Chemistry of Nuclear Reactor Systems*, Berlin, Germany, 2008.
- [130] A. Duval, P. Varry, E. Molerio, D. Deforge, M. Benfarah and J. L. Bretelle, "Primary Shutdown Chemistry Guidelines for EDF PWRs: A New Approach for Better Results," in *International Conference on Water Chemistry of Nuclear Reactor Systems*, Sapporo, Japan, 2014.
- [131] M. L. Calvar, J. L. Bretelle, J. P. Cailleaux, R. Lacroix, M. Guivarch, N. Gay, S. Taunier, F. Gressier, P. Varry, G. Corredera, O. Alos-Ramos and M. Dijoux, "Effect of Water Chemistry on Deposition for PWR Plant Operation," in *International Conference on Water Chemistry of Nuclear Reactor Systems*, Paris, France, 2012.
- [132] S. Taunier, P. Varry, M. Wintergerst, M. Bahet and J. Bretelle, "The Successful Use of an Acid Reducing Chemistry for the Resolution of Flow Variations in the RCS," in *International Conference on Water Chemistry of Nuclear Reactor Systems*, Paris, France, 2012.
- [133] C. Marks, K. Fruzzetti and J. Deshon, "Reaction Kinetics of Primary Coolant Deposit Materials," in *International Conference on Water Chemistry of Nuclear Reactor Systems*, Berlin, Germany, 2008.
- [134] B. Fellers, J. Barnette, J. Stevens and D. Perkins, "Optimization of Reactor Coolant Shutdown Chemistry Practices for Crud Inventory Management," in *International Conference on Water Chemistry of Nuclear Reactor Systems*, Avignon, France, 2002.
- [135] C. Marks, L. Ferrara, C. Gregorich and J. McElrath, "Optimization of Reactor Coolant Pump Operation during PWR Shutdowns," in *International Conference on Water Chemistry of Nuclear Reactor Systems*, Brighton, UK, 2016.
- [136] E. Fernandez Lillo, J. P. Barrios, S. Maldonado and E. Capafons, "Reduction in Dose Rates during Refuelling by Oxygenating the RCS with the Reactor Coolant Pumps Stopped," in *International Conference on Water Chemistry of Nuclear Reactor Systems*, Brighton, UK, 2016.
- [137] P. Mondit, J. Bonnefon, S. Blond and C. Dinse, "Study of the Impact of the Criteria to

Take Offline the Last Reactor Coolant Pump," in *International Conference on Water Chemistry of Nuclear Reactor Systems*, Sapporo, Japan, 2014.

- [138] EPRI, "Development of a Successful Reactor Cavity Decontamination Plan," EPRI, Report: 1009576, 2004.
- [139] C. Marks, "Characterization of Reactor Cavity Water Contamination (poster number 132)," in *International Conference on Water Chemistry of Nuclear Reactor Systems*, Brighton, UK, 2016.
- [140] C. Marks, J. Dingee, P. Saunders, J. Varnam, P. Tran, D. Hussey and J. McElrath, "Chemistry of Cavity Decontamination," in *International Conference on Water Chemistry of Nuclear Reactor Systems*, Brighton, UK, 2016.
- [141] N. Henzel, "Influence of Water Chemistry on Fuel Cladding Behaviour," in *Proceedings of a Technical Committee Meeting Held in Rez, Czech Republic, 4-8 October 1993: Alternative Water Chemistry for the Primary Loop of PWR Plants*, IAEA-TECDOC-927, 1997.
- [142] EPRI, "Potassium Hydroxide: A Potential Mitigation for AOA," EPRI, Report: TE-114158, 1999.
- [143] K. Fruzzetti, C. Marks, J. Reinders, J. McElrath and D. M. Wells, "Evaluation of Potassium Hydroxide for Reactor Coolant pHT Control in Western PWRs," in *International Conference on Water Chemistry of Nuclear Reactor Systems*, Brighton, UK, 2016.
- [144] J. Fandrich and E. Dudka, "Investigation of an Alternative Alkalization Strategy for Primary Coolant Conditioning of Pressurized Light Water Reactors," in *International Conference on Water Chemistry in Nuclear Reactor Systems*, San Francisco, USA, 2018.
- [145] L. Oliver, B. Helmersson, R. DeVito, J. Iyer and D. Hussey, "Westinghouse VVER Fuel Experience and Fuel Qualification Need for Introducing KOH in Pressurised Water Reactors," in *International Conference on Water Chemistry in Nuclear Reactor Systems*, San Francisco, USA, 2018.
- [146] K. Fruzzetti, A. Demma, P. Chou, J. Smith, D. Hussey, K. Kim, C. Gregorich and M. Burke, "Potassium Hydroxide for PWR Primary Coolant pH Control; Materials Qualification testing," in *International Conference on Water Chemistry in Nuclear Reactor Systems*, San Francisco, USA, 2018.
- [147] K. Nigmatullina, J. Rolph, K. Cothran, J. Ritchie, K. Fruzzetti, D. Perkins, P. Chou and D. Hussey, "Potassium Hydroxide for Western-Design PWRs: Plans for a Three Cycle Monitored Campaign at TVA Sequoyah," in *International Conference on Water Chemistry in Nuclear Reactor Systems*, Juan-les-Pins, France, 2023.
- [148] F. Garzarolli, S. Pohlmeier, S. Trapp Pritsching and H. G. Weidinger, "Influence of Various Additions to Water on Zircaloy 4 Corrosion in Autoclave Tests at 350 deg. C," in *IAEA, Vienna (Austria). International Working Group on Water Reactor Fuel Performance and Technology; p 275; Sep 1990, ; p. 65-72; Technical committee meeting on fundamental aspects of corrosion on zirconium base alloys in water reactor environments; Portland, OR (USA); 11-15 Sep 1989. Report: IWGFPT--34, 1990.*

- [149] Y. H. Jeong, J. H. Baek, S. J. Kim, H. G. Kim and H. Ruhmann, "Corrosion Characteristics and Oxide Microstructures of Zircaloy-4 in Aqueous Alkali Hydroxide Solutions," *Journal of Nuclear Materials*, vol. 270, no. 3. DOI: [https://doi.org/10.1016/S0022-3115\(99\)00008-2](https://doi.org/10.1016/S0022-3115(99)00008-2), pp. 322-333, 1999.
- [150] D. Pecheur, A. Giordano, E. Picard, P. Billot and J. Thomazet, "Effect of Elevated Lithium on the Waterside Corrosion of Zircaloy-4, Experimental and Predictive Studies," in *International Atomic Energy Agency, Vienna (Austria); 499 p; ISSN 1011-4289; Worldcat; Feb 1997; p. 111-130; Technical committee meeting on influence of water chemistry on fuel cladding behaviour; Rez (Czech Republic); 4-8 Oct 1993, IAEA-TECDOC-927, 1997.*
- [151] H. Arcis, D. Hussey, J. McGurk, C. Lee, S. Dickinson and J. Henshaw, "Impact of Potassium Primary Coolant Chemistry on PWRs Operating with Fuel Crud," in *International Conference on Water Chemistry in Nuclear Reactor Systems, Juan-les-Pins, France, 2023.*
- [152] K. Chen, M. R. Ickes, M. A. Burke and G. S. Was, "The Effect of Potassium Hydroxide Primary Water Chemistry on the IASCC Behaviour of 304 Stainless Steel," *Journal of Nuclear Materials*, no. DOI: <https://doi.org/10.1016/j.jnucmat.2021.153323>, p. 153323, 2022.
- [153] Z. Zhai, M. B. Toloczko, F. C. Colon and R. A. Bouffieux, "Stress Corrosion Cracking of Ni-Base Alloys in PWR Primary Water Containing KOH vs. LiOH," U.S. Department of Energy Office of Nuclear Energy, Report: M3LW-22OR0402033, 2022.
- [154] J. Dingee, C. Marks, K. Fruzzetti and J. McElrath, "Modelling Potassium Hydroxide for PHT Control in Western-Design PWRs," in *International Conference on Water Chemistry in Nuclear Reactor Systems, San Francisco, USA, 2018.*
- [155] K. Fruzzetti, C. Marks, J. Dingee, K. Kim-Stevens, D. Perkins and K. Nigmatullina, "Potassium Hydroxide for Western-Design PWRs: Chemistry and Radiation Assessments," in *International Conference on Water Chemistry in Nuclear Reactor Systems, Juan-les-Pins, France, 2023.*
- [156] EPRI, "An Evaluation of Enriched Boric Acid in European PWRs, EPRI," EPRI, Report: 1003124, 2001.
- [157] EPRI, "Update on Use of Enriched Boric Acid in Domestic Pressurized Water Reactors," EPRI, Report: 1010153, 2005.
- [158] D. Wiedenmann and K. Cook, "The Benefits of Using Enriched Boric Acid in Commercial Nuclear Power Plants," in *International Conference on Water Chemistry of Nuclear Reactor Systems, Sapporo, Japan, 2014.*
- [159] World Nuclear Association, "Mixed Oxide (MOX) Fuel (updated October 2017)," 06 03 2024. [Online]. Available: <https://world-nuclear.org/information-library/nuclear-fuel-cycle/fuel-recycling/mixed-oxide-fuel-mox.aspx>.
- [160] EPRI, "Re-Evaluation of the Benefits of Implementing Enriched Boric Acid," EPRI, Report: TR-109992, Final Report, 1998.
- [161] C. Cosse, F. Jolivel and M. Berger, "Enriched Boric Acid as an Optimized Neutron Absorber in the EPR Primary Coolant," in *International Conference on Water Chemistry*

of Nuclear Reactor Systems, Paris, France, 2012.

- [162] IAEA, "Optimization of Water Chemistry to Ensure Reliable Water Reactor Fuel Performance at High Burnup and in Aging Plant (FUWAC)," IAEA, IAEA-TECDOC-16667, 2011.
- [163] J. Chen and B. Bengtsson, *PWR Fuel Crud Characterization and CIPS Risk Assessment: A Case Study, FUWAC-2, Chennai, 2007*, IAEA-TECDOC-1666 Companion CD: https://www-pub.iaea.org/MTCD/Publications/PDF/TE_1666_Companion_CD/PDF/IAEA-TECDOC-1666_additional.pdf, 2007.
- [164] J. Chen, *Characteristics of PWR Fuel Crud and their Possible Impact on AOA, FUWAC-III, Turku, 2009*, IAEA-TECDOC-1666 Companion CD, https://www-pub.iaea.org/MTCD/Publications/PDF/TE_1666_Companion_CD/PDF/IAEA-TECDOC-1666_additional.pdf, 2009.
- [165] H. Ocken, K. Fruzzetti, P. Frattini and C. J. Wood, "Recent Developments in PWR Zinc Injection," in *International Conference on Water Chemistry of Nuclear Reactor Systems*, Avignon, 2002.
- [166] EPRI, "Overview Report on Zinc Addition in PWRs," EPRI, Report 1001020, 2001.
- [167] EPRI, "Overview Report on Zinc Addition in Pressurised Water Reactors – 2004," EPRI, Report 1009568, 2004.
- [168] B. Martin-Cabanas, F. Carrette and A. Lorin, "Experimental Determination of Zinc Behaviour in Steam Generator Tubes Inner Surface Oxide Layers," *International Conference on Water Chemistry in Nuclear Reactor Systems*, Poster 007, Juan-les-Pins, 2023, 2023.
- [169] D. Perkins, K. Fruzzetti, C. Haas and D. Wells, "An Overview of the EPRI PWR Primary Chemistry Program," in *International Conference on Water Chemistry of Nuclear Reactor Systems*, Paris, 2012.
- [170] A. Tigeras, A. Stutzmann, O. Bremnes, M. Claeys, G. Ranchoux, J. C. Segura, J. Errera and S. Bonne, "Zinc Injection Implementation Process at EDF: Risk Analysis, Chemical Specifications and Operating Procedures," in *International Conference on Water Chemistry of Nuclear Reactor Systems*, Quebec, Canada, 2010.
- [171] A. Tigeras, G. Debec, B. Jeannin and A. Rocher, "Analysis of Power Reduction Impact on the Chemistry and Radiochemistry Parameters," in *International Conference on Water Chemistry of Nuclear Reactor Systems*, Jeju, South Korea, 2006.
- [172] D. M. Wells, K. Fruzzetti, S. Garcia and J. McElrath, "Chemistry Control to Meet the Demands of Modern Nuclear Power Plant Operation," in *International Conference on Water Chemistry of Nuclear Reactor Systems*, Paper 02; Brighton, UK, 2016.
- [173] A. Tigeras, G. Debec, B. Jeannin and A. Rocher, "EDF Zinc Injection: Analysis of Power Reduction Impact on the Chemistry and Radiochemistry Parameters," in *International Conference on Water Chemistry of Nuclear Reactor Systems*, Paper 2.1; Jeju, South Korea, 2006.
- [174] A. Tigeras, B. Stellwag, N. Engler, J. L. Bretelle and A. Rocher, "Understanding the Zinc

Behaviour in PWR Primary Coolant: A Comparison between French and German Experience," in *International Conference on Water Chemistry of Nuclear Reactor Systems*, Paper L01-1; Berlin, Germany, 2008.

- [175] EPRI, "Proceedings of the August 2004 EPRI PWR Primary Zinc Addition Workshop," EPRI, Report 1011312, 2005.
- [176] J. Henshaw, J. McGurk, S. Dickinson, D. Hussey, J. Deshon, K. Garbett, J. P. B. Figeras, S. M. Sanchez and E. F. Lillo, "Modelling Zinc Behaviour in PWR Plant," in *International Conference on Water Chemistry of Nuclear Reactor Systems*, Paper O28-57; Paris, France, 2012.
- [177] C. Marks, M. Dumouchel and C. Haas, "Primary Chemistry Response to Initial Zinc Injection," in *International Conference on Water Chemistry of Nuclear Reactor Systems*, Paper 1.16P; Quebec, Canada, 2010.
- [178] R. Reid, D. Hussey, C. Marks and J. Dingee, "Effect of Corrosion Product Release Behaviour under PWR Primary System Conditions," in *International Conference on Water Chemistry of Nuclear Reactor Systems*, Paper 10072; Sapporo, Japan, 2014.
- [179] D. Hussey, A. Parsi and A. Byers, "Measurement of Steam Generator Tubing Oxide Morphology Changes after Zinc Injection," in *International Conference on Water Chemistry in Nuclear Reactor Systems*, Paper 059; Juan-les-Pins, France, 2023.
- [180] T. Terachi, T. Kuge, N. Nakano, K. Yamaguchi, T. Nakagawa, M. Murashita, T. Tanabe, T. Okada, F. Iwaki, K. Sakata, T. Nishimura, R. Umehara and Y. Shimizu, "Dose Rate Determining Factors of PWR Primary Water," in *International Conference on Water Chemistry of Nuclear Reactor Systems*, Paper 10153; Sapporo, Japan, 2014.
- [181] G. Le Meur, M. Benfarah, A.-M. Harmand, A. Stutzmann, S. Taunier, J.-L. Bretelle, A. Rocher, M. Claeys and S. Bonne, "Zinc Injection on the EDF Fleet: Monitoring the Injection on 12 Units," in *International Conference on Water Chemistry of Nuclear Reactor Systems*, Paper P1-187; Paris, France, 2012.
- [182] N. Lynch, C. Gregorich and B. Johnson, "Zinc Impact on PWR Coolant Piping Radiation Fields – A Statistical Look," in *International Conference on Water Chemistry of Nuclear Reactor Systems*, Paper 72; Brighton, UK, 2016.
- [183] C. A. Gregorich, N. Lynch and B. Johnson, "Actionable Insights for Reducing Radiation Fields in Nuclear Power Plants through Multivariate Statistical Analysis," in *International Conference on Water Chemistry of Nuclear Reactor Systems*, Paper 36; Brighton, UK, 2016.
- [184] O. Piana, A. Duval, E. Moleiro, M. Benfarah, J.-L. Bretelle and G. Chaigne, "Zinc Injection on the EDF Pressurized Light Water Reactors: Current Results and Operating Experience Feedback," in *International Conference on Water Chemistry of Nuclear Reactor Systems*, Paper 10211; Sapporo, Japan, 2014.
- [185] O. Alos-Ramos, E. Lucas, M. Bachet, R. Moll, M. Habert, H. Shneider, U. Ortega-Rodriguez and M. Pierre, "Enhance of Silica Management in French PWR Fleet," in *International Conference on Water Chemistry of Nuclear Reactor Systems*, Paper 07; Brighton, UK, 2016.
- [186] EPRI, "Behaviour of Zinc and Silica in the PWR Primary System: PWR Chemistry

Technical Strategy Group Report," EPRI, Report 3002015884, 2019.

- [187] A. Agarwal, J. McGurk, S. Dickinson, D. Wells, S. Connolly and J. Henshaw, "Zinc Chemistry in PWR Fuel Crud," International Conference on Water Chemistry of Nuclear Reactor Systems, Paper 10112; Brighton, UK, 2014.
- [188] A. Magnusson, P.-O. Aronsson, K. Lundgren and K. Stenstrom, "Characterization of ¹⁴C in Swedish Light Water Reactors," *Health Physics*, vol. 95, no. 2; DOI: <https://dx.doi.org/10.1097/01.HP.0000309765.35223.14>, pp. S110-S121, 2008.
- [189] R. Reid and M. Little, "PWR Primary System Chemistry Control during Hot Functional Testing," in *International Conference on Water Chemistry of Nuclear Reactor Systems*, Sapporo, Japan, 2014.
- [190] K. Garbett and M. Mantell, "Corrosion Product Behaviour during Hot Functional Tests and Normal Operation in Cycle 1 at Sizewell B," in *Water Chemistry of Nuclear Reactor Systems 7. BNES*, Bornemouth, UK, 1996.
- [191] J. Bates, G. A. Lancaster, M. Scrancher and K. Garbett, "Corrosion Product Monitoring during the Seventh Refuelling Ouage at Sizewell B," in *International Conference on Water Chemistry of Nuclear Reactor Systems*, Jeju, South Korea, 2006.
- [192] I. Betova, M. Bojinov, V. Karastoyanov, P. Kinnunen and T. Saario, "Optimisation of the Water Chemistry during Hot Functional Test of a PWR for Improved Stability of the Passive Film on Alloy 690," in *International Conference on Water Chemistry of Nuclear Reactor Systems*, Paris, France, 2012.
- [193] E. Yamada, S. Suzuki, T. Hirao, Y. Hashimoto, K. Hisamune and J. Yokoyama, "Corrosion Rate Reduction by Chemistry Control during Hot Functional Test," in *1991 JAIF international conference on water chemistry in nuclear power plants; Fukui (Japan); 22-25 Apr 1991*, Tokyo, Japan, 1991.
- [194] M. Bachet, "Cleaning the Primary Circuit After the First High Temperature Oxidation of Steam Generator Tubing: Why and How to Do It," in *International Conference on Water Chemistry of Nuclear Reactor Systems*, Quebec, Canada, 2010.
- [195] G. Ranchoux, M. Wintergerst, M. Bachet, S. Leclercq, J.-D. Duron, J.-P. Meunier, S. Blond and F. Dacquait, "Optimized High Temperature Oxidation and Cleaning at Bugey 3," in *International Conference on Water Chemistry of Nuclear Reactor Systems*, Paris, France, 2012.
- [196] S. Leclercq and M. Bachet, "Steam Generator Tube Pre-Oxidation and Cleaning – Effect on Release and Oxides Formation," in *International Conference on Water Chemistry of Nuclear Reactor Systems*, Paris, France, 2012.
- [197] H. Hayakawa, Y. Mino, S. Nakahama, Y. Aizawa, T. Nishimura, R. Umehara, Y. Shimuz and N. Kogawa, "Zinc Injection during Hot Functional Testing (HFT) in Tomari Unit 3," in *International Conference on Water Chemistry of Nuclear Reactor Systems*, Quebec, Canada, 2010.
- [198] Y. Aizawa, K. Ouchi, H. Hayakawa, S. Nakahama, T. Nishimura, R. Umehara, Y. Shimizu, N. Kogawa and Z. Ojima, "The Effects of Zinc Injection from HFT at Tomari Unit 3," in *International Conference on Water Chemistry of Nuclear Reactor Systems*, Sapporo, Japan, 2014.

- [199] A. Drexler, S. Schutz, J. Duca, R. Manzi, G. Galarza, G. Grasso, R. Bejarano, A. Carvalho, A. Francisco, F. Portugal, M. Oliveira, M. Menezes, M. Rubenich and W. Ferreira, "Chemistry Concept for Dose Rate Minimization Treatment of New and Decontaminated PWRs and PHWRs," in *International Conference on Water Chemistry of Nuclear Reactor Systems*, Brighton, UK, 2016.
- [200] R. L. DeVito, D. J. Buckley, W. A. Byers, R. J. Jacko and E. J. Silva, "Westinghouse Experience with AP1000 Plant Hot Functional Testing Chemistry," in *International Conference on Water Chemistry in Nuclear Reactor Systems*, San Francisco, USA, 2018.
- [201] A. Tigeras, N. Engler, M. Durel, M. Alves-Vieira and A. Blow, "Flamanville 3 – EPR Commissioning: Chemistry and Radiochemistry Roles and Interfaces," in *International Conference on Water Chemistry of Nuclear Reactor Systems*, Brighton, UK, 2016.
- [202] N. Engler, C. Brun and M. Guillodo, "Optimization of SG Tubes Prefilming Process to Reduce Nickel Release," in *International Conference on Water Chemistry of Nuclear Reactor Systems*, Berlin, Germany, 2008.
- [203] L. Guinard, C. Bates, G. Lancaster and F. Dacquit, "Characterization of Contamination: EMECC Campaign at Sizewell B and Comparison with French PWRs," in *International Conference on Water Chemistry of Nuclear Reactor Systems*, Berlin, Germany, 2008.
- [204] A. Tigeras, A. Basile, Y. Bouhlassi, M. Alves Vieira, M. Corbineau, S. Le Beguec, M. Gravouelle and C. Cosse, "Chemical Conditions during the Hot Functional Tests of EPR – Flamanville 3," in *International Conference on Water Chemistry in Nuclear Reactor Systems*, Juan-les-Pins, France, 2023.
- [205] A. Tigeras, Y. Boullassi, A. Basile and M. Alves Viera, "EPR – Flamanville 3 Hot Functional Testing: Key Insights and Lessons from Chemistry and Systems Operation," in *International Conference on Water Chemistry in Nuclear Reactor Systems*, Juan-les-Pins, France, 2023.
- [206] M. Corbineau, J. B. Doucet, L. Peng, W. Zhu, N. Engler and A. Tigeras, "Taishan EPR Commissioning: Chemistry of the Primary and Secondary Water Circuits during Hot Functional Tests," in *International Conference on Water Chemistry in Nuclear Reactor Systems*, San Francisco, USA, 2018.
- [207] N. Engler, M. H. Clinard, M. Skocic and K. Tompuri, "OL3 EPR Experience with Hot Functional Testing Chemistry," in *International Conference on Water Chemistry in Nuclear Reactor Systems*, Juan-les-pins, France, 2023.
- [208] EPRI, "Pressurized Water Reactor Fuel Cleaning Using Advanced Ultrasonics," EPRI, Report: 1001052, 2000.
- [209] EPRI, "Fuel Pellet Integrity Assessment for the EPRI Ultrasonic Fuel Cleaning Device," EPRI, Report: 1001095, 2020.
- [210] J. Blok and P. Frattini, "Advances in Ultrasonic Fuel Cleaning," in *International Conference on Water Chemistry of Nuclear Reactor Systems*, Avignon, France, 2002.

- [211] EPRI, "Application of Ultrasonic Fuel Cleaning at Two Pressurized Water Reactors," EPRI, Report: 1007856, 2003.
- [212] EPRI, "Ultrasonic Fuel Cleaning Efficacy Campaign Results at Callaway," EPRI, Report: 1003229, 2002.
- [213] EPRI, "Calculation of Dose Rate Benefits from Ultrasonic Cleaning of PWR Reload Fuel," EPRI, Report: 1003125, 2001.
- [214] EPRI, "ALARA and Low-Level Waste Impacts of Ultrasonic Fuel Cleaning," EPRI, Report: 1009570, 2004.
- [215] M. Little, "High-Efficiency Ultrasonic Fuel Cleaning (HE-UFC): Industry Experience & Adaptations in the COVID-19 Era," in *ANS DC Section Meeting – September 2020*, <http://www.dcsection.org/wp-content/uploads/2020/09/2020-09-ANS-Presentation-, 2020>.
- [216] B. Bengtsson, P. Svanberg, J. Dingee, A. Pellman and D. Wells, "Experience with High Efficiency Ultrasonic Fuel Cleaning using a Side Stream Sampling System at Ringhals Unit 4," in *International Conference on Water Chemistry of Nuclear Reactor Systems*, Sapporo, Japan, 2014.
- [217] B. Bengtsson, P. Svanberg, D. Arguelles and W. Eek, "Safety and Radiation Benefits Using Frequent and Optimised Fuel Cleaning," in *International Conference on Water Chemistry of Nuclear Reactor Systems*, Brighton, UK, 2016.
- [218] K.-S. Choi, J.-H. Kim, J.-I. Kim, Y.-H. Kim, Y.-K. Kim and J.-Y. Park, "Fuel Integrity Evaluation for Ultrasonic Fuel Cleaning," in *Transactions of the Korean Nuclear Society Spring Meeting, 25-26 May 2006*, Chuncheon, South Korea, 2006.
- [219] J. Y. Park, Y. B. Kwon, J. C. Shin, J. Y. Park, J. S. Choi, Y. K. Kim, K. S. Choi and I. K. Choi, "KNFC Crud Sampling and Fuel Cleaning Technology Development," 08 03 2024. [Online]. Available: <https://citeseerx.ist.psu.edu/document?repid=rep1&type=pdf&doi=807649f633d47481c99b7288590b19ccd36e26cb>.
- [220] K. S. Woo, S. Park, G. Kim, W. Han and S. Woo, "Ultrasonic Cleaning for Reloaded Nuclear Fuel in Domestic NPP," in *This paper appears in both Transactions of the Korean Nuclear Society Spring Meeting, Jeju, May 2018 and Transactions of the Korean Nuclear Society Spring Meeting, Jeju, May 2019*, https://www.kns.org/files/pre_paper/41/19S-544-%EA%B9%80%EC%83%81%EC%9A%B0.pdf (Accessed 08/03/2024), 2018 & 2019.
- [221] J. Deshon, K. Edsinger, P. Frattini, D. Hussey and C. J. Wood, "Ultrasonic Fuel Cleaning in PWRs and BWRs," in *International Conference on Water Chemistry of Nuclear Reactor Systems*, Jeju, South Korea, 2006.
- [222]
- [223] M. Little, J. Jaegers, J. Moser, D. Arguelles and C. Marks, "Effects of High Efficiency Ultrasonic Fuel Cleaning (HE-UFC) on Chemistry, Radiological Conditions and Fuel Performance," in *International Conference on Water Chemistry in Nuclear Reactor Systems*, Juan-les-Pins, France, 2023.
- [224] IAEA, "Review of fuel failures in water cooled reactors. Technical Report 388,"

International Atomic Energy Agency, Vienna, 1998.

- [225] IAEA, "Review of Fuel Failures in Water Cooled Reactors: IAEA Nuclear Energy Series NF-T-2.1," IAEA, Vienna, 2010.
- [226] IAEA, "Review of Fuel Failures in Water Cooled Reactors (2006-2015): No NF-T-2.5 (An update to NF-T-2.1)," IAEA, Vienna, 2019.
- [227] Nuclear Safety Analysis Center, "Analysis of Three Mile Island - Unit 2 Accident. EPRI-NSAC-80-1 (NSAC-1 Revised 1980)," Electric Power Research Institute, Palo Alto, 1980.
- [228] United States Nuclear Regulatory Commission, "Reactor Safety Study - An assessment of risks at US commercial nuclear power plants: WASH-1400 (NUREG-75/014)," USNRC, Springfield, 1975.
- [229] R. Bartel, "WASH 1400 The Reactor Safety Study: the introduction of risk assessment to the regulation of Nuclear Reactors. NUREG//KM-0010," United States Nuclear Regulatory Commission, Washington, 2016.
- [230] IAEA, "OECD - IAEA Paks Fuel Project Final Report.," International Atomic Energy Agency, Vienna, 2010.
- [231] International Experts Meeting, Vienna, 19-22 March 2012, "IAEA report on Reactor and Spent Fuel Safety in the light of the accident at the Fukushima Daiichi Nuclear Power Plant," International Atomic Energy Agency, Vienna, 2012.
- [232] IAEA, "IAEA Safety Standards: Operating Experience Feedback for Nuclear Installations. Specific Safety Guide No. SSG-50," International Atomic Energy Agency, Vienna, 2018.
- [233] ASTM, "Standard Guide for Drying Behavior of Spent Nuclear Fuel," ASTM International, C1553-08, 2008.
- [234] Y. S. Kim, J. S. Noh, S. C. Kwon and I. H. Kuk, "Effect of Hoop Stress on Corrosion of Zircaloy-4 Cladding Tube," *Journal of Nuclear Materials*, vol. 223, no. 2, DOI: [https://doi.org/10.1016/0022-3115\(94\)00679-2](https://doi.org/10.1016/0022-3115(94)00679-2), pp. 163-168, 1995.
- [235] A. W. Colldewei, M. G. Makowska, O. Tabai, D. F. Sanchez and J. Bertsch, "Zirconium Hydride Phase Mapping in Zircaloy-2 Cladding after Delayed Hydride Cracking," *Materialia*, vol. 27, no. DOI: <https://doi.org/10.1016/j.mtla.2023.101689>, p. 101689, 2023.
- [236] EPRI, "Development of a Metal/Hydride Mixture Model for Zircaloy Cladding with Mixed Hydride Structure," EPRI, 1009694, 2004.
- [237] IAEA, "Delayed Hydride Cracking of Zirconium Alloy Fuel Cladding," IAEA, IAEA-TECDOC-1649, 2010.
- [238] D. O. Northwood and R. W. Gilbert, "Hydrides in Zirconium-2.5 wt. % Niobium Alloy Pressure Tubing," *Journal of Nuclear Materials*, vol. 78, no. 1, DOI: [https://doi.org/10.1016/0022-3115\(78\)90509-3](https://doi.org/10.1016/0022-3115(78)90509-3), pp. 112-116, 1978.
- [239] V. A. Yurmanov, V. N. Belous, V. N. Vasina and E. V. Yurmanov, "Chemistry and Corrosion Issues in Supercritical Water Reactors: Paper 11.02," in *Nuclear Power*

Chemistry 2010, Quebec, 2010.

- [240] J. Killeen, "IAEA Program on nuclear fuel cycle and materials technologies," Vienna, 2009.
- [241] Office for Nuclear Regulation, "Step 4 Assessment of Chemistry for the UK Advanced Boiling Water Reactor. Assessment Report: ONR-NR-AR-17-020," Office for Nuclear Regulation, Bootle, 2017.
- [242] S. Hettiarachchi, "A Review of BWR Fuel Performance under Modern Water Chemistry Conditions," 2011. [Online]. Available: https://inis.iaea.org/collection/NCLCollectionStore/_Public/43/056/43056259.pdf. [Accessed 12 December 2023].
- [243] IAEA, "Spent fuel storage operation - Lessons Learned," IAEA, IAEA-TECDOC-1725, 2013.
- [244] H. Nagao, Y. Morikawa, K. Yamazaki, Y. Hemmi, Y. Nakayama, K. Takagi, S. Yoshikawa, Y. Suzuki and K. Otoha, "Corrosion product behaviour in low crud boiling water reactors," in *Water Chemistry of Nuclear Reactor Systems 4: Vol 2 p 59*, Bournemouth, 1986.
- [245] C. C. Lin, "Foreign Approaches to Controlling Radiation-Field Buildup in BWRs. EPRI report NP-6942-D," EPRI, Palo Alto, 1990.
- [246] K. Hisamune, T. Yamamoto, H. Takiguchi, K. Sakai, H. Igarishi, N. Usui and K. Ohsumi, "Characterisation of fuel and pipe surface deposit in Tokai-2," in *1991 JAIF International Conference on Water Chemistry in Nuclear Power Plants. Proceedings page 444.* , Fukui, Japan, 1991.
- [247] C. C. Lin, R. L. Cowan and E. Kiss, "Optimum coolant chemistry in BWRs," in *The 4th International Topical Meeting on Nuclear Thermal Hydraulics , Operations and Safety*, Taipei, 1994.
- [248] T. Kelen, K. Lundgren and B. Andersson, "Fuel corrosion and activity buildup in BWRs: Impact from metal balance," in *Water Chemistry of Nuclear Reactor Systems 8. Volume 1 p103. British Nuclear Energy Society*, Bournemouth, 2000.
- [249] H. P. Hermansson, "A Comparison of Crud Phases Appearing on Some Swedish BWR Fuel Rods Using Laser Raman Spectroscopy," in *Water Chemistry of Nuclear Reactor systems SFEN 2002. Part 2 Paper 73.* , Avignon, 2002.
- [250] C. C. Lin, "A review of corrosion product transport and radiation field buildup in boiling water reactors," *Progress in Nuclear Energy*, vol. 51, pp. 207 - 224, 2009.
- [251] H. P. Hermansson and J. Haag, "MOBILE CRUD AND TRANSPORTATION OF RADIOACTIVITY IN BWR," in *Nuclear Power Chemistry 2010. Paper 2.06*, Quebec, 2010.
- [252] A. Orlov, D. A. Kulik, C. Degueudre, G. Bart, W. Kaufmann and S. Valizadeh, "Corrosion Product Deposits on BWR Cladding: A Comparison of Thermodynamic Modelling Predictions with Experimental Analytical Results," in *Nuclear Power Chemistry 2010: Paper 8.09P*, Quebec, 2010.

- [253] J. A. Sawicki, "Analyses of fuel crud and coolant-borne corrosion products in normal water chemistry BWRs," *Journal of Nuclear Materials*, vol. 419, pp. 85-96, 2011.
- [254] L. Oliver, B. Helmersson, P. Cronstrand, G. Ledergerber and A. Kucuk, "Impact of Long Term Injection of Platinum (HWC/OLNC) on Water Chemistry, Crud Behavior and Platinum Deposition," in *Nuclear Power Chemistry 2014. Paper 10131.*, Sapporo, 2014.
- [255] P. V. Grundler, S. Ritter, L. Veleva, H. Wiese, L. Oliver, B. Helmersson, S. Allner and G. Ledergerber, "Influence of Pt Deposition on the Behaviour of Zircaloy Cladding under Boiling Conditions in Simulated BWR Environment," in *Nuclear Power Chemistry 2016. Session 8 Paper 30.*, Brighton, 2016.
- [256] M. Olsson, "Development, Identification and Inspection of 43 BWR Fuel Failures," in *The 21st International Conference on Water Chemistry in Nuclear Reactor Systems: Paper 12_2.*, San Francisco, 2018.
- [257] M. Beckman, "From Lithium to Potassium," 09 January 2020. [Online]. Available: <https://eprijournal.com/from-lithium-to-potassium/>. [Accessed 04 December 2023].
- [258] T. J. Katona, *Materials Ageing and Degradation in Light Water Reactors: Mechanisms and Management. Chapter 8.*, Woodhead Publishing, 2013.
- [259] Nuclear Engineering International, 2011 World Nuclear Industry Handbook, Sidcup: Nuclear Engineering International, 2011.
- [260] Wikipedia, "Layout of the four primary cooling circuits and the pressurizer of a VVER-1000," RusCloud, 25 September 2010. [Online]. Available: <https://en.wikipedia.org/wiki/VVER#/media/File:VVER-1000-Stereometric.svg>. [Accessed 05 December 2023].
- [261] J. Kysela, "VVER primary coolant chemistry experience and perspectives.," in *Water Chemistry of Nuclear Reactor Systems 6. British Nuclear Energy Society. Volume 1 page 1.*, Bournemouth, 1992.
- [262] J. Burclova, "Standard and hydrazine water chemistry in primary circuit of VVER 440 units," in *Water Chemistry of Nuclear Reactor Systems 6. British Nuclear Energy Society. Volume 1 page 9.*, Bournemouth, 1992.
- [263] M. Zmitko, "Investigation and modelling of corrosion product mass and activity transport in VVER and PWR primary systems. Poster 16.," in *Water Chemistry of Nuclear Reactor Systems 6. Volume 2. Page 331. British Nuclear Energy Society.*, Bournemouth, 1992.
- [264] M. Zmitko, J. Kysela, K. Roztocilova, I. Petrecky and M. Halin, "State-of-the-art in primary water chemistry and radiation control of VVERs," in *Water Chemistry of Nuclear Reactor Systems 7. British Nuclear Energy Society. Volume 2 Page 451.*, Bournemouth, 1996.
- [265] I. Smiesko, I. Petrecky and P. Marcinsky, "Factors influencing dose rate build up in Czech and Slovak NPPs," in *Water Chemistry of Nuclear Reactor Systems 8. British Nuclear Energy Society. Volume 1 page 12.*, Bournemouth, 2000.
- [266] IAEA, "Optimization of Water Chemistry to Ensure Reliable Water Reactor Fuel

Performance at High Burnup and in Ageing Plant (FUWAC):IAEA TECDOC 1666," IAEA, Vienna, 2011.

- [267] N. Vajda, Z. Molnar, Z. Maccsik, E. Szeles, P. Hargittai, A. Csordas, T. Pinter and T. Pinter, "Corrosion Particles in the Primary Coolant of VVER-440 Reactors," in *Nuclear Power Chemistry 2010: Water Chemistry of Nuclear Reactor Systems Paper 1.06*, Quebec, 2010.
- [268] V. Kritsky and I. Berezina, "Zirconium Fuel Cladding Corrosion Prediction in Fuel Assembly Operation Conditions," in *Nuclear Power Chemistry 2010: Water Chemistry of Nuclear Power Systems. Paper 4.05*, Quebec, 2010.
- [269] V. Kritsky, I. Berezina and Y. Rodionov, "Influence of Operating and Water-Chemistry Parameters on Fuel Cladding Corrosion and Deposition of Corrosion Products on Cladding Surfaces," in *Nuclear Power Chemistry 2010: Water Chemistry of Nuclear Power Systems. Paper 8.02*, Quebec, 2010.
- [270] S. Buddas and M. Makinen, "Abnormal Solid Matter Observations at Loviisa NPP Unit 2," in *Nuclear Power Chemistry 2016: Water Chemistry of Nuclear Power Systems. Poster 74*, Brighton, 2016.
- [271] IAEA Conference proceedings, Water Chemistry and Clad Corrosion / Deposition Including fuel failures. IAEA Tecdoc-CD-1692. Proceedings of a Technical Meeting Kiev, 2010., Vienna: IAEA, 2013.
- [272] Special Metals Corporation, *Incoloy Alloy 800: Publication Number SMC-046*, Special Metals Corporation, 2004, p. 12.
- [273] P. K. Sinha, M. K. Kumar and V. Kain, "Effect of microstructure of carbon steel on magnetite formation in simulated Hot Conditioning environment of nuclear reactors," *Journal of Nuclear Materials*, vol. 464, pp. 20 - 17, 2015.
- [274] P. Wu, Y. Ren, M. Feng, J. Shan, Y. Huang and W. Yang, "A review of existing SuperCritical Water reactor concepts, safety analysis codes and safety characteristics," *Progress in Nuclear Energy*, vol. 153, p. 104409, 2022.
- [275] M. Yetisir, D. Rhodes and M. J. Gaudet, "Development and integration of Canadian SCWR concept with counter-flow fuel assembly: AECL Conf Paper CW-127000-CONF-006," in *The 6th International Symposium on Supercritical Water-Cooled Reactors ISSCWR-6*, Shenzhen, China, 2013.
- [276] T. Donoclift, *The Radiolytic Steady-State and Factors Controlling H2 Production*: PhD Thesis, Manchester: University of Manchester, 2016.
- [277] Z. E. Celiz, M. Lani Saumell, R. A. Versaci and P. B. Bozzano, "Microstructural Characterization of Excel Zirconium Alloy," *Procedia Materials Science*, vol. 8, pp. 442-450, 2015.
- [278] International Atomic Energy Agency, "Status of research and technology development for supercritical water cooled reactors. IAEA TECDOC 1869," IAEA, Vienna, 2019.
- [279] R. Novotny and D. Guzonas, Material research for the supercritical water-cooled reactor - summary and open issues. In Nuclear Corrosion Research, Progress and Challenges. European Federation of Corrosion (EFC) Series, European Federation of

Corrosion, 2020.

Distribution

Name	Email Address	Location
[REDACTED]	[REDACTED]	[REDACTED]
NNL Document Controller		